Université de Montréal

Caractérisation du rôle de Citron Kinase durant la cytokinèse

par Nour El-amine

Département de Pathologie et Biologie Cellulaire
Faculté de Médecine

Thèse présentée à la Faculté des études supérieures
en vue de l'obtention du grade de Doctorat
en Pathologie et Biologie Cellulaire

Décembre, 2016

Université de Montréal

Faculté de Médecine

Cette thèse intitulée :

Caractérisation du rôle de Citron Kinase durant la cytokinèse

présentée par :

Nour El-amine

a été évaluée par un jury composé des personnes suivantes :

Dr Éric Lécuyer, président-rapporteur

Dr Gilles Hickson, directeur de recherche

Dr Jean-Claude Labbé, membre du jury

Dr Craig Mandato, examinateur externe

Dr Christian Beauséjour, représentant de la doyenne de la faculté de médecine

Résumé

La cytokinèse est un processus dont le but est une séparation de deux cellules sœurs en deux entités suite à une mitose. La cytokinèse nécessite la formation d'un anneau contractile (AC) qui va conduire un sillon de clivage vers une ingression à l'équateur de la cellule. L'une des étapes critiques de ce processus est la transition d'un AC dynamique vers une structure stable surnommée l'anneau du midbody (AM), organelle qui va guider la cellule vers l'abscision. La compréhension des mécanismes moléculaires impliqués dans cette transition nous permettrait de mieux comprendre les complexes protéiques impliqués autant au niveau de l'initiation qu'à la terminaison de la cytokinèse. Des défauts ayant lieu lors de cette transition mènent à la formation de cellules binucléées tétraploïdes qui sont observées dans plusieurs pathologies comme le cancer. Afin d'approfondir nos connaissances à ce sujet j'ai utilisé un modèle d'imagerie optique en temps réel dans un modèle cellulaire de *Drosophila melanogaster* : les cellules S2 de Schneider. Ces études ont mis l'emphase sur un nouveau mécanisme de maturation de la transition AC/AM. Nous avons pu démontrer que la kinase Citron, Sticky, et la septine, Peanut, agissent de manière opposée sur la protéine Anillin pour retenir ou éliminer, respectivement, la membrane plasmique lors de la transition AC/AM. En effet, la diminution d'expression de Sticky par ARNi engendre une perte de contrôle de rétention membranaire de l'AM. À l'inverse, la diminution d'expression de Peanut inhibe la maturation par excrétion membranaire de l'AM. La diminution d'expression simultanée de Sticky et de Peanut conduit l'AC vers des mouvements oscillatoires typiques d'une instabilité de l'AC suite à la perte de fonction de l'Anillin. Sticky est une protéine corticale lors de la cytokinèse dont le rôle et les partenaires d'interaction restent controversés. Pour approfondie nos connaissance de ce sujet, nous avons effectué une étude structurelle et fonctionnelle de Sticky. Cette étude démontre que Sticky possède deux mécanismes de localisation corticale. Le premier dépend de l'Anillin et le deuxième dépend de la petite GTPase Rho1, le régulateur maître de la cytokinèse. Sticky est capable de se localiser à l'AC en présence de l'un ou l'autre de ces deux mécanismes, mais chacun semble être essentiel pour la réussite de la cytokinèse. Le domaine minimal d'interaction entre la Sticky et l'Anillin a été identifié. Une version d'Anillin qui manque le site de liaison à la Sticky est incapable de supporter l'achèvement de la cytokinèse, et les cellules échouent la

cytokinèse d'une manière semblable aux cellules dont l'expression de Sticky est diminuée. Similairement, les cellules exprimant une protéine Sticky mutée au site d'interaction avec Rho1-GTP, sont incapables de compléter la cytokinèse lorsque les niveaux endogènes de Sticky sont diminués par ARNi. Ceci suggère que Sticky agit avec Anillin et Rho1 au niveau du cortex pour guider la transition d'un AC dynamique vers un AM stable. Par la mise en évidence et la caractérisation d'un nouveau mécanisme moléculaire essentiel à la cytokinèse, cette thèse constitue des avancements importants au niveau de la cytokinèse.

Mots-clés : Sticky, Citron Kinase, Anillin, Rho1, RhoA, Septin, Peanut, cytokinèse, cytocinèse, cytodiérèse, anneau du midbody, anneau contractile

Abstract

Cytokinesis is a multistep process that allows two sister cells to undergo complete separation following mitosis. Cytokinesis requires the formation of a contractile ring (CR) that will drive cleavage furrow ingression at the equator of the cell. One of the crucial steps in this process is the transition from a dynamic CR to a more stable structure named the midbody ring (MR), which directs the final separation or abscission. Our knowledge of the molecular mechanisms involved in the CR-to-MR transition would presumably improve our understanding of the molecular complexes involved throughout cytokinesis from initiation to abscission. Defects that occur during this transition can lead to the formation of bi-nucleate tetraploid cells that are often observed in pathological conditions such as cancer. I have used *Drosophila melanogaster* Schneider's S2 cells to study the CR-to-MR transition. My findings have highlighted a previously uncharacterized maturation process essential for the transition. More specifically, I demonstrate that the Citron Kinase, Sticky, and the Septin, Peanut, have opposing actions on the scaffold protein Anillin to either retain or extrude, respectively, membrane-positive proteins during the CR-to-MR transition. Indeed, Sticky depletion by RNAi led to uncontrolled loss of membrane-associated Anillin at the MR. Conversely, Peanut depletion led to inhibition of MR maturation by membrane extrusion. Co-depletion of Sticky and Peanut led to oscillatory movements of the CR, typical of Anillin depletion. Sticky is a cortical protein during cytokinesis whose role and interacting partners are controversial. I have performed a structure/function analysis of Sticky to better define its role and regulation during cytokinesis. My work shows that Sticky has two mechanisms of cortical localization. The first is through an Anillin interaction and the second is through the small GTPase Rho1, a master regulator of cytokinesis. Sticky can localize to the cortex in the absence of either one of these mechanisms. However, loss of both inhibits its localization. Following the identification of the minimal interaction sites of Anillin and Sticky, I expressed an Anillin mutant that lacked part of this site and found that cells failed cytokinesis in a similar manner to cells depleted of Sticky. Mutation of the Rho1 binding site on Sticky produced similar cytokinesis failures. Altogether, the results suggest that Sticky interacts with Anillin and Rho1 at the cortex to guide the transition from dynamic CR to stable MR. This thesis advances our understanding of cytokinesis by highlighting a previously

uncharacterized process of MR maturation and by defining the importance and regulation of Citron Kinase during this process.

Keywords: Cytokinesis, midbody ring, contractile ring, Citron Kinase, Sticky, Anillin, Peanut, Septin, RhoA, Rho1

Vulgarisation

Chez les organismes vivants pluricellulaires, une cellule représente une unité de l'organisme. Toutes les cellules d'un même organisme ont un ancêtre commun. Chez l'homme, c'est l'ovule fécondé par un spermatozoïde. L'être humain est composé de plusieurs trillions de cellules. Pour pouvoir se rendre à ce chiffre à partir de la cellule d'origine, il faut un processus robuste qui permet à la cellule de se multiplier. Ce processus s'appelle le cycle cellulaire, qui est un parcours pour chaque unité de l'organisme au cours duquel la cellule se trouve dans 3 états possibles : en division, en préparation pour la division ou en repos. Cette thèse se centralise sur un aspect spécifique des cellules en état de division. Plus précisément, je me concentre sur la dernière étape de la division cellulaire que l'on surnomme la cytokinèse. La cytokinèse est le processus qui permet de physiquement séparer une cellule en deux. Tous les évènements d'un cycle cellulaire qui surviennent avant la cytokinèse sont une préparation à la vie suite à la cytokinèse. Quelle importance aurait cette préparation si une cellule ne parvient à procéder à la cytokinèse? Les problèmes génétiques au niveau de la cytokinèse peuvent avoir un impact primordial au niveau du développement de l'organisme. À ces fins, l'approfondissement de nos connaissances sur la cytokinèse est d'une importance majeure. Ma thèse met en évidence un enjeu auparavant inconnu sur une période de transition entre deux étapes de la cytokinèse. En plus de cet enjeu, mes travaux réalisent un progrès nécessaire sur notre connaissance d'un gène essentiel à la cytokinèse et bien conservé lors de l'évolution surnommée Citron Kinase. Chez l'homme, des mutations dans Citron Kinase influence fortement le développement du système nerveux central manifesté par une naissance microcéphale. Ainsi, l'ensemble de cette thèse constitue un avancement important au niveau des sciences fondamentales et appliquées.

Table des matières

Liste des tableaux

CHAPITRE 3

Liste des figures

INTRODUCTION

CHAPITRE 3

CHAPITRE 4

CHAPITRE 5

CHAPITRE 6

Liste des sigles et abréviations

AC: Anneau Contractile

AM: Anneau du Midbody

ARNi: ARN interference

ARN: Acide Ribonucléique

CR: Contractile Ring

MR: Midbody Ring

RNAi: RNA interference

RNA: Ribonucleic Acid

CDK: Cyclin-Dependent Kinase

CAK: Cdk-Activating Kinase

Cdc25: phosphatase M-phase inducer phosphatase 1

CKI: Cdk Inhibiteur

MCM: Minichromosome maintenance protein complex

ATM: Ataxia Telangiectasia Mutaed

ATR: Ataxia Telangiectasia and Rad3 related

Plk1: Polo-Like Kinase

APC: Anaphase Promoting Complexe

Rho GEF: Rho Guanine Nucleotide Exchange Factor

Pbl: Pebble

Rho GAP: Rho Guanine Activating Protein

PRC1: Protein Required for Cytokinesis 1

KIF: Kinesis Family Member

Feo: Fascetto

CPC: Chromosomal Passenger Complex

Tum: Tumbleweed

MKLP1: Mitotic Kinesin-Like Protein 1

Pav: Pavarotti

INCENP: inner centromere protein

MKLP1: Mitotic Kinesin-Like Protein 1

MRLC: nonmuscle myosin regulatory light chain

Sqh: Spaghetti Squash

ROCK: Rho-associated Protein Kinase

Sti: Sticky

PH: Pleckstrin Homology

mDia: mammalian Diaphanous

Sept7: Septin 7

PNUT: Peanut

AH: Anillin Homology

PI(4, 5)P2: Phosphatidylinositol-4, 5-bisphosphate

OCRL1: ortholog of human oculocerebrorenal syndrome of Lowe 1

ESCRT: endosomal sorting complex required for transport

TSG101: Tumor susceptibility gene 101

ALIX: Apoptosis-Linked gene 2-Interacting protein

Cit-K: Citron Kinase

CNH: Nik1 homology

C1: phorbol ester/diacylglycerol-binding domain

WT: Wild Type

Rok or ROCK: Rho Kinase

CF: Cleavage Furrow

CC: Coiled Coil

LatA: Latruncuilin A

Neb: Nebbish

TUBB3: b-Tubulin isoform

NPC: Neuronal Progenitor Cells

KD: Kinase Dead

CRISPR: Clustered Regularly Interspaced Short Palindromic Repeats

ASPM: Abnormal Spindle-like Microcephaly-associated protein

RanBPM: Ran-Binding Protein Microtubule-organizing center

Dlg5: Disc Large 5

p27: Cyclin-dependent kinase inhibitor 1B

TCP1: Two Pore Channel 1

CK2a: Casein Kinase 2 Alpha

EphB2: Ephrin type-B receptor 2 precursor

Src: Proto-oncogene tyrosine-protein kinase

Ago1: Argonaute 1

HP1: Heterochromatin protein 1

mCh: mCherry

CHMP4B: Charged Multivesicular Body Protein 4B

MyoBD: Myosin Binding Domain

ActBD: Actin Binding Domain

GFP: Green Fluorescent Protein

dsRNA: double stranded RNA

FP: Fluorescent Protein

NA: Numerical Aperture

EM: Electron Microscopy

NTD: N-terminal domain

RBH: Rho Binding Homology

RBD: Rho Binding Domain

FL: Full Length

Remerciements

Je remercie tout d'abord les membres du Jury qui ont accepté de lire et juger ma thèse.

Le **Dr Éric Lécuyer**, pour avoir accepté de présider ce jury.

Le **Dr Jean-Claude Labbé**, pour avoir accepté d'être rapporteur.

Le **Dr Craig Mandato**, pour avoir accepté d'être examinateur externe. Je le remercie également pour avoir pris les mêmes fonctions lors de mon comité d'examen prédoctoral.

Le **Dr Christian Beauséjour** pour représenter la doyenne de la faculté de médecine.

Je remercie également **Dr Sébastien Carréno** et **Dre Amy Maddox** qui ont été membres de mon comité de parrainage et prédoctoral. Merci pour tous les commentaires, l'orientation du projet et la confiance mise en moi suite à l'examen prédoctoral.

Je remercie infiniment mon directeur de recherche, le **Dr Gilles Hickson**. J'ai eu l'honneur d'être votre premier étudiant au doctorat. Votre décision de m'accueillir dans votre laboratoire a affecté ma vie étudiante, professionnelle et personnelle. Vous vous êtes investis en moi pour que je devienne un meilleur étudiant et chercheur. Je me rappelle très bien à mes débuts toutes les heures passées quotidiennement ensemble, à regarder des vidéos de microscopie, à discuter d'articles et à développer ma pensée scientifique. Merci de m'avoir fait participer à plusieurs conférences internationales et au Montreal Light Microscopy Course qui m'a aidé à obtenir mon premier emploi. Je pense que nous avons développé une relation spéciale et j'espère qu'elle ne fera que s'enrichir au fil des ans

J'aimerai remercier le **Dr David Spector** et **Cold Spring Harbor Laboratory** pour leur support et compréhension lors des dernières étapes de cette thèse.

Chocolate time! Je souhaite remercier les membres du laboratoire Hickson.

Silvana Jananji, merci pour avoir gardé notre laboratoire organisé. Merci pour ta contribution dans le premier article. La majorité des techniques étaient mis en place par toi ce qui a facilité notre boulot. Merci également d'avoir pris charge des lignées cellulaires tout au long. Finalement, j'ai apprécié chaque discussion ensemble, qu'elle soit intense ou pas :).

Amel Kechad, merci d'avoir non seulement été une collègue mais également une amie. Tes critiques de mon projet étaient très importantes parce que quand tu fais des remarques c'est toujours bien réfléchi, précis et concis. Je te remercie également d'avoir été ma traductrice personnelle : quand je propose mes idées brouillonnes, tu es souvent la personne à pouvoir traduire mes pensées!

Yvonne Ruella, je n'en pourrai jamais en dire assez de toi. Tu es la personne la plus pure que j'ai jamais rencontrée. Le labo n'a jamais été le même sans toi. Une idée qui est certainement partagée par tous. Quand on était au laboratoire avec toi, ce n'était jamais du boulot, mais juste une période de récréation! Le plaisir de t'avoir côtoyé est infini.

Zlatina Dragieva, merci d'avoir accepté d'être ma stagiaire. J'ai eu du plaisir à partager mes connaissances avec toi tout au long de ton stage ainsi que ta maitrise. J'apprécie l'effort que t'a mis l'été pour créer toutes les constructions. Merci d'avoir fait des échanges western blot vs congelé mes cellules! Quand je pense à toi je me rappelle de nos pauses soleil + crème glacée!

Mélanie Diaz, c'était très plaisant de t'avoir dans le labo pendant deux ans. Toujours bien discrète dans le coin du labo je me rappellerai bien de tes super figures de mitose et cytokinèse dessinée à la main.

Denise Wernike, merci d'avoir participé au projet Citron Kinase. Ta collaboration était des plus professionnelles. Je suis content qu'on ait obtenu les mêmes résultats, ça donne beaucoup de confiance en ce projet mais ça nous fait bien paraitre aussi!

Je remercie tous les étudiants qui ont passé par le labo Hickson. **Erica Seccareccia**, je te remercie d'avoir participé au projet Citron Kinase. Même si ta présence a été courte, elle était très agréable. Seul autre membre du groupe testostérone, **Louis-Philippe Picard,** merci de nous avoir aidés à développer les protocoles de biochimie qui ont été importants pour ma thèse.

Je tiens à remercier tous les chercheurs du Centre de Recherche du CHU Sainte-Justine qui m'ont donné la chance de collaborer avec eux. Tout d'abord, **Dr Elie Haddad** qui m'a permis de travailler côte à côte avec **Simon Nicoletti**. D'ailleurs, c'était tout un honneur de travailler avec Simon qui demeure l'une des personnes les plus brillantes que j'ai rencontrées. Je suis convaincu, que sa carrière en médecine, en recherche ou en pharmaceutique sera remarquable. Je remercie également le **Dr Gregor Andelfinger** qui m'a inclus dans son excellente publication. Je soutiens à remercier les membres de son équipe avec qui j'ai eu la chance de partager mes connaissances en microscopie : **Séverine, Jessica, Carmen, Natacha, Florian et Christoph.** Je remercie le **Dr Nikolaus Heveker** pour m'avoir fait participer à un de ses projets avec mon collègue de baccalauréat **Nicolas Montpas**.

Ces groupes et leurs collaborations ont été très importants pour l'obtention de poste à CSHL. Encore une fois je vous remercie énormément. Ces travaux mon permis d'approfondir mes expertises en microscopie, un atout important pour tout biologiste cellulaire.

Je remercie tous les étudiants et post-doc avec qui j'ai eu le plaisir de côtoyer pendant des années. Nos voisins du labo Sinnett, les labos Haddad, Beauséjour et Di Cristo. Merci pour les activités sociales et sportives. Avec certains d'entre vous, j'ai eu le courage de sauter d'un avion! Ce sont des souvenirs inoubliables!

À mes deux meilleurs amis **Dr Elie Baho** et **Dre Patricia Nora Awad**. On s'est rencontré en biochimie. Notre amitié continue de grandir. Votre présence avant moi au CHU Ste-Justine a influencé ma décision de joindre le labo Hickson. Je me considère privilégié d'avoir fait le bon choix de labo d'accueil d'autant plus que d'avoir partagé la même institution que vous deux. Vous avez votre marque sur cette thèse et dans mes souvenirs de mon doctorat. Merci!

J'aimerai remercier ma famille. Ma **maman** et mon **papa** vous êtes une source d'inspiration. Je base ma vie sur votre modèle. Ma sœur **Farah**, je suis très fier de ton étique de travail et ta persévérance, tu m'inspires à ce niveau. Je remercie **Aurora**, **Ralph**, **Christine** et **Diana** pour leur support tout au long de ce processus. À mes **neveux et ma nièce**, votre énergie a été contagieuse!

Je remercier mon frère **Wael** et sa femme **Stephanie** qui m'ont accueilli dans leur maison pendant mes études graduées. Je ne pourrai jamais vous repayer votre dévouement tout au long de ces années mais j'en suis éternellement reconnaissant. **Wael**, je n'aurai pas été où je suis sans toi. Même à distance, tu demeures ma personne de ressources et de réconfort. Je te remercie d'être le meilleur grand frère que je puisse avoir.

À mon amour, **Erica** tu es la raison pourquoi je n'ai jamais lâché. Tu m'as poussé et tu continues de le faire malgré que ceci vienne toujours en détriment de sacrifices. Tu as également été et tu continues d'être une source d'inspiration et un exemple à suivre pour moi. Merci pour ton support tout au long de mes 11 années universitaires. Merci de m'aimer inconditionnellement. Je t'aime et j'ai hâte d'écrire, ensemble, les prochains chapitres de notre vie!

1. Introduction

Le cycle cellulaire est un terme utilisé pour décrire le parcours d'une cellule. En état de prolifération, la cellule peut passer à travers 4 phases M, G1, S et G2. La phase M ou mitose est la phase durant laquelle la cellule se divise en deux. Lors de la mitose, la cellule a besoin de séparer en deux son matériel génétique. La cytokinèse suit la mitose pour séparer physiquement son contenu cytoplasmique. Une cellule en prolifération, qui sort de la mitose, entre en interphase. La première phase de l'interphase s'appelle G1. C'est une période d'écart et de préparation pour la réplication de l'ADN. L'initiation de la réplication de l'ADN marque la transition vers la phase S (S pour synthèse). La dernière partie de l'interphase s'appelle G2. Durant G2, la cellule est dans une phase de croissance et de synthèse protéique rapides qui la prépare à la mitose. La mitose suit la phase G2 pour compléter le cycle. Ce cycle est soumis en tout temps à un processus de régulation stricte qui est fortement associée avec l'expression de différents types de cyclines et de cyclin-dependent kinases (CDKs).

1.1. Le cycle cellulaire

Un nouveau cycle cellulaire débute en G1. Tôt dans cette phase, il y a accumulation de la CDK4 et la CDK6 qui s'associent à la cycline D (Cdk4-cyclin D). Plus tard en G1, les complexes CDK 4,6-cyclin D conduisent à l'activation de la transcription de la CDK2 et cycline E (*Cdk2-cyclin E*). Ensemble, les complexes CDK4,6-cyclin D et CDK2-cyclin E mènent à l'initiation de la réplication de l'ADN ce qui marque la transition de la phase G1 à la phase S. La progression à travers la phase S dépend de l'association de la CDK2 à la cycline A (*Cdk2-cyclin A*). Une fois l'ADN correctement répliqué, la phase G2 est initiée par l'association de la CDK1 à la cycline A. Finalement, la cellule passe en mitose suite à l'association de la CDK1 à la cycline B (Figure 1).Malgré le rôle spécifique de chaque CDK, il existe une redondance entre certaines classes CDKs. Seule la CDK1 semble être essentiel à la prolifération cellulaire puisque l'absence des CDK2, 4 ou 6 peut être compensée par certain facteur redondant (Santamaria et al., 2007).

1.1.1. La régulation des complexes CDK-cyclin

La régulation du cycle cellulaire dépend fortement de l'état d'activation des complexes CDK-cyclin. L'association des cyclines aux CDKs marque la première étape de cette activation. Les CDKs ont un résidu activateur qui doit être phosphorylé par la Cdk-activating kinase (CAK) formée de Cdk7-cyclin H-Mat1 (*Cdk7-cyclin H/Mat1*) (Lolli and Johnson, 2005). De plus, la CDK1 et la CDK2 ont deux résidus inhibiteurs qui sont phosphorylés par la protéine Wee1 (*Wee*) (Parker et al., 1995). Cependant, la phosphatase M-phase inducer phosphatase 1 (cdc25, *String*) déphosphoryle ces deux résidus pour activer les complexes reliés à la CDK1 et la CDK2 (Hoffmann et al., 1993). Finalement, il existe des CDK inhibiteurs (CKI) qui s'associent directement aux complexes CDK-cyclin pour inhiber ces complexes (Bendris et al., 2015).

1.2. L'interphase

1.2.1. La phase G1, G0 et point de restriction

Tôt en G1, la cellule est soumise à des facteurs extrinsèques favorables à la progression du cycle cellulaire. Lorsque ces facteurs sont absents, la cellule peut devenir quiescente et entrer en G0, une phase de la cellule qui lui permet d'être en arrêt cellulaire, mais avec le potentiel de rentrée dans le cycle (Schafer, 1998). En G1, la progression du cycle cellulaire se rend à un point de restriction R qui représente une situation de non-retour où la cellule est disposée à continuer le cycle cellulaire indépendamment des facteurs extrinsèques. Pour passer ce point de restriction, la cellule a besoin d'activer la transcription d'ADN (Schafer, 1998). L'association graduelle en G1, du complexe CDK-cyclin spécifique à cette phase, permet à ce complexe d'activer certains facteurs essentiels à l'initiation de la transcription et ainsi le passage à travers le point de restriction. Vers la fin de G1, lorsque les niveaux de CDK-cyclin de la phase G1 aient atteint un niveau seuil, ces complexes activent Minichromosome maintenance protein complex (MCM, *MCM*), une hélicase qui se lie à l'origine de la réplication pour dérouler les deux brins d'ADN et ainsi initier la réplication de l'ADN (Machida et al., 2005).

1.2.2. L'initiation de la transcription et la Phase S

Avant d'entamer la réplication de son ADN en phase S, la cellule a besoin de vérifier l'intégrité de son ADN. Lorsque la cellule détecte un dommage ou stress à l'ADN, elle va retarder sa progression. Ceci a lieu indépendamment de son passage à travers le point de restriction. Ce premier point de contrôle est surnommé G1/S checkpoint. L'initiation de la réplication de l'ADN marque la transition vers la phase S. La cellule en phase S duplique son matériel génétique pour passer de deux copies homologues de chaque chromosome (2n) à quatre copies (4n). L'initiation de la réplication de l'ADN ne se fait pas simultanément partout dans l'ADN. Au contraire la réplication sera initiée à différentes origines de la réplication tout au long de la phase S (Machida et al. 2005). La MCM nécessitera donc l'activité de CDK-cyclines de la phase S. Tard en phase S, on observe une association entre la cycline A et la CDK1. Lorsque l'ADN sera complètement répliqué, le complexe CDK1-cyclin A permet à la cellule de passer en phase G_2 (Hochegger et al., 2008).

1.2.3. La phase G_2 et la transition G_2/M

En G_2, le contenu en ADN de la cellule est maintenant de 4n. Cette phase est une période de croissance cellulaire pour la préparation à la mitose. G_2 est marquée par l'association de la cycline B à la CDK1. L'activation du complexe CDK1-cyclin B est responsable du passage en mitose (Hochegger et al., 2008). Cependant, tout au long de G_2, le complexe CDK1-cyclin B s'accumule dans un état inactivé suite à une phosphorylation inhibitrice par la protéine Wee1 (Hochegger et al., 2008). Lorsque la cellule sera prête pour son passage en mitose la protéine cdc25 déphosphoryle les résidus cible de la Wee1 pour activer le complexe CDK1-cyclin B (Hochegger et al., 2008). En G2, la cellule vérifie que l'entièreté de son ADN est répliquée et qu'aucun dommage n'est détecté. La cellule est capable d'arrêter sa progression en G2 afin de corriger ces erreurs.

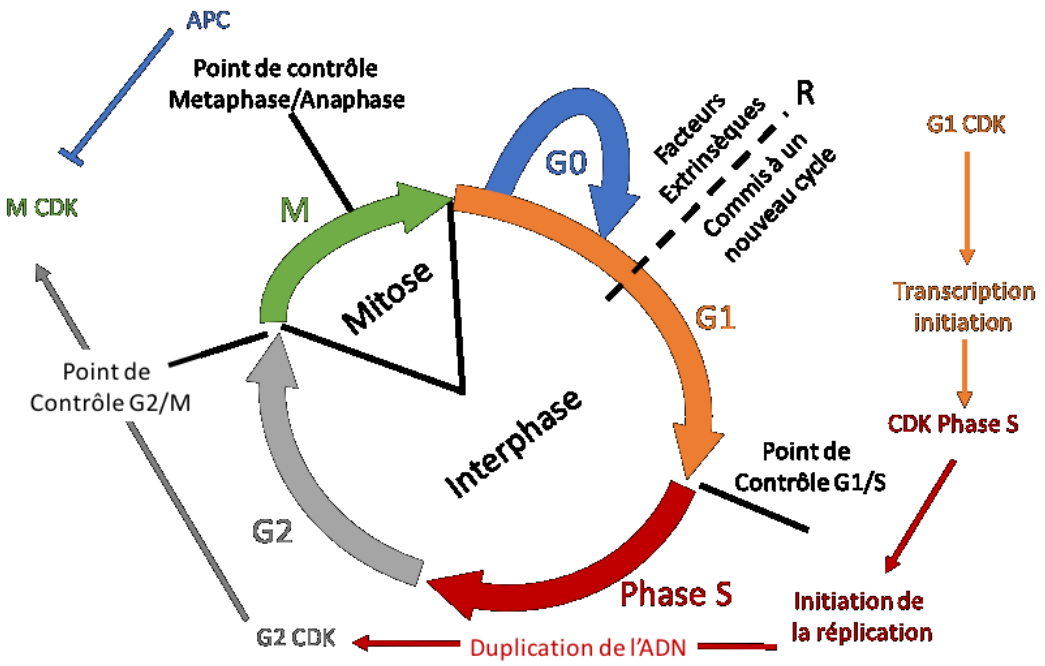

Figure 1. Le cycle cellulaire et les complexes CDK-cyclin.

1.3. La mitose

Lorsque la cellule passe le point de contrôle G2 en activant la Cdc25, le complexe CDK1-cyclin B sera à son tour activé et la cellule entre en mitose. Le complexe CDK1-cyclin B activé permettra l'activation de plusieurs protéines mitotiques dont les kinases Aurora A et B (*Aurora kinase*) ainsi que la Polo-like kinase (Polo-like kinase, *Plk1*) (Salaun et al., 2008). Ensemble ces kinases et le complexe CDK1-cyclin B, participeront dans l'établissement de processus clefs de la mitose. Les cellules qui entrent en mitose se trouvent en prophase. Durant cette phase, l'ADN prend la forme de chromosome, une structure ultra condensée formée de deux chromatides identiques issues de la réplication de l'ADN en phase S. De plus, les centrosomes se séparent et commencent à former le fuseau mitotique qui est une structure du cytosquelette qui permettra la ségrégation des chromatides vers deux pôles de la cellule. La prométaphase marque la désintégration de l'enveloppe nucléaire. Durant cette phase, les chromosomes s'associent aux microtubules du fuseau mitotique. Ensuite, la cellule se trouve en métaphase, période durant laquelle les chromosomes s'alignent correctement à l'équateur de la

cellule pour se préparer à la séparation des chromatides. Cet alignement est très important et les cellules ne peuvent procéder aux prochaines étapes avant de passer au troisième point de contrôle surnommé Spindle Assembly Checkpoint (SAC). Suite à ce point de contrôle, la cellule entre en anaphase. Durant cette partie de la mitose, le lien attachant les chromatides sœurs est brisé et la ségrégation de l'ADN vers les deux pôles débute. Vers la fin de l'anaphase, chaque chromatide identique se trouve à un pôle de la cellule. En télophase le noyau commence à se reformer et la cellule se trouve dans les premières étapes de la cytokinèse.

1.3.1. La prophase

L'ADN en interphase est sous une forme peu condensée, un état favorable à sa transcription. Cependant l'ADN dupliqué doit prendre la forme d'un chromosome, une structure ultra condensée formée de deux chromatides identiques liées par un centromère. Les complexes protéiques Cohesin et Condensin jouent un rôle clef dans l'obtention de cette morphologie d'ADN. Les deux chromatides d'un chromosome ont besoin d'être séparées vers chaque pôle de la cellule pour diviser son matériel génétique également. Le fuseau mitotique est une structure dense en microtubules qui constitue la machinerie permettant une telle séparation. Le fuseau mitotique est principalement composé de deux centrosomes, des chromosomes et leurs kinétochores, des microtubules couplés à des protéines motrices et associés à certaines protéines (Winey and Bloom, 2012). Le centrosome est un organelle qui représente le centre cellulaire organisateur des microtubules. Il contient un matériel péricentriolaire qui entoure une paire de centrioles. En interphase, les deux centrioles se séparent et sont dupliqués à l'intérieur du même matériel péricentriolaire. La nucléation et l'ancrage des microtubules du fuseau mitotique a lieu à partir des γ-tubulin présents dans le matériel péricentriolaire. On appelle centromère la région d'ancrage des chromosomes aux microtubules. Cet ancrage a lieu grâce à un complexe protéique appelé kinétochore. Chaque chromatide contient un kinétochore. À partir des centrosomes, les microtubules s'organisent en trois catégories pour former le fuseau mitotique. Les microtubules astraux se dirigent du centrosome vers l'extérieur des pôles pour aider à positionner le fuseau mitotique. Au centre de la cellule se trouvent les microtubules interpolaires et des kinétochores. Les microtubules des kinétochores de chaque pole s'attachent aux chromatides sœurs pour

entamer leur séparation plus tard en anaphase. Les microtubules interpolaires s'étendent à partir de chaque centrosome et se chevauchent à l'équateur de la cellule (Winey and Bloom, 2012).

1.3.2. La prométaphase

En prophase, la présence de l'enveloppe nucléaire empêche la finalisation de la formation du fuseau mitotique. La transition en prométaphase est marquée par la désintégration de l'enveloppe nucléaire. Les chromosomes, libres de l'enveloppe nucléaire, pourront ainsi s'attacher aux microtubules du fuseau mitotique. Lorsque l'enveloppe nucléaire est désintégrée, les chromosomes sont la cible des microtubules très dynamiques issus des centrosomes. Il est important que chaque kinétochore soit connecté par un seul pôle de la cellule. Ainsi, la cellule s'assure que chaque chromatide n'est connectée que par un pôle du fuseau mitotique. Vers la fin de la prométaphase, tous les chromosomes sont correctement attachés aux microtubules et les centrosomes sont bien positionnés aux pôles de la cellule (Cheeseman and Desai, 2008).

1.3.3. La métaphase et la transition à l'anaphase

Les chromosomes attachés de manière bipolaire se déplacent vers l'équateur du fuseau mitotique grâce aux forces opposées générées par les microtubules. À ce point, les deux chromatides sont fortement attachées l'une à l'autre par la protéine Cohesin. Pour séparer les deux chromatides, Cohesin doit être dissociée des chromatides par la protéine Separase (Peters et al., 2008). La Separase est sous forme inactive par liaison à sa protéine inhibitrice Securin jusqu'à la transition métaphase-anaphase. La dégradation de la Securin requiert l'activation de l'Anaphase Promoting Complexe (*APC*) qui est un complexe protéique initiateur de la transition en anaphase. L'APC agit par ubiquitination de ses protéines cibles qui seront ensuite marquées pour dégradation par le protéasome (Peters et al., 2008). Outre la Securin, plusieurs protéines régulatrices de la mitose comme le complexe CDK1-cyclin B, les Aurora et la Plk1, sont des cibles de l'APC (Li and Zhang, 2009). Une fois déclenchées, les actions de l'APC marquent évidemment un tournant dans la cellule qui est maintenant soumise à entamer la ségrégation des chromosomes en anaphase. Vu l'importance de ces actions, la cellule se trouve un point de

contrôle centré sur la formation d'un fuseau mitotique correctement attaché à tous les kinétochores des chromosomes. Lorsqu'un des kinétochores n'est pas attaché aux microtubules, un signal inhibiteur de l'APC empêche la cellule de passer en anaphase. Ce mécanisme de contrôle est très robuste puisque la cellule peut résister au passage en anaphase pendant de longues périodes de temps jusqu'à ce que les conditions de passage à l'anaphase soient satisfaites.

1.3.4. L'anaphase et la télophase

En anaphase, les chromatides se séparent et chaque chromatide sœur est tirée vers un pôle opposé de la cellule grâce aux forces générées par les microtubules du fuseau mitotique. L'anaphase est répartie en deux étapes Anaphase A et B qui peuvent dans certains cas avoir lieu simultanément. En anaphase A, les microtubules des kinétochores rétrécissent pour permettre la ségrégation des chromosomes. En Anaphase B, le fuseau mitotique est en élongation pour permettre une séparation des pôles du fuseau mitotique eux même. Pour ce faire, les microtubules astraux rétrécissent pour tirer le fuseau vers les pôles, tandis que les microtubules interpolaires s'étendent pour pousser le fuseau vers les pôles de la cellule (Maiato and Lince-Faria, 2010). Les chromatides nouvellement séparées par ségrégation lors de l'anaphase ont besoin d'être empaquetées en télophase. Des fragments de membranes nucléaires se forment à l'entour des chromosomes et fusionnent ensemble au fur à mesure pour reformer l'enveloppe nucléaire. La structure du noyau reprend ensuite forme par formation de la lamina nucléaire et l'incorporation de pores nucléaires. Le matériel génétique étant bien sécurisé, il ne reste qu'un objectif à la cellule : séparer son contenu cytoplasmique par cytokinèse.

1.4. La cytokinèse

Une division cellulaire est complétée par la cytokinèse (Figure 2). C'est l'étape qui permet à la cellule de physiquement séparer son contenu cytoplasmique aux deux cellules sœurs. Suite à l'anaphase, un réarrangement de microtubules a lieu entre les deux centrosomes pour former le fuseau central. Grâce à ce réarrangement, un signal moléculaire va définir le plan de

division de la cellule. Ce plan est une zone corticale à l'équateur de la cellule qui sera formé de complexes protéiques activés par la protéine GTPase RhoA (*Rho1)*. Ces complexes protéiques sont associés aux composants du cytosquelette et forment l'anneau contractile (AC) qui relie ce cytosquelette à la membrane plasmique ainsi qu'aux microtubules du fuseau mitotique. L'anneau contractile est soumis à une force motrice qui conduit à l'ingression du sillon de clivage. Cette ingression qui a lieu en parallèle avec la formation du fuseau central continue à se condenser graduellement. La nouvelle architecture à l'équateur de la cellule est une structure ultra dense en protéines, composée du successeur de l'anneau contractile surnommé l'anneau du midbody (AM). L'AM est fortement joint à un corps intermédiaire de protéines reliés aux microtubules qu'on appelle le midbody (MB) et des microtubules centraux du fuseau mitotique. Cette structure aura comme fonction de continuer la séparation cytoplasmique et de conduire les deux cellules filles vers leur rupture finale par l'abscision (revue dans (Green et al., 2012)). Cette thèse se concentre sur la transition de l'anneau contractile à l'anneau du midbody. Cette transition est souvent vue comme un processus binaire. Cependant, nos résultats mettent en évidence un nouveau mécanisme de maturation de cette transition qui est essentiel à la cytokinèse.

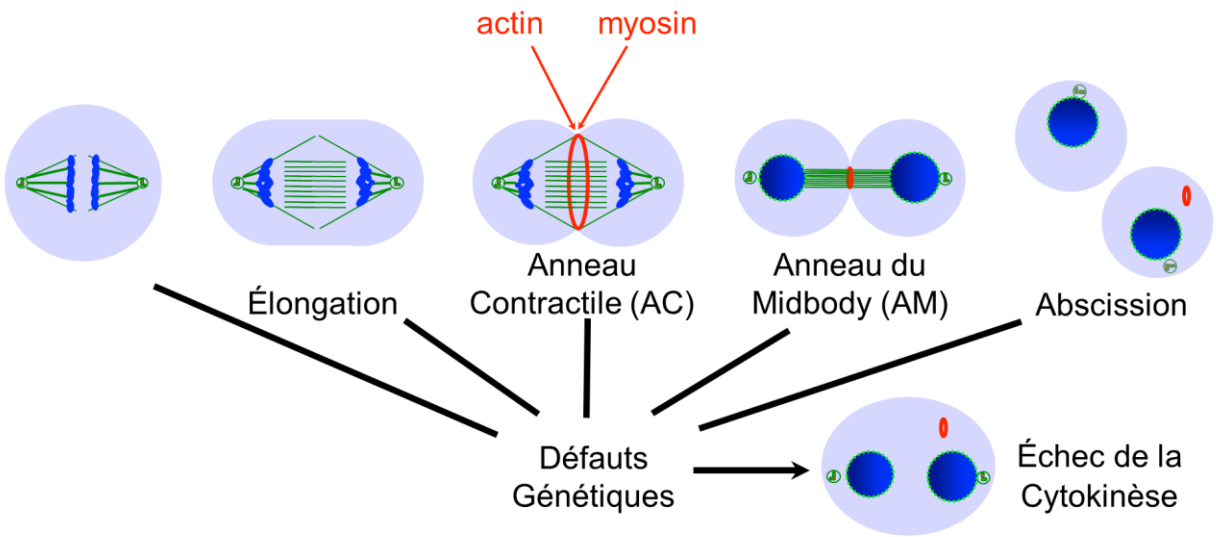

Figure 2. De l'anaphase à l'abscission : un processus à plusieurs étapes.

1.4.1. Le positionnement du fuseau mitotique

1.4.1.1. La division symétrique versus asymétrique

Une séparation égale du contenu cytoplasmique est le résultat d'une division symétrique. Par contre, le développement d'un organisme requiert plus qu'une simple prolifération linéaire d'une cellule mère identique à ses deux cellules filles. En effet, la différenciation cellulaire de cellules souches tout au long du développement est le résultat de divisions asymétriques. Tout comme la division symétrique, la division asymétrique reste fidèle au partage identique en contenu d'ADN répliqué. Cependant, la division asymétrique se distingue par une séparation inégale en contenu cytoplasmique et/ou cortical. Parmi les protéines séparées inégalement se trouvent certaines qui permettent de déterminer des destins de différenciation cellulaire distincts pour chacune des deux cellules filles (Hyenne et al., 2010).

1.4.1.2. Les facteurs extrinsèques versus facteurs intrinsèques

Durant le développement d'un organisme, les cellules se trouvent dans un contexte tridimensionnel. Ce contexte crée des environnements diversifiés qui peuvent influencer l'orientation de la prochaine division cellulaire. Des facteurs extrinsèques sont donc responsables d'une division symétrique ou asymétrique. D'autre part, les cellules elles-mêmes ne sont pas toujours uniformes autant au niveau de leur contenu cortical que cytoplasmique. L'orientation du plan de division, de manière à générer une inégalité entre les deux cellules filles est considérée comme un facteur intrinsèque à l'origine d'une division asymétrique. L'orientation du fuseau mitotique *a priori* de la cytokinèse d'une division symétrique ou asymétrique est donc d'une importance cruciale pour un organisme tout au long de sa vie. Des études dans différents modèles de développement, mais notamment dans la division de *Caenorhabditis elegans* ont permis d'identifier des complexes moléculaires bien conservés qui influencent cette orientation du fuseau mitotique qui ultimement détermine le destin d'une cellule (revue dans (Hyenne et al., 2010; Lu and Johnston, 2013; Morin and Bellaiche, 2011; Siller and Doe, 2009)).

1.4.2. Détermination du plan de division

Le positionnement du fuseau mitotique spécifie le plan de division de la cytokinèse (Rappaport, 1996). Deux populations de microtubules semblent coexister pour établir ce plan de division. Dépendamment du type cellulaire en question, l'une est souvent plus dominante que l'autre. Malgré la présence simultanée de ces deux signaux, leur séparation physique a été démontrée expérimentalement. Ces résultats suggèrent que leur occurrence a possiblement lieu de manière subséquente (Bringmann and Hyman, 2005; von Dassow, 2009). Pour une revue de l'impact du fuseau mitotique sur l'établissement du plan de division voir figure 3 (von Dassow, 2009).

1.4.2.1. La relaxation polaire

Un de ces mécanismes microtubules dépendant (astral relaxation), propose que la formation d'un sillon de clivage nécessite une inhibition des forces contractiles aux pôles de la cellule par les microtubules astraux. Ainsi, un sillon pourrait se former uniquement au niveau de l'équateur. Ceci a entre autres été démontré par la formation d'un sillon de clivage en présence exclusive de microtubules astraux de deux fuseaux mitotiques adjacents. Une distance minimale serait requise pour permettre au sillon de clivage de se former. (Oegema and Mitchison, 1997; Rappaport, 1996).

1.4.2.2. La stimulation équatoriale

Le deuxième modèle (astral and central spindle stimulation) suggère qu'un signal originaire des microtubules centraux du fuseau mitotique stimule la contraction équatoriale. Une preuve de cette stimulation a été démontrée en établissant une barrière entre les microtubules centraux et le cortex en métaphase. Suite à l'anaphase, cette barrière empêche la formation d'un sillon de clivage de ce côté du cortex (Cao and Wang, 1996).

1.4.2.3. L'établissement d'une région activée en RhoA

Outre l'implication de ses microtubules directement dans l'établissement du plan de division, le fuseau mitotique est essentiel à la concentration et l'activation de la petite GTPase RhoA (*Rho1*) dans une zone étroite à l'équateur de la cellule (Bement et al., 2005). Cette forme active de RhoA agit en amont de protéines nécessaires à la formation d'un anneau contractile, structure responsable de l'ingression du sillon de clivage (Green et al., 2012). Deux expériences clefs démontrent l'importance du fuseau mitotique dans l'établissement de cette zone RhoA. Premièrement, la perturbation des microtubules en utilisant un inhibiteur de polymérisation de microtubules (Nocodazole) élargit la zone active de RhoA (Bement et al., 2005). Deuxièmement, le déplacement du fuseau central redéfinit la zone active de RhoA (Bement et al., 2005).

RhoA étant une GTPase, son activité dépend d'une GEF ainsi que d'une GAP. L'activation de RhoA dépend de la GEF, ECT-2 (*Pebble, Pbl*) (Yüce et al., 2005) dont la localisation au fuseau central nécessite une interaction avec MgcRacGAP activé par Plk1 (Wolfe et al., 2009). Le domaine GAP de MgcRacGAP joue un rôle essentiel à la cytokinèse, mais l'importance de l'activité GTPase de GAP dans la cytokinèse reste controversée (Green et al., 2012). Un modèle (Rho flux) propose que l'activation locale de RhoA soit contrée par une inactivation globale GAP dépendante. En anaphase, une réduction globale de l'activité GAP de RhoA permet la formation d'une région équatoriale RhoA activée par une GEF équatoriale (Miller and Bement, 2009). En d'autres mots, ceci propose que malgré l'importance du fuseau mitotique dans l'établissement d'un signal d'activation pour déterminer le plan de division, une action globale d'inactivation de GAP soit nécessaire.

1.4.2.4. D'autres mécanismes?

Il est important de noter qu'en plus de ces mécanismes reliés au fuseau mitotique, une étude a démontré que dans un modèle de neuroblastes de la *Drosophile* qui n'ont pas de fuseau mitotique, une ingression du sillon de clivage peut toujours avoir lieu (Cabernard et al., 2010). Ceci a donc introduit un nouveau mécanisme de positionnement du sillon de clivage indépendamment du fuseau mitotique (Cabernard et al., 2010).

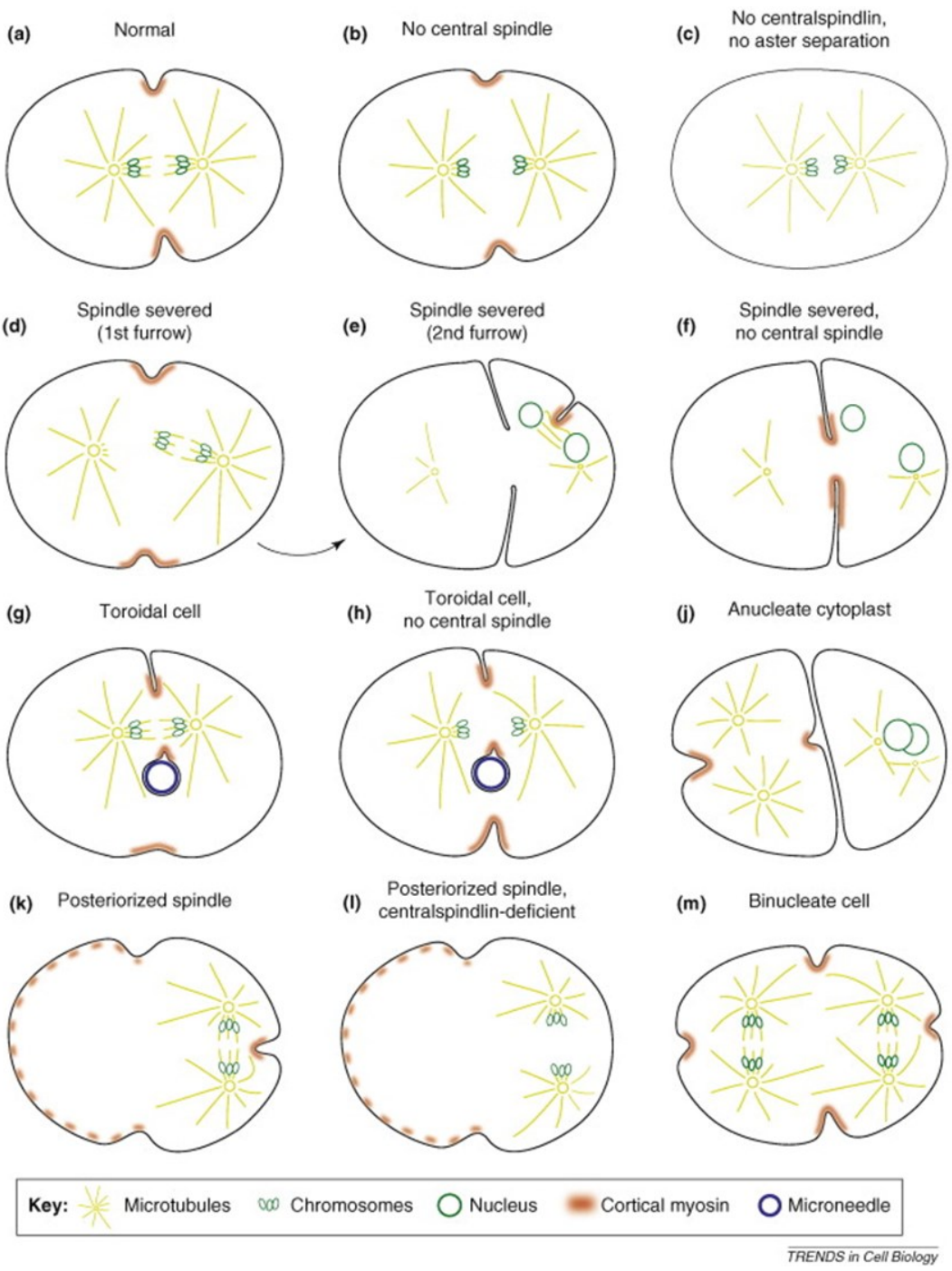

Figure 3. Représentation schématique d'expériences classiques de conditions de formation d'un sillon de clivage.

Tiré de (von Dassow, 2009) : Figure 2. Geometrical conditions supporting cleavage-furrow formation in C. elegans zygotes.

1.4.3. La formation du fuseau central

Suite à l'anaphase, les microtubules interpolaires et des nouveaux microtubules fraichement formés constituent le fuseau central. Les pôles positifs de ces microtubules provenant de chaque centrosome s'intercalent au centre de la cellule et sont regroupés ensemble. La diminution de l'activité de la CDK1 en anaphase, est responsable de l'activation de protéines essentielles à la formation du fuseau central (Figure 4), notamment Protein Required for Cytokinesis 1 (PRC1 / *Fascetto, Feo*), Centralspindlin et Chromosomal Passenger Complex (*CPC*) (Glotzer, 2009) et Augmin (*mitotic spindle density 1, Msd1*) (Uehara et al., 2016).

1.4.3.1. PRC1

PRC1 est une protéine capable de lier et de regrouper ensemble les microtubules antiparallèles du fuseau central (Mollinari et al., 2002). Une étude de reconstitution du fuseau central *in vitro* démontre que PRC1 est capable de se localiser aux microtubules antiparallèles formés de manière spontanément. Ceci suggère que PRC1 n'a pas besoin d'aucun autre facteur pour se localiser aux microtubules du fuseau central. Cependant, PRC1 est requis pour recruter la kinésine KIF4A (*Klp3a*) (Bieling et al., 2010). KIF4A est nécessaire pour la formation du fuseau central en limitant la longueur des microtubules antiparallèles du fuseau central (Hu et al., 2012). En début de mitose, PRC1 est cytoplasmique. Lors de la formation du fuseau mitotique, KIF4A est responsable de la translocation de PRC1 vers les microtubules du fuseau (Jiang et al., 1998; Zhu and Jiang, 2005). Avant le début de l'anaphase, CDK1 phosphoryle PRC1 ce qui inhibe sont interaction avec KIF4A. Suite au début de l'anaphase, Aurora B phosphoryle KIF4A spécifiquement au niveau du fuseau central pendant que CDK1 continue d'inhiber KIF4 aux microtubules astraux. Ceci permet la translocation de PRC1 spécifiquement au fuseau central. Ensemble, la présence de KIF4A actif et de PRC1 spécifiquement aux microtubules centraux permet de promouvoir la formation d'un fuseau central (Nunes Bastos et al., 2013; Voets et al., 2015).

1.4.3.2. Centralspindlin

MgcRacGAP (*Tumbleweed, Tum*) et mitotic kinesin-like protein 1 (MKLP1 / *Pavarotti, Pav*) forment un complexe tétramérique composé d'un dimère de chaque sous-unité, surnommé centralspindlin. Tout comme PRC1, MKLP1 est essentiel au regroupement des microtubules au niveau du fuseau central (Lee et al., 2012). Les deux sous unités de centralspindlin sont essentielles à la formation du fuseau central (Mishima et al., 2002). De plus, l'interaction de centralspindlin avec les microtubules est inhibée par une phosphorylation de MKLP1 par CDK1 avant l'anaphase (Mishima et al., 2004). Cependant, l'accumulation d'Aurora B kinase au niveau des microtubules centraux, permet à centralspindlin de se localiser au fuseau central en stimulant la relâche de sa protéine inhibitrice 14-3-3 qui se localise spécifiquement au niveau des microtubules centraux (Douglas et al., 2010).

1.4.3.3. Chromosomal Passenger Complex

CPC est un complexe protéique composé des protéines inner centromere protein (INCENP / *INCENP*), borealin (*Borr*), survivin et Aurora B kinase. Comme décrit plus tôt, Aurora B influence la localisation de centralspindlin et PRC1. En début d'anaphase, CPC est relocalisé des centromères au fuseau central (Glotzer, 2009). Ce transfert de CPC au fuseau central est évidement important pour l'activité d'Aurora B kinase sur MKLP1 et PRC1. La translocation de CPC au fuseau central dépend de mitotic kinesin-like protein 2 (MKLP2 / *Subito, Sub*) (Neef et al., 2006). En métaphase, INCENP est phosphorylé par CDK1 et cette phosphorylation joue un rôle inhibiteur dans l'interaction MKLP2/CPC (Kitagawa et al., 2014). Suite à l'anaphase, les niveaux réduits de CDK1 stimulent l'association de MKLP2 à CPC permettant ainsi la localisation d'Aurora B au fuseau central (Kitagawa et al., 2014).

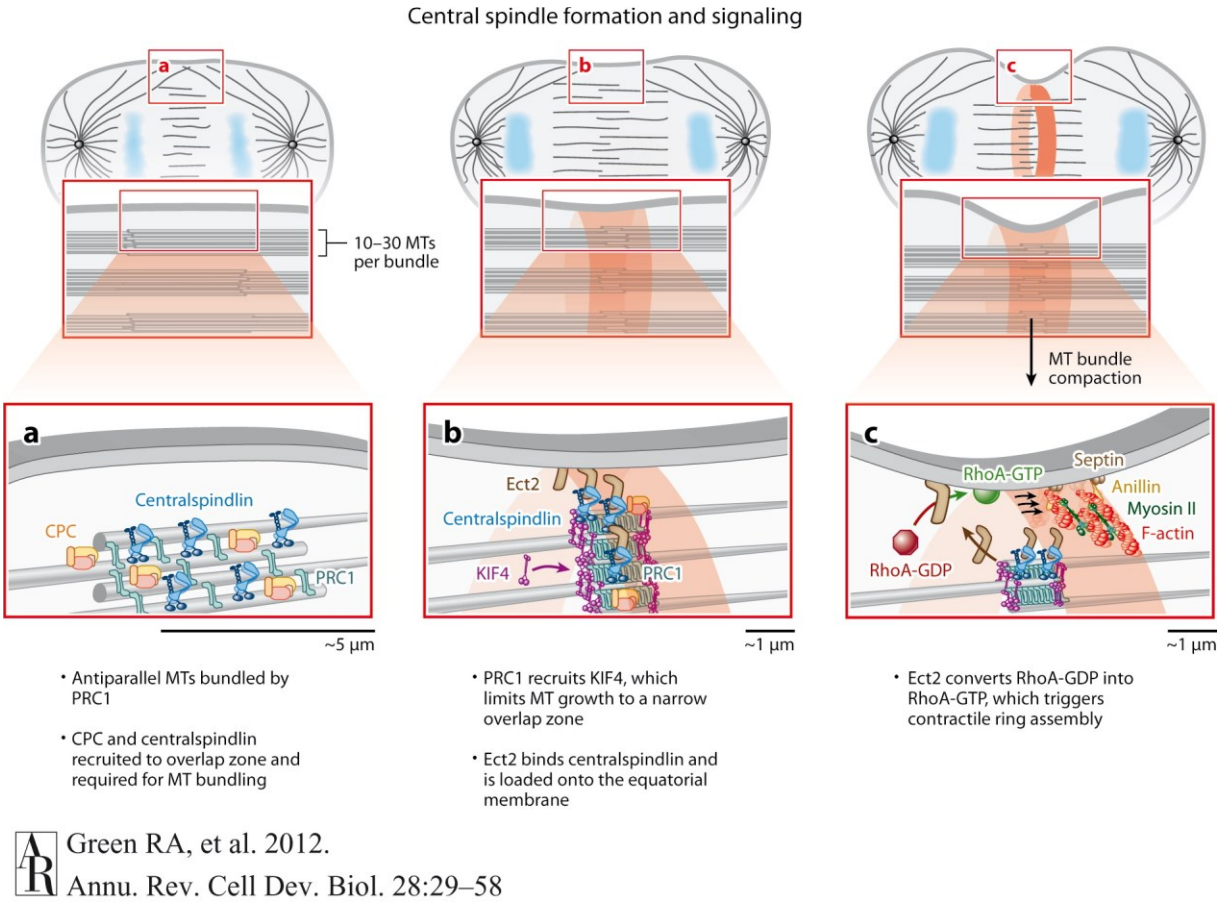

Figure 4. Complexes moléculaires impliqués dans la formation et la constriction du fuseau central.

Tiré de (Green et al., 2012) : Figure 2. Central spindle formation and signaling.

En résumé, au niveau moléculaire, la réduction des niveaux de CDK1-cyclin B à la transition métaphase-anaphase stimule la relocalisation de ces trois éléments clefs à la formation du fuseau central vers les microtubules centraux. Par la suite, la présence d'Aurora B aux microtubules centraux stimule une activation locale de centralspindlin et PRC1 au fuseau central.

1.4.3.4. Augmin

Un nouvel élément important c'est joint à la famille des organisateurs du fuseau central. Augmin est une protéine essentielle pour la formation des microtubules acentrosomaux du fuseau central. En effet la majorité des microtubules qui forment ce fuseau central constituent ce type de microtubules. À noter que ce type de microtubules nécessite également PRC1 pour le regroupement de ces microtubules acentrosomaux (Uehara et al., 2010). L'absence de ces microtubules acentrosomaux Augmin-dépendant affecte les étapes subséquentes de la cytokinèse, dont l'ingression du sillon de clivage (Uehara et al., 2016).

1.4.4. La formation d'un anneau contractile

L'activation de RhoA dans une zone étroite permet de recruter plusieurs protéines nécessaires à la formation d'un anneau contractile (Figure 5) (Piekny et al., 2005). L'anneau contractile est une structure d'épaisseur bien conservée qui se trouve tout juste au-dessous de la membrane plasmique équatoriale. La force motrice de l'anneau contractile provient de son organisation en Actine et Myosine. Cette organisation nécessite une activation de la formine mDia2 (*Diaphanous*) par RhoA afin de former des filaments d'Actine non ramifiés (Watanabe et al., 2010). D'autre part, la sous-unité régulatrice de la protéine motrice de Myosine II (nonmuscle myosin regulatory light chain, MRLC / *Spaghetti squash, Sqh*) est activée par phosphorylation. La Rho-kinase (ROCK / *Rho-kinase, rok*) est une protéine effectrice de RhoA responsable de la phosphorylation de MRLC (Amano et al., 2010). D'ailleurs, RhoA inhibe la Myosin Phosphatase Targeting Protein (MYPT) qui est responsable de la déphosphorylation de MRLC (Kimura et al., 1996). L'anneau contractile est également composé de plusieurs éléments clefs dans l'ingression du sillon comme Anillin, les septines et la kinase Citron (*Sticky, Sti*) (Echard et al., 2004). Ensemble, ces protéines doivent permettre la communication avec le fuseau central, l'ancrage à la membrane plasmique, mais également la constriction de l'anneau contractile.

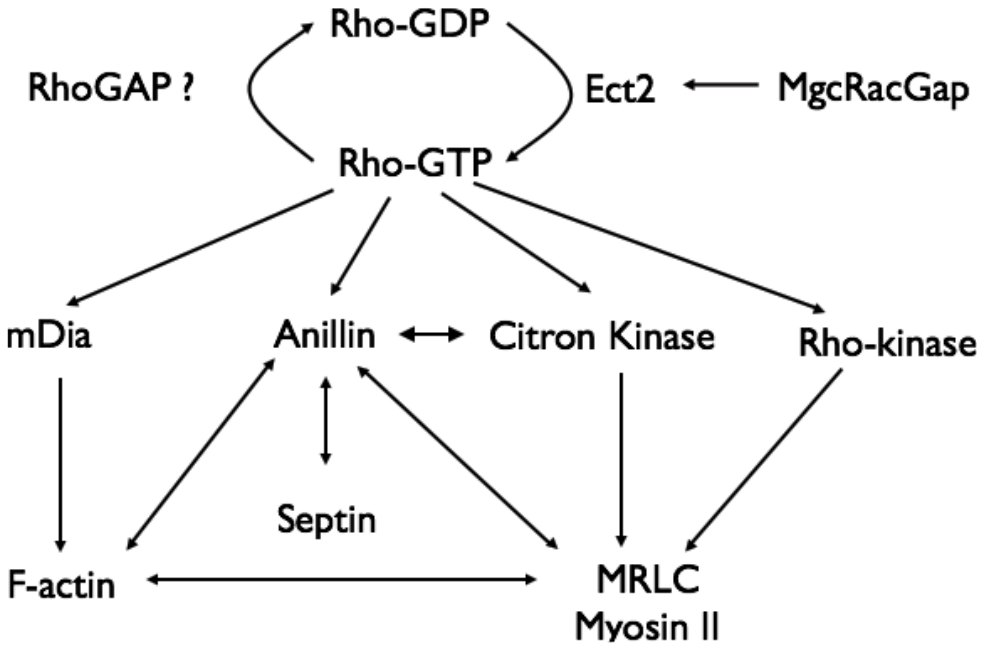

Figure 5. RhoA est une protéine qui agit en amont de plusieurs éléments essentiels à la cytokinèse

1.4.5. La constriction de l'anneau contractile

1.4.5.1. Une force motrice d'actomyosine?

Le mécanisme de contraction de l'anneau contractile est encore ambigu. Cependant, la constriction est souvent attribuée à la contribution de l'Actine et Myosine comme facteurs intégraux dans la génération d'une force motrice. L'organisation de l'actomyosine au niveau de l'anneau contractile reste controversée (Eggert et al., 2006). Différents modèles d'organisation ont été suggérés, mais il est difficile d'en tirer une conclusion aujourd'hui. Les modèles les plus précoces proposent que les filaments d'Actine et de Myosine s'organisent le long de l'anneau contractile de manière à pouvoir produire des glissements des filaments d'Actines grâce à l'activité de sa protéine motrice Myosin II (Schroeder, 1972). Une telle organisation n'a jamais été clairement démontrée (Eggert et al., 2006; Green et al., 2012). Au contraire, l'orientation de ces filaments d'Actines n'est pas toujours le long du plan de division, mais plutôt de directions mixtes (Kamasaki et al., 2007). De même pour Myosine II qui s'organise également en fibres et

peut se trouver dans différentes orientations dans l'anneau contractile (DeBiasio et al., 1996). De plus, des nouvelles molécules Myosines sont continuellement recrutées lors de la constriction suggérant un remodelage de l'organisation du cytosquelette de l'anneau contractile durant la constriction (Uehara et al., 2010). D'ailleurs, une étude a démontré que la phosphorylation de MRLC affecte le renouvellement de la Myosine II et de l'Actine au niveau de l'anneau contractile (Kondo et al., 2011). Finalement, une étude dans *Caenorhabditis elegans* démontre que les composants de l'anneau contractile sont éliminés à un niveau proportionnel au périmètre de l'anneau contractile tout au long de la constriction (Carvalho et al., 2009). Ceci indique que peu importe la taille d'un anneau contractile, le temps de constriction sera égal. Malgré le recrutement de nouvelles protéines lors de la constriction, une diminution nette de ces niveaux a lieu ce qui suggère que la constriction a possiblement lieu par perte de complexes protéiques au niveau de l'anneau contractile (Carvalho et al., 2009; Green et al., 2012).

1.4.5.2. Une relaxation polaire?

Une contraction à l'équateur de la cellule devrait être accompagnée par une relaxation ailleurs dans le cortex. D'où la proposition d'un modèle de relaxation polaire lors de la contraction de l'anneau contractile (Fededa and Gerlich, 2012; Ramkumar and Baum, 2016). En effet, lors de la constriction on observe souvent un bourgeonnement membranaire polaire dont le but proposé est de servir comme source de relâche de pression (Sedzinski et al., 2011). L'importance de la relaxation des forces contractiles polaires est indéniable puisque si les pôles sont perturbés cela génère des oscillations de l'anneau contractile le long de la cellule ce qui dirige la cellule vers l'échec de la cytokinèse (Sedzinski et al., 2011).

1.4.5.3. Rien d'autre que RhoA?

Malgré le fait que le mécanisme de constriction reste controversé, RhoA est identifiée comme le régulateur ultime dans la génération et la constriction de l'anneau contractile en passant par sa voie effectrice de nucléation et d'activation d'Actine et Myosine respectivement. D'ailleurs, une étude optogénétique récente démontre qu'une activation locale de RhoA, par

recrutement induite des domaines GEFs du RhoGEF LARG, à n'importe quel endroit du cortex est suffisante pour stimuler une ingression partielle (Wagner and Glotzer, 2016). Sous ces conditions, cette ingression partielle pouvait même avoir lieu dans certaines cellules en interphase (Wagner and Glotzer 2016). Ceci met encore plus d'emphase sur l'importance de RhoA dans ce processus, mais plusieurs questions restent encore en doute dans notre compréhension de ce mécanisme de contraction (revue dans (Liu and Weiner, 2016)).

1.4.5.4. Une ingression asymétrique

La constriction de l'anneau contractile n'est pas symétrique. En effet, suite à l'élongation de la cellule, un plan vertical le long de la cellule montre une asymétrie de constriction favorisant un bord de la cellule. Cette asymétrie dépend de deux protéines corticales essentielles à la cytokinèse, Anillin et Septin (Maddox et al., 2007). L'asymétrie semble avoir lieu par rétroaction de la courbure membranaire, l'alignement du cytosquelette et la contractilité (Dorn et al., 2016). L'importance de l'asymétrie de l'ingression du sillon de clivage n'est toujours pas claire, mais ce modèle pourrait rendre la cytokinèse encore plus robuste et moins susceptible à des variations de contractilité (Menon and Gaestel, 2015).

1.4.6. La formation de l'anneau du midbody et du midbody

La constriction progresse en compactant les microtubules centraux, la membrane plasmique, la structure d'actomyosine et les protéines reliées à l'anneau contractile pour former une structure ultra dense qu'on surnomme l'anneau du midbody (Figure 4). La nomenclature est très variée en ce qui concerne la région entourant la structure cellulaire au niveau de l'anneau du midbody. Dans cette thèse, l'anneau du midbody représente la région corticale issue directement de l'anneau contractile. Elle forme une structure dense qui entoure les microtubules compactés à l'équateur de la cellule. Certains composants initiaux qui forment l'anneau contractile comme RhoA, la Myosine, Anillin, les septines et Citron Kinase sont toujours présents dans l'anneau du midbody (Green et al., 2012). Vers la fin de la constriction de l'anneau

contractile, le fuseau central est formé d'une structure de microtubule centré par l'anneau du midbody qui relie les deux cellules, que l'on surnomme le midbody. Ainsi, toute référence à une protéine qui se localise au midbody signifie une localisation spécifiquement aux microtubules compactés du fuseau central. Suite à l'anaphase, le fuseau mitotique se détériore graduellement et ceci est accompagné par la reformation du noyau. Au milieu du midbody se trouve une région dense en protéines dont les microtubules sont indétectables par immunofluorescence indirecte, mais visible par microscopie électronique (Mullins and Biesele, 1977). On retrouve au midbody des protéines essentielles à la formation du fuseau central comme PRC1, KIF4A et Plk1 (Hu et al., 2012). Certaines protéines comme Aurora B et MKLP2 se localisent à une région adjacente à cette structure dense que l'on appelle le midbody flanquant (Green et al., 2012; Hu et al., 2012). Ces deux régions flanquant le midbody sont constituées de la machinerie responsable de l'abscission. Le terme pont intercellulaire définit l'ensemble de ces différentes régions : le midbody, l'anneau du midbody, les microtubules du fuseau central et leur liaison à la membrane plasmique. Pour une publication détaillée de la localisation de protéines au midbody revoir (Hu et al., 2012).

1.4.7. Le rôle des éléments clefs au niveau du cortex

La transition de l'anneau contractile à l'anneau du midbody nécessite un effort synchronisé au niveau de la membrane plasmique, le cytosquelette d'actomyosine équatorial ainsi que les microtubules du fuseau mitotique. Un mouvement collectif de ces trois composants a lieu lors de cette transition afin de s'assurer que tous les trois restent connectés et se métamorphosent sous forme de la structure du midbody. Cette transition nécessite un enjeu protéique à ces 3 niveaux pour guider la cellule vers l'abscision et ainsi garantir une séparation cytoplasmique adéquate. Parmi les protéines impliquées dans cet enjeu on retrouve RhoA, les septines, l'Anillin ainsi que la Citron Kinase.

1.4.7.1. RhoA

L'arrondissement cellulaire RhoA-dépendant

L'un des rôles les plus précoces de RhoA dans la mitose est son implication dans l'arrondissement de la cellule, un processus qui a lieu en cooccurrence avec la désintégration de l'enveloppe nucléaire (Maddox and Burridge, 2003). Suite à la désintégration de la membrane nucléaire, ECT-2 se trouve au cytoplasme ce qui permet d'augmenter les niveaux de RhoA activés (Matthews et al., 2012). RhoA nécessite son activation pour remodeler le cytosquelette d'Actine afin de conférer une rigidité accrue au cortex de la cellule (Chircop, 2014; Maddox and Burridge, 2003; Matthews et al., 2012)

L'activation de RhoA

Ce remodelage s'intensifie suite à l'anaphase, lorsque RhoA est recrutée et ensuite activée plus fortement à l'équateur de la cellule. L'activation de RhoA à l'équateur de la cellule nécessite l'interaction Plk1-dépendant de sa GEF, ECT-2 avec le composant MgcRacGAP de centralspindlin au niveau du fuseau central (Wolfe et al., 2009; Yüce et al., 2005). Ceci permet la localisation d'ECT-2 dans une région étroite à l'équateur de la cellule, augmentant ainsi la présence de RhoA activée dans cette région (Su et al., 2011; Yüce et al., 2005). Bien que ECT-2 soit recruté majoritairement au niveau des microtubules du fuseau central, une présence membranaire a été signalée par le biais de son domaine PH (Su et al., 2011). Cette localisation membranaire d'ECT2 nécessite l'activité de Cdk1. Ceci pourrait être dû à centralspindlin qui peut se lier à la membrane plasmique grâce au domaine C1 de MgcRacGAP et ce, malgré le fait que sa localisation est exclusive au fuseau central (Lekomtsev et al., 2012a). La présence d'ECT-2 cytoplasmique est suffisante pour induire une activation de RhoA mais l'ingression du sillon de clivage nécessite une activation de RhoA par ECT-2 membranaire (Su et al., 2011).

La réponse à RhoA activée en cytokinèse

À son tour, RhoA activée gouverne plusieurs actions essentielles à la cytokinèse. Tout d'abord, RhoA activée induit le recrutement de la formine mDia responsable de la nucléation

des filaments d'Actines de l'anneau contractile (Li and Higgs, 2003). Plus spécifiquement, RhoA se lie à mDia pour la relâcher de sa forme auto-inhibitrice, lui permettant ainsi de se localiser à l'anneau contractile (Jordan and Canman, 2012; Otomo et al., 2005). De plus, RhoA est nécessaire pour l'activation et le recrutement de Citron Kinase et ROCK à l'anneau contractile (Dean et al., 2005; Kamijo et al., 2006; Matsumura et al., 2006). Ces deux kinases sont responsables de la phosphorylation de MRLC (Yamashiro et al., 2003). En effet, l'inhibition de RhoA par la C3 exoenzyme empêche l'accumulation de phospho-MRLC à l'anneau contractile (Kamijo et al., 2006). Finalement, l'activation de RhoA est responsable de la concentration équatoriale de la protéine d'échafaudage Anillin (Hickson and O'Farrell, 2008b). Le recrutement d'Anillin par RhoA est crucial pour la cytokinèse vu qu'Anillin a plusieurs partenaires d'interactions qui sont essentiels à la cytokinèse. Ainsi, RhoA joue le rôle ultime durant la cytokinèse puisque sa présence et son état d'activation semble agir en amont de la machinerie responsable de la formation et de la constriction de l'anneau contractile.

1.4.7.2. Les septines

Les septines sont des protéines GTPase associées à la membrane qui forment des structures de multiples ordres de grandeur par attachements combinatoires de plusieurs monomères des différents groupes de septines (Menon and Gaestel, 2015). Lors de l'ingression du sillon de clivage, les septines se localisent à l'anneau contractile et ensuite au midbody (Estey et al., 2010; Renshaw et al., 2014). La présence à l'anneau contractile de Septin 7 (Sept7 / *Peanut, PNUT*) dépend de l'Anillin et PNUT joue un rôle essentiel dans la cytokinèse (Field et al., 2005; Kechad et al., 2012; Neufeld and Rubin, 1994). PNUT permet à l'anneau du midbody de s'ancrer à la membrane plasmique (Kechad et al., 2012). Cette liaison a lieu grâce à l'interaction des septines avec la portion C-terminale d'Anillin qui est attachée au cortex (Field et al., 2005; Kechad et al., 2012). Cependant, les septines sont également capables de se lier directement aux filaments d'Actines et même de polymériser l'Actine, ce qui n'écarte pas la possibilité d'une interaction directe avec le cortex au niveau de l'anneau contractile (Mavrakis et al., 2014). Chez les mammifères, outre Sept7, la Septin 2 (*Septin 2, Sep2I*) et Septin 11 semblent également jouer un rôle essentiel dans la cytokinèse. Cependant, Septin 9 est important

pour le mécanisme d'abscision (Estey et al., 2010). À noter que la cytokinèse de différents types cellulaires n'est pas toujours dépendante des septines. (Pour une revue, voir (Menon and Gaestel, 2015)).

1.4.7.3. Anillin

Du noyau aux cortex et autres localisations

L'Anillin est une protéine d'échafaudage de l'anneau contractile (Figure 6 et 7). Elle possède plusieurs partenaires d'interaction (Figure 6) (Piekny and Maddox, 2010). En G_1, l'Anillin s'accumule dans le noyau tandis que la désintégration de l'enveloppe nucléaire coïncide avec son intégration au cortex (Field and Alberts, 1995). Suite à l'anaphase, on observe une accumulation d'Anillin à l'anneau contractile RhoA-dépendent suivi par une transition à l'anneau du midbody où elle restera localisée jusqu'à l'abscision (Field and Alberts, 1995). Une rentrée en G_1 marque le début de relocalisation d'Anillin au noyau accompagné par une dégradation cytoplasmique par l'APC (Field and Alberts, 1995; Zhao and Fang, 2005). Outre cette localisation typique, dans des cellules neuroepitheliales, Anillin est observée dans des structures qui sont excrétées vers la lumière apicale du tissu (Dubreuil et al., 2007). Ces excrétions sont entourées de membranes plasmiques et contiennent un marqueur de cellules souches surnommé Prominin-1/CD133 (Dubreuil et al., 2007). Finalement, Anillin se trouve concentré dans les jonctions cellulaires épithéliales ou elle joue un rôle essentiel dans la réorganisation du cytosquelette pour la formation de jonctions serrées et d'ancrages (Reyes et al., 2014).

Une interaction actomyosine

La partie N-terminale d'Anillin contient un domaine de liaison à la Myosine suivit par un domaine de liaison à l'Actine. Cette partie N-terminale est non seulement capable de se lier aux filaments d'Actine mais également de les regrouper ensemble (Field and Alberts, 1995; Straight et al., 2005). Malgré que le recrutement d'Anillin et d'Actine ne soit pas interdépendant, la présence de filaments d'Actine influence en partie la localisation d'Anillin (Hickson and

O'Farrell, 2008a; Hickson and O'Farrell, 2008b). De plus, chez les mammifères, Anillin interagit avec la formine mDia2 et cette interaction est essentielle pour la localisation de mDia2 mais aussi pour ses fonctions dans la cytokinèse (Watanabe et al., 2010).

Congestion en C-terminal

Le rôle d'échafaudage d'Anillin est impliqué dans la machinerie responsable de l'activation de RhoA. La partie C-terminale d'Anillin contient un domaine Pleckstrin Homology (PH) et une séquence de conservation Anillin spécifique nommé domaine Anillin Homology (AH) (Piekny and Maddox, 2010). C'est à travers le domaine AH qu'Anillin interagit avec RhoA (Piekny and Glotzer, 2008; Sun et al., 2015). Cette interaction est mutuellement importante pour la localisation et/ou la stabilisation de ces deux protéines (Piekny and Glotzer, 2008). Chez l'humain, le domaine PH d'Anillin interagit avec ECT-2 (Frenette et al., 2012). Par contre, en *Drosophile*, Anillin semble interagir avec RacGAP50C/Tum via son domain AH (D'Avino et al., 2008; Gregory et al., 2008). Outre ces trois protéines, Anillin interagit également avec les septines à travers une combinaison de ses domaines AH et PH (Oegema et al., 2000). Cette interaction semble mutuellement importante pour la localisation de ces deux protéines à l'anneau contractile (Piekny and Maddox, 2010). Finalement, Anillin est capable d'interagir directement avec les Phosphatidylinositol-4, 5-bisphosphate (PI(4,5)P2) dans la membrane par le biais de son domaine PH (Liu et al., 2012).

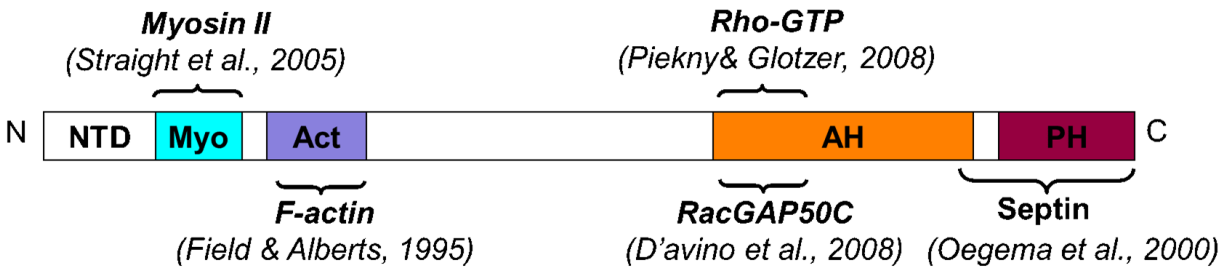

Figure 6. Structure d'Anillin et partenaires d'interactions lors de la cytokinèse

Lier le cortex à la membrane

La portion N terminal d'Anillin se lie à l'anneau d'actomyosine tandis que la partie C-terminale se lie à la membrane plasmique directement ainsi qu'à travers sa liaison aux septines. Nos études ont montré qu'Anillin sert de lien entre le cortex et la membrane plasmique (Kechad et al., 2012). D'autre part, une diminution d'expression d'Anillin inhibe l'attachement de l'anneau contractile aux septines et génère des mouvements oscillatoires de l'anneau contractile le long de la cellule ce qui empêche la réussite de la cytokinèse (Hickson and O'Farrell, 2008b; Kechad et al., 2012).

1.4.7.4. Citron Kinase

Une kinase qui interagit avec Rho

Citron Kinase est une protéine d'interaction avec Rho qui se localise à l'anneau contractile ainsi qu'à l'anneau du midbody lors de la cytokinèse (Madaule et al., 1998). Citron Kinase est essentiel à la cytokinèse seulement dans certains types cellulaires (Cunto et al., 1998). Ainsi, la souris knockout de Citron Kinase meurt avant l'âge adulte à cause de défaut de développement du système nerveux central (Cunto et al., 1998). Originalement identifié comme protéine effectrice de Rho, Citron possède un domaine Serine/Thréonine kinase qui peut phosphoryler la MRLC ainsi que INCENP (McKenzie et al., 2016; Yamashiro et al., 2003). Cependant, il n'existe aucune preuve qui démontre un lien direct entre la phosphorylation de MRLC par Citron Kinase et la cytokinèse (Dean and Spudich, 2006; McKenzie et al., 2016).

Une ressemblance à Anillin?

Le domaine kinase est suivi par une région de superhélice et ensuite une portion C-terminale qui diffère entre les espèces (D'Avino et al., 2004). Des études ont démontré que la surexpression de Citron Kinase manquant la partie C-terminale génère des mouvements oscillatoires de l'anneau contractile de manière similaire à l'Anillin (Madaule et al., 1998). Cependant, la diminution d'expression de Citron Kinase affecte l'organisation de l'anneau du midbody plutôt que l'anneau contractile (Bassi et al., 2011; Echard et al., 2004). Entre autres,

cette réduction d'expression de Citron Kinase affecte la localisation d'Anillin qui devient aberrante à l'anneau du midbody (Bassi et al., 2011; Gai et al., 2011).

Une interaction avec le pont intercellulaire

Citron Kinase interagit également avec les kinésines MKLP1 et KIF14 (Nebbish, Neb) (Bassi et al., 2013; Gruneberg et al., 2006a; Watanabe et al., 2013). Cette interaction entre Citron Kinase/KIF14 ainsi que Citron Kinase/MKLP1 permet à KIF14, MKLP1 et PRC1 d'interagir ensemble (Figure 7) (Bassi et al., 2013). Le recrutement à l'anneau du midbody de Citron Kinase et KIF14 est interdépendant et essentiel pour celui de PRC1 et MKLP1 (Bassi et al., 2013). Cette interaction avec KIF14 a lieu à travers la partie N-terminal du domaine coiled coil de Citron Kinase (Bassi et al., 2013). Ce domaine permet aussi une interaction directe avec les composants du CPC (McKenzie et al., 2016). D'ailleurs, Aurora B phosphoryle Citron Kinase (McKenzie et al., 2016). Toutes ces interactions entre Citron Kinase et les protéines associées aux microtubules semblent être importantes pour l'organisation du midbody (Bassi et al., 2013; Bassi et al., 2011; Watanabe et al., 2013). L'importance de cette architecture du midbody Citron Kinase-dépendant pour le succès de la cytokinèse, demeure inconnue.

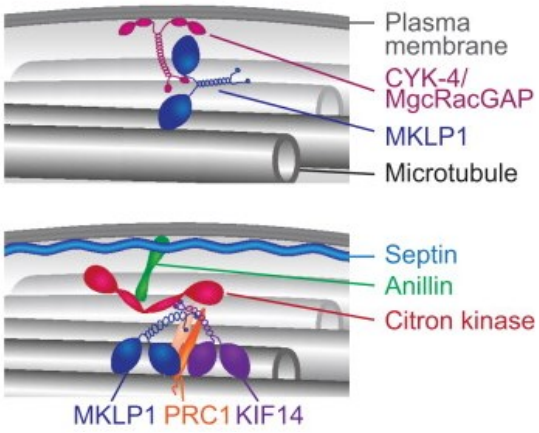

Figure 7. Principaux mécanismes moléculaires de liaison de la membrane plasmique aux microtubules du fuseau central.

Tiré de (Mierzwa and Gerlich, 2014) : Figure 3. Anchorage of the Cell Cortex in the Intercellular Bridge.

Une controverse au niveau de Rho

Citron Kinase affecte également la localisation ainsi que l'état d'activation de RhoA (Bassi et al., 2011; Gai et al., 2011). Ceci a mené certains groupes à suggérer que Citron Kinase pourrait agir en amont de RhoA malgré le fait que la localisation de Citron Kinase au sillon de clivage soit Rho-dépendant (D'Avino et al., 2015). Pour plus de détails sur Citron Kinase lors de la cytokinèse, consulter le Chapitre 3: *Citron Kinase in cytokinesis : A Sticky situation*.

1.4.7.5. La composition de la membrane plasmique

Plusieurs changements au niveau du contenu lipidique sont observés lors de la cytokinèse (Atilla-Gokcumen et al., 2014). Ces changements se manifestent au niveau d'une spécificité globale de la membrane plasmique, de l'anneau contractile et de l'anneau du midbody (Atilla-Gokcumen et al., 2014). Ainsi, les études sur le rôle de la constitution lipidique lors de la cytokinèse démontrent une implication à toutes les étapes de cette réorganisation lipidique. Suite à l'anaphase, on observe une redistribution de la localisation uniforme des PI(4, 5)P2 pour se concentrer au niveau du sillon de clivage (Ben El Kadhi et al., 2011; Zhang et al., 2000). Plusieurs enzymes de modification de la phosphatidylinositol sont impliqués dans la cytokinèse. Pour une revue sur ce chapitre (Echard, 2012) et la figure 8. Un exemple intéressant de cette implication est une étude chez la *Drosophile*. De l'enzyme *Drosophila* ortholog of human oculocerebrorenal syndrome of Lowe 1 (dOCRL1) qui est notamment impliqué dans le processus de relocalisation des PI(4, 5)P2 (Ben El Kadhi et al., 2011). En absence de ORCL1, de larges vacuoles cytoplasmiques se forment et le sillon de clivage est incapable de se positionner correctement. Au niveau moléculaire la réduction d'expression de ORCL1 démontre une localisation aberrante d'Anillin et Sqh (Ben El Kadhi et al., 2011). Ainsi, une spécificité de composition lipidique au niveau du sillon de clivage joue un rôle important dans l'organisation moléculaire des composants essentiels à la cytokinèse. Ceci n'est d'ailleurs pas surprenant vu l'abondance d'informations qui supporte l'importance d'interactions spécifiques de phosphatidylinositol avec les différents composants de l'anneau contractile. Entre autres, les phosphatidylinositol jouent un rôle clef au niveau (Figure 8, revue dans (Echard, 2012)):

- De l'association du cytosquelette d'Actine à la membrane (Echard, 2012; Logan and Mandato, 2006);
- Du recrutement membranaire d'Ect2 (Frenette et al., 2012; Su et al., 2011) ainsi qu'Anillin (Liu et al., 2012) par le biais de leur domaine PH
- Du recrutement membranaire de MgcRacGap par le biais de son domaine C1 (Lekomtsev et al., 2012b)
- De la liaison du cortex à la membrane par activation des protéines Ezrin, Radixin, moesin (ERM, *moesin*) (Carreno et al., 2008; Fehon et al., 2010)
- Dans la localisation appropriée des septines au niveau de l'anneau contractile (Chesneau et al., 2012)

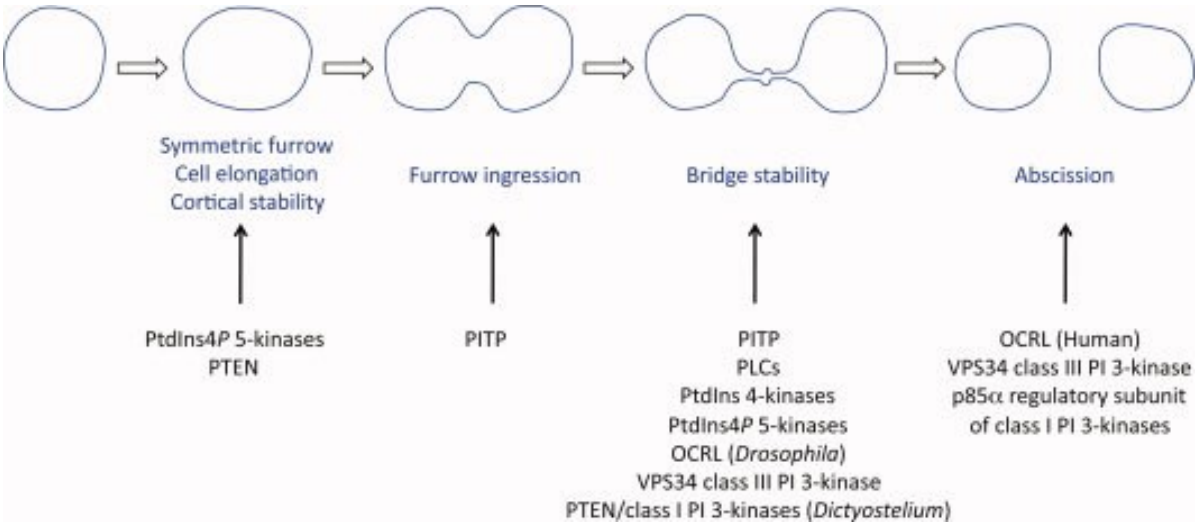

Figure 8. Rôle des enzymes de modification des phosphatidylinositols lors de la cytokinèse.

Tiré de (Echard, 2012) : Figure 2. Phosphoinositide-modifying enzymes are required at different steps of cytokinesis.

1.5. L'abscision

Suite à la transition vers l'anneau du midbody, ce dernier guide la cellule vers l'abscission. Il existe plusieurs modèles d'abscision dans le modèle animal. Cependant, lors des dernières années, une théorie a pris beaucoup d'ampleur comparée aux autres (Figure 9). Pour en savoir plus sur un modèle d'abscission qui impliquerait un trafic vésiculaire revoir (Neto et al., 2011).

1.5.1. ESCRT-III

Au niveau du midbody en utilisant le microscope électronique, on observe des ondulations du site d'abscission (Mullins and Biesele, 1973). Parmi les protéines recrutées à ce site, on retrouve les complexes protéiques Endosomal Sorting Complex Required for Transport-III (ESCRT-III) qui forment probablement ces filaments ondulatoires au site d'abscission (Guizetti et al., 2011; Hanson et al., 2009). Cette famille de protéine contient 11 éléments chez l'homme et 7 chez la *Drosophile* (Capalbo et al., 2012). Le complexe ESCRT-III est essentiel au mécanisme d'abscission et ses fonctions dans la cytokinèse sont très bien conservées lors de l'évolution (Bhutta et al., 2014; Guizetti et al., 2011; Matias et al., 2015). L'abscission a lieu par une constriction secondaire adjacente à celle de l'anneau du midbody. Un des modèles de mécanismes responsables de cette abscission propose qu'il y ait élimination graduelle des composants du cytosquelette au niveau du midbody (Guizetti and Gerlich, 2010). Ainsi, les complexes ESCRT-III qui forment des filaments ondulatoires au niveau du site d'abscission seraient responsables du recrutement de la protéine Spastine qui est une protéine responsable de couper les microtubules (Guizetti et al., 2011). La forme spirale des filaments ondulatoires expliquerait la coupure graduelle des microtubules pour rompre le pont intercellulaire (Green et al., 2012).

1.5.2. La régulation temporelle de l'abscission

Les cellules se trouvent attachées par le midbody pour une période de temps qui varie grandement d'une cellule à l'autre et elle peut durer plusieurs heures. Ainsi, les cellules peuvent se retrouver dans différentes étapes de l'interphase avant de se séparer indéfiniment. Cependant, le moment d'abscission est bien coordonné avec le déroulement des évènements de la cytokinèse (Bhutta et al., 2014). ESCRT-III ne peut être recruté que tard dans le processus de la cytokinèse puisque son recrutement au site d'abscission dépend de la protéine Cep55 (Lee et al., 2008). Lors de la constriction de l'anneau contractile, Cep55 est phosphorylé par Plk1, ce qui empêche Cep55 de s'accumuler à l'anneau contractile (Bastos and Barr, 2010). Tout comme Plk1, Aurora B est également importante pour un bon déroulement chronologique de la cytokinèse (Capalbo et al., 2012; Norden et al., 2006). Si l'activité d'Aurora B est réduite prématurément lors de la cytokinèse, l'abscission peut également avoir lieu prématurément (Carlton et al., 2012). Aurora B est responsable de la phosphorylation d'un composant d'ESCRT-III pour retarder l'abscission (Capalbo et al., 2012).

Cep55 peut médier lui-même un recrutement coordonné des composants requis pour l'abscission. Ainsi, Cep55 interagit directement Tumor susceptibility gene 101 (TSG101) et apoptosis-linked gene 2-interacting protein (ALIX), pour permettre leur recrutement à l'anneau du midbody (Eikenes et al., 2015). Ces deux protéines sont un composant du complexe ESCRT-I et une protéine associée à ce complexe respectivement (Eikenes et al., 2015). ALIX et TSG101 à leur tour recrutent certains composants d'ESCRT-III (Eikenes et al., 2015; Guizetti et al., 2011). La protéine VPS4 serait impliquée dans la redistribution d'ESCRT-III sous forme spirale dans un bord de la cellule ce qui aboutirait à une organisation conforme à l'abscission (Bhutta et al., 2014)

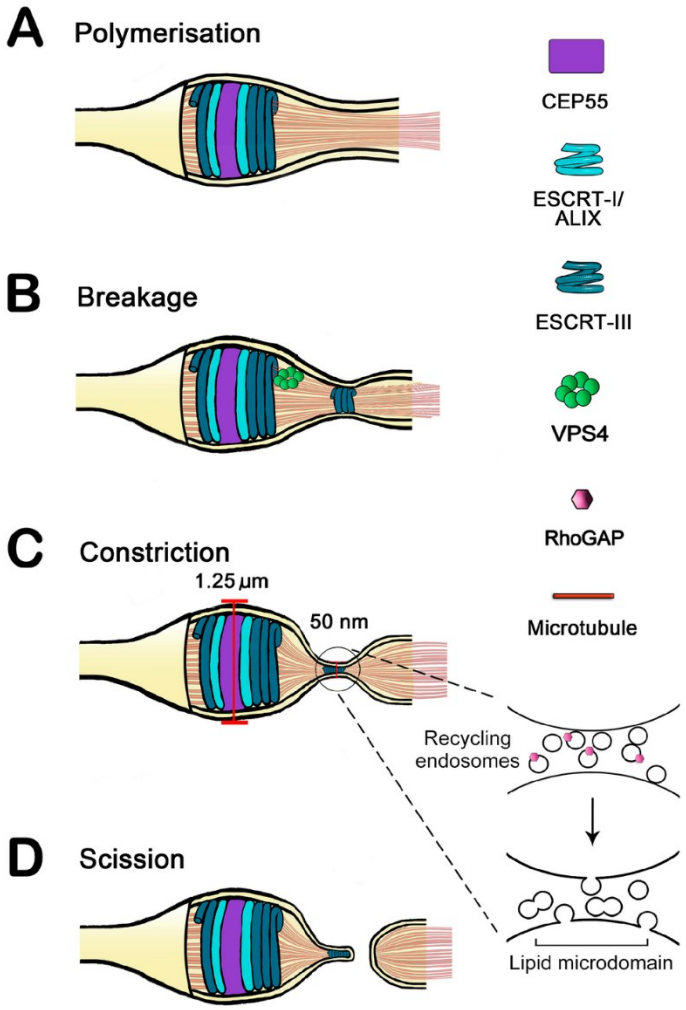

Figure 9. Modèle d'abscission des cellules mammifères.

Tiré de (Bhutta et al., 2014) : Figure 1. Schematic model for abscission in mammalian cells.

1.5.3. Le midbody ''remnant''

Une vue classique de la conséquence de l'abscission qui a lieu de manière asymétrique est qu'une des deux cellules se retrouve avec un midbody résiduel qu'on appelle le midbody remnant. Ce remnant est formé de composants qui se retrouvent dans l'anneau du midbody et au midbody tard en cytokinèse. La présence d'un remnant soulève plusieurs interrogations comme l'origine de l'héritage asymétrique, l'impact de cet héritage ainsi que le destin du remnant (Schink and Stenmark, 2011).

1.5.3.1. Un mécanisme aléatoire?

Plusieurs études démontrent que l'héritage du midbody n'est pas aléatoire. Chez *Caenorhabditis elegans*, l'héritage du remnant a une distribution stéréotypée (Ou et al., 2014). Une autre étude démontre que le midbody remnant est hérité par la cellule qui possède le centrosome le plus vieux (Kuo et al., 2011). De plus, les cellules souches accumulent préférentiellement le remnant (Ettinger et al., 2011; Kuo et al., 2011) tandis que les cellules différenciées éliminent le remnant (Crowell et al., 2014; Ettinger et al., 2011). Une accumulation de midbody dans des cellules cancéreuses a également été observée (Crowell et al., 2014; Ettinger et al., 2011; Kuo et al., 2011). Tous ces indices semblent indiquer que l'héritage n'est pas aléatoire et pourrait donc influencer le destin de différenciation d'une cellule (Crowell et al., 2014).

1.5.3.2. Deux coupures et phagocytose

Même si l'abscission a lieu d'un bord de la cellule, une étude démontre qu'une deuxième coupure a lieu à l'autre bout du pont intercellulaire (Crowell et al., 2014). Dans plusieurs lignées cellulaires, le midbody se retrouve majoritairement relâché dans le milieu extracellulaire ou repris par une des cellules (Crowell et al., 2014; Ettinger et al., 2011; Mullins and Biesele, 1973). Ce midbody peut également être récupéré par une cellule autre qu'une des deux cellules filles (Crowell et al., 2014). Une dégradation lysosome-dépendant a lieu suite à une recapture du midbody remnant par phagocytose (Crowell et al., 2014; Kuo et al., 2011).

1.6. L'impact clinique

La cytokinèse se doit d'être un processus rigoureux. Lorsqu'elle est compromise, les deux cellules filles risquent de se fusionner pour former une cellule tétraploïde. Les cellules dans le corps humain sont d'habitude diploïdes. Ce qui veut dire que physiologiquement, les cellules sont capables de procéder à une cytokinèse avec succès. On observe dans certains cas physiologiques, des échecs programmés de la cytokinèse (pour plus de détail se référer à (Lacroix and Maddox, 2012; Normand and King, 2010; Tormos et al., 2015)).

Cependant, des défauts non régulés de la cytokinèse sont observés dans plusieurs pathologies graves. Dans certains cas, la cytokinèse en est la cause et dans d'autre elle en est la conséquence, mais peu importe le cas, la conséquence de polyploïdie en est problématique (Lacroix and Maddox, 2012). À titre d'exemple, il a été démontré que dans des souris p53 -/- les cellules tétraploïdes issues de cytokinèses défectueuses peuvent promouvoir le développement de tumeurs (Fujiwara et al., 2005). D'ailleurs, la détection de cellules tétraploïdes dans le cancer est très bien documentée et souvent utilisée comme outil pronostic (Lacroix and Maddox, 2012). Anillin a également été démontré comme protéine surexprimée dans plusieurs tumeurs (Hall et al., 2005). Pour plus de détail sur la cytokinèse et les différentes pathologies, consultez (Lacroix and Maddox, 2012; Tormos et al., 2015)

1.6.1. Le cas de Citron Kinase

Citron Kinase est une protéine intéressante d'un point de vue pathologique. Contrairement aux à plusieurs protéines essentielles à la cytokinèse, Citron Kinase ne l'est pas pour tous les tissus ou type cellulaire (Cunto et al., 1998). Principalement, Citron Kinase affecte le développement du system nerveux central ainsi que le développement testiculaire (Cunto et al., 2000). Chez l'homme, la microcéphalie est associée avec des mutations de Citron Kinase qui cause des défauts de cytokinèse menant au sous-développement du système nerveux central (Basit et al., 2016; Gai and Di Cunto, 2016; Harding et al., 2016; Shaheen et al., 2016). Ces mutations associées peuvent être non-sens ou faux sens dans le domaine kinase (Basit et al., 2016; Harding et al., 2016).

1.7. Vers la stabilité d'un anneau contractile

La cytokinèse est un processus très complexe. C'est un mécanisme cellulaire qui requiert plusieurs éléments à travailler ensemble pour s'assurer de la séparation des deux cellules filles. La partie la plus critique et probablement la plus étudiée de la cytokinèse est celle qui est le plus dynamique : l'ingression du sillon de clivage. Malgré tous les efforts mis en place afin d'améliorer notre compréhension de cette étape, une incertitude règne toujours sur les

mécanismes de base. Suite à une période de contraction, l'anneau contractile passe vers la structure de l'anneau du midbody. Les cellules peuvent rester attachées ensemble pendant plusieurs heures avant de se séparer définitivement. Cette vue typique et parfois binaire de la transition d'anneau contractile à l'anneau du midbody est très primitive. Comment une organelle si dynamique tel que l'anneau contractile dynamique peut passer vers une structure si stable, l'anneau du midbody? Cet aspect de la cytokinèse est très peu étudié. Mais si l'on comprend les processus moléculaires permettant à la cellule de passer d'un anneau contractile dynamique vers un anneau du midbody stable, ceci nous donnerait des informations importantes autant au niveau de la formation de l'anneau contractile, la force contractile, qu'au niveau des mécanismes requis pour former un anneau du midbody prêt à entreprendre l'abscission (Figure 10).

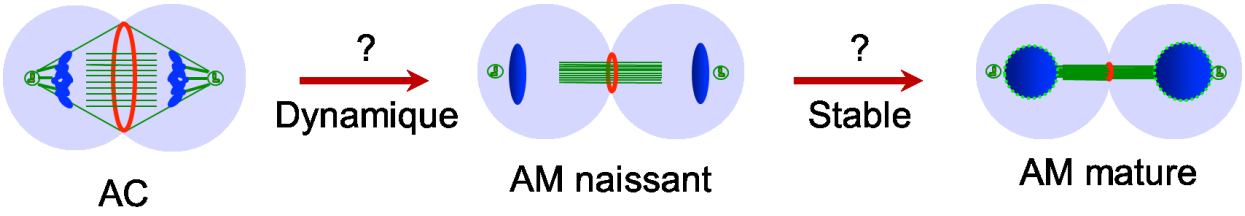

Figure 10. Les mécanismes transition de l'anneau contractile dynamique vers un anneau du midbody stable ne sont pas encore bien élucidés.

2. Rationnel

Hypothèse

Comment l'anneau contractile (AC) passe d'un état dynamique à un état stable pendant la formation de l'anneau du midbody (AM), tout en maintenant l'ancrage de la membrane plasmique, reste inconnu. Plusieurs évidences supportent l'hypothèse centrale que la Citron Kinase participe à ce processus, notamment la perte de fonction de Citron Kinase déstabilise le pont intercellulaire à cette étape (Bassi et al., 2013; Echard et al., 2004; Madaule et al., 1998; McKenzie et al., 2016; Sgro et al., 2016; Watanabe et al., 2013).

Objectif

L'objectif global de cette thèse est de définir le rôle de la Citron Kinase, Sticky, dans la transition AC-AM.

Le système expérimental

Les cellules S2 de Schneider de *Drosophila melanogaster* ont été utilisées comme modèle. Cette lignée bénéficie d'un génome simple et non redondant et elle est très sensible aux ARNs double-brins (dsRNAs) pour des études d'ARNi. De plus les cellules S2 sont très faciles à maintenir et bien adaptées pour faire de la microcopie optique à temps réel (Hickson and O'Farrell, 2008b; Kechad and Hickson, 2016). Ce système est très adéquat pour l'étude de la cytokinèse. De plus, la génération de lignées cellulaires stables qui contiennent des vecteurs d'expression de protéines fusionnées à différentes protéines fluorescentes est routine. L'expression de ces vecteurs est bien contrôlée puisqu'elle est inductible en présence de $CuSO_4$.

Sommaire des articles

- Le Chapitre 3 s'agit d'une revue de la littérature sur Citron Kinase, pour mettre à jour nos connaissances à ce sujet.

- Le Chapitre 4 s'agit d'un article publié qui décrit une étude approfondie sur les phénotypes associés à la perte de fonction du Citron Kinase, Sticky, ainsi que la documentation de phénomènes importants à la maturation de l'AM.
- Le Chapitre 5 s'agit d'un manuscrit en préparation qui décrit une étude de structure/fonction de Sticky, et qui démontre comment Sticky interagit avec d'autres régulateurs clés de la transition AC-AM, tel que Rho1 et Anillin.

3. Citron Kinase in cytokinesis: A Sticky situation

Nour El Amine[1, 2] and Gilles R.X. Hickson[1, 2]

1 Centre de Cancérologie Charles Bruneau, Centre Hospitalier Universitaire Sainte-Justine Centre de Recherche, Montréal, Québec H3T 1C5, Canada

2Département de Pathologie et Biologie Cellulaire, Université de Montréal, Montréal, Québec H3C 3J7, Canada

Manuscript in preparation

Contributions : NE et GH ont rédigé l'article.

3.1. Abstract

Citron Kinase (Cit-K) is a conserved protein involved in cytokinesis. Mutations in Cit-K can have major effects on organism development, especially in the central nervous system where loss of Cit-K function can lead to microcephaly. The cellular roles of Cit-K have been extensively studied in mammals and *Drosophila*. While, Cit-K was originally suspected to function early during cytokinesis, it is now clear that Cit-K acts primarily at later stages of cytokinesis, during the formation and stabilization of the intercellular bridge. However, some results regarding the regulation of Cit-K appear to be contradictory and the precise roles of Cit-K during cytokinesis have remained obscure. However, recent studies on Cit-K in cytokinesis have clarified our understanding of the function and role of Cit-K during this process. Here, we review the most significant findings and discuss how they collectively contribute to our understanding of cytokinesis.

3.2. The roots

Murine Citron-N, which lacks a kinase domain, was first identified in 1995 by Madaule et al. as a Rho/Rac effector using the yeast two hybrid system and overlay assay (Madaule et al., 1995). The same group later identified Citron Kinase as a splice variant of Citron-N that contains an additional Serine/Threonine kinase domain in its N-terminus (Madaule et al., 1998). Citron Kinase exogenously expressed in HeLa cells localized to the cleavage furrow (CF) and a donut shaped midbody ring (MR) (Madaule et al., 1998). The sequence of Citron Kinase was confirmed shortly after by Di Cunto et al. who also demonstrated that active Rho modulates the kinase activity of Citron Kinase while Rac had more limited effects (Cunto et al., 1998). The essential function of Citron Kinase in cytokinesis was detected very early on (Cunto et al., 1998; Madaule et al., 1998). Intriguingly, over-expression of a Kinase Dead mutant of Citron Kinase caused oscillation of the contractile ring before cells would regress and form a binucleate cell (Madaule et al., 1998). This suggested that Citron Kinase could have an early role in furrowing.

3.3. The structure

Cit-K is well conserved from flies to humans, both in terms of predicted domains and their organization. Human Citron Kinase comprises 2027 amino acids, while the *Drosophila melanogaster* Cit-K orthologue, Sticky, comprises 1854 amino acids (Figure 1). In both species, the N-terminus contains the kinase domain and is followed by a central coiled coil (CC) region. The C-terminus of both orthologues have conserved Citron and Nik1 homology (CNH) domains. However, the region between the Coiled Coil and the CNH differs amongst the two species. In humans, there is a predicted Pleckstrin Homology domain (PH) as well as a Protein kinase C-like, phorbol ester/diacylglycerol-binding domain (C1 domain). The *Drosophila* Sticky only has a C1 but is missing the PH domain. Finally, human Citron Kinase has an 80-90 amino acid extension predicted to contain a PDZ domain that is not present in Sticky.

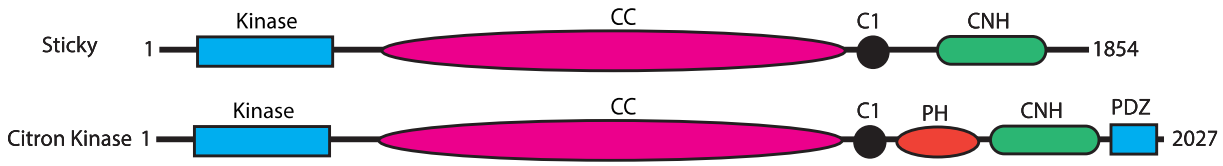

Figure 1. Citron Kinase/Sticky structure

3.4. Citron Kinase *in vivo*

The first studies of the role of Citron Kinase *in vivo* were done in embryonic mouse development. The long Citron Kinase isoform was found to be the predominantly expressed in proliferating neuronal precursors of early brain development whereas the short Citron-N isoform was found to be predominantly expressed in differentiated neurons (Cunto et al., 2000). Citron Kinase -/- mice displayed normal growth until P8 where they would display severe ataxia. The mice died before P21 from epileptic seizures and exhibited a 50% reduction in total brain weight. Specifically, the olfactory bulbs, the hippocampus, and the cerebellum had the most abnormal development. These defects were associated with apoptosis likely initiated by increased cytokinesis failures. Interestingly, some tissues that showed high expression of Citron Kinase in

wild type mice did not show any defects in knockout mice, suggesting that the non-redundant essential role of Citron Kinase in cytokinesis is tissue specific (Cunto et al., 2000).

Another major developmental defect of Cit-K knockout mice was found in testis. Mice express Cit-K in the testis from at least P4 to P40 (Cunto et al., 2002). However, no protein levels were detected at P4 ovaries (Cunto et al., 2002). Cit-K knockout mice displayed a severe reduction in testis size at p14 compared to Wild Type (WT) control whereas ovaries in female mice did not show any significant size reduction or morphological changes (Cunto et al., 2002). Histological sections of testis revealed a great reduction in the number of germ cells due to gradual depletion by apoptosis (Cunto et al., 2002). Furthermore, the presence of multi-nucleated spermatogenic precursors of Cit-K knockout mice indicates that they had failed cytokinesis and re-entered the cell cycle. (Cunto et al., 2002). These early *in vivo* studies highlighted the importance of Cti-K in cytokinesis. However, an important question arose: why do only some cell types appear to require Citron Kinase?

3.5. Citron Kinase is cell cycle regulated

Lack of Cit-K mRNA in adult mouse liver, heart and skeletal muscle studies had suggested that Cit-K expression is tissue specific (Cunto et al., 1998). However, it was later shown that Cit-K expression is not detectable because the cells in these tissues are probably present in a quiescent form (Liu et al., 2003). In an elegant study, where liver cells were induced to re-enter the cell cycle after hepatectomy, Liu et al. demonstrated that Cit-K expression is increased after Cyclin B1 levels are expressed suggesting that Cit-K is expressed between end of S phase and early G2. Conversely, Cit-K levels decreased gradually during post-natal rat liver development (Liu et al., 2003). Thus, it seems that an apparent lack of Cit-K mRNA in some adult organs may reflect exit from the cell cycle. These observations originally attempted to justify how Cit-K is potentially important for all tissue but it is not sufficient as organ development is mostly normal in Cit-K deficient rodents for the exceptions of the brain and the testis. In our opinion, how Citron Kinase is selectively important is still not fully understood but recent cues discussed later could shed light onto potential mechanisms.

3.6. Citron Kinase and Myosin phosphorylation

Cit-K has been show to phosphorylate both Ser-18 and Thr-19 of the Myosin Regulatory Light Chain (MRLC) (Yamashiro et al., 2003). The phosphorylation of these two specific sites is crucial for activation of the motor activity of Myosin II (Matsumura, 2005). Even though Cit-K seems to be favoring the promotion of the diphosphorylated form of MRLC to the cleavage furrow, the importance of this phosphorylation by Cit-K in cytokinesis is still unclear (Yamashiro et al., 2003). Cit-K shares structural similarities with Rho Kinase (ROCK) (Yamashiro et al., 2003). The latter is also responsible for the phosphorylation of MRLC and this attribute of ROCK has been shown to be essential for cytokinesis. Unlike Cit-K, ROCK is also capable of inhibiting MRLC dephosphorylation through Myosin Phosphatase inhibition (Dean and Spudich, 2006; Matsumura, 2005; Yamashiro et al., 2003). Furthermore, the only essential role of ROCK in cytokinesis is the phosphorylation of MRLC since expression of a phosphomimetic mutant of MRLC rescued depletion of ROCK (Dean and Spudich, 2006). On the contrary, a phosphomimetic version of MRLC still localizes to the cleavage furrow and cannot rescue cytokinesis upon Cit-K depletion (Dean and Spudich, 2006). This led to the conclusion that MRLC phosphorylation cannot be the only essential role of Cit-K during cytokinesis (Dean and Spudich, 2006). Perhaps we could add the possibility that the phosphorylation of MRLC by Cit-K cannot be the only essential role of Cit-K in cytokinesis. It is important to understand that what seems like a more limited role in cytokinesis of MRLC's phosphorylation by Cit-K does not deny its biological importance. Indeed, this has been elegantly demonstrated by a Sticky RNAi in the *Drosophila melanogaster* eye imaginal disc leads to a rough eye phenotype that can be rescued by the presence of a single copy of the phosphomimetic form of Spaghetti Squash (Sqh) the orthologue of MRLC (D'Avino et al., 2004). However, this still raises the question of whether the kinase domain of Cit-K could play an essential role in cytokinesis.

3.7. Sticky the orthologue of Citron Kinase

In 2004 a series of 4 papers described the role of the *sticky* gene the orthologue of Citron Kinase in *Drosophila melanogaster*. Sticky depletion led to formation of multinucleated cells indicating that it also has an essential role in cytokinesis (D'Avino et al., 2004; Echard et al., 2004; Naim et al., 2004; Shandala et al., 2004). Although Sticky localizes to the contractile ring (CR) before it is found in the midbody ring (MR) (Figure 2), Sticky depleted cells did not show major defects in furrowing, but rather showed unstable intercellular bridges after furrowing. These findings suggested that the essential role of Sticky is in late cytokinesis and not early events (D'Avino et al., 2004; Echard et al., 2004; Naim et al., 2004; Shandala et al., 2004). Furthermore, Sticky depletion from *Drosophila* S2 cells led to abnormal localization of CR proteins like Anillin and the septin Peanut at the MR (D'Avino et al., 2004; Naim et al., 2004). Antibody staining of Sticky revealed localization to the CF, CR as well as early and late midbody ring (MR) (D'Avino et al., 2004).

Analysis of *Drosophila* harboring mutant sticky alleles that introduced stop codons in the CC domain around the Rho binding domain, demonstrates that in late cytokinesis of neuroblasts, Anillin and Fascetto (Feo), the PRC1 orthologue, displayed a longer localization along the central spindle (Naim et al., 2004). This was some of the first indications of potential involvement of Citron Kinase with microtubule associated proteins and its importance in the maintenance of a proper midbody and midbody ring in late cytokinesis.

3.8. Citron Kinase/Rho/Anillin in cytokinesis

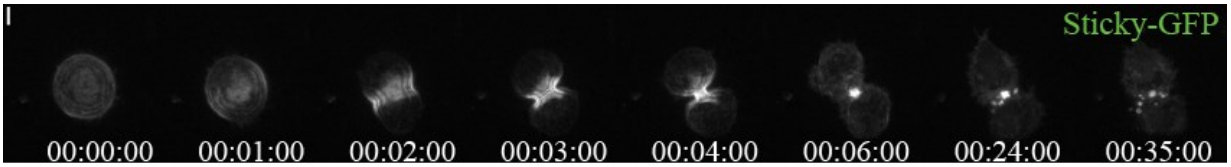

Figure 2. Citron Kinase/Sticky localization during cytokinesis.

Time-lapse sequence of cells expressing Sticky–GFP, acquired with a 63x, 1.4 NA objective. Times are h:min:sec. Bar is 3 μm.

3.8.1. A role in early cytokinesis?

In a similar fashion to Citron Kinase-induced cleavage furrow oscillations previously discussed (Madaule et al., 1998), Anillin knockdown was later discovered to cause similar defects in cytokinesis (Zhao and Fang, 2005). This led the field to believe in a possible interplay between these 2 proteins early in cytokinesis. Although this phenotype was prominently displayed in multiple Anillin studies (Kechad et al., 2012; Piekny and Glotzer, 2008; Sedzinski et al., 2011), Sticky induced oscillations were only confirmed in HeLa cells overexpressing Citron Kinase that caused oscillation of the contractile ring in 35% of the cells and also led to early abscission in the other 65% of cells that underwent cytokinesis (Gai et al., 2011). In both Madaule et al. 1998 and Gai et al. 2011, an overexpression led to the phenotype and no loss of function had demonstrated such phenotypes until our study confirmed this possibility albeit redundantly as discussed later in this manuscript (El-Amine et al., 2013). Further insight into potential Citron/Anillin interplay was gained by the finding that Citron Kinase and Anillin are present in the same physical complex (Gai et al., 2011). GST fused to the N-terminal portion of Anillin containing the Myosin and Actin binding domains was sufficient to pull down Citron Kinase from Hela cell lysates (Gai et al., 2011).

3.8.2. A Rho controversy

Recently data from a couple of publications challenged the prevailing view that Citron Kinase/Sticky should function downstream of RhoA. First, Anillin and RhoA both failed to localize to the late midbody ring in Citron Kinase/Sticky depleted cells (Bassi et al., 2011; Gai et al., 2011). On the contrary, RhoA inactivation by C3 exoenzyme in late cytokinesis does not perturb Citron Kinase localization at the midbody ring (Gai et al., 2011). Furthermore, Citron Kinase can modulate the activity of RhoA, as well being able to bind to RhoA independent of its activation state (Bassi et al., 2011). Together this led to the suggestion that Citron Kinase localization to the midbody ring could be upstream of RhoA or at least that it is acting as a non-canonical effector of RhoA. A challenge to this notion came from an experiment where cells expressing a Citron Kinase point mutant in the putative amino acid that would form the interface to Rho-GTP, partially rescued cytokinesis failures following Citron Kinase depletion (Watanabe

et al., 2013). This Citron Kinase mutant also weakly localized to the contractile ring. This is further supported by early treatment in mitosis of C3 exoenzyme that would shift Citron Kinase localization from the cortex to the spindle indicating that Rho is acting upstream of Citron Kinase before cytokinesis onset (Eda et al., 2001). A middle ground to this controversy, is the possibility that Citron Kinase could be downstream of RhoA in early cytokinesis but that order is reversed or lost in later stages of cytokinesis.

3.8.3. The transition needs Citron Kinase

Our understanding of the transition from a dynamic CR to a stable MR is limited. The presence of Citron Kinase at the CR, the observations that modulation of its expression levels could affect contractility and indications pointing towards a more important role later in cytokinesis at the midbody level made Sticky an ideal candidate to understand the transition from CR to MR. Although rarely discussed, membrane extrusion from the MR as it transitions from the CR can often be observed and has been described in the past (Mullins and Biesele, 1973). Our own work has shown that Sticky depleted S2 cells not only fail to stabilize their MRs, but they also fail to limit (and rather enhance) the extrusions and shedding of membrane associated Anillin that normally accompanies MR formation (El-Amine et al., 2013). Thus, Sticky is required to retain MR components such as Anillin, and in the absence of Sticky, shedding of MR components continues unchecked until cytokinesis failure results. On the contrary the septin Peanut was essential for extrusions to occur and thus for proper thinning of the MR during its maturation (El-Amine et al., 2013). Even though depletion of either Peanut or Sticky alone did not destabilize cleavage furrows, their co- depletion led to oscillating furrows, in a manner that was reminiscent of Anillin depletion phenotypes (El-Amine et al., 2013; Zhao and Fang, 2005). We had previously shown that the N-terminus of Anillin was sufficient to form a MR-like structure, but that was incapable of anchoring the plasma membrane (Kechad et al., 2012). We subsequently showed that the formation of these MR-like structures also required Sticky and therefore concluded that Sticky acts to specifically retain the N-terminus of Anillin and form the MR, while Peanut acts to extrude/shed Anillin via its C-

terminus. Coordination of these two opposing processes of retention and removal seems essential for the maturation and stabilization of the MR (El-Amine et al., 2013).

3.9. Localization to the contractile ring and midbody ring via the Coiled Coil domain

When the CR has almost completely closed, the MR forms at the midpoint of the central spindle as it becomes the midbody. Accordingly, for MR formation to occur correctly, there needs to be communication between both cortical proteins and the proteins of the central spindle. Citron Kinase is well placed to fulfill this role. A structure function analysis of Sticky led to the identification of the domains responsible for its CF and midbody localization. Coiled Coil (CC) probability analysis of Sticky shows 2 possible regions that were identified as CC1 and CC2 (Bassi et al., 2011). Imaging of these truncations showed localization to the CF was through CC2 whereas CC1 localized to the spindle midzone. Sticky CC1 domain stayed in the central spindle until abscission. CC2 contains an area with a high Rho binding homology (RBH) at its C-terminus which they named CC2b. The amino part of CC2 was thus named CC2a. CC2a was able to pull down Actin and MRLC suggesting a possible localization to the CR via this interaction. However, CC2a was not able to pull down Rho1 suggesting a possible localization to the CR independent of a direct Rho1 interaction. Furthermore, Citron Kinase fails to be recruited to the CR by disrupting Actin filaments using Latruncuilin A (LatA). In this same condition, Rho1 localizes to a partial furrow. Similar results were observed with zipper RNAi (Myosin II RNAi). Together these data indicated that Citron Kinase could localized to the contractile ring via the CC2 and this localization seems to be dependent on actomyosin. On the other hand, CC2b alone was cytoplasmic and unable to pull down any form of WT, active or inactive Rho. However the CNH domain was able to pull down WT, the active and inactive form of Rho (Bassi et al., 2011). This is coherent with what has been reported by Shandala et al. in 2004. Using a yeast two hybrid assay a Rho-Sticky interaction occurs only through the C-terminal region that encompasses the CNH domain and not the putative coiled coil region (Shandala et al., 2004).

Similar conclusions regarding the functions of the CC domain in *Drosophila* Sticky were also reached for human Citron Kinase (Watanabe et al., 2013). The N-terminal region of CC domain was responsible for localization to the spindle midzone microtubules whereas the C-terminal region of CC localized to the CF. Furthermore, Citron Kinase CC domain was sufficient for rescue of the Citron Kinase depletions but the C-terminal end of CC only partially rescued cytokinesis failure. This suggested that the essential role of Citron Kinase in cytokinesis is independent of its kinase, PH or CNH domains. Intriguingly, Citron Kinase has been reported to form aggregates (Eda et al., 2001). These aggregates seem to be dependent on a C-terminal region of CC domain distinct from the one responsible for its localization to the cleavage furrow (Watanabe et al., 2013).

3.10. Binding partners at the central spindle via the Coiled Coil domain

KIF14 was identified as an essential cytokinesis protein shown by formation of binucleate cells following RNAi depletion in HeLa cells (Gruneberg et al., 2006a). Interestingly depletion of KIF14 only affected the localization of Citron Kinase and no other CR or midbody associated protein that was tested (Gruneberg et al., 2006a). Furthermore, immunoprecipitation assays demonstrated that Citron Kinase was found in KIF14 as well as PRC1 precipitates. The reverse experiment failed to show KIF14 and PRC1 being pulled down by Citron Kinase immunoprecipitation. However, a kinase dead mutant of Citron Kinase was unable to pull down KIF14, indicating that the kinase domain is essential for the regulation of this interaction (Gruneberg et al., 2006a). This discovery was followed by increased focus on Citron Kinase's involvement at the central spindle.

These reports were later confirmed by showing that Citron Kinase depletion altered localization of KIF14 and PRC1 (Watanabe et al., 2013). Specifically, KIF14 localization was shown as a double band on the outer region of the midbody instead of a focused midbody localization. As for PRC1, Citron Kinase depletion resulted in a broader localization of PRC1 (Watanabe et al., 2013). These data along with those found in *Drosophila* mutants previously

discussed, indicate a possible role of Citron Kinase in proper midbody formation (Naim et al., 2004; Watanabe et al., 2013).

Studies in *Drosophila* introduced further insight into this interaction between Sticky and KIF14 orthologue Nebbish (Neb) (Bassi et al., 2013). Direct pull downs assay suggest that although Citron Kinase and PRC1 orthologue Fascetto (Feo) are present in the same physical complex, they do not directly interact (Bassi et al., 2013). On the other hand, Sticky was able to pull down the orthologue of MKLP1, Pavarotti (Pav). All these interactions are mediated via the CC1 of the coiled coil domain of Sticky (Bassi et al., 2013). Localization of Pav and Feo at midbody are disturbed upon Sticky depletion, but Neb cannot localize to the midbody in this condition. Interestingly, Neb depletion caused similar mislocalization of Feo and Pav to those observed in Sticky depletion (Bassi et al., 2013). Together these data, clearly identify a major role of Citron Kinase in proper midbody organization through microtubule associated proteins. Importantly, this function seems to be important through an evolutionarily conserved interaction with Neb.

3.11. Citron Kinase interacts with the CPC

With the potential of many Citron Kinase interacting partners, the D'Avino group did a mass spectrometry analysis of a Flag tagged Citron Kinase in HeLa cells to identify the interactome of Cit-K (McKenzie et al., 2016). The assay showed that Cit-K interacts with the chromosomal passenger complex (CPC) components (McKenzie et al., 2016). The authors also demonstrate that Cit-K directly binds the CPC components Aurora B, Borealin and INCENP. Citron Kinase depletion disturbed localization of INCENP and a kinase dead version of Citron Kinase failed to rescue this phenotype. Cit-K phosphorylates INCENP at the site responsible for Aurora B activation. Conversely, Aurora B phosphorylates Cit-K at S699 and this phosphorylation regulates Citron Kinase localization to the central spindle by limiting its accumulation at this site (McKenzie et al., 2016). This is another sign that Cit-K plays a role in maintaining proper midbody formation but how and to what importance this is contributing to cytokinesis remains unclear. Aurora B has been shown to be a critical player in abscission whereby maintaining an active Aurora B could lead to delay in abscission (Steigemann and

Gerlich, 2009). This offers a potential explanation to the Cit-K overexpression delayed abscissions. Indeed, if Cit-K overexpression would increase the activation state of Aurora B, this should lead to delayed abscission. Assuming that this function is conserved in *Drosophila*, because lack of Sticky would lead to an inactive Aurora B that could accelerate the cytokinesis process and this would in turn explain why sticky depletion leads to either failed cytokinesis or early abscission events at a similar timing as previously documented (El-Amine et al., 2013; McKenzie et al., 2016).

3.12. TUBB3 a critical downstream target of Citron Kinase

A recent discovery by the Di Cunto group could be the most significant finding so far concerning the specific role of Cit-K in cytokinesis (Sgro et al., 2016). The authors demonstrate the importance of a beta-Tubulin isoform TUBB3 in the mechanism of action of Citron Kinase. This was the first study that showed data of full Cit-K RNAi rescue by another protein which could be a great indication of the direct functional role of such a protein. The data suggest that the roles of Cit-K in cytokinesis are mainly through modulation of midbody microtubule stability. Low doses of nocodazole to partially destabilize microtubules were able to rescue abscission delays induced by Cit-K overexpression. More importantly, Cit-K RNAi caused cytokinesis failures that could be rescued by stabilizing microtubules using paclitaxel. Moreover, the authors identified TUBB3 as the indirect downstream effector of Cit-K responsible for the stabilization of midbody microtubules at the MR. Indeed, co-depletion of TUBB3 rescued for Cit-K depletion induced cytokinesis failures and midbody microtubule instability. To do so, Citron Kinase seems to play an important but indirect role in phosphorylation of S444 of TUBB3 which is crucial for the specific role of TUBB3 in midbody microtubule stabilization. Finally, TUBB3 is known to be phosphorylated at S444 through a kinase called CK2a. Depletion of CK2a caused cytokinesis failures that could be rescued by expressing a phosphomimetic form of TUBB3 which suggests that the only essential role of CK2a is its phosphorylation of this site. The authors propose a model whereby the role of Cit-K in microtubule stability is through maintaining CK2a at the midbody, a protein that they confirmed is present in the same physical complex as Cit-K. It is worth noting that this role of

Cit-K seems to be independent of its relationship with KIF14 since KIF14 depletion did not change the state of microtubules at the midbody (Sgro et al., 2016).

3.13. Is the kinase domain required for cytokinesis?

This question has generated conflicting results and it is difficult to make a decisive conclusion. In HeLa cells, expression of the Citron kinase coiled coil domain (i.e. lacking the kinase domain and C-terminus) was sufficient to rescue cytokinesis in Citron Kinase depleted cells (Watanabe et al., 2013). *Drosophila* S2 cells co-expressing Anillin-GFP and a kinase dead (KD) Sticky mutant largely succeeded cytokinesis even when endogenous Sticky was depleted (El-Amine et al., 2013). Cells imaged live in the same field of view that lacked expression of Sticky KD either failed cytokinesis or underwent abscission in an abnormally fast manner, similar to that observed in cells depleted of all sources of Sticky (El-Amine et al., 2013). A similar experiment also in S2 cells was reported by a Bassi et al. in 2011, who claimed that the KD mutant only partially rescues cytokinesis in Sticky depleted cells, suggesting that the kinase function is important (Bassi et al., 2011). In the human models, one study in HeLa cells has shown that a mutant bearing only the CC domain and thus lacking the kinase domain can fully rescue cytokinesis. Finally, neuronal progenitor cells (NPC) derived from patients with mutations in Citron Kinase that affect the kinase activity, failed cytokinesis in about 25% of the cells and delayed abscission in the rest (Li et al., 2016). Perhaps this study is well suited for interpreting the essential role of the kinase domain because their expression system of an endogenous biallelic mutant cannot have variations in expression levels due to exogenous expression of a mutant. Nonetheless, because this is a homogenous cell line lacking Citron Kinase how can we explain that cytokinesis is failing in only this percentage of cells? As no full rescue of a KD mutant has been demonstrated in any system and biallelic KD mutant is responsible for only 25% of failures, perhaps the best conclusion is that the kinase domain cannot be the only essential role of Sticky in cytokinesis. This is supported by the authors of the NPC study who claim that in another publication of patients that had a stop codon mutations in the Kinase domain, the patient had more severe phenotypes then the ones in their study (Harding et al., 2016)

3.14. Citron Kinase in abscission: to stop or go?

As previously mentioned the NPC study showed that 75% of cells that didn't fail cytokinesis, delayed abscission (Li et al., 2016). This adds a level of complexity in our understanding of Citron Kinase because it is contradicting with the current literature. This phenotype has been observed with Citron Kinase overexpression studies and not loss of function (Gai et al., 2011; Sgro et al., 2016). However, from the NPC study, the phenotypes observed were rescued by CRISPR gene editing indicating that these phenotypes are directly due to the mutant and not any other patient specific differences (Li et al., 2016). In *Drosophila,* we have demonstrated that Sticky depletion could lead to either cytokinesis failures or quick abscission that occurs at a similar timing then those failures. Our Sticky KD experiments also show that rescued cells did not delay abscission (El-Amine et al., 2013). Furthermore, Sgro et al. show that Citron Kinase's essential actions in cytokinesis come from stabilizing the midbody which is coherent with many other results (Bassi et al., 2013; Naim et al., 2004; Sgro et al., 2016; Watanabe et al., 2013). Therefore, any essential loss of function results would presumably destabilize the MR and would not lead to an abscission delay. Finally, abscission delays were rescued by stabilizing microtubules at the central spindle with nocodazole (Sgro et al., 2016). All indications that Citron Kinase abscission delays with loss of function could occur through a midbody stabilization process. This suggests that the Citron Kinase role in cytokinesis of NPC is operating through a much different mechanism than previously reported. It would be interesting to test out whether nocodazole can rescue these abscission delays in NPC derived from those patients with a biallelic mutation of Citron Kinase.

3.15. The lost and found

For brevity, only some of the key Citron kinase interactions and findings are described above. However, we have generated two tables that provide comprehensive, chronological summaries of all reported Cit-K phenotypes and interacting partners in cytokinesis of mammals (Table I) and *Drosophila melanogaster* (Table II). It is hoped that these will serve as a useful guide to help redirect the reader to the original articles

Tableau I. Citron Kinase interacting partners in cytokinesis.

Protein	Method	Region	Notes /Claims	Reference
Rac	Yeast two hybrid / Overlay assay	1167-1345	This was not tested for Citron Kinase but only for Citron-N isoform	(Madaule et al., 1995)
RhoA	Yeast two hybrid / Overlay assay	1167-1345	This was not tested for Citron Kinase but only for Citron-N isoform	(Madaule et al., 1995)
Histone H1	Kinase assay	Kinase	Increase kinase activity with Cit-K against Histone H1.	(Cunto et al., 1998)
RhoA	C3 exoenzyme	N/A	Potential indication of Rho acting upstream of Cit-K	(Eda et al., 2001)
MRLC	Kinase assay	N/A	Kinase assay shows Citron Kinase phosphorylated MRLC at Ser19 and but preferentially at both Ser-19 Thr18.	(Yamashiro et al., 2003)
Myosin Binding Subunit (MBS)	Kinase assay **NO INTERACTION**	N/A	Cit-K FAILED to phosphorylate MBS indicating that it does not inhibit Myosin Phosphatase contrary to ROCK	(Yamashiro et al., 2003)
KIF14	RNAi /IP	N/A	Only Citron Kinase localization to the MR is affected by KIF14 RNAi. Citron Kinase was found in KIF14 IPs and vice-versa. This interaction is enhanced with KD Cit-K	(Gruneberg et al., 2006b)
PRC1	IP	N/A	Citron Kinase was found in PRC1 Immuno Precipitates	(Gruneberg et al., 2006b)
Myosin	RNAi – Rescue **NO INTERACTION**	N/A	Interaction denied upon phosphomimetic MRLC failing to rescue Citron Kinase depletion	(Dean and Spudich, 2006)
Ect2	RNAi	N/A	Cit-K failed to localize to the contractile ring when Ect2 was depleted.	(Gruneberg et al., 2006b)
ASPM	IP	N/A	ASPM was found in Citron Kinase precipitates of rat brains	(Paramasivam et al., 2007)
RanBPM	Yeast two hybrid	N/A	RanBPM RNAi alters Cit-K asymmetric localization in metaphase of neuronal precursors. RanBPM RNAi cells accumulation in mitosis is nullified in absence of a function Cit-K	(Chang et al., 2010)
Disc Large 5 (Dlg5)	IP	PDZ	Dlg5 RNAi alters Cit-K asymmetric localization in metaphase of neuronal precursors.	(Chang et al., 2010)
Anillin	RNAi/overexpression	N/A	Cit-K RNAi cells alter Anillin localization in early cytokinesis and fails to maintain it at the MR. Cit-K overexpression alters Anillin localization during cytokinesis	(Gai et al., 2011)
RhoA	RNAi/overexpression	N/A	Cit-K RNAi cells alter RhoA localization in early cytokinesis and fails to maintain it at the MR. Cit-K overexpression alters RhoA localization during cytokinesis	(Gai et al., 2011)
RhoA/Anillin	C3 exoenzyme **NO INTERACTION**	N/A	RhoA does not alter localization of Cit-K in late cytokinesis even though it does so for anillin. This indicates that Cit-K is maintained at the MR independently of Anillin and RhoA	(Gai et al., 2011)
Anillin	Pull down	RBD-3'	The N-term of Anillin (5'-ActBD) interacts with an extensive region of Sticky from RBD onwards.	(Gai et al., 2011)

p27	Pull down	HR1	The HR1 domain of Cit-K interacts with the C-terminal region of p27. p27 overexpression cytokinesis failures are inhibited by Cit-K HR1 overexpression.	(Serres et al., 2012)
RhoA	Pull down	RBD	Expression of p27 greatly affected HR1-RBD but not RBD interaction.	(Serres et al., 2012)
p27	Overexpression / Structure-Function	HR1	p27 phosphomutant failed to interact with Cit-K and did not cause multinucleation. p27 phosphomimetic which interacts with Cit-K caused multinucleation.	(Serres et al., 2012)
Anillin	RNAi	N/A	Cit-K RNAi cells fail to maintain Anillin at the MR.	(Watanabe et al., 2013)
Septin 6	RNAi	N/A	Cit-K RNAi cells fail to maintain Septin 6 at the MR.	(Watanabe et al., 2013)
Septin 7	RNAi	N/A	Cit-K RNAi cells fail to maintain Septin 7 at the MR.	(Watanabe et al., 2013)
PRC1	RNAi	N/A	Cit-K RNAi cells alters localization of PRC1 at the midbody.	(Watanabe et al., 2013)
KIF14	RNAi	N/A	Cit-K RNAi cells alters localization of KIF14 at the midbody. KIF14 only affects the maintenance of Cit-K at later stages of cytokinesis	(Watanabe et al., 2013)
Tubulin	RNAi	N/A	Cit-K alters intracellular bridge morphology	(Watanabe et al., 2013)
KIF14	Direct binding / Rescue	429-835	Coiled Coil region 429-835 directly binds KIF14. A Cit-K lacking this area fails to rescue Cit-K RNAi cytokinesis failures.	(Watanabe et al., 2013)
MKLP1	Pull down / RNAi	Coil Coiled	Cit-K coiled coil region corresponding to 463-783 pulled down MKLP1. MKLP1 abnormally localized to the midbody in Cit-K RNAi	(Bassi et al., 2013)
PRC1	RNAi	N/A	PRC1 abnormally localized to the midbody in Cit-K RNAi	(Bassi et al., 2013)
Two Pore Channel 1 (TCP1)	Mass Spectrometry / IP	N/A	TCP1 caused multinucleation. Cit-K was identified as an interacting partner by MS suggesting a possible pathway for TCP1 in involvement cytokinesis	(Horton et al., 2015)
a-Tubulin	RNAi / Nocodazole /Paclitaxel	N/A	Cit-K RNAi reduces microtubule stability leading to higher turnover of tubulin at the midbody. Paclitaxel reduced Cit-K RNAi failures. Nocodazole decreased Cit-K over expression abscission delays.	(Sgro et al., 2016)
TUBB3	RNAi/overexpression / IP	N/A	TUBB3 overexpression increases Cit-K RNAi failures. TUBB3 RNAi decreases them. TUBB3 RNAi also rescues the increase of dynamic tubulin induced by Cit-K RNAi. Reciprocal co-IP of TUBB3 and Cit-K.	(Sgro et al., 2016)
TUBB3	2D gel / Kinase assay	N/A	Cit-K RNAi doesn't alter TUBB3 levels. Cit-K promotes phosphorylation of TUBB3 at S444. This an indirect effect.	(Sgro et al., 2016)
CK2a	IP	N-term	CK2a but not GRK2 is co-IP with Cit-K. Cit-K RNAi inhibits CK2a localization to the midbody. The only essential role of CK2a in cytokinesis is to phosphorylate TUBB3 at S444	(Sgro et al., 2016)
Aurora B	Pull down / Direct binding / RNAi / ZM447439 treatment	See data	Aurora B was detected in Cit-K pull-down assay. Multiple domains of Cit-K were able to directly bind Aurora B. Cit-K RNAi altered localization of Aurora B at the midbody. Cit-K RNAi reduces total phosphorylated Aurora B at the midbody. Aurora B drug inhibition altered Cit-K localization.	(McKenzie et al., 2016)

KIF14	Pull down	N/A	Aurora B was detected in Cit-K pull-down assay	(McKenzie et al., 2016)
KIF23	Pull down / RNAi	N/A	Aurora B was detected in Cit-K pull-down assay. Cit-K RNAi altered localization of KIF23 at the midbody	(McKenzie et al., 2016)
KIF20A	Pull down / RNAi	N/A	Aurora B was detected in Cit-K pull-down assay. Cit-K RNAi altered KIF20A localization at the midbody.	(McKenzie et al., 2016)
Borealin	Direct binding	See data	Multiple domains of Cit-K were able to directly bind Borealin	(McKenzie et al., 2016)
INCENP	Direct binding / RNAi / Phosphorylation assay	See data	Multiple domains of Cit-K were able to directly bind INCENP. Cit-K RNAi altered INCENP localization at the midbody and reduced its phosphorylation state. KD Cit-K failed to rescue normal localization of INCENP in Cit-K depleted cells. Cit-K phosphorylates INCENP.	(McKenzie et al., 2016)
Aurora B	Phosphorylation assay	S699 / 1385-1387	Aurora B phosphorylates Cit-K at its S699 residue and this phosphorylation alters interaction between Cit-K and CPC which in turn limits the amount of Cit-K at the midbody.	(McKenzie et al., 2016)
EphB2	Pull down / RNAi	N/A	EphB2 tagged lysate pulled down Cit-K. EphB2 RNAi alters Cit-K localization.	(McKenzie et al., 2016)
Src	Kinase assay	Y1237 / Y1246	Src phosphorylated Cit-K at Y1237 and Y1246 of the RBD domain	(McKenzie et al., 2016)
ASPM	IP / RNAi / overexpression	See data	Multiple fragments of Cit-K could be found in ASPM precipitates. ASPM RNAi reduces localization of Cit-K to centrosomes. Cit-K overexpression rescues spindle orientation changes and total number of astral microtubule decreased by ASPM RNAi.	(Gai and Di Cunto, 2016)
Tubulin	RNAi / overexpression	N/A	Cit-K RNAi alters orientation of the mitotic spindle. Cit-K RNAi reduces number, length, stability and nucleation of astral microtubules.	(Gai and Di Cunto, 2016)

Tableau II. Sticky interacting partners in cytokinesis

Protein	Method	Region	Notes /Claims	Reference
RhoA	Genetic interaction in analysis of ommatidia	N/A	Rho enhanced Sticky mutant or RNAi phenotypes	(D'Avino et al., 2004)
Rac	Genetic interaction in analysis of ommatidia	N/A	Rac suppressed Sticky mutant or RNAi phenotypes	(D'Avino et al., 2004)
Anillin	Sticky RNAi	N/A	Extended Anillin signal and membrane protrusion at the membrane site	(Naim et al., 2004)
Tubulin	Sticky RNAi	N/A	Intracellular bridge does not display a dark band in the middle	(Naim et al., 2004)
Tubulin	Sticky RNAi	N/A	Sticky depletion destabilized intracellular bridge	(Echard et al., 2004)
Pebble (RhoGEF/Ect2)	Pebble mutant	N/A	Sticky fails to localize to the CR in Pbl mutant background	(Shandala et al., 2004)

RhoA	Yeast two hybrid	1439-1854	Data not shown. Interaction between domain and RhoA-G14V	(Shandala et al., 2004)
Argonaute 1 (Ago1)	Genetic interaction in analysis of ommatidia	N/A	Sticky mutant dominantly suppresses Ago1 overexpression phenotype / Ago mutant enhances sticky mutant phenotype	(Sweeney et al., 2008)
HP1	Temperature sensitive Sticky mutant	N/A	Sticky mutants altered localization of HP1 in the nuclei to chromocenters. These Sticky mutants also diminished methylation of histone H3K-K9. This effect seems to be cytokinesis independent	(Sweeney et al., 2008)
Fragile-X mental retardation-1 (dFmr1)	Genetic interaction in analysis of ommatidia	N/A	Sticky mutant dominantly suppresses dFmr1 overexpression phenotype / dFmr1 mutant enhances sticky mutant phenotype	(Bauer et al., 2008)
Rho1	RNAi	N/A	Sticky fails to localize to the CR in Rho1 RNAi. Rho1 localizes normally in CF but not MR in Sitcky RNAi.	(Bassi et al., 2011)
Zipper (Myosin II)	RNAi / Pull down	774-1227	Sticky fails to localize to the CR in Zipper RNAi. Coiled Coil region 774-1227 pulls down Sqh	(Bassi et al., 2011)
Actin	RNAi / Pull down	774-1227	Sticky fails to localize to the CR in LatA (actin polymerization inhibitor. Coiled Coil region 774-1227 pulls down actin	(Bassi et al., 2011)
Rho1	Pull down	1437-1854	Sticky Coiled Coil region 774-1227 and 1150-1331 failed to pull down Rho1 but CNH domain did.	(Bassi et al., 2011)
Sqh	RNAi	N/A	Sticky depletion altered Sqh mono and dephosphorylated ratios only in late cytokinesis	(Bassi et al., 2011)
N/A	RNAi	Kinase	Sticky-KD only partially rescues Sticky RNAi cytokinesis failures.	(Bassi et al., 2011)
Nebbish, Neb (KIF14)	Mass Spectrometry / Pull down / Direct Binding	463-783	Sticky pulled down Neb. Neb depletion prevented Sticky 463-783 from localization to the midzone. Neb can interact with Feo.	(Bassi et al., 2013)
Pavarotti, Pav (MKLP1)	Mass Spectrometry / Pull down / Direct Binding	463-783	Sticky pulled down Pav. The Pac and Neb regions that bind to 463-783 do not compete for Sticky binding. Pav can interact with Feo.	(Bassi et al., 2013)
Fascetto, Feo (PRC1)	Pull down **NO INTERACTION**	463-783	Sticky failed to pull down Feo. However the Feo interactions with Neb and Pav indicates that Sticky and Feo are in the same physical complex.	(Bassi et al., 2013)
Neb	RNAi	N/A	Neb failed to localize to the midbody in early and late cytokinesis in Sticky RNAi	(Bassi et al., 2013)
Pav	RNAi	N/A	Pav abnormally localized to the midbody in Sti RNAi	(Bassi et al., 2013)
Feo	RNAi	N/A	Feo abnormally localized to the midbody in Sti RNAi	(Bassi et al., 2013)
Anillin	RNAi	N/A	Sticky RNAi increased Anillin extrusion from the MR. Sticky RNAi on Anillin N-term expressing cells fail to form a stable furrow or MR structures.	(El-Amine et al., 2013)
Peanut	RNAi	N/A	Codepletion of Sticky and Peanut leads to CF destabilization though actions on Anillin N-term and C-term respectively. Peanut was present in Sticky RNAi enriched extrusions	(El-Amine et al., 2013)
Actin	RNAi	N/A	Actin was present in Sticky RNAi enriched extrusions	(El-Amine et al., 2013)

Rho1	RNAi	N/A	Rho1 was present in Sticky RNAi enriched extrusions	(El-Amine et al., 2013)
N/A	RNAi	Kinase	Sticky-KD only failed to rescues Sticky RNAi cytokinesis failures.	(El-Amine et al., 2013)

3.16. Discussion

A growing interest in the role of Citron Kinase in cytokinesis has uncovered much needed information about its implication in this process. First, we now understand that Citron Kinase localizes to the CR and MR through a portion of its coiled coil domain (Bassi et al., 2011). Citron is not just a passenger at membrane and cortex level, it can associate with proteins such as Anillin but more importantly its presence modulates the maturation process of the MR by limiting the gradual elimination of such cortical proteins (El-Amine et al., 2013; Gai et al., 2011).

Second, Citron Kinase is also capable of interacting with the midbody and directly binding many microtubules associated proteins such as KIF14, INCENP, Borealin and Aurora B (Bassi et al., 2013; Watanabe et al., 2013). These interactions must link it indirectly to other microtubule associated proteins such as PRC1. Once again, Citron Kinase's presence at the midbody is not passive since it is critical for proper midbody organization. Functionally, Citron Kinase is also capable of phosphorylating INCENP (McKenzie et al., 2016). In turn, reducing this phosphorylation by depleting Citron Kinase results in a decreased Aurora B activation state (McKenzie et al., 2016). It would be reasonable to think that this finding can explain the impact of Citron Kinase on abscission timing, which is known to be regulated by Aurora B. Another downstream target of Citron Kinase would be TUBB3 (Sgro et al., 2016). Modulation of the phosphorylation state of TUBB3 seems to rescue the essential role of Citron Kinase in cytokinesis (Sgro et al., 2016). Citron Kinase is important for microtubule stabilization at the intracellular bridge (Sgro et al., 2016). Perhaps a redundant role on this phosphorylation of TUBB3 can explain how Citron Kinase is essential for cytokinesis in a tissue specific manner (Cunto et al., 2000). If there is a redundant mechanism of TUBB3 regulation that is only active in certain cell types, then loss of Citron Kinase could be rescued by these mechanisms.

Citron Kinase localizes to the CR and MR but can also interact with microtubule associated proteins. We have shown that Sticky plays an essential role in a mechanism of retention of cortical proteins at the MR that guide the ring for a correct maturation process required for abscission. On the other hand, most essential roles of Citron Kinase are pointing towards a stronger implication at the midbody. Independent of the kinase domain having a partial of fully important role in cytokinesis, the only known kinase target would be Aurora B which ultimately seems to be important for a Citron Kinase role at the midbody. Furthermore, Citron Kinase seems to play an important role in modulating midbody stability through TUBB3. Together this raises the question of how Citron Kinase influences cytokinesis from cortex to central spindle. Perhaps one indication is that the TUBB3 mechanism does not involve KIF14, a well-established microtubule associated protein target of Citron Kinase (Bassi et al., 2013; Gruneberg et al., 2006a; Watanabe et al., 2013). In addition, data in HeLa cells demonstrate that C-term CC domain of Citron Kinase (responsible for cortical localization) but not N-term CC (responsible for midbody localization) can rescue cytokinesis upon Citron Kinase depletion (Watanabe et al., 2013). This suggests that scaffolding roles of Citron Kinase at the cortex may be more important for cytokinesis than scaffolding roles at the midbody. Moreover, the CPC components have a stronger interaction with Citron Kinase through the C-terminal portion of the CC domain rather than the N-terminal portion (McKenzie et al., 2016). However, this does not exclude the possibility that in a cellular context, Citron Kinase may rely on the N-terminal portion of its CC domain to localize to the midbody in order to interact with the CPC which would perhaps explain how could the C-terminal CC domain rescue cytokinesis (Watanabe et al., 2013). Together all these cues offer circumstantial evidence that the cortical localization of Citron Kinase plays a major role in cytokinesis and is potentially important for its role at the microtubule-based midbody also.

3.17. Concluding remarks

The story of Citron Kinase has been a bumpy ride and it does not look like the path is still very clear. On the positive side the important advances on the molecular level are starting to give us greater understanding of its impact *in vivo* development. The findings on microtubule

stability at the midbody proposes some models into how it can be selectively essential for cytokinesis *in vivo* (Cunto et al., 2000; Sgro et al., 2016). More importantly, the undeniable importance on neuronal development of Citron Kinase in human is now very well documented (Harding et al., 2016; Li et al., 2016). This major impact is likely originating from its role in cytokinesis but our understanding of this role in those developmental conditions is still limited. Even though the debate of direct relationship between the kinase domain and cytokinesis is not over, the impact of kinase mutations in humans is undeniably important for cytokinesis and neuronal development. This highlights the importance of ongoing efforts towards understanding the roles of Citron Kinase at the molecular level and in a variety of model systems and cell types.

3.18. References

Bassi, Z. I., M. Audusseau, M. G. Riparbelli, G. Callaini and P. P. D'Avino (2013). "Citron Kinase controls a molecular network required for midbody formation in cytokinesis." Proc Natl Acad Sci U S A **110**(24): 9782-9787.

Bassi, Z. I., K. J. Verbrugghe, L. Capalbo, S. Gregory, E. Montembault, D. M. Glover and P. D'Avino (2011). "Sticky/Citron Kinase maintains proper RhoA localization at the cleavage site during cytokinesis." The Journal of Cell Biology **195**(4): 595-603.

Bauer, C. R., A. M. Epstein, S. J. Sweeney, D. C. Zarnescu and G. Bosco (2008). "Genetic and systems level analysis of Drosophila sticky/Citron Kinase and dFmr1 mutants reveals common regulation of genetic networks." BMC Syst Biol **2**: 101.

Chang, Y., O. Klezovitch, R. S. Walikonis, V. Vasioukhin and J. J. LoTurco (2010). "Discs large 5 is required for polarization of Citron Kinase in mitotic neural precursors." Cell Cycle **9**(10): 1990-1997.

Cunto, D. F., E. Calautti, J. Hsiao, L. Ong, G. Topley, E. Turco and G. P. Dotto (1998). "Citron rho-interacting kinase, a novel tissue-specific ser/thr kinase encompassing the Rho-Rac-binding protein Citron." The Journal of biological chemistry **273**(45): 29706-29711.

Cunto, F., S. Imarisio, P. Camera, C. Boitani, F. Altruda and L. Silengo (2002). "Essential role of Citron Kinase in cytokinesis of spermatogenic precursors." Journal of Cell Science **115**(24): 4819-4826.

Cunto, F., S. Imarisio, E. Hirsch, V. Broccoli, A. Bulfone, A. Migheli, C. Atzori, E. Turco, R. Triolo, G. Dotto, L. Silengo and F. Altruda (2000). "Defective Neurogenesis in Citron Kinase Knockout Mice by Altered Cytokinesis and Massive Apoptosis." Neuron **28**(1): 115-127.

D'Avino, P., M. S. Savoian and D. M. Glover (2004). "Mutations in sticky lead to defective organization of the contractile ring during cytokinesis and are enhanced by Rho and suppressed by Rac." The Journal of Cell Biology **166**(1): 61-71.

Dean, S. O. and J. A. Spudich (2006). "Rho kinase's role in myosin recruitment to the equatorial cortex of mitotic Drosophila S2 cells is for myosin regulatory light chain phosphorylation." PLoS One **1**: e131.

Echard, A., G. R. X. Hickson, E. Foley and P. H. O'Farrell (2004). "Terminal cytokinesis events uncovered after an RNAi screen." Current biology : CB **14**(18): 1685-1693.

Eda, M., S. Yonemura, T. Kato, N. Watanabe, T. Ishizaki, P. Madaule and S. Narumiya (2001). "Rho-dependent transfer of Citron-kinase to the cleavage furrow of dividing cells." Journal of cell science **114**(Pt 18): 3273-3284.

El-Amine, N., A. Kechad, S. Jananji and G. Hickson (2013). "Opposing actions of septins and Sticky on Anillin promote the transition from contractile to midbody ring." The Journal of Cell Biology **203**(3): 487-504.

Gai, M., P. Camera, A. Dema, F. Bianchi, G. Berto, E. Scarpa, G. Germena and F. Cunto (2011). "Citron Kinase controls abscission through RhoA and anillin." Molecular biology of the cell **22**(20): 3768-3778.

Gai, M. and F. Di Cunto (2016). "Citron Kinase in spindle orientation and primary microcephaly." Cell Cycle: 1-2.

Gruneberg, U., R. Neef, X. Li, E. Chan, R. B. Chalamalasetty, E. A. Nigg and F. A. Barr (2006). "KIF14 and Citron Kinase act together to promote efficient cytokinesis." The Journal of Cell Biology **172**(3): 363-372.

Gruneberg, U., R. Neef, X. Li, E. H. Chan, R. B. Chalamalasetty, E. A. Nigg and F. A. Barr (2006). "KIF14 and Citron Kinase act together to promote efficient cytokinesis." J Cell Biol **172**(3): 363-372.

Harding, B. N., A. Moccia, S. Drunat, O. Soukarieh, H. Tubeuf, L. S. Chitty, A. Verloes, P. Gressens, V. El Ghouzzi, S. Joriot, F. Di Cunto, A. Martins, S. Passemard and S. L. Bielas (2016). "Mutations in Citron Kinase Cause Recessive Microlissencephaly with Multinucleated Neurons." Am J Hum Genet **99**(2): 511-520.

Horton, J. S., C. T. Wakano, M. Speck and A. J. Stokes (2015). "Two-pore channel 1 interacts with Citron Kinase, regulating completion of cytokinesis." Channels (Austin) **9**(1): 21-29.

Kechad, A., S. Jananji, Y. Ruella and G. R. Hickson (2012). "Anillin acts as a bifunctional linker coordinating midbody ring biogenesis during cytokinesis." Curr Biol **22**(3): 197-203.

Li, H., S. L. Bielas, M. S. Zaki, S. Ismail, D. Farfara, K. Um, R. O. Rosti, E. C. Scott, S. Tu, N. C. Chi, S. Gabriel, E. Z. Erson-Omay, A. G. Ercan-Sencicek, K. Yasuno, A. O. Caglayan, H. Kaymakcalan, B. Ekici, K. Bilguvar, M. Gunel and J. G. Gleeson (2016). "Biallelic Mutations in Citron Kinase Link Mitotic Cytokinesis to Human Primary Microcephaly." Am J Hum Genet **99**(2): 501-510.

Liu, H., F. Di Cunto, S. Imarisio and L. M. Reid (2003). "Citron Kinase is a cell cycle-dependent, nuclear protein required for G2/M transition of hepatocytes." J Biol Chem **278**(4): 2541-2548.

Madaule, P., M. Eda, N. Watanabe, K. Fujisawa, T. Matsuoka, H. Bito, T. Ishizaki and S. Narumiya (1998). "Role of Citron Kinase as a target of the small GTPase Rho in cytokinesis." Nature **394**(6692): 491-494.

Madaule, P., T. Furuyashiki, T. Reid, T. Ishizaki, G. Watanabe, N. Morii and S. Narumiya (1995). "A novel partner for the GTP-bound forms of rho and rac." FEBS letters **377**(2): 243-248.

Matsumura, F. (2005). "Regulation of myosin II during cytokinesis in higher eukaryotes." Trends in Cell Biology **15**(7): 371-377.

McKenzie, C., Z. I. Bassi, J. Debski, M. Gottardo, G. Callaini, M. Dadlez and P. P. D'Avino (2016). "Cross-regulation between Aurora B and Citron Kinase controls midbody architecture in cytokinesis." Open Biol **6**(3).

Mullins, J. M. and J. J. Biesele (1973). "Cytokinetic activities in a human cell line: the midbody and intercellular bridge." Tissue Cell **5**(1): 47-61.

Naim, V., S. Imarisio, F. Di Cunto, M. Gatti and S. Bonaccorsi (2004). "Drosophila Citron Kinase is required for the final steps of cytokinesis." Mol Biol Cell **15**(11): 5053-5063.

Paramasivam, M., Y. J. Chang and J. J. LoTurco (2007). "ASPM and Citron Kinase co-localize to the midbody ring during cytokinesis." Cell Cycle **6**(13): 1605-1612.

Piekny, A. J. and M. Glotzer (2008). "Anillin is a scaffold protein that links RhoA, Actin, and myosin during cytokinesis." Curr Biol **18**(1): 30-36.

Sedzinski, J., M. Biro, A. Oswald, J.-Y. Tinevez, G. Salbreux and E. Paluch (2011). "Polar actomyosin contractility destabilizes the position of the cytokinetic furrow." Nature **476**(7361): 462-466.

Serres, M. P., U. Kossatz, Y. Chi, J. M. Roberts, N. P. Malek and A. Besson (2012). "p27(Kip1) controls cytokinesis via the regulation of Citron Kinase activation." J Clin Invest **122**(3): 844-858.

Sgro, F., F. T. Bianchi, M. Falcone, G. Pallavicini, M. Gai, A. M. Chiotto, G. E. Berto, E. Turco, Y. J. Chang, W. B. Huttner and F. Di Cunto (2016). "Tissue-specific control of midbody microtubule stability by Citron Kinase through modulation of TUBB3 phosphorylation." Cell Death Differ **23**(5): 801-813.

Shandala, T., S. L. Gregory, H. E. Dalton, M. Smallhorn and R. Saint (2004). "Citron Kinase is an essential effector of the Pbl-activated Rho signalling pathway in Drosophila melanogaster." Development **131**(20): 5053-5063.

Steigemann, P. and D. W. Gerlich (2009). "Cytokinetic abscission: cellular dynamics at the midbody." Trends in Cell Biology **19**(11): 606-616.

Sweeney, S. J., P. Campbell and G. Bosco (2008). "Drosophila sticky/Citron Kinase is a regulator of cell-cycle progression, genetically interacts with Argonaute 1 and modulates epigenetic gene silencing." Genetics **178**(3): 1311-1325.

Watanabe, S., T. De Zan, T. Ishizaki and S. Narumiya (2013). "Citron Kinase mediates transition from constriction to abscission through its coiled-coil domain." J Cell Sci **126**(Pt 8): 1773-1784.

Yamashiro, S., G. Totsukawa, Y. Yamakita, Y. Sasaki, P. Madaule, T. Ishizaki, S. Narumiya and F. Matsumura (2003). "Citron Kinase, a Rho-dependent kinase, induces di-phosphorylation of regulatory light chain of myosin II." Mol Biol Cell **14**(5): 1745-1756.

Zhao, W.-m. and G. Fang (2005). "Anillin Is a Substrate of Anaphase-promoting Complex/Cyclosome (APC/C) That Controls Spatial Contractility of myosin during Late Cytokinesis." Journal of Biological Chemistry **280**(39): 33516-33524.

4. Opposing actions of septins and Sticky on Anillin promote the transition from contractile to midbody ring

Nour El Amine[1, 2], Amel Kechad[1, 2], Silvana Jananji[1] and Gilles R.X. Hickson[1, 2]

1 Centre de Cancérologie Charles Bruneau, Centre Hospitalier Universitaire Sainte-Justine Centre de Recherche, Montréal, Québec H3T 1C5, Canada

2 Département de Pathologie et Biologie Cellulaire, Université de Montréal, Montréal, Québec H3C 3J7, Canada

Corresponding author: gilles.hickson@umontreal.ca

Manuscript #: 201305053, August 28th 2013

Contributions :

NE et GH ont conçu le projet

NE et GH ont rédigé l'article.

Les expériences ont été effectués par :

NE dans Fig. 1, 2, 6, 7, 8, S2, S3, S4, S5

GH dans Fig. 3, 9, S1

AK dans Fig. 4, 5, S1

SJ dans la génération de certains vecteurs utilisés dans l'article

4.1. Abstract

During cytokinesis, closure of the actomyosin contractile ring (CR) is coupled to the formation of a midbody ring (MR), through poorly understood mechanisms. Using time-lapse microscopy of *Drosophila melanogaster* S2 cells, we show that the transition from the CR to the MR proceeds via a previously uncharacterized maturation process that requires opposing mechanisms of removal and retention of the scaffold protein Anillin. The septin cytoskeleton acts on the C terminus of Anillin to locally trim away excess membrane from the late CR/nascent MR via internalization, extrusion, and shedding, whereas the citron kinase Sticky acts on the N terminus of Anillin to retain it at the mature MR. Simultaneous depletion of septins and Sticky not only disrupted MR formation but also caused earlier CR oscillations, uncovering redundant mechanisms of CR stability that can partly explain the essential role of Anillin in this process. Our findings highlight the relatedness of the CR and MR and suggest that membrane removal is coordinated with CR disassembly.

4.2. Introduction

During cytokinesis of animal cells, an actomyosin-based contractile ring (CR) forms and drives the ingression of a cleavage furrow that bisects the cell at the midpoint of the microtubule-based spindle (Glotzer, 2005; Eggert et al., 2006; Barr and Gruneberg, 2007; Pollard, 2010; Green et al., 2012). The CR is a dynamic, membrane-bound structure that requires continuous Rho-dependent signaling (Bement et al., 2005) and contains many cytoskeletal proteins, including actin, myosin II, Anillin, septins, and their regulators. CR closure occurs via disassembly and proceeds until reaching a diameter of 1–2 μm (Schroeder, 1972; Carvalho et al., 2009). The CR then transforms itself into the midbody ring (MR), a long-lived, dense structure that forms around the center of the midbody as it matures from the antiparallel midzone microtubules that become compacted during CR closure (Mullins and Biesele, 1977; Hu et al., 2012). The MR is essential for cementing the efforts of the CR and for specifying where, and presumably when, abscission ultimately occurs (Steigemann and Gerlich, 2009; Green et al., 2012).

Our previous work showed that the transition from the CR to the MR requires the scaffold protein Anillin (Kechad et al., 2012). Anillin-depleted CRs are unstable and oscillate back and forth across the equator (Straight et al., 2005; Zhao and Fang, 2005; Hickson and O'Farrell, 2008b; Piekny and Glotzer, 2008; Goldbach et al., 2010), but even CRs that do not oscillate fail to close completely and fail to form a stable MR (Kechad et al., 2012). Anillin can bind many other cytokinesis proteins, including F-actin (Field and Alberts, 1995), myosin (Straight et al., 2005), septins (Oegema et al., 2000; Field et al., 2005; Liu et al., 2012), and RacGAP50c (D'Avino et al., 2008; Gregory et al., 2008), among others (Hickson and O'Farrell, 2008a; D'Avino, 2009; Piekny and Maddox, 2010). It remains unclear how Anillin acts to dampen the inherent instabilities of cleavage furrows (Dorn and Maddox, 2011; Sedzinski et al., 2011), and how it subsequently guides MR formation after CR closure.

Here, we show that the CR gives rise to the MR via a previously uncharacterized maturation process involving opposing mechanisms acting on Anillin: the septin Peanut (Pnut) acts with the C terminus of Anillin to locally remove membrane, whereas the Citron kinase (Cit-K) Sticky acts to retain the N terminus of Anillin at ring structures. Furthermore, Pnut and Sticky redundantly stabilize the earlier CR. The data lead to the proposal that septin-dependent removal of membrane-associated Anillin during disassembly of the actomyosin ring contributes to CR stability and closure, whereas Sticky-dependent retention of Anillin also contributes to CR stability and limits the removal of Anillin from the mature MR.

4.3. Results

4.3.1. Maturation of the MR is accompanied by removal and retention of Anillin

To better define the process of MR formation and maturation, we have monitored the localization of Anillin-GFP (Hickson and O'Farrell, 2008b) using time-lapse spinning-disc confocal microscopy. Anillin-GFP localized to the CR and MR throughout cytokinesis and to the MR remnant that remained associated with one of the sister cells after abscission (Fig. 1 A). Induced expression of Anillin-GFP under the control of the metallothionein promoter resulted

in a fourfold overexpression of Anillin (Fig. S1, A–C). This fully rescued for loss of endogenous Anillin (Hickson and O'Farrell, 2008b) and had no consequence on the duration of furrowing or the timing of abscission when compared with other markers, such as GFP-tubulin or the myosin regulatory light chain (MRLC) Spaghetti squash–GFP (myosin-GFP; unpublished data). However, during formation of the MR, we observed a gradual thinning of the MR structure that was unexpectedly accompanied by extrusion and internalization of Anillin-GFP (Fig. 1, A–C). Extrusion originated from blebs or tubules that formed either at late stages of furrowing (Fig. 1 B and Video 1) or at the nascent MR soon after furrowing (Fig. 1 C). The extruded material persisted for several minutes and in some cases was clearly shed completely from the cell (Fig. 1, B and C, arrowheads). During internalization, Anillin-containing structures budded from the cytokinetic apparatus and were internalized into the cytoplasm as punctate vesicular structures (Fig. 1 E and Video 2). At the nascent MR, Anillin-FP sometimes labeled plasma membrane folds that had been gathered up during CR closure (Fig. S1 E). Such plasma membrane folds were also evident by EM (Fig. S1 F). Mature MRs, however, were more uniform in shape, had more closely opposed plasma membranes, and exhibited a double ring ultrastructure with a more electron-dense outer layer and a less dense inner layer (Fig. S1 F), similar to that described for intercellular canals in *Drosophila melanogaster* embryos (Haglund et al., 2011). The extruded structures labeled with a plasma membrane marker, myristoylated palmitoylated–GFP (myrpalm-GFP; Fig. S1), although this revealed many additional plasma membrane protrusions associated with the nascent MR that did not contain Anillin–fluorescent protein (FP; Fig. S1 G). These membrane protrusions accumulated during furrowing but then gradually dissipated during MR maturation, indicating that excess plasma membrane is gathered by the CR and then removed from the nascent MR (Fig. S1 H).

Extrusion/shedding and internalization of Anillin occurred during the ∼1-h period that followed CR closure and coincided with a progressive decline in total Anillin-FP intensity measured at the nascent MR (n = 20; Fig. 1 E). Beyond this time, the appearance and intensity of MRs remained constant until after abscission. We examined the dynamic nature of Anillin-GFP at different stages of MR biogenesis using FRAP. When the entire MR region was bleached within 15 min of CR closure (Fig. 1 F, top), 30 ± 13% of Anillin-GFP fluorescence recovered within 4 min (n = 16; Fig. 1 G). However, when bleached >45 min after CR closure (Fig. 1 F,

bottom), only 10 ± 6% recovery was observed within 4 min (n = 9; Fig. 1 G), indicating that the potential to restore Anillin to the MR declined as it matured. Photoconversion of an Anillin-Dendra2-FP revealed that the recovery occurred preferentially at the flanking regions, whereas less exchange occurred at the central region of the MR (Fig. S1 H). We conclude that nascent MRs mature over the course of ∼1 h into stable MRs, during which they progressively extrude, shed, and internalize Anillin.

4.3.2. Nascent MRs shed numerous cytokinesis proteins but not F-Actin

We wished to determine whether other cytokinesis proteins were also shed with Anillin during MR maturation. Immunofluorescence analysis revealed that the septin, Pnut (Fig. 2 A), and Rho1 (Fig. 2 B) were also enriched on the extruded membranes. Similarly, the Cit-K, Sticky-FP, was extruded with Anillin-FP (Fig. 2 C), as were the components of the centralspindlin complex, RacGAP50C/Tumbleweed (Tum)-FP (Fig. 2 D) and the kinesin-6 motor Pavarotti-FP (Fig. 2 E). Aurora B–GFP, which also localizes primarily to the central spindle and midbody microtubules (Fig. 2 F), was also extruded from the center of the midbody soon after CR closure.

Cells expressing myosin-GFP showed no evidence of extrusion, shedding, or internalization (Fig. 2 G), unless Anillin-mCherry (mCh) was also coexpressed, in which case some myosin-GFP colocalized with shed Anillin-mCh (Fig. 2 H). However, the F-actin probe LifeAct-GFP (Riedl et al., 2008), although enriched at the late CR, did not colocalize with extruded Anillin-FP (Fig. 2 I). Phalloidin staining of fixed cells also revealed that the extruded Anillin-positive membranes were labeled poorly for F-actin (Fig. 2 J). Thus, although numerous key components of the cytokinesis machinery were removed via extrusion and shedding, actin was specifically not. We next designed experiments to further understand the mechanisms of Anillin removal from the late CR/nascent MR.

.

4.3.3. Shedding from the nascent MR requires Anillin but not ESCRT-III or the proteasome

Aurora B–GFP and Tum-GFP showed evidence of shedding even when Anillin was not overexpressed (Fig. 3, A and C). We therefore used these markers to test whether Anillin was itself required for shedding. In Anillin-depleted cells, Aurora B–GFP was no longer extruded compared with controls but still disappeared from the cleavage site over a similar time course to controls ($n > 20$; Fig. 3, A and B). Similarly, no evidence of Tum-GFP extrusion was observed from Anillin-depleted late CRs/nascent MRs ($n > 20$; Fig. 3, C and D). Thus, Anillin is required for extrusion, although we note that this may reflect a direct requirement for Anillin in the extrusion process, an indirect consequence of the requirement for Anillin in complete CR closure (Kechad et al., 2012), or both.

The membrane topology during extrusion/shedding is the same as the abscission event that occurs later. We therefore tested whether shedding, like abscission, requires ESCRT-III complexes. A 3–4-d depletion of Shrub, the *Drosophila* orthologue of CHMP4B, a key ESCRT-III component (Elia et al., 2011; Carlton et al., 2012), delayed abscission well beyond the 3 h and 48 s ± 1 h and 57 s (mean ± SD; $n = 12$) observed for untreated controls, although cells never became binucleated. Shrub-depleted cells remained paired for so long that they could not be reliably followed from furrowing to abscission, as the cells, being poorly adherent, would often move out of the imaging field over time. However, we noted that 30% of Shrub-depleted cells initiated cytokinesis while still connected to their sister cells from the previous attempt ($n = 110$ pairs; Fig. 3, E–G), whereas control cells had always undergone abscission before reaching the next metaphase ($n > 55$ pairs). Daisy chains of Shrub-depleted cells were sometimes observed, consistent with abscission failure in multiple rounds of division. Even in the most extreme cases, normal MR maturation was observed, including extrusion, shedding, and internalization of Anillin-GFP (Fig. 3 H, Fig. S2 A, and Video 4). Similar results were obtained upon depletion of dIST1 (unpublished data), another ESCRT-III component required for cytokinesis (Agromayor et al., 2009). Thus, ESCRT-III is required for abscission, as expected, but not for MR maturation.

Human Anillin is subject to anaphase-promoting complex/cyclosome–mediated degradation (Zhao and Fang, 2005). We tested whether degradation of *Drosophila* Anillin might contribute to its decline during MR maturation, by treating cells expressing Anillin-GFP with the proteasome inhibitor MG132. When added early in mitosis, 5 µM MG132 induced widespread metaphase arrest, as expected. Cells that successfully underwent the metaphase/anaphase transition during the 5 min before or after MG132 addition, however, furrowed normally (Fig. S2 B). However, although untreated control cells typically exhibited a net loss of Anillin-GFP soon after the end of furrowing, MG132-treated furrows accumulated Anillin-GFP during the subsequent 15–20 min after closure (n = 14; Fig. S2 C), before exhibiting a profile of net loss that was similar to controls (n = 20; Fig. S2 D) and that ended with a mature MR that was indistinguishable from controls (Fig. S2 E). Extrusion and shedding of Anillin-GFP during MR maturation continued in MG132 (Fig. S2 E). We conclude that proteasomal degradation is not required for extrusion/shedding of Anillin and does not provide a major contribution to the loss of Anillin from the MR during its maturation. However, proteasomal degradation, directly or indirectly, appears to limit the extent or accelerate the rate of Anillin-GFP accumulation at the late CR/nascent MR.

A third population of cells displayed a highly aberrant exit from mitosis that was seen 5–40 min after MG132 addition. Slow and excessive spindle elongation, slow and broad furrows, and a failure of nuclear envelope reformation and/or nuclear import of Anillin-GFP characterized this (Fig. S2 F). We interpret these cells as having degraded only a subset of anaphase-promoting complex/cyclosome substrates, resulting in a partial arrest. Remarkably, most of these cells succeed to a midbody-like stage, although they were not followed until completion.

Collectively, these experiments show that cortical extrusion/shedding during the transition from CR to MR requires Anillin but does not depend on ESCRT-III or the proteasome. We next performed a structure–function analysis of Anillin to further define the requirements for its extrusion and shedding.

4.3.4. Removal of Anillin from the nascent MR is mediated via its C terminus, whereas retention at the mature MR is mediated via its N terminus

Anillin is a large multidomain protein (Fig. 4 A) that can bind to many other cytokinesis proteins (D'Avino, 2009; Piekny and Maddox, 2010). We analyzed truncation mutants lacking domains to determine which mediate its retention and removal at the nascent MR. Anillin-Δactin-binding and -bundling domain (ActBD)-GFP, which lacks the ActBD identified by Field and Alberts (1995), was no longer recruited to the actin-rich cortex in mitosis, similar to the behavior of full-length Anillin-GFP in Latrunculin A–treated cells (Hickson and O'Farrell, 2008b). However, Anillin-ΔActBD-GFP was still recruited to the furrow, nascent MR, and mature MR and exhibited dramatic extrusion and shedding (Fig. S3 A). Anillin-Δmyosin-binding domain (MyoBD)-GFP, which lacks the region adjacent to the ActBD that is homologous to the *Xenopus laevis* myosin II–binding domain (Straight et al., 2005), still localized to the cortex at metaphase, indicating a functional ActBD, and to the CR and nascent MR during cytokinesis (Fig. S3 B). It was also readily extruded and shed and localized to mature MRs, although these appeared smaller than MRs containing full-length Anillin-GFP. Anillin-ΔN, in which the entire N terminus was deleted, leaving only the Anillin homology domain (AHD) and Pleckstrin homology (PH) domain (PHD), was still extruded and shed. Constructs expressing only the AHD or PHD were poorly recruited and showed no evidence of shedding, and deletion of either domain blocked extrusion and shedding. Thus, the C-terminal AHD and PHD are each required and together sufficient for extrusion and shedding.

Conversely, a mutant comprising only the extreme N-terminal domain and the ActBD and MyoBD (Anillin-N) was still recruited to the MR (Fig. S3 C) and behaved similarly to the larger Anillin-ΔC (Kechad et al., 2012). The reciprocal mutants lacking these domains (Anillin-ΔN and Anillin-ΔN with the central domain [CD; Anillin-ΔN+CD]) failed to be retained at the mature MR despite localizing to the nascent MR and readily being extruded and shed (Fig. 4 B). Thus, the Anillin N terminus is both necessary and sufficient for retention at the mature MR.

Coexpressing N- and C-terminal truncations fused to different FPs in the same cells did not alter their respective behaviors and made their differences even more apparent. Fig. 4 B shows

Anillin-ΔC-GFP incorporating into the MR without being extruded or internalized, whereas Anillin-ΔN+CD-mCh is completely shed from the nascent MR without incorporating into the mature MR (Fig. 4 B and Video 5). Collectively, our data indicate that distinct mechanisms of removal and retention act on the C and N termini of Anillin, respectively. We next aimed to better understand the removal mechanisms acting on the C terminus of Anillin.

4.3.5. Maturation of the MR requires septin-dependent removal of Anillin via its C-terminal PHD

The Anillin PHD is known to bind septins (Field and Alberts, 1995; Oegema et al., 2000; Liu et al., 2012) and phosphoinositides (Liu et al., 2012), and septins are required for the recruitment of Anillin-ΔN to the cleavage furrow (Kechad et al., 2012). We further evaluated the requirement for the PHD and septins in Anillin removal during MR maturation. Anillin-ΔPH-FP localized efficiently to the CR and MR but showed little, if any, evidence of extrusion or internalization from the nascent MR, whether or not endogenous Anillin was depleted (Fig. 5, A and C). Anillin-ΔPH-GFP MRs also appeared larger than controls of the same age (Fig. 5 E). Measuring MR volumes over time revealed that Anillin-ΔPH-GFP MRs did not thin to the same extent as Anillin-GFP controls (Fig. 5 F). This effect was dominant, suggesting that the PHD is autonomously required for Anillin removal. A 7–8-d incubation with double-stranded RNAs (dsRNAs) targeting the septin Pnut (Neufeld and Rubin, 1994), which results in >94% depletion in S2 cells (Fig. 5 B), also blocked extrusion/ shedding of Anillin-GFP (Fig. 5 A) and inhibited the thinning of the MR during its maturation (Fig. 5, D–F). Thus, the PHD of Anillin and Pnut are each required for cortical removal during MR maturation.

In the 30% (Anillin-ΔPH-GFP + Anillin dsRNA, $n = 75$) and 34% (Anillin-GFP + Pnut dsRNA) of attempts at cytokinesis that failed, deletion of the PHD or depletion of Pnut produced similar phenotypes: at 1 h and 10 min ± 12 min (mean ± SD; $n = 50$) and 1 h and 23 min ± 33 min (mean ± SD; $n = 50$) after anaphase onset, respectively, the plasma membrane regressed, leaving internal MR-like structures (Fig. 5 G; Kechad et al., 2012). However, in the cells that succeeded, Anillin-ΔPH-FP delayed abscission, which occurred 10 h and 42 min ± 6 h and 7 min (mean ± SD; $n = 50$) after furrowing, whereas Pnut depletion led to premature abscission

that occurred 2 h and 19 min ± 0 h and 42 min (mean ± SD; *n* = 50) after furrowing compared with 4 h and 54 min ± 1 h and 36 min (mean ± SD; *n* = 75) for Anillin-FP–expressing controls (Fig. 5 G). Given that the PHD binds both the membrane and septins (Liu et al., 2012), this difference in abscission timing could reflect the difference between loss of septin binding (Pnut depletion) and the additional loss of membrane binding (deletion of the entire PHD). Accordingly, membrane binding by the Anillin PHD may facilitate abscission.

These experiments show that the PHD of Anillin and the septin Pnut are required for the normal thinning of the nascent MR and the extrusion and shedding of membrane-associated Anillin. We next sought to better understand the mechanism of Anillin retention at the MR.

4.3.6. Sticky acts to limit extrusion and shedding and retains Anillin at the MR

Cit-K, Sticky in *Drosophila*, is a conserved Rho-associated kinase required for a late step of cytokinesis (Di Cunto et al., 2000, 2002; D'Avino et al., 2004; Echard et al., 2004; Naim et al., 2004; Shandala et al., 2004; Gruneberg et al., 2006). Human Cit-K and Anillin can be coimmunoprecipitated, and Cit-K has been suggested to maintain Anillin at the MR (Gai et al., 2011; Watanabe et al., 2013). Cit-K/Sticky and Anillin depletion phenotypes also bear some similarities, such as plasma membrane blebbing (Somma et al., 2002; Echard et al., 2004; Naim et al., 2004; Gai et al., 2011). However, because the relationship between Anillin and Cit-K/Sticky remains unclear, we reexamined Sticky depletion phenotypes. Immunoblot analysis revealed that 3-d incubation of S2 cells with Sticky dsRNAs led to a >90% depletion of both major migrating forms of Sticky (Fig. S5 A), similar to that described previously (D'Avino et al., 2004).

Time-lapse sequences captured at 1-min intervals with a 63× objective revealed that Sticky-depleted CRs closed with normal kinetics and morphology (Fig. 6, A and B; and Videos 6 and 7), consistent with previous studies (Echard et al., 2004; Bassi et al., 2011). The midbody microtubules also adopted their characteristic compacted morphology at the close of furrowing (Fig. 6, A and B), unlike Anillin-depleted cells (Fig. 3, B and D; Kechad et al., 2012). However, measuring Anillin-GFP intensities revealed that Anillin levels continued to increase after the

close of furrowing, such that the peak intensity of the nascent MR was ~10 min later than that of control cells (Fig. 6 C). At the time of normal MR formation and maturation, Anillin-GFP displayed enhanced extrusion and internalization events (Fig. 6 D). As in controls, blebs and tubules of Anillin-positive membranes formed and subsequently left the MR region by lateral movement or outright shedding (Fig. 6, A and B; and Videos 6 and 7). Although we observed clear examples of both internalization and extrusion/shedding in both control and Sticky-depleted cells, it was often difficult to differentiate between the two in any given case, especially as extruded material could subsequently be internalized. We therefore simply quantified removal (by either mechanism). This revealed that more Anillin-GFP was removed from Sticky-depleted nascent MRs and over a longer period than in controls (Fig. 6 D). Removal continued until Anillin-GFP was no longer detectable at the MR site, and furrows either regressed within a few minutes or underwent abscission prematurely (Fig. 6, A and B; and Videos 6 and 7).

To better define the outcomes of cytokinesis attempts upon Sticky depletion, we acquired time-lapse sequences at 2–4-min intervals over longer periods using a 40× objective. 77% of attempts failed, whereas 23% succeeded ($n > 65$; Fig. 6 E). Interestingly, successes occurred earlier and with much less variability than untreated controls (Fig. 6 E), confirming our earlier inference of premature abscission in Sticky-depleted cells obtained from scoring the frequency of paired S2 cells (Echard et al., 2004). These successful divisions probably represent a hypomorphic phenotype, as they were more prevalent at earlier times after dsRNA addition, with failures predominating later. Failures resulted from rapid furrow regression 77 ± 15 min (mean ± SD; $n = 50$) after CR closure (Fig. 6 E). Thus, ~75 min after furrowing, Sticky-depleted nascent MRs either quickly resolved or regressed and failed. In both cases, a persistent Anillin-GFP–positive MR structure failed to form in >90% of division attempts ($n > 58$ per condition; Fig. 6, A and B).

Analysis of fixed cells revealed that Pnut (Fig. 6 F) and Rho1 (Fig. 6 G) were also enriched in the extruded Anillin-positive membranes, whereas F-actin was depleted (Fig. 6 H), as had been observed for extrusion in cells that were not depleted of Sticky (Fig. 2). Importantly, nascent MRs of Sticky-depleted untransfected cells also revealed markedly enhanced extrusion of endogenous Anillin compared with controls (Fig. 6, I and J), confirming that Sticky limits

extrusion and that extrusion is not simply a consequence of Anillin-FP overexpression. We conclude that Sticky acts to retain Anillin at the mature MR.

4.3.7. Sticky acts with the N terminus of Anillin to promote both MR formation and CR stability

Sticky depletion had no effect on the recruitment or removal of Anillin-ΔN-FP (Fig. 7 A) but greatly diminished the localization of Anillin-ΔC-FP to the nascent MR (Fig. 7 B) and prevented it from forming stable MR-like structures, whether or not endogenous Anillin was codepleted (Fig. 7 C). Furthermore, a functional Sticky-mCh localized to internal Anillin-ΔC-GFP–dependent MR-like structures that resulted upon depletion of endogenous Anillin (Fig. 7 D) but did not colocalize with Anillin-ΔN-GFP–positive structures that accumulate around the nascent MR when endogenous Anillin is present (Fig. 7 E). Thus, Sticky is specifically required to retain the N terminus of Anillin at the mature MR.

Cleavage furrows are inherently unstable (Sedzinski et al., 2011) and oscillate after certain perturbations, including Anillin depletion (Straight et al., 2005; Zhao and Fang, 2005; Hickson and O'Farrell, 2008b; Piekny and Glotzer, 2008; Goldbach et al., 2010) and overexpression of full-length or truncated Cit-K (Madaule et al., 1998; Gai et al., 2011). Remarkably, cells expressing Anillin-ΔC-FP and depleted of endogenous Anillin, which furrow slowly without oscillating and form stable MR-like structures (Kechad et al., 2012), also became prone to oscillate when Sticky was codepleted (Fig. 7, F and H). This indicates that Sticky promotes the ability of the Anillin N terminus to stabilize furrows.

Because Pnut depletion blocked Anillin removal from the MR and Sticky depletion blocked Anillin retention, we tested the effects of codepleting Sticky and Pnut. Little, if any, evidence of extrusion or internalization of Anillin-GFP was observed, indicating that the enhanced extrusion observed upon Sticky depletion was still Pnut dependent (Fig. 7 G and Video 8). In 39% (n = 46) of cells, the formation of stable MR-like structures was abolished, as expected (Fig. 7 I). The remaining 61% exhibited an intermediate phenotype whereby Anillin-positive MR structures persisted, but unlike control or Pnut-depleted cells (Fig. S4, A and B), these often did not label for myosin (Fig. S4, C and D). This partial destabilization

of the MR suggests that Sticky acts to retain myosin at the MR. Furthermore, some of the structures were clearly not closed rings but had less well-defined shapes (e.g., Fig. 7 G and Video 8). Persistence of Anillin at these structures may reflect the existence of other Sticky-independent mechanisms that contribute to Anillin retention at the midbody.

Strikingly, cells codepleted of Sticky and Pnut were prone to oscillate during furrowing (53% oscillations, $n = 135$), whereas singly depleted cells were much less so (<10% oscillations; Fig. 7, G and H; and Video 8). During oscillations, Anillin-FP migrated laterally in repeated cycles, much like myosin does upon Anillin depletion. The fact that codepletion of Sticky and Pnut destabilized furrows and caused Anillin to oscillate suggests that Pnut contributes to a stabilizing influence of the Anillin C terminus. Anillin-ΔN-FP, comprising only the Anillin C terminus, failed to rescue oscillations but was completely disconnected from actomyosin (Kechad et al., 2012), underscoring the importance of the linkage to actomyosin. These data show that Anillin stabilizes furrows in part by linking actomyosin to the membrane-associated septin cytoskeleton and in part via a distinct Sticky-dependent action of its N terminus.

4.3.8. Sticky's essential role during MR formation is as a scaffold

We next wished to test whether Sticky kinase activity is required to retain Anillin-GFP at the MR. We generated inducible cell lines that coexpressed Anillin-GFP and mCh-tagged wild-type or kinase-dead (KD) versions of Sticky, at roughly endogenous levels (Fig. 8 A). Both Sticky-mCh and Sticky-KD-mCh were faithfully recruited to the CR and MR, although both also led to the formation of Anillin-GFP–negative, intracellular aggregates, similar to those described by others (Fig. 8, C and D; and Videos 9 and 10; Eda et al., 2001). Expression of either Sticky-mCh or Sticky-KD-mCh rescued the widespread failures of cytokinesis induced by depletion of endogenous Sticky using a dsRNA directed against the Sticky 3′ UTR (Fig. 8 B). That formation of Sticky- and Anillin-positive MRs (Fig. 8, C–E; and Video 10) were rescued in Sticky-KD-mCh cells indicates that Sticky kinase activity is dispensable for both MR formation and abscission (Fig. 8, B and E). However, abscission timing was slightly accelerated for Sticky-KD-mCh MRs (128 ± 49 min, mean ± SD; $n = 28$) than for Sticky-mCh MRs (196 ±

67 min, mean ± SD; $n = 26$). Furthermore, the majority of cells that failed did not recruit detectable levels of Sticky-mCh (7/8 failures) or Sticky-KD-mCh (18/24 failures) to the CR/MR, consistent with failures reflecting the lack of Sticky rather than the lack of kinase function (Fig. 8 B and Fig. S3 B). In addition, excess Sticky-mCh and Sticky-KD-mCh were both also internalized and extruded/shed with Anillin-GFP (Fig. 8, C–E; and Videos 9 and 10), indicating that Sticky must itself be subject to retention at the midbody. We conclude that the essential role of Sticky in these cells is as a scaffold that serves to retain Anillin and stabilize the MR.

4.4. Discussion

The organization of the cell cortex during closure of the CR and formation of a stable MR remains poorly defined. We show in *Drosophila* S2 cells that the late CR/nascent MR thins via a maturation process that lasts ∼1 h and that involves a molecular tug of war between stable retention and dynamic removal of the membrane- and cytoskeleton-associated scaffold Anillin. Retention requires a scaffold function of the Cit-K Sticky and the N terminus of Anillin, whereas removal requires septins and the C terminus of Anillin and includes dramatic extrusion and shedding of membranes. Simultaneous perturbation of these antagonistic processes disrupts not only MR maturation but also CR stability, supporting our previous proposal that the CR and MR represent different stages of the same structure (Kechad et al., 2012). The work provides novel insight into the elusive mechanisms of CR closure and its maturation to the MR (Fig. 9).

4.4.1. Anillin-septin–dependent membrane removal

The extrusion and shedding of membrane from the nascent MR was unexpected; however, it is highly reminiscent of Anillin- and prominin-1–positive, membrane-bound particles that shed from apical MRs in the vertebrate neuroepithelium (Dubreuil et al., 2007). EM has also revealed budding of membranous structures from the MR of human D98S cells

(Mullins and Biesele, 1977) and prominent membrane microvilli in cleavage stage sea urchin embryos (Schroeder, 1972). We have also observed extrusion of Anillin from the nascent MRs of human HeLa and neuroblastoma cells (unpublished data). Finally, we note that tubules of Anillin- and Pnut-positive membranes are shed from the newly formed cells at the close of cellularization of the *Drosophila* embryo, a process mechanistically related to cytokinesis (unpublished data; Adam et al., 2000; Field et al., 2005). Thus, membrane extrusion may be a universal feature of animal cell cytokinesis.

4.4.2. Is membrane removal the cause or consequence of CR closure?

Key questions arise concerning the mechanism of Anillin-septin membrane extrusion and whether it is a cause or consequence of CR closure or both. In mammalian interphase cells, membrane blebs recruit septins, after F-actin, to facilitate bleb retraction (Gilden et al., 2012). However, the membrane protrusions/tubules that we describe are enriched in Anillin from their first emergence, they are poor in actin and they never retract. Thus, rather than being recruited to or trapped in preexisting blebs, we favor the model that Anillin directs septin-dependent membrane tubulation. Septins are capable of tubulating membranes (Tanaka-Takiguchi et al., 2009), although the topology of such structures is reversed compared with the extrusions that we describe. However, it remains unclear how Rho1 and Anillin (and potentially other cytokinesis proteins) might alter septin behaviors. Experimentally disconnecting the N terminus of Anillin from the actomyosin network, either by deleting the N terminus of Anillin (Kechad et al., 2012) or by disrupting the actin cytoskeleton with Latrunculin A (Hickson and O'Farrell, 2008b), triggers the C terminus of Anillin to induce Pnut-dependent remodeling of the plasma membrane, resulting in either punctate or tubular protrusions that extend outwards from the cell. These data argue that the extrusions at the late CR/nascent MR may simply reflect the local disassembly of actin, thereby liberating Anillin N termini and allowing Anillin C termini/septins to tubulate membranes in such a dramatic fashion. Indeed, membrane extrusion is most obvious at the time when the MR is becoming resistant to Latrunculin A (Echard et al., 2004), suggesting coordination with disassembly of the actin ring. Finally, actin and Anillin-ΔC were notably

absent from the extruded and shed membranes, indicating that not all CR components are removed in this way.

4.4.3. Can furrow oscillations result from impeding CR disassembly?

The CR closes by disassembly (Schroeder, 1972; Carvalho et al., 2009). Our results suggest that this involves both depolymerization and membrane-associated removal. Accordingly, Anillin and septins may sequester the excess membrane that is liberated upon actomyosin depolymerization. Anillin-depleted CRs fail to close to completion and become unstable and oscillate (Straight et al., 2005; Zhao and Fang, 2005; Hickson and O'Farrell, 2008b; Piekny and Glotzer, 2008; Goldbach et al., 2010). Our findings raise the possibility that this phenotype reflects a failure to sequester membrane (via septins) that impedes the normal disassembly of the actin ring, combined with the loss of an additional Sticky-dependent scaffolding role of the N terminus of Anillin.

We note that Sticky and Pnut codepletion did not completely phenocopy Anillin depletion. The latter is more severe with a proportion of cells that undergo wild oscillations that are too unstable to allow ingression beyond 50% closure (Kechad et al., 2012). Sticky- and Pnut-codepleted cells, although they oscillated, mostly ingressed to completion and then failed at the MR stage (this study). Thus, Anillin likely has additional inputs into furrow stability that are independent of Sticky and Pnut. RacGAP50C/Tum is a strong candidate known to interact with the AHD (D'Avino et al., 2008; Gregory et al., 2008).

4.4.4. The essential role of Sticky is as a scaffold for the mature MR, but it also functions during furrowing

We show that Sticky is required to retain the N terminus of Anillin at the mature MR. Human Cit-K can phosphorylate the MRLC (Yamashiro et al., 2003), and MRLC is another component of the MR in S2 cells (Dean and Spudich, 2006; Kechad et al., 2012). Expression of phosphomimetic MRLC (Spaghetti squash–E20E21) in S2 cells cannot rescue for Sticky

depletion, indicating that myosin phosphorylation cannot be the only essential role of Sticky (Dean and Spudich, 2006). Our results further show that kinase activity is completely dispensable for the essential function of Sticky because a KD version is still able to form a stable MR and rescue cytokinesis. In agreement with this, the central coiled-coil region of human Cit-K is sufficient to support cytokinesis in HeLa cells (Watanabe et al., 2013). The fact that Sticky was extruded and shed with Anillin suggests that Sticky itself must be retained by additional, saturable mechanisms at the midbody, likely via KIF14-dependent mechanisms (Gruneberg et al., 2006; Bassi et al., 2013; Watanabe et al., 2013).

Although Cit-K/Sticky localizes to the CR (Madaule et al., 1998; Eda et al., 2001; D'Avino et al., 2004; Bassi et al., 2011), whether it acts there is a long-standing enigma. Our findings confirm that it does, albeit redundantly. First, unlike control furrows, Sticky-depleted furrows continued to accumulate Anillin-GFP for 10 min after closure, indicating that Sticky normally functions at this time. Second, Sticky depletion caused furrow oscillations in cells codepleted of Pnut or in cells expressing Anillin-ΔC and codepleted of endogenous Anillin. This indicates that Sticky plays a role in furrow stability that is redundant with the C terminus of Anillin and Pnut. We attempted to test whether kinase activity was required for this role. However, rescuing Sticky depletion in the context of Pnut codepletion was problematic. The longer induction times required by the fact that Pnut depletion takes many days resulted in poor recruitment of Sticky-mCh and Sticky-KD-mCh to CRs, with both proteins preferring to form ectopic aggregates. Thus, although kinase activity is dispensable for Sticky's essential role at the MR, it remains possible that its kinase activity contributes to CR stability.

4.5. Concluding remarks

Current models for CR closure focus on the cytoskeletal proteins and pay little attention to the plasma membrane to which these elements are anchored. Although net membrane addition may be required during furrow ingression (Albertson et al., 2005; McKay and Burgess, 2011; Neto et al., 2011), our findings highlight a need for membrane removal from the furrow apex that must be coordinated with CR disassembly and MR assembly. Extrusion and shedding

is one way of achieving this; other potential mechanisms include internalization and lateral outflow within the lipid bilayer. Theoretical and experimental analyses in different systems will be needed to fully test this novel perspective.

4.6. Materials and methods

4.6.1. Constructs, cell lines, and RNAi

All constructs were generated by PCR amplification of the ORF, without stop codons, followed by cloning into pENTR-D-TOPO (Invitrogen) followed by recombination using LR Clonase into appropriate destination vectors (Drosophila Gateway Vector Collection; T. Murphy, Carnegie Institution for Science, Washington, DC). Anillin-GFP (pMT-WG, driven by the metallothionein promoter), Anillin-mCh (pAc-WCh, driven by the constitutive *Act05C* promoter), mCh-tubulin (pAc-ChW), $MRLC^{Sqh}$-GFP (endogenous *spaghetti squash* promoter), Anillin-ΔC-FP (pMT-WG or pMT-WCh), Anillin-ΔN-FP (pMT-WG or pMT-WCh), and Pavarotti-GFP (pMT-WG) have been described previously (Echard et al., 2004; Hickson and O'Farrell, 2008b; Kechad et al., 2012). Internal deletions and site-directed mutagenesis were performed by PCR by overlap extension followed by cloning into pENTR-D-TOPO and subsequent recombination into pMT-WG and pMT-WCh. All Anillin constructs derive from clone LD23793 (Berkeley Drosophila Genome Project Gold collection; Drosophila Genomics Resource Center) that encodes the CG2092-RB polypeptide. Note that CG2092-RB has an additional 27 residues within the actin-binding domain that is absent in CG2092-RA (Field and Alberts, 1995), but CG2092-RB is better supported by sequencing data. Anillin-ΔN+CD-FP encodes amino acids 410–1,239 and lacks all N-terminal domains up to and including the ActBD. Anillin-ΔPH-FP encodes amino acids 1–1,104 and thus lacks the last 135 residues comprising the entire PHD. Anillin-ΔActBD encodes amino acids 1–255 and 410–1,239 and lacks the minimal ActBD defined in Field and Alberts (1995). Anillin-ΔMyoBD encodes amino acids 1–145 and 238–1,239 and lacks 92 amino acids homologous to the *Xenopus* MyoBD defined in Straight et al. (2005). The *sticky* (CG10522) ORF was PCR

amplified from clone RE26327 (Drosophila Gene Collection release 2 collection; Drosophila Genomics Resource Center). The Sticky KD mutant was generated by site-directed mutagenesis using primers 5′-GACATATACGCCATGGCGGCGATCAAAAAGTCGGTG-3′ and 5′-CACCGACTTTTTGATCGCCGCCATGGCGTATATGTC-3′, which introduced K142A and K143A mutations in the kinase domain. The Aurora B ORF was amplified by RT-PCR from S2 cell cDNA and was described in Smurnyy et al. (2010). Myrpalm-GFP (in pAc-WG) was a gift from S. Carreno (Institut de Recherche en Immunologie et Cancérologie, Université de Montréal, Montréal, Quebec, Canada) and encodes the first 16 amino acids of Lyn (MGCIKSKRKDNLNDDE), including myristoylation and palmitoylation signals, upstream of GFP and driven by the *act05C* promoter. LifeAct-GFP encodes the 17-amino sequence described by Riedl et al. (2008) cloned upstream of GFP (pMT-WG). The Dendra2 sequence was subcloned from pDendra2-N1 (Takara Bio Inc.) into pAc-WG, replacing GFP, to generate pAc-WD2 and allowing subsequent generation of Anillin-Dendra2 by Gateway recombination. All constructs were verified by sequencing.

Plasmids were used to transfect *Drosophila* Schneider's S2 cells using Cellfectin reagent (Invitrogen), together with pCoHygro and additional plasmids as needed to generate stable, hygromycin-resistant cell lines following established protocols (Invitrogen). After selection, cells were cultured in Schneider's medium supplemented with 10% fetal calf serum (Invitrogen) and penicillin/streptomycin.

dsRNAs were generated using in vitro transcription kits (RiboMAX; Promega), and DNA templates were generated in a two-step PCR amplification from cDNA or genomic DNA, as described previously (Echard et al., 2004). In brief, in the first round PCR, gene-specific primer sequences included a 5′ anchor sequence (5′-GGGCGGGT-3′), whereas the second round PCR used a universal T7 anchor primer (5′-TAATACGACTCACTATAGGGAGACCACGGGCGGGT-3′). Gene-specific primer sequences were previously described for *anillin* dsRNA (Echard et al., 2004; Hickson and O'Farrell, 2008b), *anillin* 3′ UTR dsRNA (Hickson and O'Farrell, 2008b), *pnut* dsRNA (Hickson and O'Farrell, 2008b), and *sticky* dsRNAs (Echard et al., 2004). *shrub/CHMP4/CG8055* and *dIST1/CG10103* dsRNAs were generated using primer pairs 5′-GGGCGGGTTCGATACAAAGCTAAGACTGCG-3′ and 5′-

GGGCGGGTATGATCCAGACATGAAGAGCAGC-3′ (Shrub) and 5′-GGGCGGGTGTTGGTGTTCAGATCCTTCTCC-3′ and 5′-GGGCGGGTCTACAGAGCGATATAGCCGAGC-3′ (dIST1). The *sticky* 3′ UTR dsRNA was generated using primer sequences 5′-GGGCGGGTGCATATAGATGAAGGATATAT-3′ and 5′-GGGCGGGTTTTAAAATATTATGCGACTTC-3′.

RNAi experiments were performed as follows: cells were plated in 96-well dishes and incubated with ∼1 μg/ml dsRNA. 12–24 h before imaging or fixation, cells were transferred to 8-well chambered coverglass dishes (Lab-Tek; Thermo Fisher Scientific). Live imaging was performed between 30 and 72 h for Anillin dsRNAs, between 30 and 48 h for Sticky dsRNAs, and between 144 and 192 h for Pnut dsRNA, in which case cells were split and fresh dsRNA added on the fourth day. These dsRNA incubation times were maintained for codepletion experiments, but the individual dsRNA incubations were performed in the presence of irrelevant LacI control dsRNAs to control for possible effects of combining dsRNAs.

4.6.2. Live-cell microscopy

Live-cell imaging of *Drosophila* S2 cells in Schneider's medium was performed at room temperature using a spinning-disc confocal system (UltraVIEW Vox; PerkinElmer) using a scanning unit (CSU-X1; Yokogawa Corporation of America) and a charge-coupled device camera (ORCA-R2; Hamamatsu Photonics) fitted to an inverted microscope (DMI6000 B; Leica) equipped with a motorized piezoelectric stage (Applied Scientific Instrumentation). Image acquisition was performed using Volocity versions 5 and 6 (PerkinElmer). Routine and long-time course imaging was performed using a Plan Apochromat 40×, 0.85 NA air objective with camera binning set to 2 × 2, high-resolution imaging was performed using Plan Apochromat 63 or 100× oil immersion objectives, NA 1.4, with camera binning set to 2 × 2 unless otherwise described in the figure legends.

Expressions of FP fusions under the control of the metallothionein promoter (pMT plasmids) were induced with 250 μM CuSO4 at the time of dsRNA addition in the case of rescue experiments, or when cells were transferred to imaging dishes, 12–24 h before the start of

imaging. Where described, MG132 (Enzo Life Sciences) was added to a final concentration of 5 μM directly to the culture medium.

4.6.3. Immunofluorescence microscopy

Live-cell imaging of *Drosophila* S2 cells in Schneider's medium was performed at room temperature using a spinning-disc confocal system (UltraVIEW Vox; PerkinElmer) using a scanning unit (CSU-X1; Yokogawa Corporation of America) and a charge-coupled device camera (ORCA-R2; Hamamatsu Photonics) fitted to an inverted microscope (DMI6000 B; Leica) equipped with a motorized piezoelectric stage (Applied Scientific Instrumentation). Image acquisition was performed using Volocity versions 5 and 6 (PerkinElmer). Routine and long-time course imaging was performed using a Plan Apochromat 40×, 0.85 NA air objective with camera binning set to 2 × 2, high-resolution imaging was performed using Plan Apochromat 63 or 100× oil immersion objectives, NA 1.4, with camera binning set to 2 × 2 unless otherwise described in the figure legends.

Expressions of FP fusions under the control of the metallothionein promoter (pMT plasmids) were induced with 250 μM $CuSO_4$ at the time of dsRNA addition in the case of rescue experiments, or when cells were transferred to imaging dishes, 12–24 h before the start of imaging. Where described, MG132 (Enzo Life Sciences) was added to a final concentration of 5 μM directly to the culture medium.

4.6.4. FRAP and image analysis

FRAP was performed using the PhotoKinesis module (PerkinElmer) controlled through Volocity software. 5-μm-thick stacks of four z sections were acquired with a 63× objective and 2 × 2 camera binning. Acquisition was at maximum speed (exposure time of 200 ms) for the first 15 s after bleaching (representing cytoplasmic recovery) and then at one image per 15 s for 5 min. Percent recovery = percentage (maximum intensity after bleach − intensity at bleach)/(intensity before bleach − intensity at bleach). All intensity values in FRAP experiments

were normalized to the first time point of acquisition. For statistical analysis, an unpaired *t* test was performed using Prism (GraphPad Software).

MR volume measurements were obtained as follows: cells were imaged using a 63×, 1.4 NA objective (12 z sections at 1-min intervals) during ≥1 h after furrowing using Volocity acquisition. Datasets were then exported as Openlab LIFF files (PerkinElmer) and analyzed using Imaris 7 quantification module (Bitplane) as follows: a surface around the MR was selected using intensity threshold, and the volume of this surface was determined empirically for each MR. These values were then expressed as percentages relative to the value of MR volume at the end of furrowing (the first time point of analysis). Relative fold differences in MR volume were calculated relative to the volume of control Anillin-GFP MRs for each given time point after furrowing. The same process was applied for intensity measurements of each extrusion, internalization, or shedding (Fig. 6 D).

Intensity measurements of MRs were performed using the Volocity select objects by percent intensity tool. Optimal percentage values were determined empirically for each MR, and the resulting sum intensity values were then expressed as percentages relative to the highest value within the given time series (usually, t = 0). Datasets were background corrected. Quantification of the Anillin-GFP loss in Fig. 6 C was performed using Imaris 7 after export from Volocity as Openlab LIFF files. Individual shedding events were selected by creating surfaces using variable thresholds between different cells. Intensity values of individual shedding events were expressed as percentages relative to the total intensity associated with the MR at the start of the given time series. Images were processed for publication using Photoshop CS (Adobe) and assembled as figures using Illustrator CS (Adobe). Video files were exported from Volocity as QuickTime videos (Apple).

4.6.5. Immunoblotting

S2 cells were grown in 12-well dishes, treated with the indicated dsRNAs, and harvested by centrifugation. Cells were lysed in lysis buffer (50 mM Tris-HCl, pH 7.5, 150 mM NaCl, and 1% Triton X-100 completed with protease inhibitor cocktail [Roche]), and total cell lysates were subjected to SDS-PAGE (8–15% polyacrylamide). Proteins were transferred to a nitrocellulose

membrane and blocked with 5% milk in TBS containing 0.2% Tween 20 (TBST). The membrane was cut at the appropriate molecular weight marker with the upper molecular weight part immunoblotted with affinity-purified anti-Anillin antibodies (1:1,000; generated in rabbits against amino acids 1–409 of Anillin fused to GST; a gift from J. Brill, The Hospital for Sick Children [SickKids], Toronto, Ontario, Canada; Goldbach et al., 2010) or anti-Sticky antiserum (1:3,000, generated in rabbits against a fragment of the Sticky protein [amino acids 531–742] fused to a C-terminal 6×His tag, a gift from P. D'Avino, Cambridge University, Cambridge, England, UK; D'Avino et al., 2004), whereas the lower molecular weight part was blotted with mAb anti-tubulin antibody (clone DM1A; 1:1,000; Sigma-Aldrich). For anti-Pnut (1:1,000; concentrated supernatant from clone 4C9H4; Developmental Studies Hybridoma Bank; Neufeld and Rubin, 1994), immunoblotting was performed in duplicate in which one membrane was immunoblotted with anti-Pnut and the other with mAb anti-tubulin (as indicated in this paragraph). The blots were washed in TBST, incubated with horseradish peroxidase–coupled donkey anti–rabbit or anti–mouse secondary antibodies (1:5,000; GE Healthcare), and washed again before detection of signals using Western ECL substrate (Clarity; Bio-Rad Laboratories).

4.6.6. EM

Drosophila S2 cells were gently pelleted by centrifugation, incubated for an hour at room temperature in a fixative consisting of 2.5% glutaraldehyde, 4% paraformaldehyde, and 5 mM $CaCl_2$in 0.1 M cacodylate buffer, pH 7.4 (Caco), and in 1% OsO_4 in Caco for postfixation. The pellet was stained in 2% uranyl acetate overnight at 4°C, dehydrated in a graded series of ethanol, and embedded in Epon 812. Ultrathin tissue sections were cut using an ultramicrotome (Ultracut; Reichert) and mounted on copper grids. Ultrathin sections were stained with uranyl acetate and lead citrate and examined with an electron microscope (CM100; Philips).

4.7. Online supplemental material

Fig. S1 shows Anillin immunoblots demonstrating efficacy of RNAi and level of Anillin-GFP overexpression as well as additional images of membrane morphology at the nascent MR. Fig. S2 shows additional cells treated with Shrub/CHMP4 dsRNAs or MG132. Fig. S3 show behaviors of additional Anillin truncations during MR maturation. Fig. S4 shows the effects of codepletion of Sticky and Pnut on MR formation. Fig. S5 shows a Sticky immunoblot demonstrating efficacy of RNAi as well as images of Sticky-KD-mCh cytokinesis failure. Video 1 shows extrusion of Anillin-GFP from the nascent MR. Video 2 shows internalization of Anillin-GFP from the nascent MR. Video 3 shows the behavior of coexpressed Anillin-mCh and LifeAct-GFP at the nascent MR. Video 4 shows cells expressing Anillin-GFP undergoing cytokinesis after depletion of Shrub/CHMP4B. Video 5 shows a cell expressing Anillin-ΔN+CD-mCh and Anillin-ΔC-GFP undergoing cytokinesis. Video 6 shows a Sticky-depleted Anillin-GFP–expressing cell undergoing premature abscission. Video 7 shows a Sticky-depleted Anillin-GFP–expressing cell failing cytokinesis. Video 8 shows an Anillin-GFP–expressing cell codepleted of Sticky and Pnut attempting cytokinesis. Video 9 shows a cell expressing Anillin-GFP and Sticky-mCh undergoing cytokinesis after endogenous Sticky depletion. Video 10 shows a cell expressing Anillin-GFP and Sticky-KD-mCh undergoing cytokinesis after endogenous Sticky depletion. Online supplemental material is available at http://www.jcb.org/cgi/content/full/jcb.201305053/DC1. Additional data are available in the JCB DataViewer at http://dx.doi.org/10.1083/jcb.201305053.dv.

4.8. Acknowledgments

We thank Patrick O'Farrell, in whose laboratory this work was initiated (supported by National Institutes of Health grant R01-GM037193) and for comments on an early version of the manuscript. We thank Christine Field, Julie Brill, Paolo D'Avino, and the Developmental Studies Hybridoma Bank for antibodies, Ron Vale, Sébastien Carreno, and Yvonne Ruella for

constructs, Raphaëlle Cadenas for generating ESCRT-III dsRNAs, and Diane Gingras for help with EM.

G.R.X. Hickson thanks the Fonds de Recherche du Québec–Santé (FRQS) for a Junior 1 scholarship. A. Kechad thanks the Fondation du Centre Hospitalier Universitaire Sainte-Justine/Fondation des Étoiles and the FRQS for graduate fellowships. This work was supported by grants from the Canadian Institutes of Health Research (MOP-97788), the Canadian Fund for Innovation, and the FRQS to G.R.X. Hickson.

4.9. References

Adam, J.C., J.R. Pringle, and M. Peifer. 2000. Evidence for functional differentiation among Drosophila septins in cytokinesis and cellularization. Mol. Biol. Cell. 11:3123–3135. http://dx.doi.org/10.1091/mbc.11.9.3123

Agromayor, M., J.G. Carlton, J.P. Phelan, D.R. Matthews, L.M. Carlin, S. Ameer-Beg, K. Bowers, and J. Martin-Serrano. 2009. Essential role of hIST1 in cytokinesis. Mol. Biol. Cell. 20:1374–1387. http://dx.doi.org/10.1091/mbc.E08-05-0474

Albertson, R., B. Riggs, and W. Sullivan. 2005. Membrane traffic: a driving force in cytokinesis. Trends Cell Biol. 15:92–101. http://dx.doi.org/10.1016/j.tcb.2004.12.008

Barr, F.A., and U. Gruneberg. 2007. Cytokinesis: placing and making the final cut. Cell. 131:847–860. http://dx.doi.org/10.1016/j.cell.2007.11.011

Bassi, Z.I., K.J. Verbrugghe, L. Capalbo, S. Gregory, E. Montembault, D.M. Glover, and P.P. D'Avino. 2011. Sticky/Citron Kinase maintains proper RhoA localization at the cleavage site during cytokinesis. J. Cell Biol. 195:595–603. http://dx.doi.org/10.1083/jcb.201105136

Bassi, Z.I., M. Audusseau, M.G. Riparbelli, G. Callaini, and P.P. D'Avino. 2013. Citron Kinase controls a molecular network required for midbody formation in cytokinesis. Proc. Natl. Acad. Sci. USA. 110:9782–9787. http://dx.doi.org/10.1073/pnas.1301328110

Bement, W.M., H.A. Benink, and G. von Dassow. 2005. A microtubule-dependent zone of active RhoA during cleavage plane specification. J. Cell Biol. 170:91–101. http://dx.doi.org/10.1083/jcb.200501131

Carlton, J.G., A. Caballe, M. Agromayor, M. Kloc, and J. Martin-Serrano. 2012. ESCRT-III governs the Aurora B-mediated abscission checkpoint through CHMP4C. Science. 336:220–225. http://dx.doi.org/10.1126/science.1217180

Carvalho, A., A. Desai, and K. Oegema. 2009. Structural memory in the contractile ring makes the duration of cytokinesis independent of cell size. Cell. 137:926–937. http://dx.doi.org/10.1016/j.cell.2009.03.021

D'Avino, P.P. 2009. How to scaffold the contractile ring for a safe cytokinesis - lessons from Anillin-related proteins. J. Cell Sci. 122:1071–1079. http://dx.doi.org/10.1242/jcs.034785

D'Avino, P.P., M.S. Savoian, and D.M. Glover. 2004. Mutations in sticky lead to defective organization of the contractile ring during cytokinesis and are enhanced by Rho and suppressed by Rac. J. Cell Biol. 166:61–71. http://dx.doi.org/10.1083/jcb.200402157

D'Avino, P.P., T. Takeda, L. Capalbo, W. Zhang, K.S. Lilley, E.D. Laue, and D.M. Glover. 2008. Interaction between Anillin and RacGAP50C connects the actomyosin contractile ring with spindle microtubules at the cell division site. J. Cell Sci. 121:1151–1158. http://dx.doi.org/10.1242/jcs.026716

Dean, S.O., and J.A. Spudich. 2006. Rho kinase's role in myosin recruitment to the equatorial cortex of mitotic Drosophila S2 cells is for myosin regulatory light chain phosphorylation. PLoS ONE. 1:e131. http://dx.doi.org/10.1371/journal.pone.0000131

Di Cunto, F., S. Imarisio, E. Hirsch, V. Broccoli, A. Bulfone, A. Migheli, C. Atzori, E. Turco, R. Triolo, G.P. Dotto, et al. 2000. Defective neurogenesis in Citron Kinase knockout mice by altered cytokinesis and massive apoptosis. Neuron. 28:115–127. http://dx.doi.org/10.1016/S0896-6273(00)00090-8

Di Cunto, F.D., S. Imarisio, P. Camera, C. Boitani, F. Altruda, and L. Silengo. 2002. Essential role of Citron Kinase in cytokinesis of spermatogenic precursors. J. Cell Sci. 115:4819–4826. http://dx.doi.org/10.1242/jcs.00163

Dorn, J.F., and A.S. Maddox. 2011. Cytokinesis: cells go back and forth about division. Curr. Biol. 21:R848–R850. http://dx.doi.org/10.1016/j.cub.2011.09.012

Dubreuil, V., A.M. Marzesco, D. Corbeil, W.B. Huttner, and M. Wilsch-Bräuninger. 2007. Midbody and primary cilium of neural progenitors release extracellular membrane particles enriched in the stem cell marker prominin-1. J. Cell Biol. 176:483–495. http://dx.doi.org/10.1083/jcb.200608137

Echard, A., G.R. Hickson, E. Foley, and P.H. O'Farrell. 2004. Terminal cytokinesis events uncovered after an RNAi screen. Curr. Biol. 14:1685–1693. http://dx.doi.org/10.1016/j.cub.2004.08.063 Eda, M., S. Yonemura, T. Kato, N. Watanabe, T. Ishizaki, P. Madaule, and S.

Narumiya. 2001. Rho-dependent transfer of Citron-kinase to the cleavage furrow of dividing cells. J. Cell Sci. 114:3273–3284.

Eggert, U.S., T.J. Mitchison, and C.M. Field. 2006. Animal cytokinesis: from parts list to mechanisms. Annu. Rev. Biochem. 75:543–566. http://dx.doi.org/10.1146/annurev.biochem.74.082803.133425

Elia, N., R. Sougrat, T.A. Spurlin, J.H. Hurley, and J. Lippincott-Schwartz. 2011. Dynamics of endosomal sorting complex required for transport (ESCRT) machinery during cytokinesis and its role in abscission.

Proc. Natl. Acad. Sci. USA. 108:4846–4851. http://dx.doi.org/10.1073/pnas.1102714108

Field, C.M., and B.M. Alberts. 1995. Anillin, a contractile ring protein that cycles from the nucleus to the cell cortex. J. Cell Biol. 131:165–178. http://dx.doi.org/10.1083/jcb.131.1.165

Field, C.M., M. Coughlin, S. Doberstein, T. Marty, and W. Sullivan. 2005. Characterization of Anillin mutants reveals essential roles in septin localization and plasma membrane integrity. Development. 132:2849–2860. http://dx.doi.org/10.1242/dev.01843

Gai, M., P. Camera, A. Dema, F. Bianchi, G. Berto, E. Scarpa, G. Germena, and F. Di Cunto. 2011. Citron Kinase controls abscission through RhoA and Anillin. Mol. Biol. Cell. 22:3768–3778. http://dx.doi.org/10.1091/mbc.E10-12-0952

Gilden, J.K., S. Peck, Y.C. Chen, and M.F. Krummel. 2012. The septin cytoskeleton facilitates membrane retraction during motility and blebbing. J. Cell Biol. 196:103–114. http://dx.doi.org/10.1083/jcb.201105127

Glotzer, M. 2005. The molecular requirements for cytokinesis. Science. 307:1735–1739. http://dx.doi.org/10.1126/science.1096896

Goldbach, P., R. Wong, N. Beise, R. Sarpal, W.S. Trimble, and J.A. Brill. 2010. Stabilization of the actomyosin ring enables spermatocyte cytokinesis in Drosophila. Mol. Biol. Cell. 21:1482–1493. http://dx.doi.org/10.1091/mbc.E09-08-0714

Green, R.A., E. Paluch, and K. Oegema. 2012. Cytokinesis in animal cells. Annu. Rev. Cell Dev. Biol. 28:29–58. http://dx.doi.org/10.1146/annurevcellbio-101011-155718

Gregory, S.L., S. Ebrahimi, J. Milverton, W.M. Jones, A. Bejsovec, and R. Saint. 2008. Cell division requires a direct link between microtubule-bound RacGAP and Anillin in the contractile ring. Curr. Biol. 18:25–29. http://dx.doi.org/10.1016/j.cub.2007.11.050

Gruneberg, U., R. Neef, X. Li, E.H. Chan, R.B. Chalamalasetty, E.A. Nigg, and F.A. Barr. 2006. KIF14 and Citron Kinase act together to promote efficient cytokinesis. J. Cell Biol. 172:363–372. http://dx.doi.org/10.1083/jcb.200511061

Haglund, K., I.P. Nezis, and H. Stenmark. 2011. Structure and functions of stable intercellular bridges formed by incomplete cytokinesis during development. Commun. Integr. Biol. 4:1–9.

Hickson, G.R., and P.H. O'Farrell. 2008a. Anillin: a pivotal organizer of the cytokinetic machinery. Biochem. Soc. Trans. 36:439–441. http://dx.doi.org/10.1042/BST0360439

Hickson, G.R., and P.H. O'Farrell. 2008b. Rho-dependent control of Anillin behavior during cytokinesis. J. Cell Biol. 180:285–294. http://dx.doi.org/10.1083/jcb.200709005

Hu, C.K., M. Coughlin, and T.J. Mitchison. 2012. Midbody assembly and its regulation during cytokinesis. Mol. Biol. Cell. 23:1024–1034. http://dx.doi.org/10.1091/mbc.E11-08-0721

Kechad, A., S. Jananji, Y. Ruella, and G.R. Hickson. 2012. Anillin acts as a bifunctional linker coordinating midbody ring biogenesis during cytokinesis. Curr. Biol. 22:197–203. http://dx.doi.org/10.1016/j.cub.2011.11.062

Liu, J., G.D. Fairn, D.F. Ceccarelli, F. Sicheri, and A. Wilde. 2012. Cleavage furrow organization requires PIP(2)-mediated recruitment of Anillin. Curr. Biol. 22:64–69. http://dx.doi.org/10.1016/j.cub.2011.11.040

Madaule, P., M. Eda, N. Watanabe, K. Fujisawa, T. Matsuoka, H. Bito, T. Ishizaki, and S. Narumiya. 1998. Role of Citron Kinase as a target of the small GTPase Rho in cytokinesis. Nature. 394:491–494. http://dx.doi.org/10.1038/28873

McKay, H.F., and D.R. Burgess. 2011. 'Life is a highway': membrane trafficking during cytokinesis. Traffic. 12:247–251. http://dx.doi.org/10.1111/j.1600-0854.2010.01139.x

Mullins, J.M., and J.J. Biesele. 1977. Terminal phase of cytokinesis in D-98s cells. J. Cell Biol. 73:672–684. http://dx.doi.org/10.1083/jcb.73.3.672

Naim, V., S. Imarisio, F. Di Cunto, M. Gatti, and S. Bonaccorsi. 2004. Drosophila Citron Kinase is required for the final steps of cytokinesis. Mol. Biol. Cell.15:5053–5063. http://dx.doi.org/10.1091/mbc.E04-06-0536

Neto, H., L.L. Collins, and G.W. Gould. 2011. Vesicle trafficking and membrane remodelling in cytokinesis. Biochem. J. 437:13–24. http://dx.doi.org/10.1042/BJ20110153

Neufeld, T.P., and G.M. Rubin. 1994. The Drosophila Peanut gene is required for cytokinesis and encodes a protein similar to yeast putative bud neck filament proteins. Cell. 77:371–379. http://dx.doi.org/10.1016/0092-8674(94)90152-X

Oegema, K., M.S. Savoian, T.J. Mitchison, and C.M. Field. 2000. Functional analysis of a human homologue of the Drosophila actin binding protein Anillin suggests a role in cytokinesis. J. Cell Biol. 150:539–552. http://dx.doi.org/10.1083/jcb.150.3.539

Piekny, A.J., and M. Glotzer. 2008. Anillin is a scaffold protein that links RhoA, actin, and myosin during cytokinesis. Curr. Biol. 18:30–36.http://dx.doi.org/10.1016/j.cub.2007.11.068

Piekny, A.J., and A.S. Maddox. 2010. The myriad roles of Anillin during cytokinesis. Semin. Cell Dev. Biol. 21:881–891. http://dx.doi.org/10.1016/j.semcdb.2010.08.002

Pollard, T.D. 2010. Mechanics of cytokinesis in eukaryotes. Curr. Opin. Cell Biol. 22:50–56. http://dx.doi.org/10.1016/j.ceb.2009.11.010

Riedl, J., A.H. Crevenna, K. Kessenbrock, J.H. Yu, D. Neukirchen, M. Bista, F. Bradke, D. Jenne, T.A. Holak, Z. Werb, et al. 2008. Lifeact: a versatile marker to visualize F-Actin. Nat. Methods. 5:605–607. http://dx.doi.org/10.1038/nmeth.1220

Schroeder, T.E. 1972. The contractile ring. II. Determining its brief existence, volumetric changes, and vital role in cleaving Arbacia eggs. J. Cell Biol. 53:419–434. http://dx.doi.org/10.1083/jcb.53.2.419

Sedzinski, J., M. Biro, A. Oswald, J.Y. Tinevez, G. Salbreux, and E. Paluch. 2011. Polar actomyosin contractility destabilizes the position of the cytokinetic furrow. Nature. 476:462–466. http://dx.doi.org/10.1038/nature10286

Shandala, T., S.L. Gregory, H.E. Dalton, M. Smallhorn, and R. Saint. 2004. Citron Kinase is an essential effector of the Pbl-activated Rho signalling pathway in Drosophila melanogaster. Development. 131:5053–5063. http://dx.doi.org/10.1242/dev.01382

Smurnyy, Y., A.V. Toms, G.R. Hickson, M.J. Eck, and U.S. Eggert. 2010. Binucleine 2, an isoform-specific inhibitor of Drosophila Aurora B kinase, provides insights into the mechanism of cytokinesis. ACS Chem. Biol. 5:1015–1020. http://dx.doi.org/10.1021/cb1001685

Somma, M.P., B. Fasulo, G. Cenci, E. Cundari, and M. Gatti. 2002. Molecular dissection of cytokinesis by RNA interference in Drosophila cultured cells. Mol. Biol. Cell. 13:2448–2460. http://dx.doi.org/10.1091/mbc.01-12-0589

Steigemann, P., and D.W. Gerlich. 2009. Cytokinetic abscission: cellular dynamics at the midbody. Trends Cell Biol. 19:606–616. http://dx.doi.org/10.1016/j.tcb.2009.07.008

Straight, A.F., C.M. Field, and T.J. Mitchison. 2005. Anillin binds nonmuscle myosin II and regulates the contractile ring. Mol. Biol. Cell. 16:193–201. http://dx.doi.org/10.1091/mbc.E04-08-0758

Tanaka-Takiguchi, Y., M. Kinoshita, and K. Takiguchi. 2009. Septin-mediated uniform bracing of phospholipid membranes. Curr. Biol. 19:140–145. http://dx.doi.org/10.1016/j.cub.2008.12.030

Watanabe, S., T. De Zan, T. Ishizaki, and S. Narumiya. 2013. Citron Kinase mediates transition from constriction to abscission through its coiled-coil domain. J. Cell Sci. 126:1773–1784. http://dx.doi.org/10.1242/jcs.116608

Yamashiro, S., G. Totsukawa, Y. Yamakita, Y. Sasaki, P. Madaule, T. Ishizaki, S. Narumiya, and F. Matsumura. 2003. Citron Kinase, a Rho-dependent kinase, induces di-phosphorylation of regulatory light chain of myosin II. Mol. Biol. Cell. 14:1745–1756. http://dx.doi.org/10.1091/mbc.E02-07-0427

Zhao, W.M., and G. Fang. 2005. Anillin is a substrate of anaphase-promoting complex/cyclosome (APC/C) that controls spatial contractility of myosin during late cytokinesis. J. Biol. Chem. 280:33516–33524. http://dx.doi.org/10.1074/jbc.M504657200

4.10. Figures and legends

El Amine Fig. 1

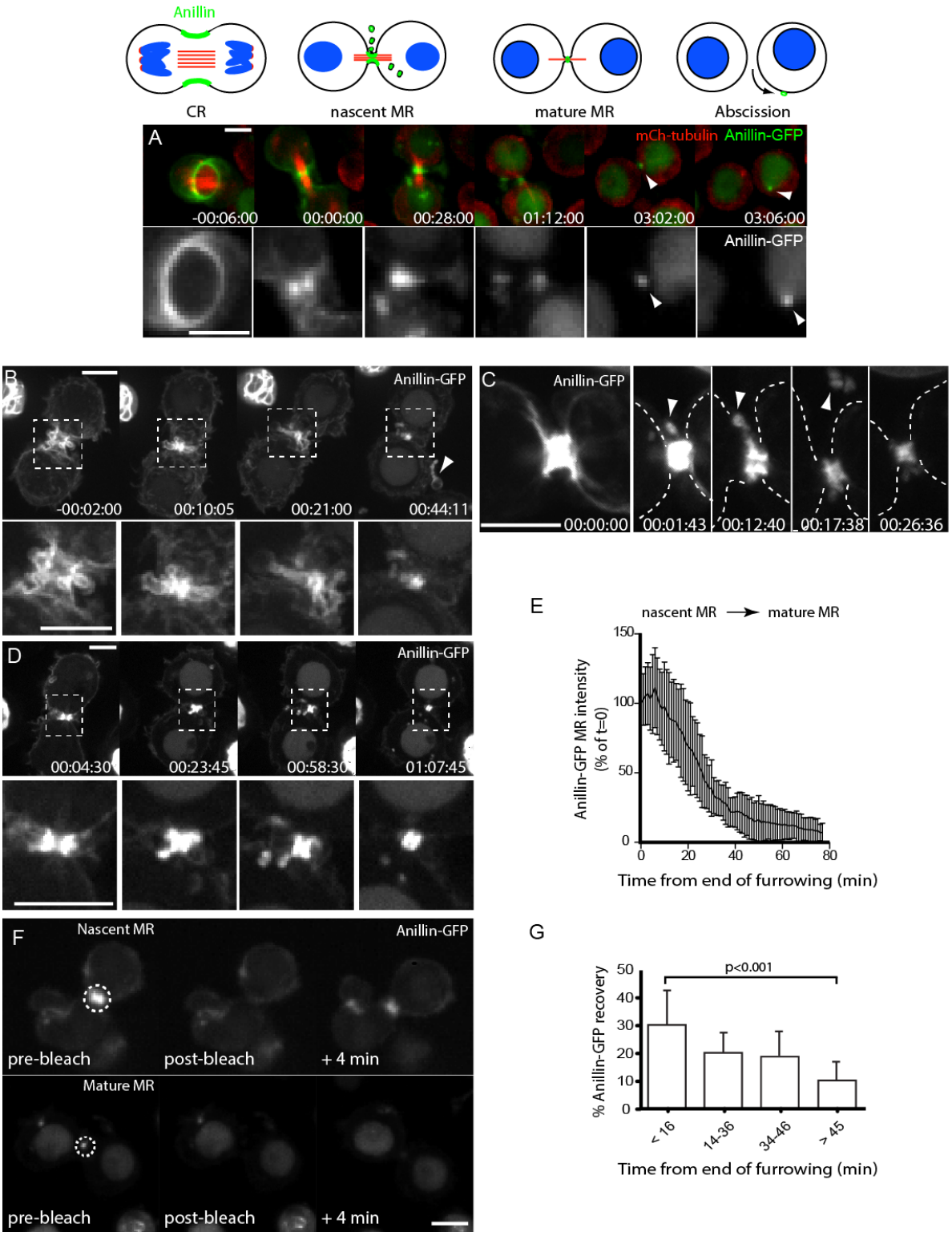

Figure 1. Maturation of the MR is accompanied by both removal and retention of Anillin.

(A) Time-lapse sequence of a cell expressing Anillin-GFP and mCh-tubulin (40× objective). Arrowheads mark the mature MR before and after abscission MR release. (B–D) Time-lapse sequence of cells expressing Anillin-GFP and mCh-tubulin (not depicted) acquired with 40× objective, showing extrusion and shedding (B and C) and internalization (D). Boxed regions in B and D are shown magnified at the bottom; dashed lines in C mark the cell boundary; arrowheads mark shed material. (E) Relative Anillin-GFP fluorescence (sum intensity) at nascent MRs measured from the end of furrowing (means ± SD; $n = 20$). (F) FRAP experiments of nascent and mature MRs, showing images acquired immediately before (prebleach), after (bleach), and 4 min after high-intensity illumination of the outlined region of interest (63× objective and 2 × 2 camera binning). (G) The percent recovery of GFP fluorescence within 4 min of bleaching is shown for MRs of different ages ($n = 9–17$ each, means ± SD). P-value is for an unpaired *t* test. Times are hours, minutes, and seconds from the end of furrowing. Bars, 5 μm. See also Videos 1 and 2.

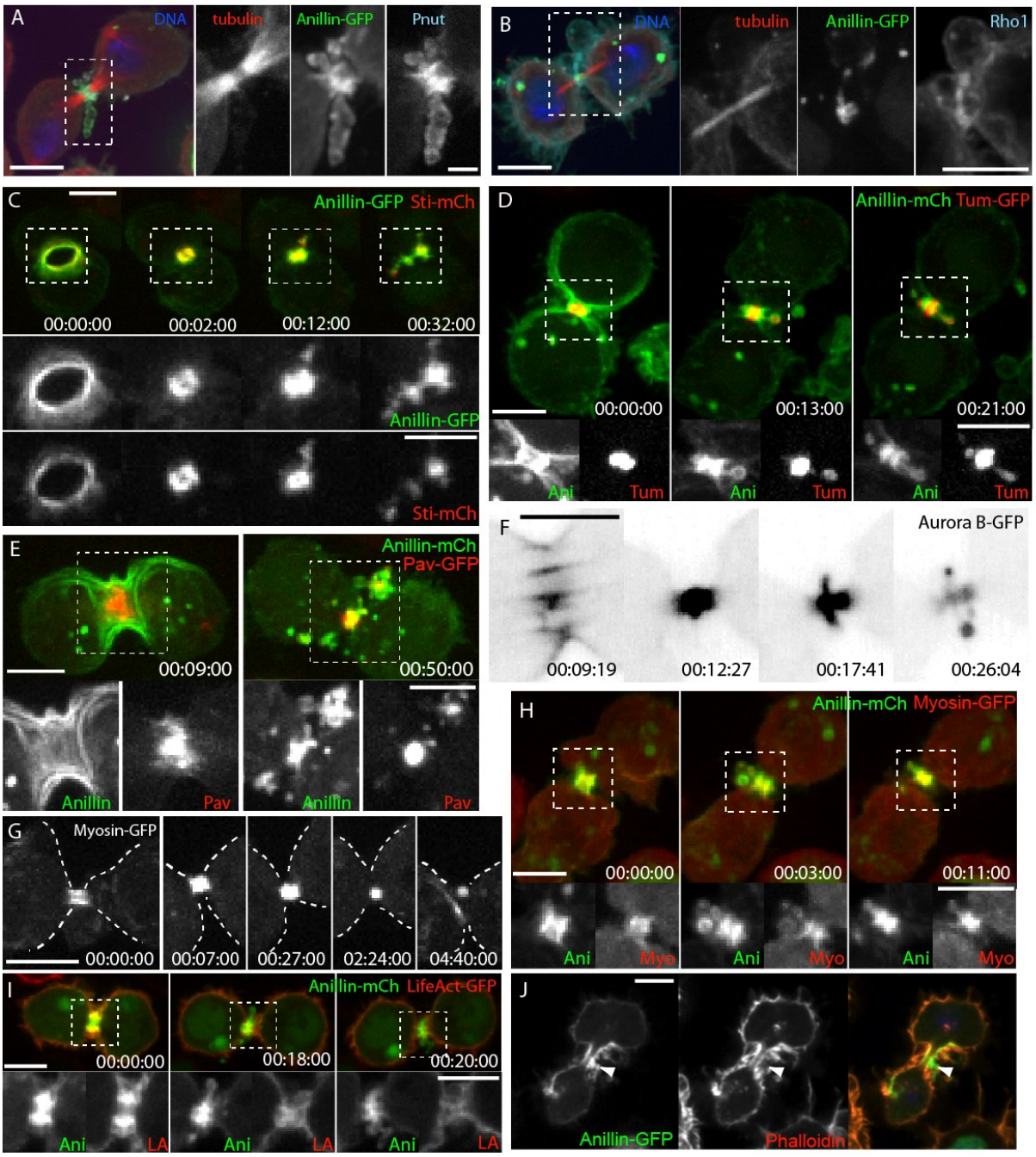

Figure 2. Nascent MRs shed numerous CR components, except F-Actin.

(A and B) Fixed cells expressing Anillin-GFP and tubulin-mCh stained for anti-Pnut (A) and anti-Rho1 (B) by immunofluorescence. Separated channels of boxed regions are shown

magnified on the right. (C) Cell expressing Anillin-GFP and Sticky (Sti)-mCh. (D) Cell expressing Anillin-mCh and Tum-GFP. (E) Cell expressing Anillin-mCh and Pavarotti (Pav)-GFP. (F) Inverted look-up table of the nascent MR of an Aurora B–GFP-expressing cell. (G) The nascent MR of a myosin-GFP–expressing cell. Dashed lines mark the cell boundary. (H) The nascent MR of a cell expressing myosin-GFP (Myo) and Anillin-mCh (Ani). (I) The nascent MR of a cell expressing LifeAct-GFP (LA) and Anillin-mCh. (C, D, E, H, and I) Separated channels of boxed regions are shown magnified at the bottom. (J) The nascent MR of a cell expressing Anillin-GFP fixed and stained with rhodamine-phalloidin. Arrowhead points to an extrusion enriched in Anillin-GFP but lacking actin. Times are hours, minutes, and seconds. Bars: (A [main image] and B–J) 5 μm; (A, magnified images) 1 μm. See also Video 3.

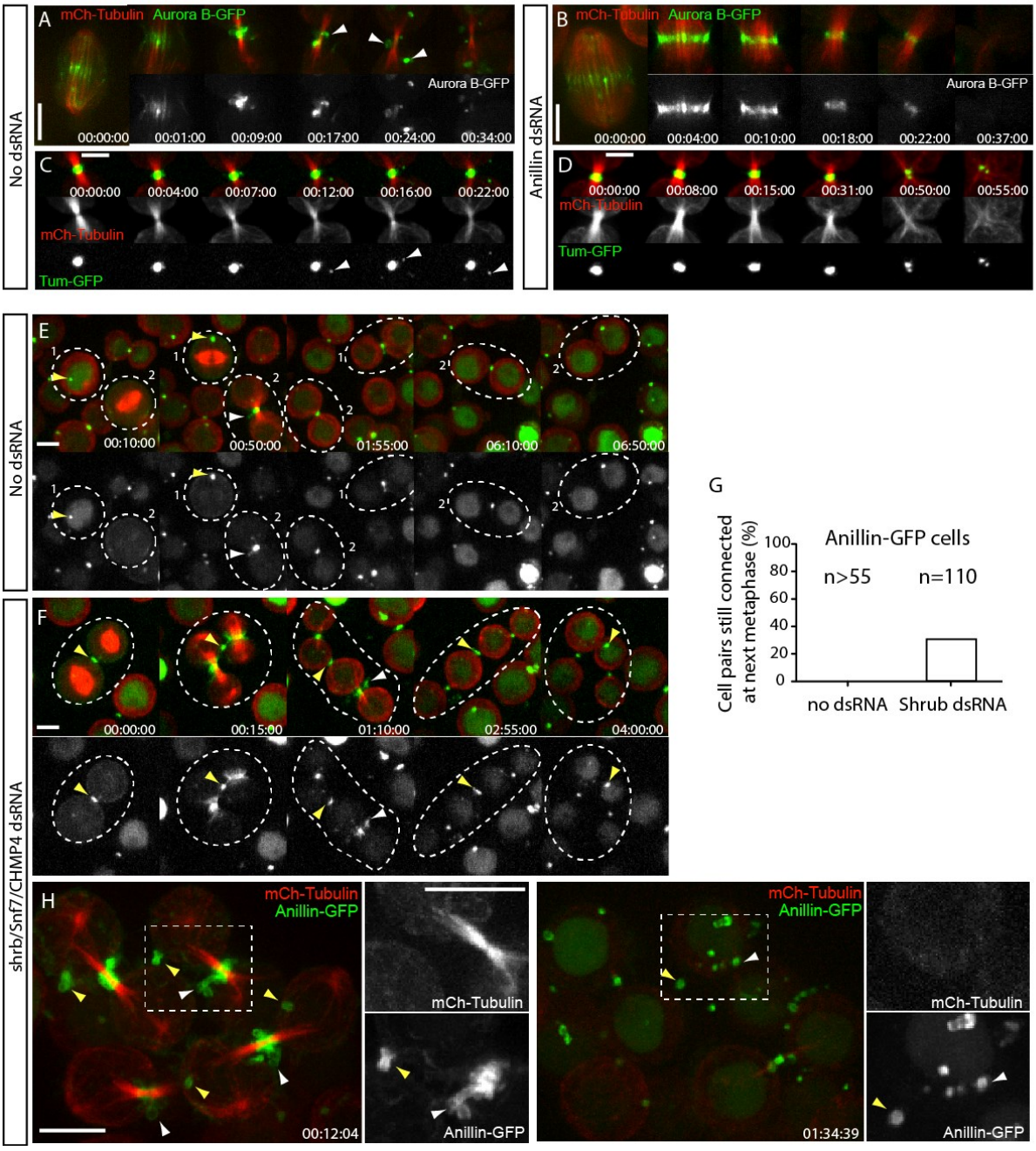

Figure 3. Shedding from the nascent MR requires Anillin but not ESCRT-III.

(A and B) Time-lapse sequence of cells expressing Aurora B–GFP and mCh-tubulin after a 3-d incubation without (A) or with (B) Anillin dsRNAs, acquired with a 100×, 1.4 NA objective. Arrowheads in A mark shedding events. (C and D) Time-lapse sequence of cells expressing Tum-GFP and mCh-tubulin after a 3-d incubation without (C) or with (D) Anillin dsRNAs.

Arrowheads in C mark shedding events. (E and F) Selected frames from a time-lapse sequence of Anillin-GFP cells after a 4-d incubation without (E) or with (F) *shrub* dsRNAs, acquired with a 40× objective. Dotted circles highlight sister cells; yellow arrowheads mark mature MRs/MR remnants from previous divisions; and white arrowheads mark MRs from the current division. (G) Quantification of Anillin-GFP–expressing cells that have failed to undergo abscission and thus remain paired at metaphase in control and Shrub-depleted cells. Data are from two independent experiments. (H) Selected frames from a time-lapse sequence of Anillin-GFP cells, acquired with a 100× objective, after a 4-d incubation with *shrub* dsRNAs. Boxed regions are shown magnified and with separated channels on the right; yellow arrowheads mark mature MRs from previous divisions; and white arrowheads mark nascent MRs from the current division that are shedding Anillin-GFP. Times are given in hours, minutes, and seconds. Bars, 5 μm. See also Video 4.

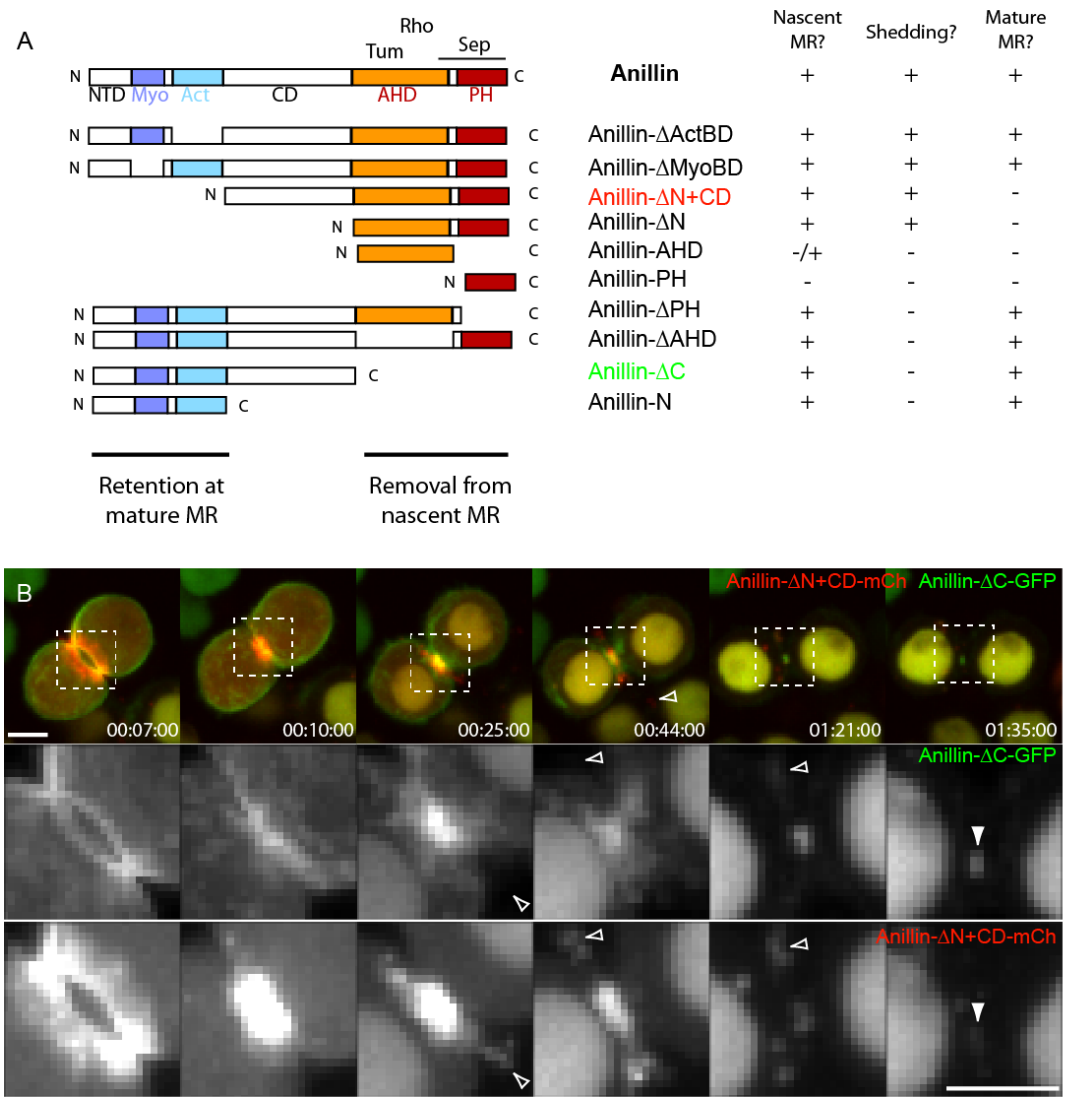

Figure 4. Removal of Anillin from the nascent MR is mediated via its C-terminal domains, whereas retention requires its N-terminal domains.

(A) Domain organization of Anillin and truncation mutant analyses for their localization to the nascent MR, their ability to be extruded and shed, and their retention at the mature MR. Myo, myosin; Act, actin; NTD, N-terminal domain; Sep, septin; C, C terminus; N, N terminus. (B) Time-lapse sequence of a cell coexpressing Anillin-ΔC-GFP and Anillin-ΔN+CD-mCh. Open arrowheads mark shed material, and closed arrowheads mark the mature MR. Separated channels and magnified images of the boxed regions are shown at the bottom. Times are given in hours, minutes, and seconds. Bars, 5 µm. See also Video 5.

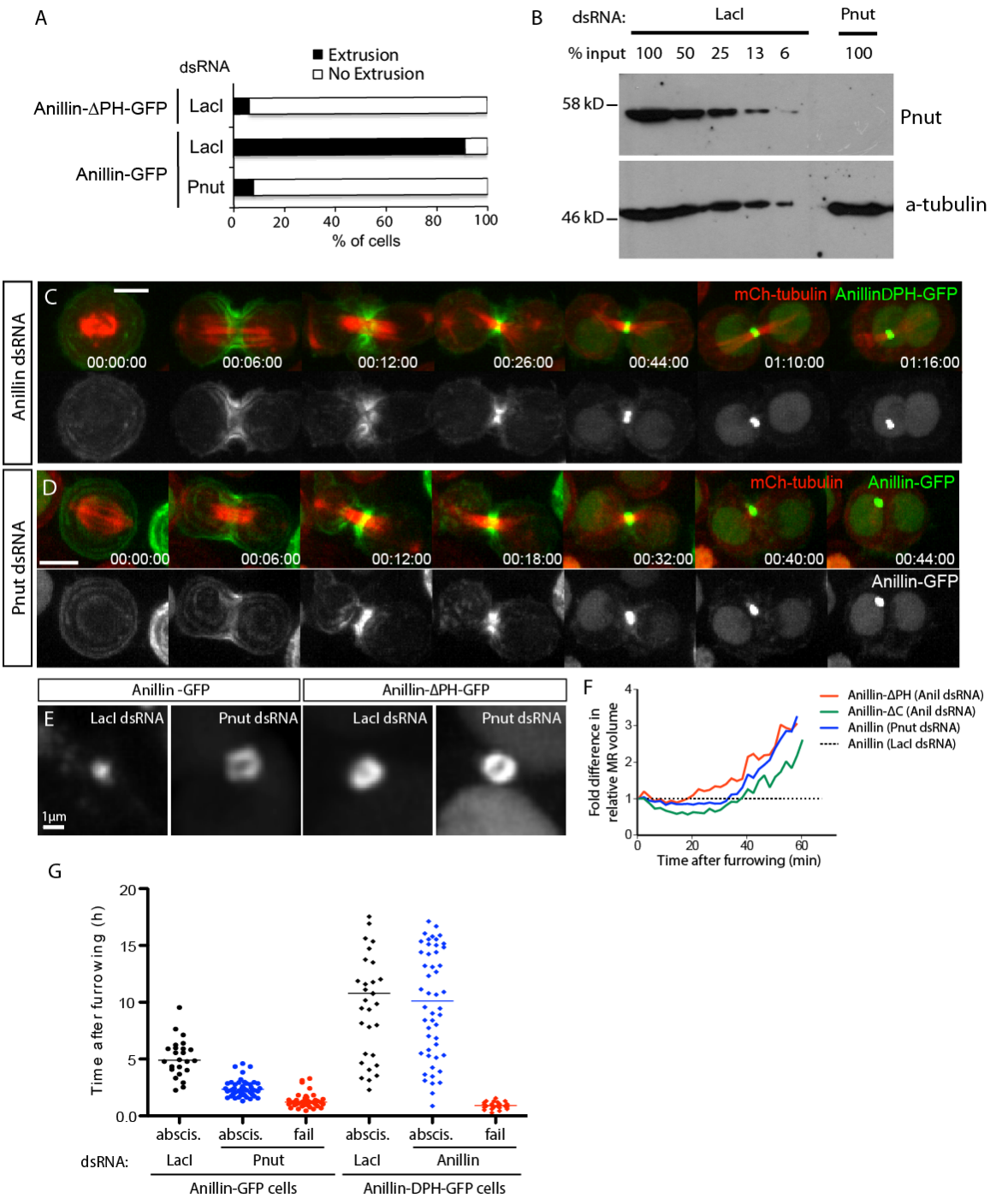

Figure 5. Proper maturation of the MR requires septin-dependent removal of Anillin via its C-terminal PHD.

(A) Frequency of extrusion from time-lapse sequences of Anillin-ΔPH-GFP and of Anillin-GFP after 8-d Pnut RNAi. (B) Anti-Pnut immunoblot of S2 cell lysates serially diluted after LacI control dsRNA incubation or after Pnut dsRNA incubation; anti-tubulin is the loading control. (C) Time-lapse sequences of cells expressing Anillin-ΔPH-GFP depleted of endogenous Anillin. (D) Time-lapse sequence of an Anillin-GFP–expressing cell after 8-d Pnut RNAi. (E) Representative images of age-matched MR structures from Anillin-GFP or Anillin-ΔPH-GFP cells treated with the indicated dsRNAs. (F) Volume measurements of the nascent MR of cells expressing Anillin-ΔPH-GFP, Anillin-ΔC-GFP, or Anillin-GFP treated with the indicated dsRNAs, from the end of furrowing, normalized at each time point to equivalently aged Anillin-GFP controls (n = 10 per condition from two independent experiments). (G) Timing of abscission (abscis.) or furrow regression (fail) of Anillin-GFP cells treated for 7–9 d with LacI (control, n = 30) or Pnut dsRNAs (n = 75) and of Anillin-ΔPH-GFP cells treated for 3 d with LacI (control, n = 30) or Anillin dsRNAs (n = 75). Mean values are shown; data are from a single representative experiment out of three repeats. Times are given in hours, minutes, and seconds. Bars: (C and D) 5 µm; (E) 1 µm.

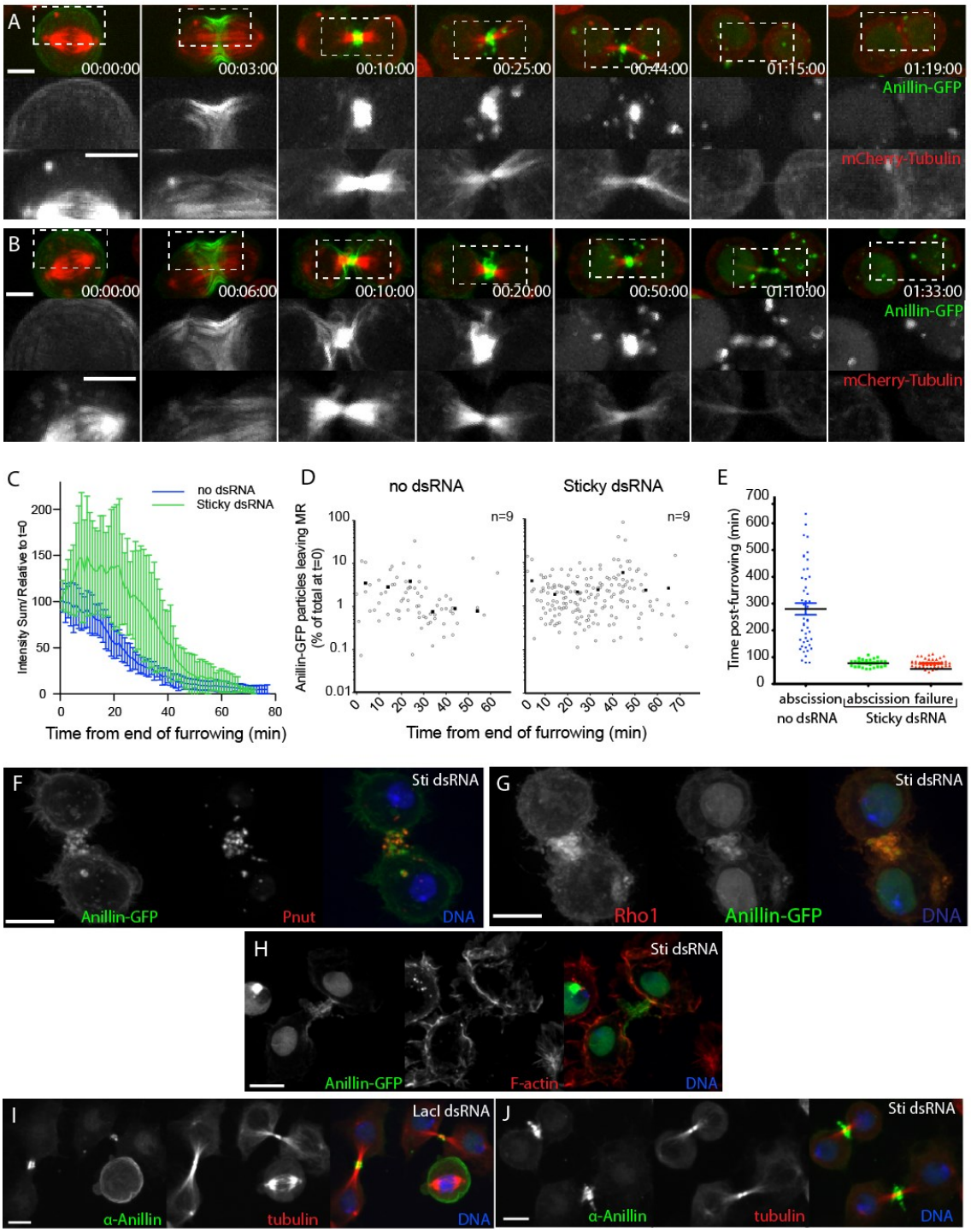

Figure 6. Sticky acts to limit extrusion/shedding and retain Anillin at the MR.

(A and B) Sticky-depleted cells expressing Anillin-GFP and mCh-tubulin failing cytokinesis (A) or prematurely abscising (B) (63× objective). Boxed regions are shown magnified and with separated channels below. (C) Quantification of relative Anillin-GFP intensities (sum intensity) at the MR from the time of midbody formation in control (n = 9) and Sticky-depleted cells (n = 17). (D) Quantification of individual extrusion or internalization events (open circles) plotted as a function of time and associated Anillin-GFP $\log_{10}$ intensity (as a measure of total intensity at the close of furrowing, t = 0). Closed circles represent mean values for each 10-min interval (n = 9 cells each, from one experiment representative of two repeats). (E) Timing of abscission or furrow regression (failure) events of individual Anillin-GFP cells treated for 30–48 h with or without Sticky dsRNAs. Data are from two independent experiments, horizontal lines mark the mean times, and error bars show the SDs. (F–H) Confocal images of Sticky-depleted cells expressing Anillin-GFP (left), stained for Pnut (F, center), Rho1 (G, left), or F-actin (H, center) and DNA. (I and J) Confocal images of untransfected S2 cells treated with LacI control dsRNA (I) or Sticky dsRNA (J) and stained for endogenous Anillin (left), tubulin (center), and DNA (63× objective). Times are given in hours, minutes, and seconds. Bars, 5 µm. See also Videos 6 and 7.

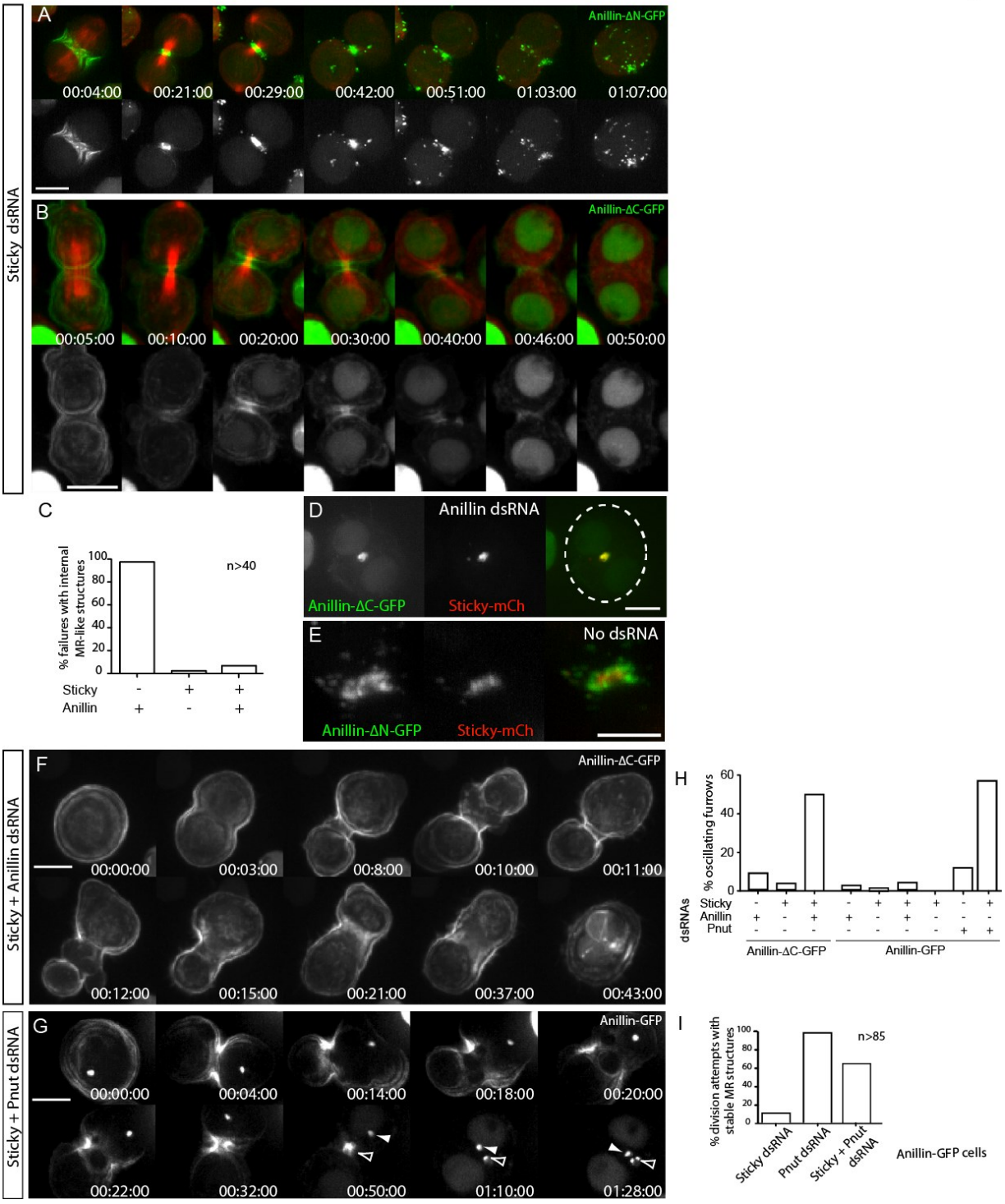

Figure 7. Sticky acts with the N terminus of Anillin to promote both MR formation and CR stability.

(A and B) Time-lapse sequence of cells expressing mCh-tubulin and Anillin-ΔN-GFP (A) or Anillin-ΔC-GFP (B) after a ∼30-h incubation with Sticky dsRNAs (63× objective and 2 × 2 camera binning). (C) Quantification from time-lapse records of failed attempts at cytokinesis that form internal Anillin-ΔC-FP–positive MR-like structures after incubation with the indicated dsRNAs. Data are from two independent experiments. (D and E) Confocal images of cells coexpressing Sticky-mCh and Anillin-ΔC-GFP (D) or Anillin-ΔN-GFP (E) after endogenous Anillin depletion. Dotted line in D marks the cell boundary (63× objective and no camera binning). (F) Time-lapse sequence of a cell expressing Anillin-ΔC after codepletion of Sticky and Anillin. (G) Time-lapse sequence of a cell expressing Anillin-GFP after codepletion of Pnut (144–162-h RNAi) and Sticky (30–48-h RNAi), captured with a 63× objective with 2 × 2 camera binning. Closed arrowheads mark a presumed MR remnant from a previous division. Open arrowheads mark failing MR from the current division attempt. (H) Quantification from time-lapse records (40× objective and 2 × 2 camera binning) of the percentage of Anillin-GFP and Anillin-ΔC-GFP cells displaying oscillating furrows during CR closure after incubation with the indicated dsRNAs ($n > 78$ per condition from two independent experiments). (I) Quantification from time-lapse records (40× objective and 2 × 2 camera binning) of attempts at cytokinesis that result in Anillin-GFP–positive MR structures after incubation with indicated dsRNAs ($n > 45$ per condition, from two independent experiments). Times are given in hours, minutes, and seconds. Bars, 5 µm. See also Video 8.

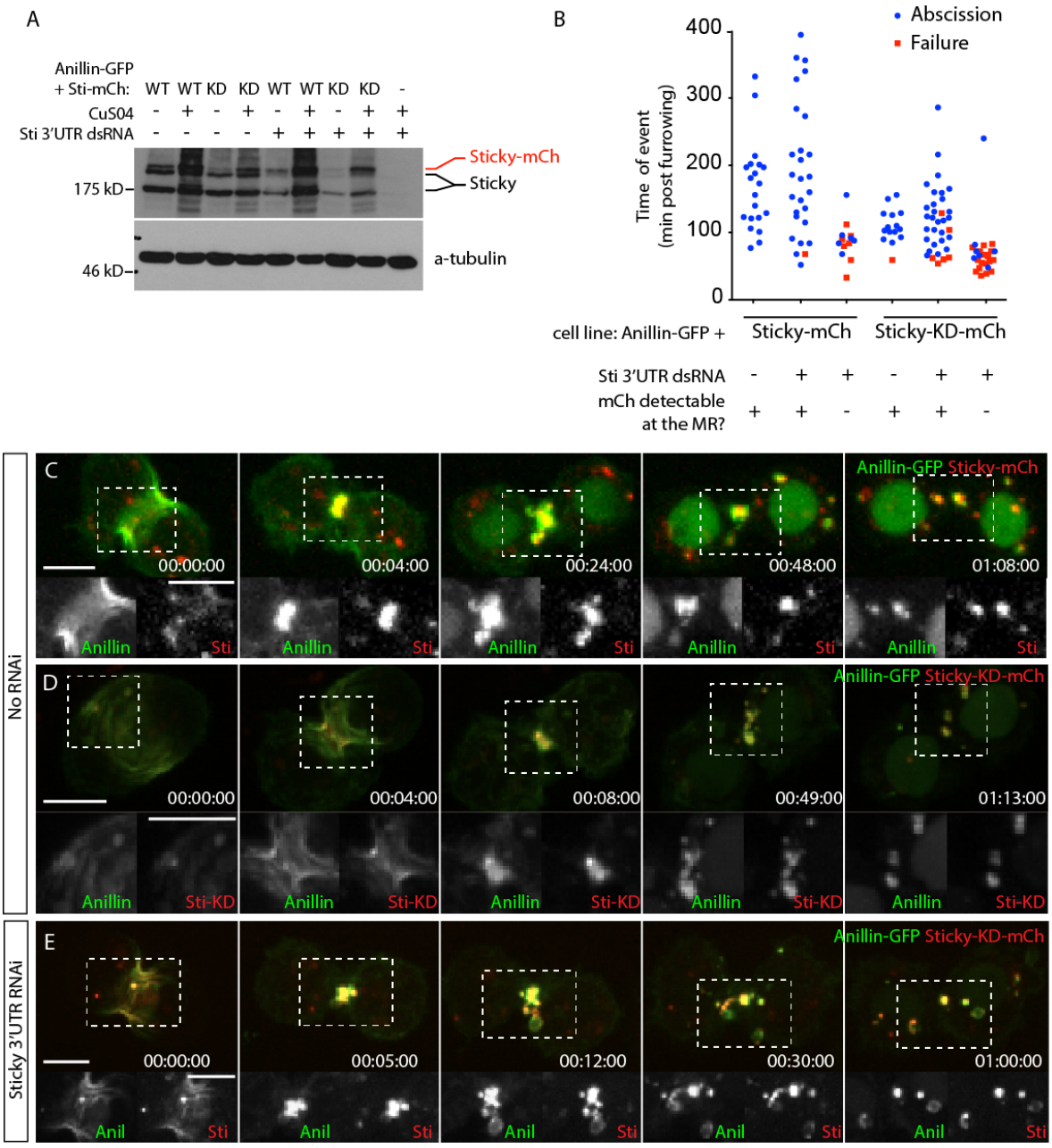

Figure 8. Sticky's essential role during MR formation is as a scaffold.

(A) Anti-Sticky (Sti) immunoblot of cell lysates from indicated cell lines after Sticky 3′ UTR dsRNA or LacI control dsRNA incubation, with anti-tubulin blot as a loading control. WT, wild type. (B) Timing of abscission or furrow regression (failure) of cells coexpressing Anillin-GFP

and Sticky-mCh or Sticky-KD-mCh, treated for 3–5 d with or without Sticky 3′ UTR dsRNAs. Data are from two independent experiments. (C and D) Time-lapse sequence of a cell coexpressing Anillin-GFP and Sticky-mCh (C) or Sticky-KD-mCh (D). Separated channels of the boxed regions are shown magnified at the bottom. (E) Time-lapse sequence of a cell coexpressing Anillin (Anil)-GFP and Sticky-KD-mCh after depletion of endogenous Sticky. Times are given in hours, minutes, and seconds. Bars, 5 µm. See also Videos 9 and 10.

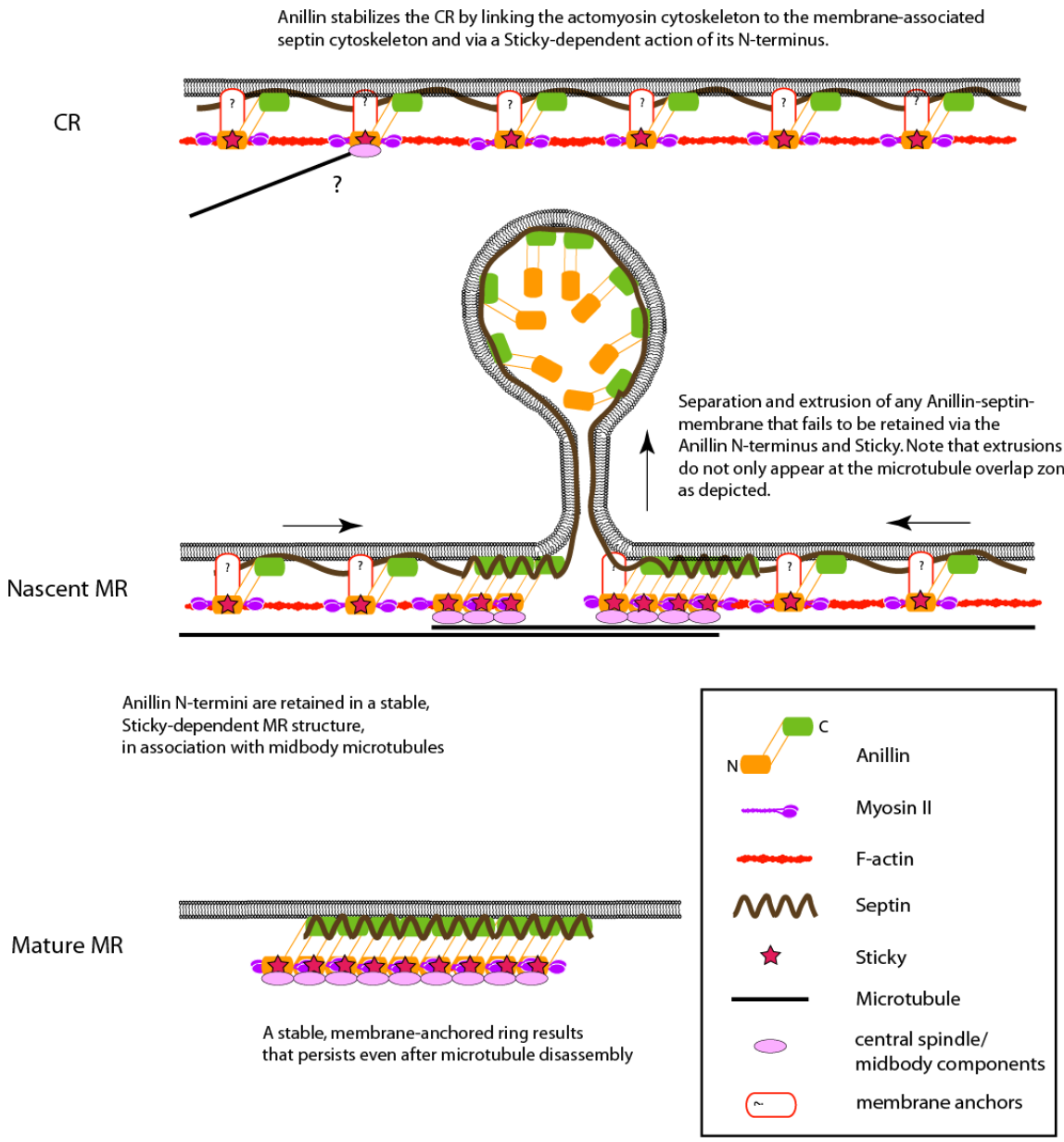

Figure 9. Model for the maturation of the CR and MR.

(top) At the CR stage, Anillin links the plasma membrane–associated septin cytoskeleton to actomyosin, stabilizing the furrow. Anillin also stabilizes the furrow via a separate Sticky-dependent action of its N terminus. (middle) At the nascent MR, Sticky, myosin, and the Anillin N terminus are retained at the midbody, where they will form a mature MR structure. Septins

act on the C terminus of Anillin to remove membrane-associated Anillin molecules, whose N termini are liberated upon disassembly of the F-actin ring. Note that this removal does not only occur at the center of the midbody as depicted. (bottom) Septins and the C termini of Anillin molecules that are retained also act as membrane anchors for the mature MR that persists beyond ~1 h after furrowing.

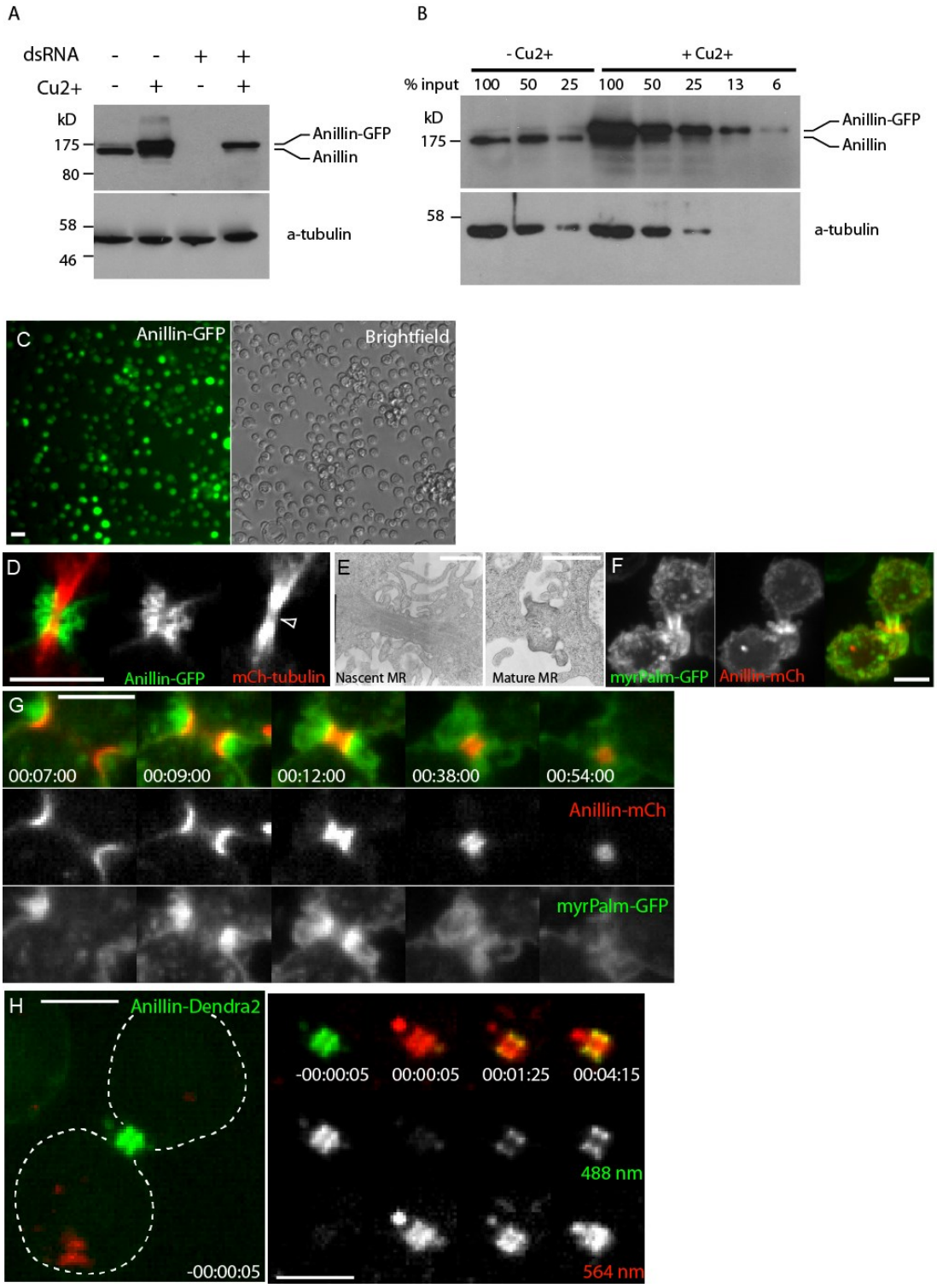

Figure S1. Anillin-FP expression and localization during MR maturation.

(A) Anti-Anillin immunoblot analysis of cell lysates after 3-d treatment with or without Anillin dsRNAs, with or without CuSO4 induction of Anillin-GFP. The same blot was cut and probed with an anti-tubulin antibody as a loading control. (B, top) Serial dilutions of Anillin-GFP cell lysates with or without CuSO4 induction, probed with anti-Anillin antibodies. (bottom) The same blot was cut and probed with an anti-tubulin antibody as a loading control. From this, it can be estimated that Anillin-GFP is expressed at approximately fourfold higher levels than endogenous Anillin, although we note that this is likely an overestimate in mitotic cells because endogenous Anillin expression is cell cycle regulated, accumulating in G2 (Field and Alberts, 1995), whereas Anillin-GFP expression is not. (C) Fluorescence and bright-field images of Anillin-GFP expression, showing that close to 100% of the cells express Anillin-GFP. (D) Single confocal sections of a nascent MR from a cell expressing Anillin-GFP and mCh-tubulin. Arrowhead marks the midbody region. (E) Transmission electron micrographs of Anillin-GFP–expressing S2 cells. (F and G) Single confocal sections of a nascent MR expressing Anillin-mCh and myrpalm-GFP. (H) Single confocal sections of Anillin-Dendra2–expressing nascent MR before and after photoconversion, imaged using both 488- and 564-nm light. Dotted lines mark the cell boundary, and separated channels of the MR region are shown at the right (63× objective and 2 × 2 camera binning used throughout, except in C, which is a 20× objective). Times are given in hours, minutes, and seconds. Bars: (C, D, and F–H) 5 μm; (E) 1 μm.

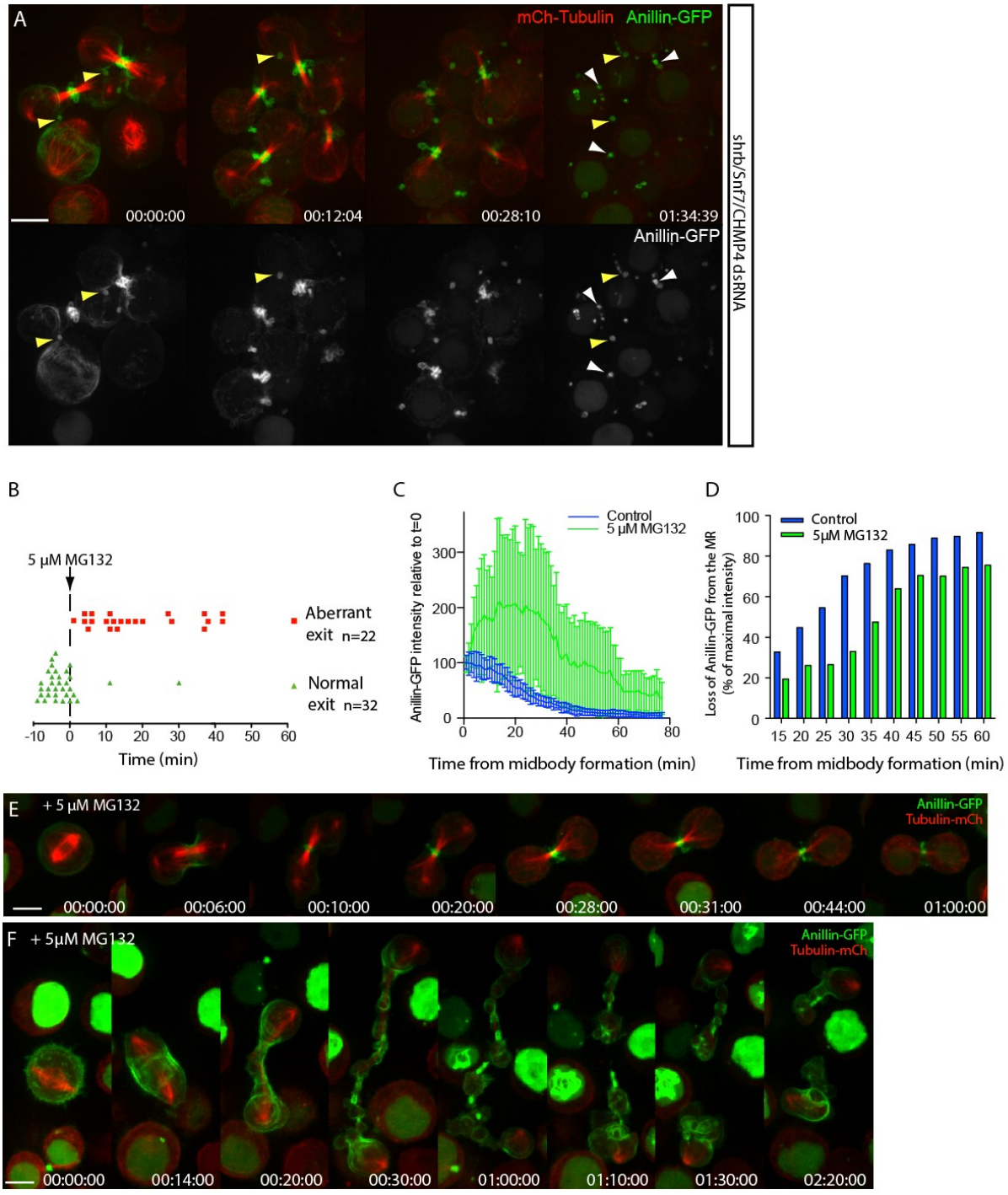

Figure S2. Additional cells treated with Shrub/CHMP4 dsRNAs or MG132.

(A) Anillin-GFP–expressing S2 cells incubated for 3 d with Shrub (shrb)/CHMP4 dsRNAs. Yellow arrowheads depict MR from a previous division that still connects sister cells. White

arrowheads depict shedding from the nascent MRs of the current division. Same cells as shown in Fig. 3 H. (B) Consequences of acute administration of 5 μM MG132 to mitotic cells expressing Anillin-GFP and mCh-tubulin. Points represent individual cells undergoing anaphase at the indicated times relative to MG132 addition. Data are from three independent experiments. (C) Changes in Anillin-GFP intensities at the MR in cells undergoing "normal" exit in the presence or absence of 5 μM MG132, relative to the time of midbody formation (t = 0; mean values ± SD; n = 14 and 11, respectively). (D) Anillin-GFP sum intensity values at the MR are plotted at 5-min intervals relative to the maximal sum intensity value for each cell, regardless of when during MR maturation this occurred. Mean values are shown for cells in the presence (n = 14) or absence (n = 11) of 5 μM MG132. Data are from three independent experiments. (E) Selected frames from a time-lapse sequence of an AnillinGFP cell in the presence of 5 μM MG132. (F) Example of an Anillin-GFP–expressing cell exhibiting aberrant mitotic exit and cytokinesis in the presence of 5 μM MG132 added just before the metaphase/anaphase transition. Times are given in hours, minutes, and seconds. Bars, 5 μm.

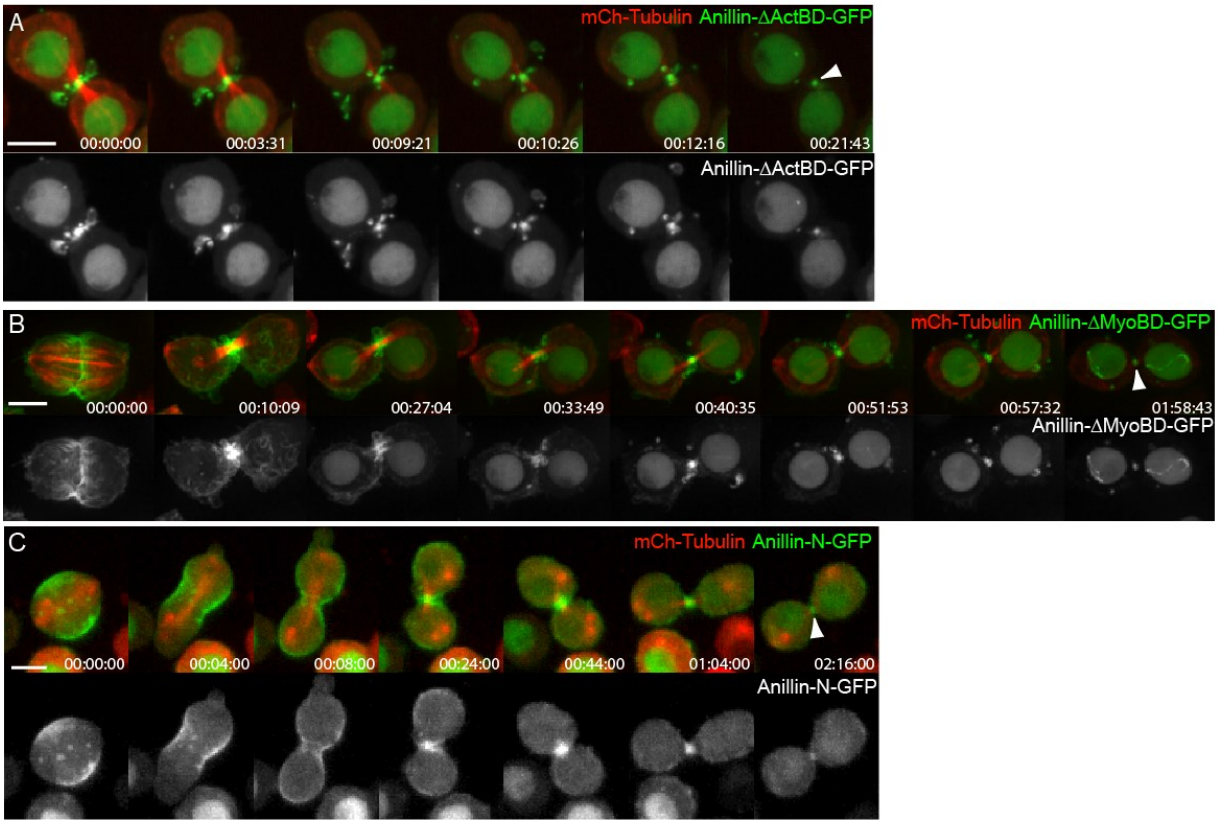

Figure S3. Behaviors of additional Anillin truncations during MR maturation.

(A) Cell coexpressing Anillin-ΔActBD-GFP and mCh-tubulin. (B) Cell coexpressing Anillin-ΔMyoBD-GFP and mCh-tubulin. (C) Cell coexpressing Anillin-N-GFP and mCh-tubulin. Arrowheads point to the mature MRs. Times are given in hours, minutes, and seconds. Bars, 5 µm.

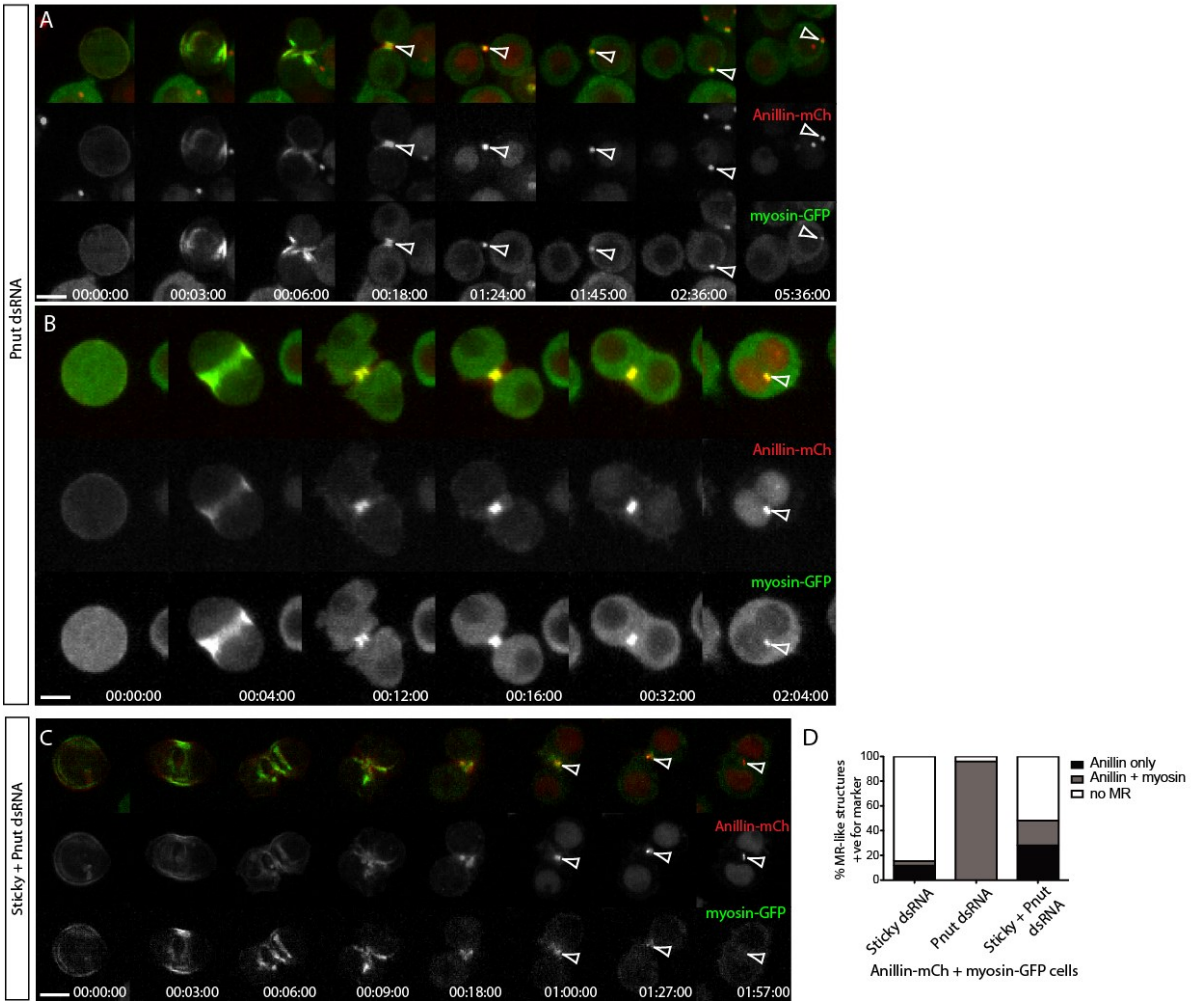

Figure S4. Codepletion of Sticky and Pnut disrupts MR formation.

(A–C) Time-lapse sequences of cells coexpressing Anillin-mCh and myosin-GFP attempting cytokinesis after incubation with Pnut dsRNA (A and B) or Sticky and Pnut dsRNAs (C). Arrowheads mark the MR structures that result after successful (A) or failed (B and C) division attempts. (D) Quantification from time-lapse records (40× objective and 2 × 2 camera binning) of failed division attempts resulting in the presence or absence of internal MR-like structures positive for Anillin-mCh alone or Anillin-mCh and myosin-GFP after depletion of Sticky (n = 25), Pnut (n = 28), or both (n = 46). Data are from one experiment representative of three repeats. Times are given in hours, minutes, and seconds. Bars, 5 µm.

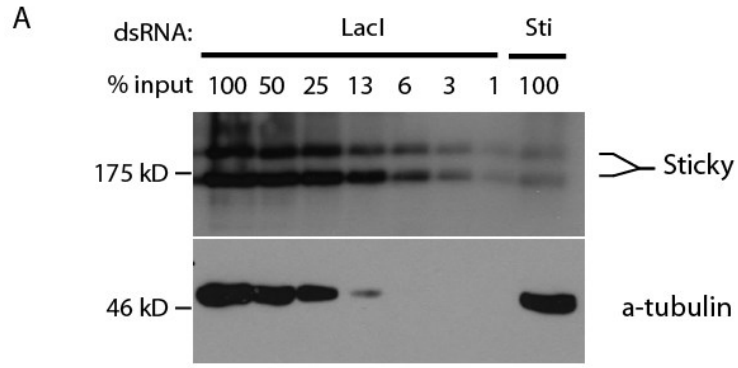

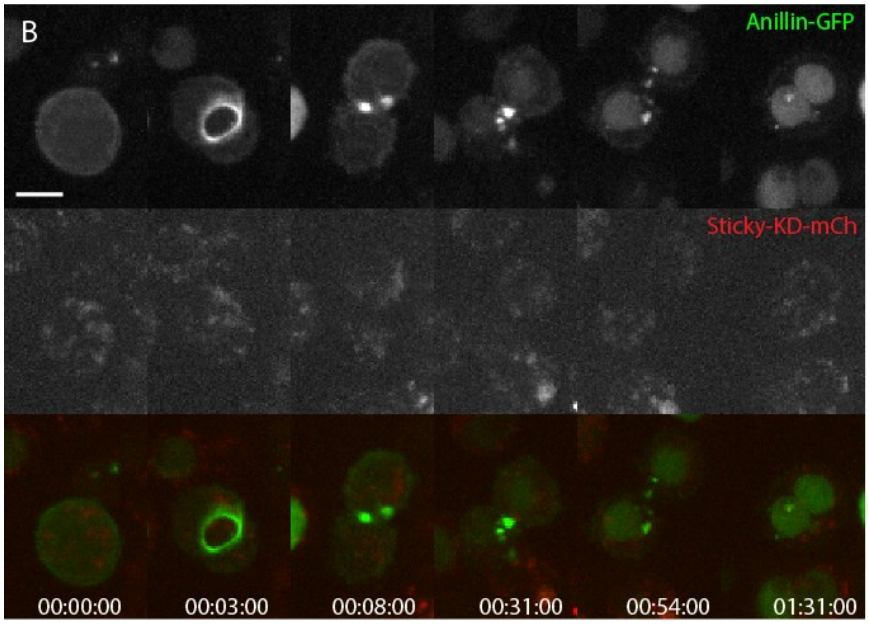

Figure S5. Sticky immunoblot and example of cell Sticky-KD-mCh failure.

(A) Anti-Sticky immunoblot analysis of S2 cell lysates after a 3-d treatment with LacI or Sticky (Sti) dsRNA. A serial dilution of the LacI lysate demonstrates the extreme sensitivity of detection of the antibody and the efficacy of the RNAi. (bottom) The same blot was cut and probed with an anti-tubulin antibody as a loading control. (B) Example of a cell expressing Anillin-GFP and Sticky-KDmCh, depleted of endogenous Sticky, which failed to recruit any Sticky-KD-mCh and failed cytokinesis. Times are given in hours, minutes, and seconds. Bar, 5 µm.

Video 1. Extrusion of Anillin-GFP from the nascent MR. *Drosophila* S2 cells stably expressing Anillin-GFP (green) and mCh-tubulin (red). Images were acquired by time-lapse spinning-disc confocal microscopy, with frames taken every 38 s for 1 h and 5 min. A maximum intensity projection of multiple confocal sections is shown. The cell at the top left corresponds to Fig. 1 B. Times are shown in hours, minutes, and seconds.

http://movie.rupress.org/video/10.1083/jcb.201305053/video-1

Video 2. Internalization of Anillin-GFP from the nascent MR. *Drosophila* S2 cell stably expressing Anillin-GFP (green) and mCh-tubulin (red). Images were acquired by time-lapse spinning-disc confocal microscopy (63×, 1.4 NA objective) with frames taken every 45 s for 2 h. Single confocal sections are shown. Video corresponds to Fig. 1 D. Times are shown in hours, minutes, and seconds.

http://movie.rupress.org/video/10.1083/jcb.201305053/video-2

Video 3. F-Actin is not extruded from the nascent MR. *Drosophila* S2 cell stably expressing LifeAct-GFP (center, green in merged) and Anillin-mCh (left, red in merged). Images were acquired by time-lapse spinning-disc confocal microscopy (63×, 1.4 NA objective) with frames taken every 60 s for 1 h and 35 min. A maximum intensity projection of multiple confocal sections is shown. Video corresponds to the cell in Fig. 2 I. Times are shown in hours, minutes, and seconds.

http://movie.rupress.org/video/10.1083/jcb.201305053/video-3

Video 4. Cells expressing Anillin-GFP undergoing cytokinesis after depletion of Shrub/CHMP4B. *Drosophila* S2 cells stably expressing Anillin-GFP (left, green in merged) and mCh-tubulin (center, red in merged) treated with Shrub dsRNAs for 4 d. Images were acquired by time-lapse spinning-disc confocal microscopy (100×, 1.4 NA objective) with frames taken every 2 min for 2 h and 45 min. A maximum intensity projection of multiple confocal

sections is shown. Video corresponds to Fig. 3 H. Times are shown in hours, minutes, and seconds.

http://movie.rupress.org/video/10.1083/jcb.201305053/video-4

Video 5. Cell expressing Anillin-ΔN+CD-mCh and Anillin-ΔC-GFP undergoing cytokinesis. A *Drosophila* S2 cell stably expressing Anillin-ΔN+CD-mCh (center, red in merged) and Anillin-ΔC-GFP (left, green in merged) undergoing cytokinesis. Images were acquired by time-lapse spinning-disc confocal microscopy with frames taken every 60 s for 2 h and 12 min. A maximum intensity projection of multiple confocal sections is shown. Video corresponds to Fig. 4 B. Times are shown in hours, minutes, and seconds.

http://movie.rupress.org/video/10.1083/jcb.201305053/video-5

Video 6. Sticky-depleted cell expressing Anillin-GFP succeeding at cytokinesis. *Drosophila* S2 cell stably expressing Anillin-GFP (green) and mCh-tubulin (red) after a 48-h incubation with Sticky dsRNA. Images were acquired by time-lapse spinning-disc confocal microscopy with frames taken every 60 s for 1 h and 33 min. A maximum intensity projection of multiple confocal sections is shown. Video corresponds to Fig. 6 A. Times are shown in hours, minutes, and seconds.

http://movie.rupress.org/video/10.1083/jcb.201305053/video-6

Video 7. Sticky-depleted cell expressing Anillin-GFP failing cytokinesis. *Drosophila* S2 cell stably expressing Anillin-GFP (green) and mCh-tubulin (red) after a 48-h incubation with Sticky dsRNA. Images were acquired by time-lapse spinning-disc confocal microscopy with frames taken every 60 s for 2 h and 9 min. A maximum intensity projection of multiple confocal sections is shown. Video corresponds to Fig. 6 B. Times are shown in hours, minutes, and seconds.

http://movie.rupress.org/video/10.1083/jcb.201305053/video-7

Video 8. Cell expressing Anillin-GFP attempting cytokinesis after Sticky and Pnut codepletion. *Drosophila* S2 cell expressing Anillin-GFP attempting cytokinesis after Pnut and Sticky codepletion. Images were acquired by time-lapse spinning-disc confocal microscopy with frames taken every 2 min for 2 h. A maximum intensity projection of multiple confocal sections is shown. Video corresponds to Fig. 7 G. Times are shown in hours, minutes, and seconds.

http://movie.rupress.org/video/10.1083/jcb.201305053/video-8

Video 9. Cell expressing Anillin-GFP and Sticky-mCh undergoing cytokinesis after endogenous Sticky depletion. Cell expressing Anillin-GFP (left, green in merged) and Sticky-mCh (center, red in merged) incubated with Sticky 3′UTR dsRNA for 3 d. Images were acquired by time-lapse spinning-disc confocal microscopy with frames taken every 4 min for 3 h and 4 min. A maximum intensity projection of multiple confocal sections is shown. Video corresponds to Fig. 8 C. Times are shown in hours, minutes, and seconds.

http://movie.rupress.org/video/10.1083/jcb.201305053/video-9

Video 10. Cell expressing Anillin-GFP and Sticky-KD-mCh undergoing cytokinesis after endogenous Sticky depletion. Cell expressing Anillin-GFP (left, green in merged) and Sticky-KD-mCh (center, red in merged) incubated with Sticky 3′UTR dsRNA for 3 d. Images were acquired by time-lapse spinning-disc confocal microscopy with frames taken every 60 s for 2 h and 2 min. A maximum intensity projection of multiple confocal sections is shown. Video corresponds to Fig. 8 E. Times are shown in hours, minutes, and seconds.

http://movie.rupress.org/video/10.1083/jcb.201305053/video-10

5. Distinct Anillin- and Rho-dependent contributions to Citron Kinase localization and function are required for cytokinesis.

Nour El Amine[1, 2], Denise Wernike[1] and Gilles R.X. Hickson[1, 2]

1 Centre de Cancérologie Charles Bruneau, Centre Hospitalier Universitaire Sainte-Justine Centre de Recherche, Montréal, Québec H3T 1C5, Canada

2 Département de Pathologie et Biologie Cellulaire, Université de Montréal, Montréal, Québec H3C 3J7, Canada

Contributions :

NE et GH ont conçu le projet

NE et GH ont rédigé l'article.

Les expériences ont été effectués par :

NE dans Fig. 1A, 2, 3, 4A-B, 5A, 5C-N, 6A-E, S1, S2, S3, S4, S5, S6, S7

DW dans Fig. 1B, 4A-B, 5A-F, 6G-H, S5F-G

NE a généré tous les vecteurs utilisés dans cet article sauf dans 5B et 6H.

Les expériences dans 1A, 3A, 4A, 5C et 5E ont été effectué par NE originalement et répliqués indépendamment par DW. Les résultats obtenus entre NE et DW sont identiques.

5.1. Abstract

Cytokinesis is a multi-step process that results in the physical separation of two daughter cells following mitosis. It begins by the formation of an actomyosin contractile ring (CR) at the equator of the cell, which then constricts to form a midbody ring (MR) around the densely packed microtubules of the midbody. Finally abscission occurs on one side of the MR. A network of Rho-dependent proteins control progress through cytokinesis, yet how these proteins work together to insure a successful cytokinesis is still under heavy investigation. Here, we conduct a structure-function analysis of the Citron Kinase, Sticky, in *Drosophila* S2 cells. Sticky is known to be required for the formation of a stable MR, but the mechanisms of its regulation and function are poorly understood. We find that Sticky has two distinct mechanisms of localization to the CR. The first mechanism is Anillin-dependent and occurs through residues 774-1228 of Sticky. Pull-down assays identified and mapped a biochemical interaction between the N-terminus of Anillin and a sub-region of the coiled-coil domain of Sticky. The second input into the cortical localization of Sticky mapped to residues 1074-1370, which encompass a well conserved putative Rho1 binding domain (RBD). Fine-mapping analysis revealed that the Anillin-dependent and RBD-dependent inputs were separable, although directly adjacent. Sticky mutants with disrupted RBDs failed to support cytokinesis when endogenous Sticky was depleted and failed to form MR structures. Remarkably, a similar phenotype was observed when the Anillin-Sticky interaction was disrupted using an Anillin truncation lacking its N-terminal domain. Collectively, the data show that Sticky has two distinct Anillin- and Rho1-dependent mechanisms of localization to the CR and that these are both essential for the transition to the MR.

5.2. Introduction

In animal cells, cytokinesis succeeds mitosis by forming a cleavage furrow at the equator of the dividing cell. Furrow ingression is driven at its base by a contractile ring (CR), a dynamic, membrane-anchored assembly of cytoskeletal proteins that constricts to reduce the cell equator

to a diameter of 1-2 µm. At this point, the CR has gathered the bundled microtubules of the central-spindle and it must transition into a stable structure called the midbody ring (MR) (Schroeder, 1972). The CR-to-MR transition is a crucial step in cell division, essential for maintaining the integrity of the intercellular bridge and for setting the stage for the final abscission event that will irrevocably separate the cells. The CR-to-MR transition occurs via a maturation process that includes a gradual thinning of the nascent MR and removal of cortical material through shedding and internalization (El-Amine et al., 2013; Renshaw et al., 2014). A complex machinery is involved in organizing the succession of events during cytokinesis and for ensuring that they proceed with high fidelity (Green et al., 2012). Activation of RhoA is an early event essential for furrow initiation and CR formation (Piekny et al., 2005). The CR comprises cytoskeletal proteins including actin, myosin II and septins, along with many other proteins that insure CR contractility, attachment to the membrane and interaction with the central spindle (D'Avino et al., 2015). Among these proteins is the Citron Kinase, named Sticky in *Drosophila melanogaster*. Originally identified as a Rho interacting protein (Cunto et al., 1998; Madaule et al., 1998; Madaule et al., 1995), Citron kinase was initially expected to play a role in Myosin activation and furrowing (Bassi et al., 2011; D'Avino et al., 2004; Yamashiro et al., 2003). However, it has since become clear that the major function, and requirement for Citron kinase during cytokinesis, is during the CR-to-MR transition. Although there is evidence of redundant contributions of Citron kinase/Sticky during furrowing (El-Amine et al., 2013; Gai et al., 2011; Madaule et al., 1998), as well as suggestions of a role during abscission (Gai et al., 2011; Sgro et al., 2016), loss of function studies have clearly shown that Citron kinase/Sticky is required for the stabilization of the MR in a variety of cell types (Bassi et al., 2011; El-Amine et al., 2013; Sgro et al., 2016; Watanabe et al., 2013). How Sticky is regulated and how it acts to stabilize the MR, remain controversial and unclear. Although Citron kinase is a cortical protein, numerous studies indicate that it can interact with microtubule-associated proteins of the midbody, such as KIF14/Nebbish and MKLP1/Pavarotti, and that these interactions are important for intracellular bridge stability (Bassi et al., 2013; Gruneberg et al., 2006a; McKenzie et al., 2016; Watanabe et al., 2013). Furthermore, an important outstanding question concerns the nature of the relationship between Citron kinase/Sticky and the Rho GTPase. Recently, the assumption that Sticky acts as a canonical downstream effector of Rho has been challenged by suggestions that mammalian Citron Kinase may act upstream of RhoA to modulate its activity,

and by evidence of *Drosophila* Sticky interacting with Rho independently of its nucleotide status (Bassi et al., 2011; Gai et al., 2011).

Here we show that Sticky is capable of localizing to the cleavage furrow through two distinct mechanisms: one dependent on Anillin, the other dependent on Rho1. Perturbing either the Anillin/Sticky or the Rho1/Sticky interaction led to failures in MR formation that resembled loss of Sticky. We also confirm that Sticky can connect with microtubules of the midbody and provide evidence that this ability is independent of both Anillin/Sticky and Rho1/Sticky inputs. Collectively, these data lead us to propose that Rho1 and Anillin act cooperatively to recruit Sticky to the CR and that in turn Sticky acts to stabilize Rho1 and Anillin in the subsequent MR as it forms around the midbody, to which Sticky is also connected.

5.3. Results

5.3.1. Sticky acts on the N-terminus of Anillin.

We previously showed that Sticky acts to retain Anillin at the midbody ring and that this is necessary for cytokinesis (El-Amine et al., 2013). We therefore wished to better understand the nature of Sticky-Anillin interactions. First, we mapped the region of Anillin that mediates interactions with Sticky by performing pull-down experiments using recombinant GST fused to fragments of Anillin. A fragment that included the N-terminal domain (NTD) and adjacent Myosin-binding domain (MyoBD) of Anillin robustly pulled-down Sticky from S2 cell lysates, indeed so effectively that the supernatant was depleted of Sticky (Fig. 1A, S1). GST fused to a fragment containing both the MyoBD and the adjacent Actin-binding domain (ActBD) also pulled down Sticky, but to a much lesser extent, while GST-ActBD alone was unable to pull down any Sticky (Fig. 1A, S1). GST alone, or fused to a construct containing the Central domain (CD), Anillin homology domain (AHD) and Pleckstrin Homology domains (PH), were also unable to pull down Sticky (Fig. 1A, S1). Thus, although the MyoBD of Anillin can interact with Sticky, inclusion of the Anillin NTD leads to a markedly stronger interaction. This result is consistent with the finding that mammalian Citron kinase can be co-precipitated from mammalian cells in complex with the Anillin N-terminus (Gai et al., 2011), and suggests that,

despite poor sequence conservation of the NTD between flies and mammals, a Anillin-Sticky interaction has been conserved during evolution.

We next used time lapse, spinning disk confocal microscopy of *Drosophila* S2 cells to test the abilities of GFP-tagged Anillin mutants lacking the NTD or MyoBD to support cytokinesis of S2 cells. In a rescue assay that we have used extensively before (Hickson and O'Farrell, 2008b; Kechad et al., 2012) inducible expression of Anillin-ΔNTD-GFP failed to rescue for RNAi-induced depletion of endogenous Anillin. The cells furrowed successfully, but then the Anillin-ΔNTD was lost from the nascent MR, a stable MR failed to form and 98% of the cells became binucleate (Fig. 1B). This is highly reminiscent of the phenotype observed when Sticky is depleted in cells expressing wild-type Anillin-GFP (El-Amine et al., 2013), and is consistent with Sticky acting to retain the Anillin NTD during MR formation.

Interestingly, in cells induced to express Anillin-ΔMyoBD-GFP, only 30% failed cytokinesis compared to 80% in uninduced controls (Fig. 2D). These data suggest that, unlike the NTD, the MyoBD of Anillin is not absolutely required for cytokinesis of S2 cells. However, even in the cells that successfully divided, a comparison of age matched MR in cells expressing Anillin-ΔMyoBD-GFP or Anillin-GFP, revealed that Anillin-ΔMyoBD-GFP positive MRs were smaller than the controls and failed to form a persistent structure before undergoing abscission (Fig. 2A/A', 2B/B', 2C/C'). Surprisingly, Anillin-ΔMyoBD expression also appeared to partially rescue for loss of Sticky. In cells expressing Anillin-ΔMyoBD-GFP and depleted of Sticky, no mature MR structure formed, but rather resulted in binucleate cells in only 33% (n=297) of the division attempts which is significantly lower than the 50% (n=365) failure rate observed in uninduced cells or the 65% (n=127) failure rate of cells expressing Anillin-GFP instead (Fig. 2D). Furthermore, the division attempts that succeeded in cells expressing Anillin-ΔMyoBD-GFP, did so via premature abscission which occurred at a similar time to furrow regression in cells that failed (Fig. 2E). As we previously reported, such premature abscission is the earliest observable phenotype that precedes the onset of failed cytokinesis when Sticky is depleted from otherwise wild-type cells (El-Amine et al., 2013). Furthermore, co-depletion of Anillin and Sticky in these Anillin-ΔMyoBD expressing cell lines did not alter any of the phenotypes observed by depletion of Sticky alone (Fig. 2E).

Collectively, these data indicate that Sticky acts on the N-terminus of Anillin during the CR-to-MR transition, and suggests that both the NTD and MyoBD of Anillin are important for the Sticky-dependent formation of the MR.

5.3.2. An Anillin interaction contributes to Sticky localization.

We performed reciprocal pull down experiments to define the region of Sticky that is required for interaction with Anillin. We generated a panel of truncated Sticky constructs and purified these from *E. coli* as GST fusion proteins. After independently reviewing predictions of the coiled coil domain of Sticky with the LOGICOILS algorithm (Fig. S2A), we decided to adopt the nomenclature and boundaries defined by Bassi et al, 2011. Neither the kinase domain alone nor combined with the adjacent CC1 region showed any interaction with Anillin (Fig. 3A, S1). However, the second coiled-coil region (CC2) of Sticky, and more specifically its N-terminal (CC2a) region, robustly pulled-down endogenous Anillin from S2 cell lysates (Fig. 3A, S1). This interaction does not seem to have been conserved at the same site in mammals because a fragment that included the equivalent of CC2 was not found to co-precipitate with Anillin and it rather appeared that multiple regions of the C-terminus of Citron Kinase were involved (Gai et al., 2011).

We also generated an extended panel of Sticky truncation constructs fused to GFP for localization studies by real-time imaging. In broad agreement with Bassi et al. and an analogous study of mammalian Citron Kinase (Watanabe et al., 2013), we find that the coiled-coil domains mediate Sticky localization (Fig. 3B and Fig. S3) (Bassi et al., 2011). The CC1 domain localized to the central region of the midbody (Fig. 3B, 3C), while the CC2 domain localized to the cell cortex (Fig. 3B, 3G). Importantly, the CC2a region (residues 774-1228) was sufficient for cortical localization (Fig. 3B, 3E). All constructs that began after residue 1228 were cytoplasmic (Fig. S3), and Sticky lacking its kinase domain localized in a comparable manner to full length (FL) Sticky (Fig. S3). Finally, cells that expressed Sticky truncations of either, Kinase domain alone, Citron Nek1 Homology (CNH) domain alone or C1+CNH domains were cytoplasmic (Fig. S3). Thus, the ability of Sticky truncations to localize to the cortex correlated with the

presence of the CC2a region (residues 774-1228), which was both necessary and sufficient for cortical localization.

Given our finding that Sticky interacts with Anillin (Fig. 1A and 3A), we sought to test the consequences of depleting Anillin on the localization patterns of Sticky constructs. Sticky-CC1-GFP localization to the microtubules of the midbody was unaffected by Anillin depletion (Fig. 3D), consistent with the work of D'Avino and colleagues who showed that this localization requires Kif14/Nebbish and/or kinesin-6/Pavarotti (Bassi et al., 2013; Bassi et al., 2011). Strikingly, however, Sticky-CC2a-GFP no longer localized to the CF in Anillin dsRNA-treated cells (Fig. 3F, S5A-B), indicating that the Anillin-CC2a interaction described above contributes to localization of Sticky to the cortex.

We next studied the localization of the entire CC2 domain which extends a further 143 amino acids carboxy terminal of CC2a, to include a region named CC2b. Intriguingly, along with its normal equatorial localization at the cortex, CC2a+b-GFP exhibited a strong cortical localization even in metaphase and this persisted when cells underwent cytokinesis (Fig 3G). Importantly, in Anillin-depleted cells, Sticky CC2a+b-GFP still had a very clear localization to the CF and late CR (Fig. 3H, S5C-E). Thus, although CC2a cortical localization was Anillin-dependent, CC2a+b (CC2) localization was not, indicating that an additional contribution to Sticky localization must require the CC2b region. Further support for the existence of multiple mechanisms of cortical localization comes from the observation that full-length Sticky was still recruited to the late CR in Anillin-depleted cells (Fig. 3J).

5.3.3. Fine-mapping the Anillin-dependent domain within the Sticky CC2a region

These observations suggested the existence of 2 distinct inputs within the CC2a+b region of Sticky. We wished to better understand the nature of these inputs and determine whether they were separable events. We first sought to define the minimal region within the 450-amino acid CC2a region that is required for Anillin-dependent localization. We generated a series of GFP-tagged truncations where the CC2a region was progressively shortened by 50 amino acid deletions at the N-terminus (Fig. 4A) or C-terminus (Fig. 4 B) and expressed these in S2 cells.

This revealed that deletion of up to 200 amino acids from the N-terminus of CC2a region (i.e. resulting in a construct corresponding to residues 774-973 of Sticky) did not prevent the cortical recruitment of the Sticky CC2a (Fig. 4A, three upper panels), whereas deletion of 250 amino acids from the N-terminus did prevent cortical recruitment (Fig. 4A, lower two panels). A similar strategy of progressive deletions from the C-terminus of CC2a revealed that deletion of up to 100 amino acids did not affect the cortical recruitment (Fig. 4B, upper two panels), while deletion of 200 residues abolished the cortical recruitment (Fig. 4B, middle panel). Together, these observations define amino acid residues 974-1127 of Sticky as being necessary for the cortical localization of the CC2a region.

Interestingly, fragments with C-terminal deletions of 200 or 250 amino acids, although not recruited to the cortex during furrowing, nevertheless showed some localization to a later midbody structure (Fig. 4B). This suggests that an additional sequence conferring midbody localization may reside in the region immediately N-terminal of residue 974. Further support for this notion comes from a comparison of the behaviors of the different N-terminally truncated CC2a constructs (Fig. S4). CC2a(874-1228) localized in an Anillin-dependent manner to the CR, nascent MR and persistent midbody structures (Fig. S4 A-C). However, CC2a(974-1228), while still localizing to the CR and nascent MR, was not retained in late midbody (Fig. S4E-G), arguing for the involvement of residues 874-974 in midbody localization. The differences in midbody retention of CC2a(874-1228) and CC2a(974-1228) are apparent from line profile measurements obtained from both cell lines at different stages of the CR-to-MR transition (Fig. S4H).

5.3.4. Identification of an RBD-dependent contribution to Sticky localization.

Having defined the minimal sequence required for the Anillin-dependent cortical localization of CC2a, we wished to define the requirements for the second input into cortical localization that we had inferred to exist from examination of the CC2a+b construct. The CC2b region contains a putative Rho-binding domain, although its functionality has been questioned (Bassi et al., 2011; Gai et al., 2011). A GFP-tagged construct encoding only the CC2b region

(residues 1228-1370) was entirely cytoplasmic throughout cytokinesis (Fig. 5A), as previously reported by Bassi et al. 2011. We therefore generated constructs that progressively extended the N-terminus of CC2b (into the CC2a region). Addition of residues 1124-1227, which were dispensable for the cortical localization of CC2a (Fig. 4B), conferred the ability of the resulting CC2b(1124-1350) construct to localize to the cortex during furrowing (Fig. 5B). A slightly longer construct CC2b(1074-1370) was similarly cortical during furrowing (Fig. 5C), and in a manner that was abrogated by the introduction of a point mutation (L1246N) that is predicted to abrogate any potential Rho1 binding (Fig. 5D, S5). This point mutation was chosen based on the crystal structure of the Rho binding domain of the related ROCK kinase and based on the work by Watanabe et al. 2013 who generated the analogous mutation in human Citron Kinase (Dvorsky et al., 2004; Serres et al., 2012; Shimizu et al., 2003; Watanabe et al., 2013). This same mutation, however, did not prevent the cortical recruitment of an even longer CC2b(974-1350) construct that also included the portion of CC2a that was required for Anillin-dependent cortical localization (Fig. 5E, F, S5F-G). These data strongly suggest that the Rho-binding domain within the CC2b region also contributes to the cortical recruitment of Sticky.

The cortical localization of CC2b(1074-1370) persisted following depletion of Anillin (Fig. 5I), confirming that it is independent from the Anillin/CC2a mechanism of localization. It is also exciting to note that CC2b(1074-1370) did not localize to any structures after cytokinesis failure induced upon depletion of endogenous Sticky (Fig. 5H). This is in contrast to the longer CC2b(874-1370) construct that localized robustly to internal MR-like structures following endogenous Sticky depletion (Fig. 5K). CC2b(874-1370) includes the Anillin-dependent region of CC2a, and the additional 100 amino acids (residues 874-973) that we inferred to play a role in midbody targeting in the context of the CC2a constructs in the previous section.

It is interesting to note that CC2b(874-1370) and CC2b(1074-1370), the former containing the Anillin-dependent input and the latter lacking it, were cortically localized during metaphase (Fig. 5G, 5K) and thus prior to the normal robust activation of Rho1 that occurs at anaphase onset (Fig. S5F, S5G). Furthermore, this cortical localization was dependent on the RBD because it was abolished by the L1246N mutation (Fig. 5D). Conversely, this indicates that the presence of Anillin-dependent signal alone was insufficient for metaphase recruitment as expected from CC2a(874-1228) localization (Fig. 4). We depleted the RhoGEF, Pebble (Pbl),

to inhibit Rho1 activation at this time. This revealed that the cortical pool of these constructs persisted at metaphase for CC2a (Fig. 5N). However, no additional recruitment was observed during the ensuing anaphase where furrowing was blocked (Fig. 5J, 5N). This suggests that the initial cortical localization (at metaphase) is Pbl-independent, although it is clearly RDB-dependent and sensitive to the L1246N mutation (Fig. 5D, Fig. S5F). It may be that the RBD-dependent localization is a more constitutive Rho1-dependent event that is independent of cytokinesis-specific Rho activation.

Thus, the central CC2 coiled-coil region of Sticky includes sequences that respond to distinct and separable Anillin-dependent (residues 974-1127) and RBD-dependent (residues 1128-1370) inputs into cortical localization, and potentially includes an additional midbody targeting region that requires residues 874-973.

5.3.5. The Rho-binding domain of Sticky is essential for cytokinesis.

We next tested the consequences of abrogating the putative Rho1-dependent input in the context of the full-length Sticky. First, we examined the behavior of Sticky-ΔRBH-GFP, a mutant that lacks the most highly conserved residues (1233-1263, RBH) within the Rho-binding domain (Fig. 6A-F). Consistent with our observations of the CC2 truncations, Sticky-ΔRBH-GFP localized to the cortical MR and nascent MR during cytokinesis (Fig. 6A-B), but only in an Anillin-dependent manner. Anillin RNAi abolished this cortical localization of Sticky-ΔRBH-GFP, although in some cells Sticky localization was still detected at the inner midbody (Fig. 6D), presumably via KIF14^{Nebbish} recruitment via the intact CC1 domain (Bassi et al., 2013). Importantly, Sticky-ΔRBH-GFP failed to support successful cytokinesis when endogenous Sticky was depleted using a dsRNA targeting the 3' UTR (Fig. 6C). Analysis of time-lapse records of many division attempts revealed that 70% (n=67) of cells expressing Sticky-ΔRBH-GFP failed cytokinesis following endogenous Sticky depletion, compared to 15% (n=66) of control cells expressing full-length Sticky-GFP (Fig. 6E).

Finally, we examined a Sticky-L1246N-GFP mutant, also predicted to be incapable of binding Rho1 (Fig. 6G-H). This construct was robustly recruited to the CR and MR in control cells (Fig. 6G), but, unlike wild-type Sticky-GFP (Fig. 3J), it was no longer recruited in Anillin-

depleted cells (Fig. 6H). This further reinforces our conclusion that the extended Rho-binding domain of Sticky (defined in the current study as residues 1128-1370) contributes to the cortical localization of Sticky, in a pathway that is redundant with the Anillin-dependent recruitment of the adjacent region of the coiled-coil domain (defined in the current study as residues 974-1127).

Collectively, these data show that the putative Rho1-binding domain of Sticky is crucial for Sticky function during the CR-to-MR transition. In the absence of the Rho1 binding capacity, Anillin was completely shed and the MR failed to form, i.e. the same phenotype as that observed upon Sticky depletion. Thus, it appears that Rho1 binding to Sticky is essential for Sticky function and is specifically required for the stabilization of the MR structure that itself requires Anillin.

5.4. Discussion

Loss-of-function studies have clearly established Citron kinase/Sticky as a key mediator of intercellular bridge stability (Bassi et al., 2013; McKenzie et al., 2016; Sgro et al., 2016; Watanabe et al., 2013). Furthermore, this key role appears to involve an ability to connect the cortical nascent MR, to which Cit-K localizes, with the microtubules of the midbody, via interactions with MAPs such as KIF14, PRC1 and MKLP1 (Bassi et al., 2013; Gruneberg et al., 2006a; Watanabe et al., 2013). Long-standing enigmas regarding Citron kinase regulation and function include the relationship with the small GTPase Rho and the mechanism(s) of cortical localization. Mammalian Citron kinase was first identified through yeast two-hybrid screening for RhoA-GTP binding proteins (Madaule et al., 1998; Madaule et al., 1995). It was thus assumed that Cit-K, and its *Drosophila* ortholog Sticky, would act as canonical Rho effectors: i.e. that direct Rho-GTP binding would activate Citron kinase and drive its recruitment to the equatorial cortex, in much the same way as the related Rho-dependent kinases such as ROCK are thought to be regulated (Cunto et al., 1998; Madaule et al., 1998; Madaule et al., 2000; Thumkeo et al., 2013). However, that assumption has been recently called into question on the basis of several observations that seem at odds with such a model (Bassi et al., 2011; Gai et al., 2011). These include the findings that RhoA was unable to localize to the late MR upon Cit-K

depletion while Cit-K localization was unaffected after RhoA inactivation by C3 exoenzyme. One group has claimed that Cit-K can modulate RhoA activity (Gai et al., 2011). Sticky was shown to bind to Rho1 independent of its activation state (Bassi et al., 2011; Shandala et al., 2004) Finally, S2 cells, Sticky depletion caused weak localization of Rho1 at the MR while an increase of phosphorylated Squash was observed in this same condition. In order to test whether this functionally affected the activity of Rho1, levels of phosphorylated Squash at the CF were measured and shown to increase (Bassi et al., 2011; Dean and Spudich, 2006).

Here we report a detailed structure-function analysis of the CC2 region of the coiled-coil domain of Sticky that revealed two adjacent regions that redundantly mediate cortical localization to the cell cortex. One region requires Anillin, the other requires the Rho-binding domain, and presumably a direct interaction with Rho1-GTP. Although these two inputs are experimentally separable, they likely function together as a unit and are likely of central importance to the essential role of Sticky in the formation of a stable MR.

5.4.1. Rho/Sticky: an essential and conserved interaction in cytokinesis.

Bassi et al (2011) defined a sub-region of Sticky (CC2a) that was sufficient for cortical localization. However, on the basis of their truncation analysis, they dismissed a role for the adjacent Rho-binding domain (within CC2b). Our finer mapping analysis presented here reveals that the junction used in the Bassi et al. study to divide the CC2 region into CC2a and CC2b had removed essential sequences (residues 1124-1228) from the CC2b portion that we now show are required for the RBD-dependent mechanism of localization (Bassi et al., 2011). Using multiple coiled coil prediction algorithms revealed an inconsistency in results obtained for the residues in the region 1150-1170 indicating a possible break in the coiled coil sequence (Fig. S2B). This could possibly explain our inference that residues 1124-1228 provide an important contribution to the cortical localization of the RBD domain. However, the strongest support for the role of the RBD comes in the analysis of Sticky-ΔRBD and Sticky-L1246N mutants, which clearly show that in the context of the full-length protein, the RBD is essential for Sticky to localize in the absence of Anillin, and for the formation of the MR even in the presence of Anillin. A RhoA/Cit-K interaction seems to be evolutionarily conserved in human cells. In HeLa

cells, cytokinesis failures induced by Citron Kinase depletion can be partially rescued by over expression of the coiled coil portion corresponding to CC2 (835-1354) and in a manner that is abrogated by an L1263N mutation in the RhoA binding site (Watanabe et al., 2013). One of the arguments for Sticky being a non-canonical target of Rho1 stems from the reported ability of the C-terminal CNH domain to bind Rho1 independently its activation state (Bassi et al., 2011; Shandala et al., 2004). Therefore, there could be multiple Rho1 interaction sites in Sticky through RBD and CNH. Nonetheless, our data show that RBD is important for Sticky's role in cytokinesis and this is more consistent with Sticky being a canonical effector of Rho1. Clearly, more work is needed to fully understand the relationship between Sticky and Rho.

5.4.2. Anillin/Sticky a conserved interaction in cytokinesis?

Our Sticky pull-down analysis yielded similar results to those reported in mammalian cells for the Anillin interacting region (Gai et al., 2011). We mapped the interaction to within the NTD and the MyoBD of Anillin, which, despite poor sequence conservation within the NTD, is consistent with co-immunoprecipitation assays of HeLa cells (Gai et al., 2011). However, that same study concluded that the interacting region of Cit-K involved an extended region of the C-terminus, based on the fact that interactions were observed with multiple different truncation constructs of varying lengths (Gai et al., 2011). Our analysis in *Drosophila* cells found that the interacting region required amino acids 774-1228 of Sticky. However, when even smaller regions within Sticky-CC2a (774-1228) were imaged in S2 cells, Sticky (974-1228) and (774-1128) were found to still be capable of localizing to the cortex. Although we have not yet tested these fragments in biochemical interaction assays, they localized in an Anillin-dependent manner and we expect they will bind. Close inspection of the constructs used in the human study (Gai et al., 2011) reveals that the only construct tested that did not pull down Anillin encoded amino acids 1-955 of Cit-K. All other constructs, which did pull down Anillin, contained the equivalent sequence corresponding to residues 974-1128 of Sticky. Thus we speculate that the Anillin/Sticky interaction may be conserved through homologous regions in both humans and flies.

On the basis of the observation that GST-CC2a pulled down Actin and Myosin from cell lysates, Bassi et al., 2011 proposed that the CC2a region localizes to the cortex through interactions with Actin and Myosin. However, Actin and Myosin still localize to the cleavage furrow upon Anillin depletion (Hickson & O'Farrell, 2008), and CC2a localization seems uniquely sensitive to Anillin depletion. Although additional biochemical tests are required, it would rather seem that direct interactions with the Anillin NTD and/or MyoBD may be more centrally involved in the CC2a-mediaed recruitment of Sticky.

5.4.3. Role of Sticky's interplay in MR maturation

We have previously reported that the transition from a CR to MR requires a maturation process in which Sticky acts in the retention of membrane bound MR proteins. Sticky depletion led to uncontrolled loss of MR material until cytokinesis failure. Here, we observed a similar phenotype following either of two perturbations: one, upon expression of Anillin-ΔNTD-GFP (which is compromised in its ability to bind Sticky) in absence of endogenous Anillin (Fig. 1B); and the second, when either Sticky-ΔRBD (Fig. 6E) or Sticky-L1246N (Fig. 6F) was overexpressed in Sticky depleted cells. It is interesting that this same phenotype was independently observed when either Anillin/Sticky or Rho1/Sticky interactions were compromised. This could be an indication that the two separable Anillin and Rho1 inputs on Sticky are working together towards the same mechanism of MR stabilization during the transition from CR to MR.

5.4.4. A potential third input?

As mentioned previously in section 5.3.3 (Fig. 4, S4), we speculate that residues 874-973 participate in additional, undefined protein-protein interactions at the midbody. Interestingly, CC2b(974-1370) localized in a similar fashion to CC2b(874-1370) except that the former's expression selectively led to a marked increase in cytokinesis failure even in the presence of endogenous Sticky (Fig. S6). That CC2b(974-1370) appeared to act as a dominant-negative mutant while CC2b(874-1370) did not, might be attributable to the presence or absence

of residues 874-973, which also appeared to contribute to midbody targeting in the context of other truncations (e.g. compare Fig. S7A-E). Remarkably, cells in 30% of the cases failed to initiate furrows, which is a phenotype more associated with loss of function of either Rho1 or its GEF, Pebble, than with loss of function of Sticky, which does not block furrowing. One plausible explanation is that since residues 974-1370 exhibit Rho1-dependent localization, they may bind and sequester Rho1 in the presence of the Anillin-dependent 974-1128 cortical localization but in the absence of the putative 874-974 input. In support of this Rho1 binding and sequestration model, cells expressing Sticky(974-130) were particularly sensitive to Rho RNAi (Fig S7F). However, it was also intriguing to observe that Anillin depletion further enhanced this phenotype (Fig S7G). Although, further work is clearly required, these observations provide tantalizing hints at the complex interplay that likely exists between Rho, Sticky, Anillin and presumably other players.

5.5. Concluding remarks

Our current understanding of the functions of Sticky during cytokinesis is limited. We have previously shown how Sticky is important to retain proteins at the membrane in order to ensure a faithful transition from the CR to MR. Here we have deepened our knowledge of this situation by demonstrating that Sticky itself has multiple inputs to its cortical localization. We provide strong evidence that these mechanisms are Anillin and Rho1 dependent. We propose a model in which Sticky, Anillin and Rho1 work together to ensure proper MR formation. It was interesting to notice that results obtained from other groups are not contradictory and rather support the notion that Citron Kinase/Anillin and Citron Kinase/RhoA interactions have been conserved through evolution. It would be intriguing to conduct further experiments in mammalian models to test whether this is the case.

5.6. Figures and legends

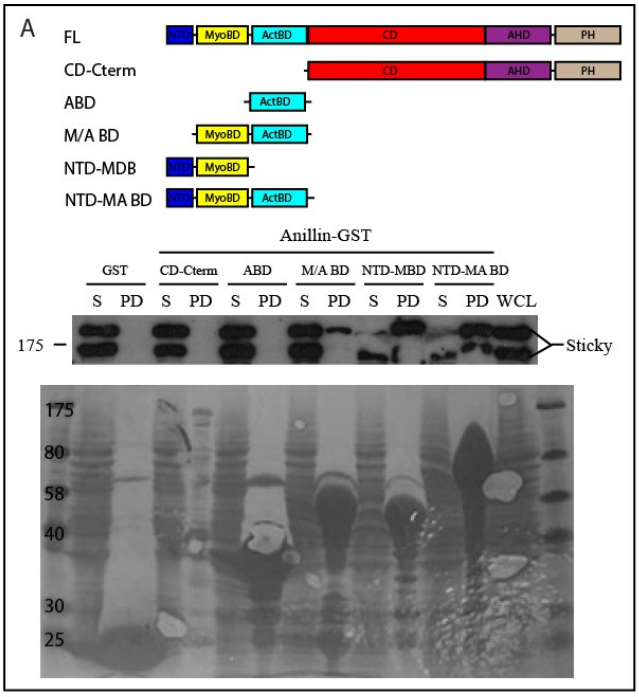

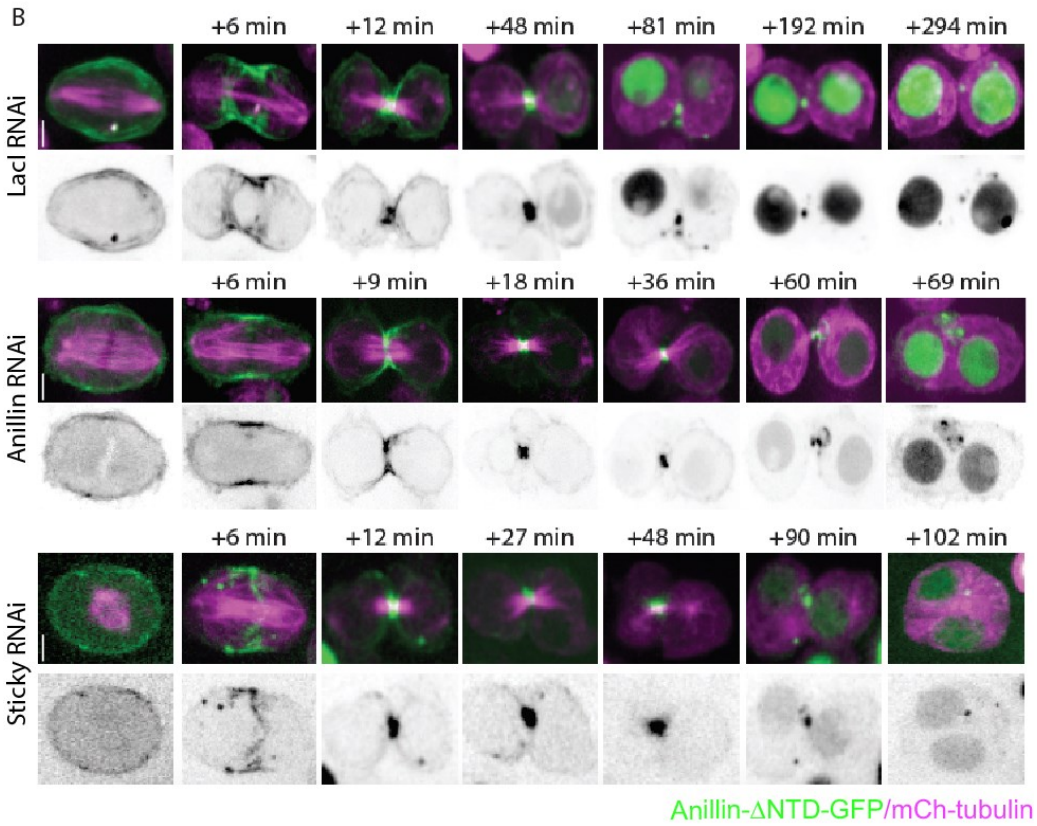

Figure 1. Sticky interacts with the N-terminus of Anillin.

(A) Top: domain organization of Anillin truncations that were tested in a Sticky pull-down from *Drosophila* S2 cell lysates. Middle: Anti-Sticky immunoblot of cell lysates pulled down from indicated recombinant GST fused to fragments of Anillin. Bottom: Ponceau-S staining of nitrocellulose membrane before immunoblot. WCL=Whole cell lysate. (B) Time-lapse sequence of a cell co-expressing Anillin-ΔNTD-GFP and Tubulin-mCherry treated with 3′ UTR Anillin dsRNA (Top), Anillin (Middle) or Sticky (Bottom) dsRNA. 100× objective 1.4 NA. Times are h:min:sec. Scale bars 3.3 μm

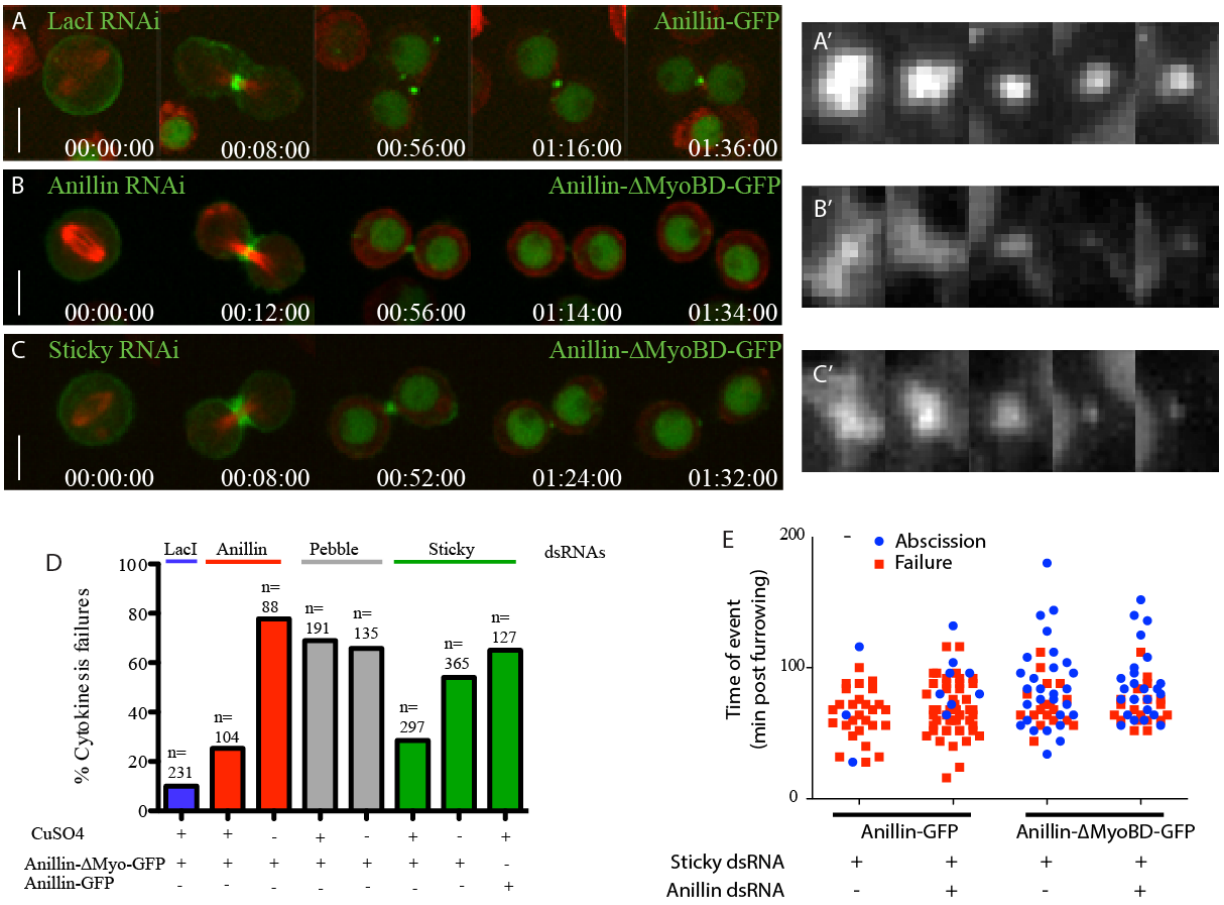

Figure 2. The MyoBD of Anillin plays a role in Sticky functions during cytokinesis.

(A) Time-lapse sequence of a cell co-expressing Anillin-GFP and Tubulin-mCherry treated with control LacI RNAi. (B and C) Time-lapse sequence of a cell co-expressing Anillin-ΔMyoBD-GFP and Tubulin-mCherry treated with 3 ′ UTR Anillin dsRNA (B) or Sticky dsRNA (C). (A', B', C') Age matched midbody rings of cells in A, B and C respectively. (D) Quantification from live time lapse imaging of failed attempts at cytokinesis in cells co-expressing Tubulin-mCherry and either Anillin-GFP or Anillin-ΔMyoBD-GFP treated with either LacI, Anillin, Pebble or Sticky dsRNA in presence or absence of CuSO4 for Anillin-GFP and Anillin-ΔMyoBD-GFP promotor induction. (E) Timing of abscission or furrow regression (Failure) of cells co-expressing Tubulin-mCherry and Anillin-GFP or Anillin-ΔMyoBD-GFP treated with either Sticky or Anillin dsRNA. Data in F and E are compiled from 3 to 5 independent experiments. 40× objective 0.85 NA, binning 2x2. Times are h:min:sec. Scale bars 8 µm.

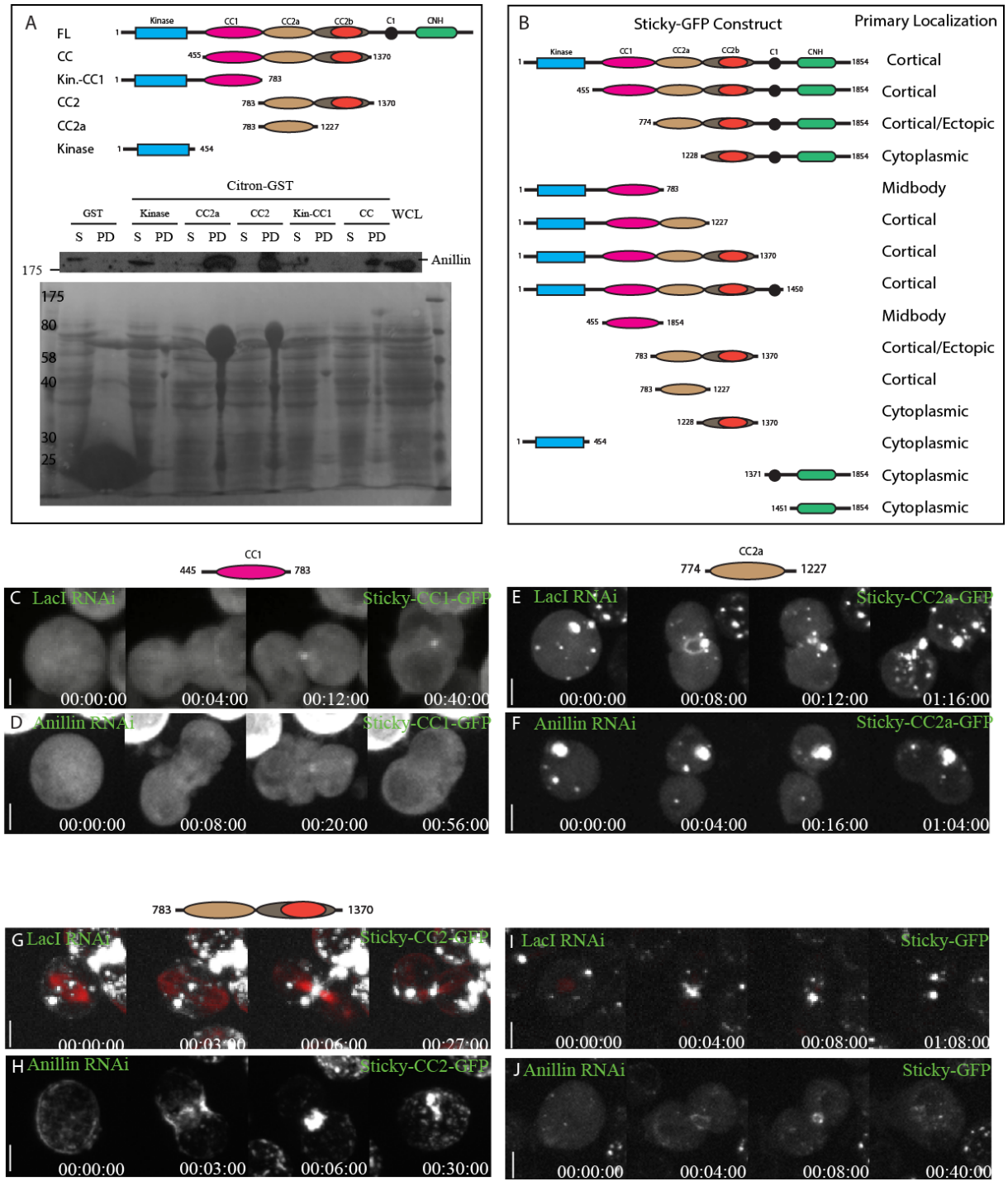

Figure 3. Anillin interacts with Sticky through its Coiled Coil domain.

(A) Top: domain organization of Sticky truncations that were tested in an Anillin pull-down from *Drosophila* S2 cell lysates. Middle: Anti-Anillin immunoblot of cell lysates pulled down from indicated recombinant GST fused to fragments of Sticky. Bottom: Ponceau-S staining of

nitrocellulose membrane before immunoblot. WCL=Whole cell lysate. (B) Summary panel of Sticky-GFP and truncation mutant's primary localization during cytokinesis. (C and D) Time-lapse sequence of a cell co-expressing Tubulin-mCherry and Sticky-CC2a-GFP treated with (C) LacI or (D) Anil dsRNA. (E and F) Time-lapse sequence of a cell co-expressing Tubulin-mCherry and Sticky-CCa-GFP treated with (E) LacI or (F) Anillin dsRNA. (G and H) Time-lapse sequence of a cell co-expressing Tubulin-mCherry and Sticky-CC2-GFP treated with (G) LacI or (H) Anillin dsRNA. (I and J) Time-lapse sequence of a cell co-expressing Tubulin-mCherry and Sticky-FL-GFP treated with (I) LacI or (J) Anillin dsRNA. 100× objective 1.4 NA. Times are h:min:sec. Scale bars 3.3 μm

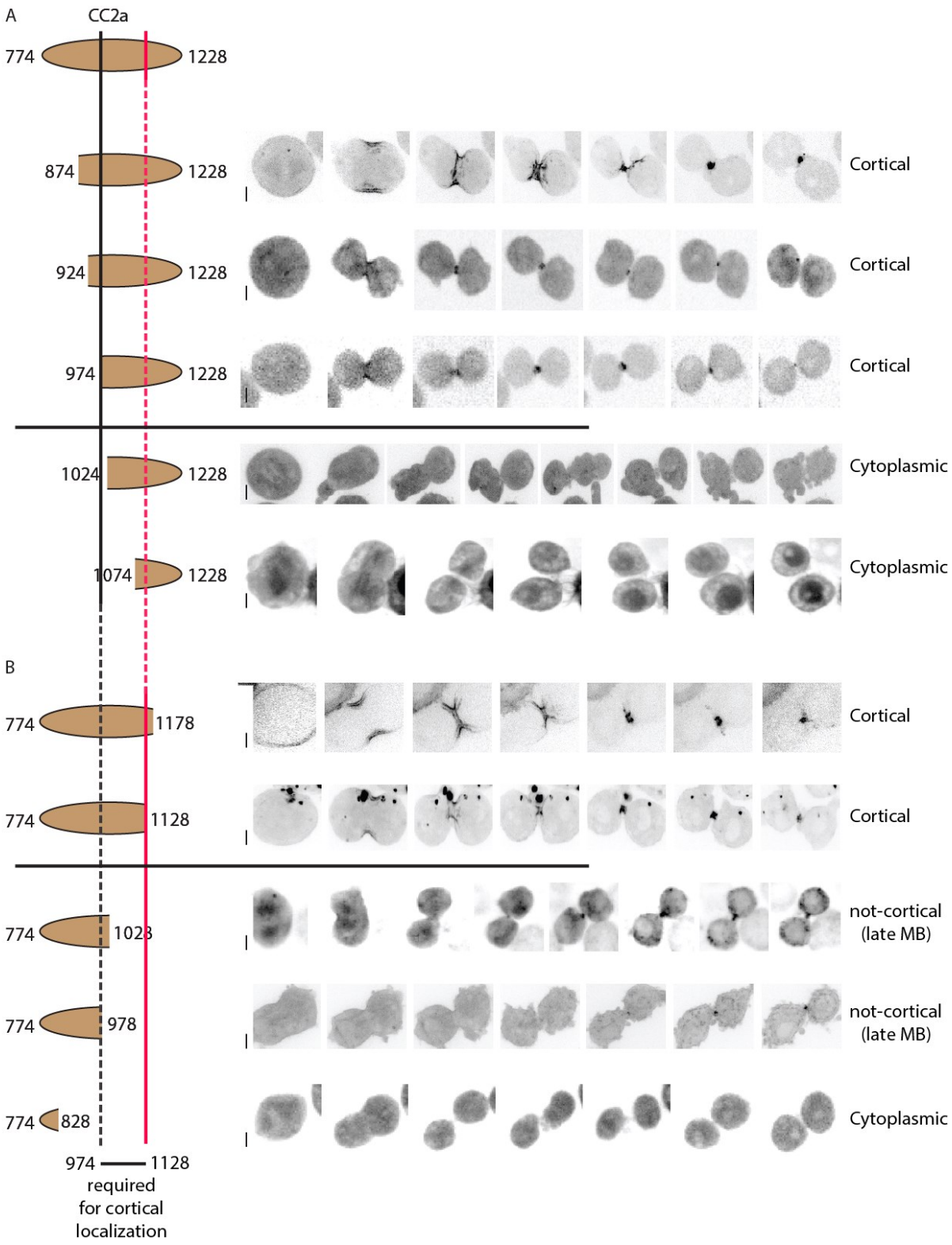

Figure 4. Fine-mapping the Anillin-dependent domain within the Sticky CC2a region.

Time-lapse sequence of a cell co-expressing Sticky-CC2a-GFP truncations. (A) Top 5 panels are truncations of 5' end of Sticky-CC2a. (B) Bottom 5 panels are truncations of 3' end of Sticky CC2a. Black and red vertical lines delimits the 5' and 3' ends respectively of the minimal Anillin-dependent domain capable of being recruited to the cortex. Black Horizontal line separates cortical vs non cortical localized Sticky-CC2a truncations. 100× objective 1.4 NA. Times are h:min:sec. Scale bars 3.3 μm

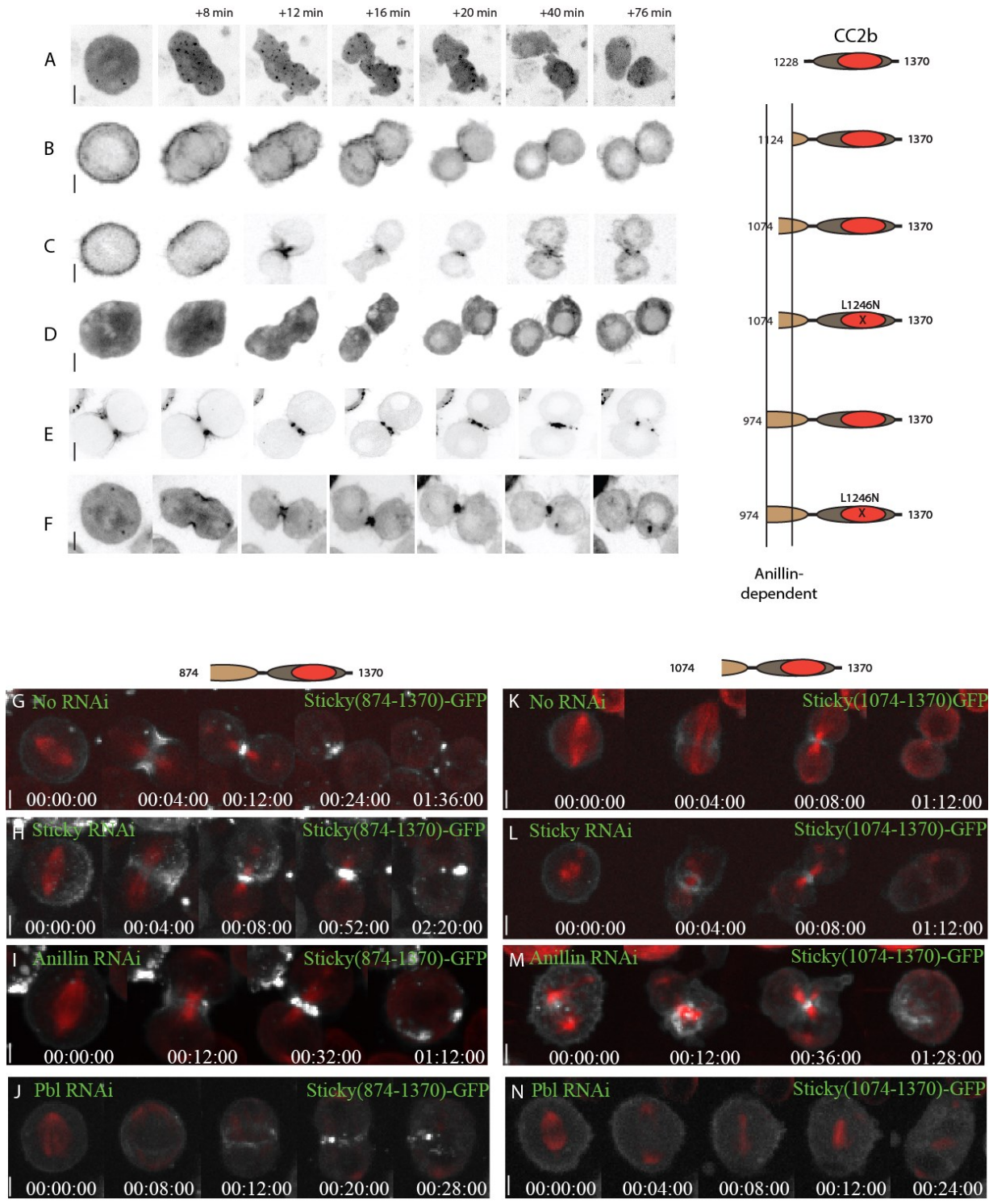

Figure 5. Identification of a RBD-dependent contribution to Sticky's localization during cytokinesis.

(A-F) Time-lapse sequence of a cell expressing (A) Sticky-CC2b-GFP, (B) Sticky(1124-1370)-GFP, (C) Sticky(1074-1370)-GFP, (D) Sticky(1074-1370)-L1246N-GFP, (E) Sticky(974-1370)-GFP, (F) Sticky(974-1370)-L1246N-GFP. (G-J) Time-lapse sequence of a cell co-expressing Tubulin-mCherry and Sticky(874-1370)-GFP treated with (G) LacI, (H) Sticky RNAi, (I) Anillin dsRNA or (J)Pebble RNAi. (K-N) Time-lapse sequence of a cell co-expressing Tubulin-mCherry and Sticky(874-1370)-GFP treated with (K) LacI, (L) Sticky, (M) Anillin or (N)Pebble dsRNA. (A-F) 100× objective 1.4 NA; (G-H) 40× objective 0.85 NA, binning 2x2. Times are h:min:sec. Scale bars 3.3 μm

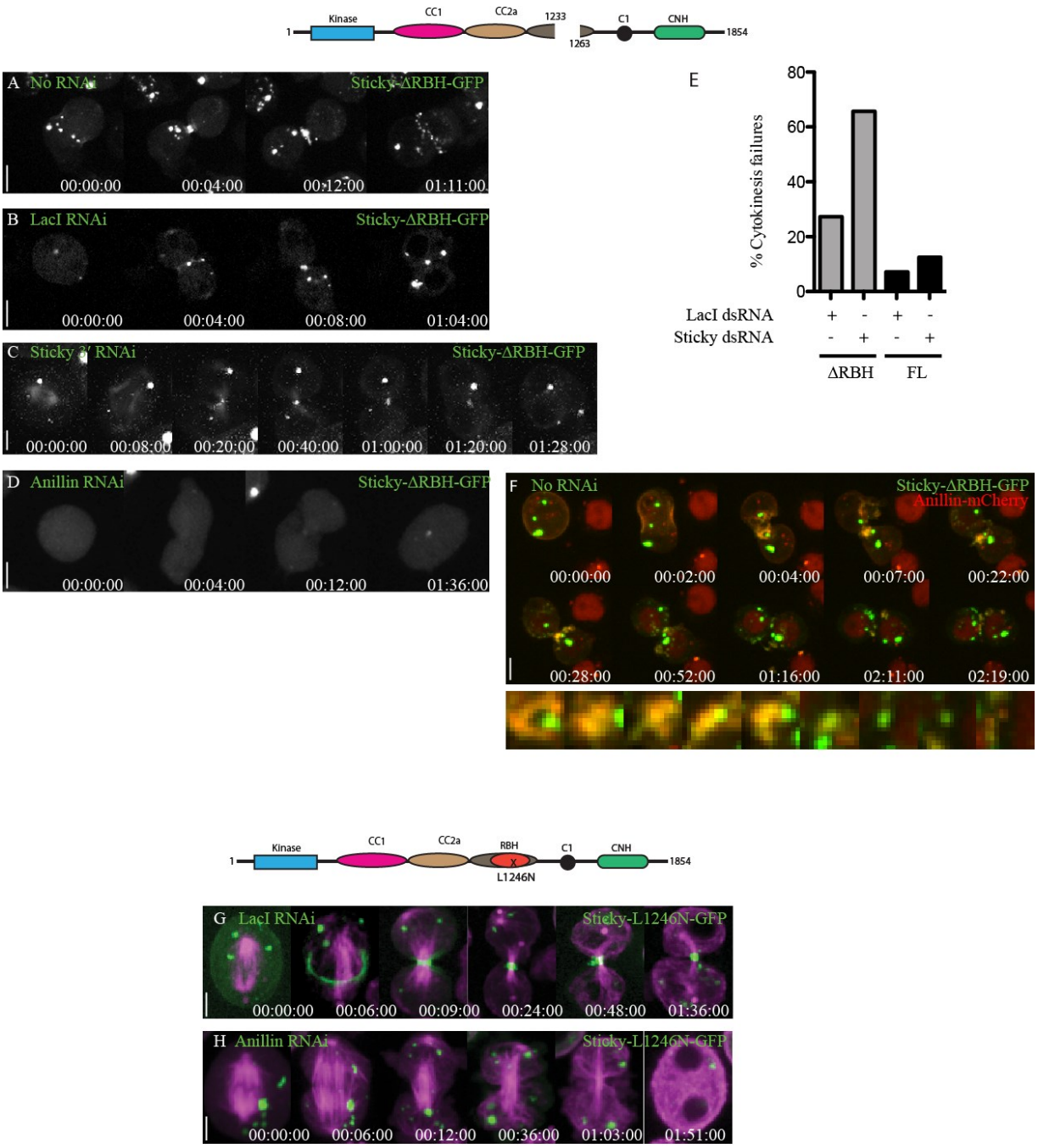

Figure 6. RBD-dependent Sticky localization is essential for MR maturation.

(A-D) Time-lapse sequence of a cell co-expressing Tubulin-mCherry and Sticky-ΔRBH-GFP that failed to form a mature MR (only Sticky-ΔRBH-GFP is displayed) treated with (A) No dsRNA, (B) LacI dsRNA, (C) Sticky 3′ UTR dsRNA or (D) Anillin dsRNA. (E) Quantification from live time lapse imaging from one representative of 3 experiments of failed attempts at

cytokinesis in cells co-expressing Tubulin-mCherry and Sticky-ΔRBH-GFP construct treated with either LacI or Sticky dsRNA (n=66). (F) Top panels: time-lapse sequence of a cell co-expressing Anillin-mCherry and Sticky-ΔRBH-GFP that failed to form a mature MR and display excess shedding. Bottom panels: blow up of the MR in top panels. (G and H) Time-lapse sequence of a cell co-expressing Tubulin-mCherry and Sticky-FL-L246N-GFP treated with (I) LacI or (J) Anillin dsRNA. (A-F) 40× objective 0.85 NA, binning 2x2; (G-H) 100× objective 1.4 NA. Times are h:min:sec. Scale bars (A-F) 8 μm; (G-H) 3.3 μm.

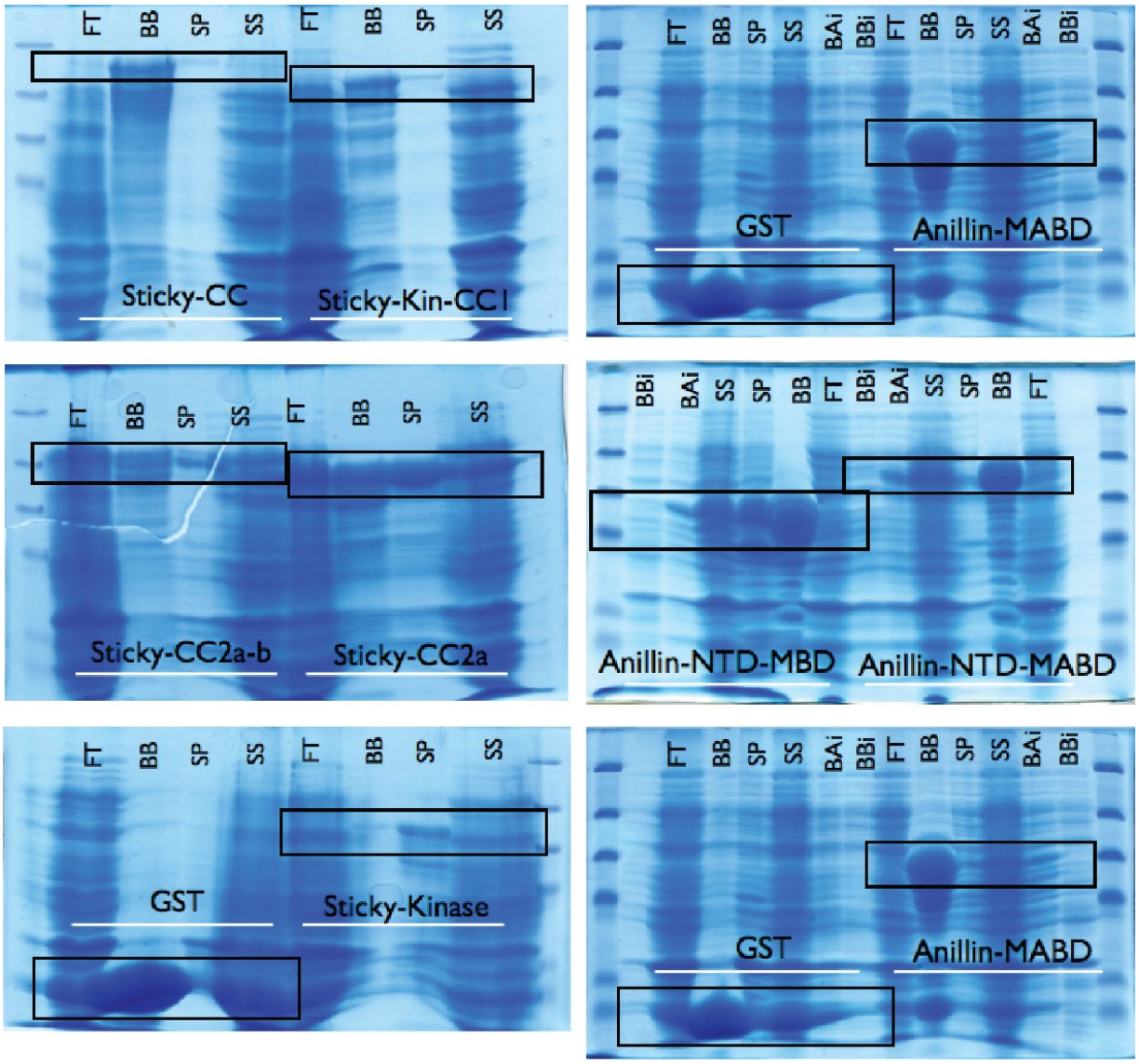

Figure S1. Protein purification

Protein purification preparation of pull-down experiments shown in (Left panels) figure 1 and (Right panels) figure 2. Samples were loaded on 8% SDS page gels stained with Coomassie blue as described in Materials and Methods. FT: Flow Through of bacteria. BBi: Bacteria Before induction. BAi: Bacteria After induction BB: Beads Bound to GST. SS: Sonicated supernatant. SP: Sonicated Pellet. MABD (Myosin-Actin binding domains; Anillin 5` to Actin binding domain)

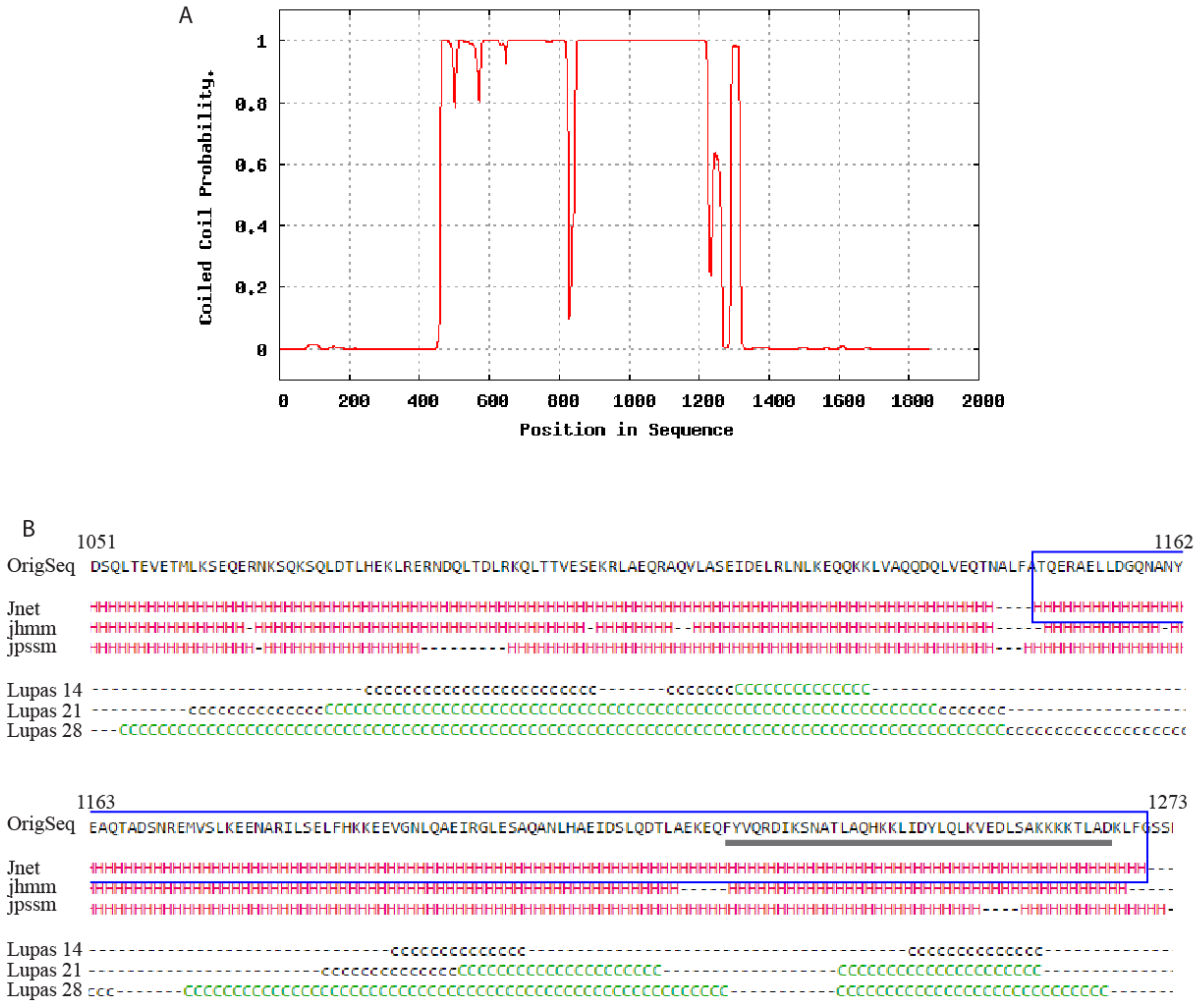

Figure S2. Sticky coiled coil domain prediction

(A) Domain prediction was performed using LOGICOILS algorithm. (B) Domain prediction was performed using Jpred 4. Grey bar designates the Rho binding homology sequence as defined by (Bassi et al. 2011). The blue square highlights a potentially newly defined coiled coil fragment.

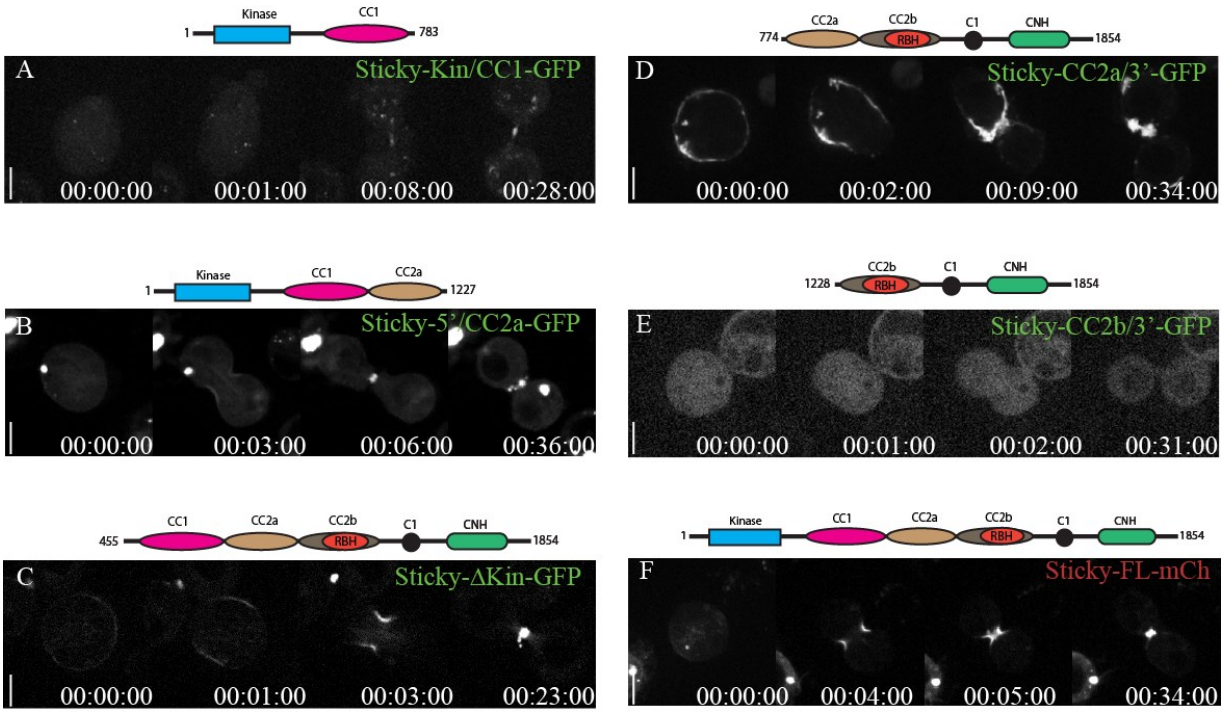

Figure S3. Localization of various Sticky truncations during cytokinesis.

(A to F) Time-lapse sequence of a cell co-expressing Tubulin-mCherry and (A) Sticky(Kin-CC1)-GFP, (B) Sticky-CC2a/3'-GFP, (C) Sticky(5'-CC2a)-GFP, (D) Sticky(CC2b-3')-GFP (E) Sticky-ΔKin-GFP or (F) Sticky-FL-mCherry.. Kin=Kinase; FL=Full Length; 5'= First residue of Sticky; 3'=Last residue of Sticky. Times are h:min:sec. 40× objective 0.85 NA. Scale bars 6.5 µm

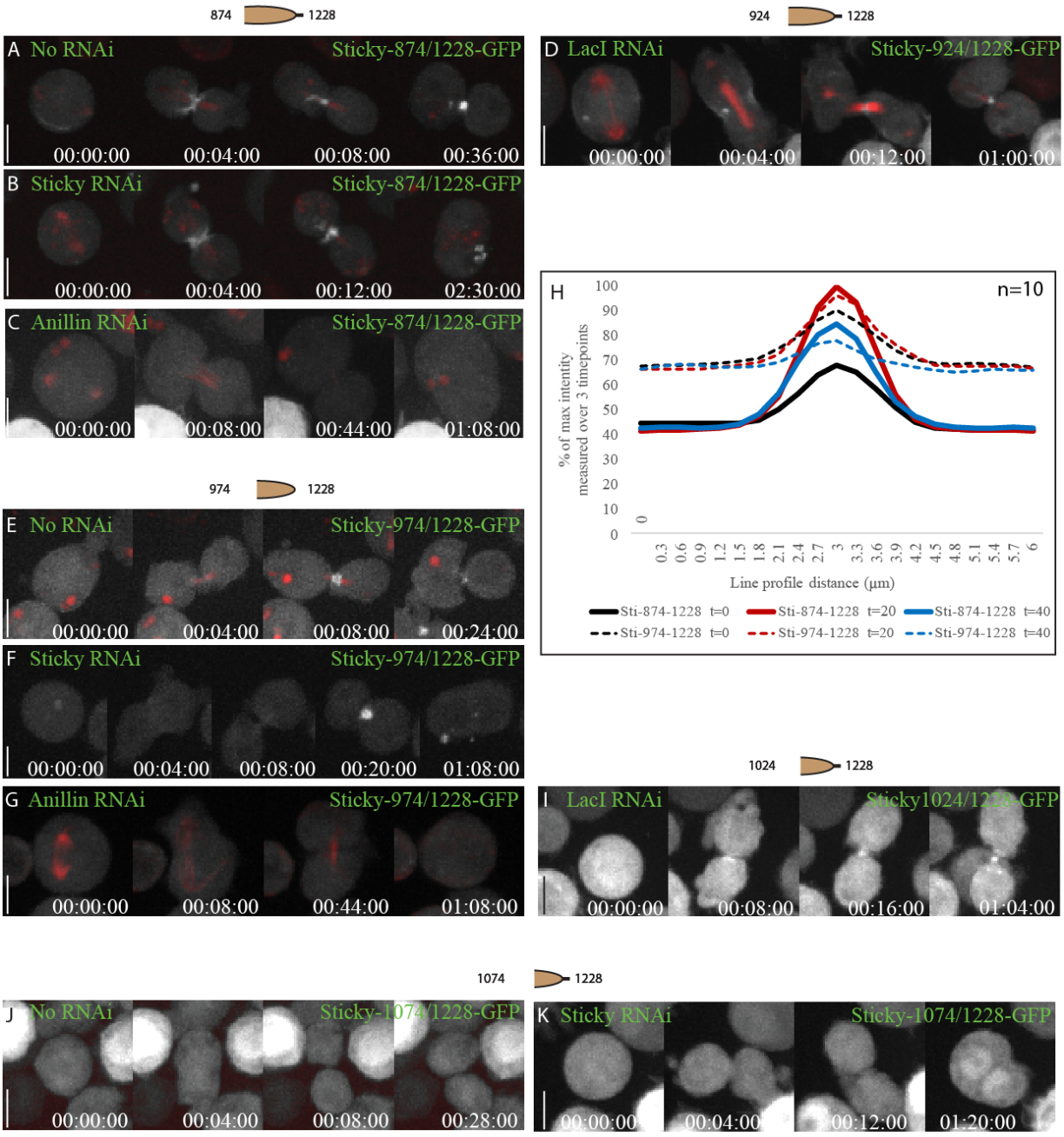

Figure S4. Identification of the minimal region of Sticky capable of Anillin-dependent cortical recruitment during cytokinesis.

(A, B and C) Time-lapse sequence of a cell co-expressing Tubulin-mCherry and Sticky-874/1228-GFP treated with (A) LacI or (B) Sticky or (C) Anillin dsRNA. (D) Time-lapse sequence of a cell co-expressing Tubulin-mCherry and Sticky(924-1228)-GFP treated with LacI dsRNA. (E, F and G) Time-lapse sequence of a cell co-expressing Tubulin-mCherry and

Sticky(974-1228)-GFP treated with (E) LacI or (F) Sticky or (G) Anillin dsRNA. (H) Line profile across the MR over time timepoints from end of furrow (t=0, 20 or 40 minutes) of cells co-expressing Tubulin-mCherry and Sticky-874/1228-GFP or Sticky-974/1228-GFP. (I) Time-lapse sequence of a cell co-expressing Tubulin-mCherry and Sticky(1074-1228)-GFP treated with LacI dsRNA. (J and K) Time-lapse sequence of a cell co-expressing Tubulin-mCherry and Sticky(874-1228)-GFP treated with (J) LacI or (K) Sticky dsRNA. Times are h:min:sec. 40× objective 0.85 NA, binning 2x2. Scale bars 8 μm

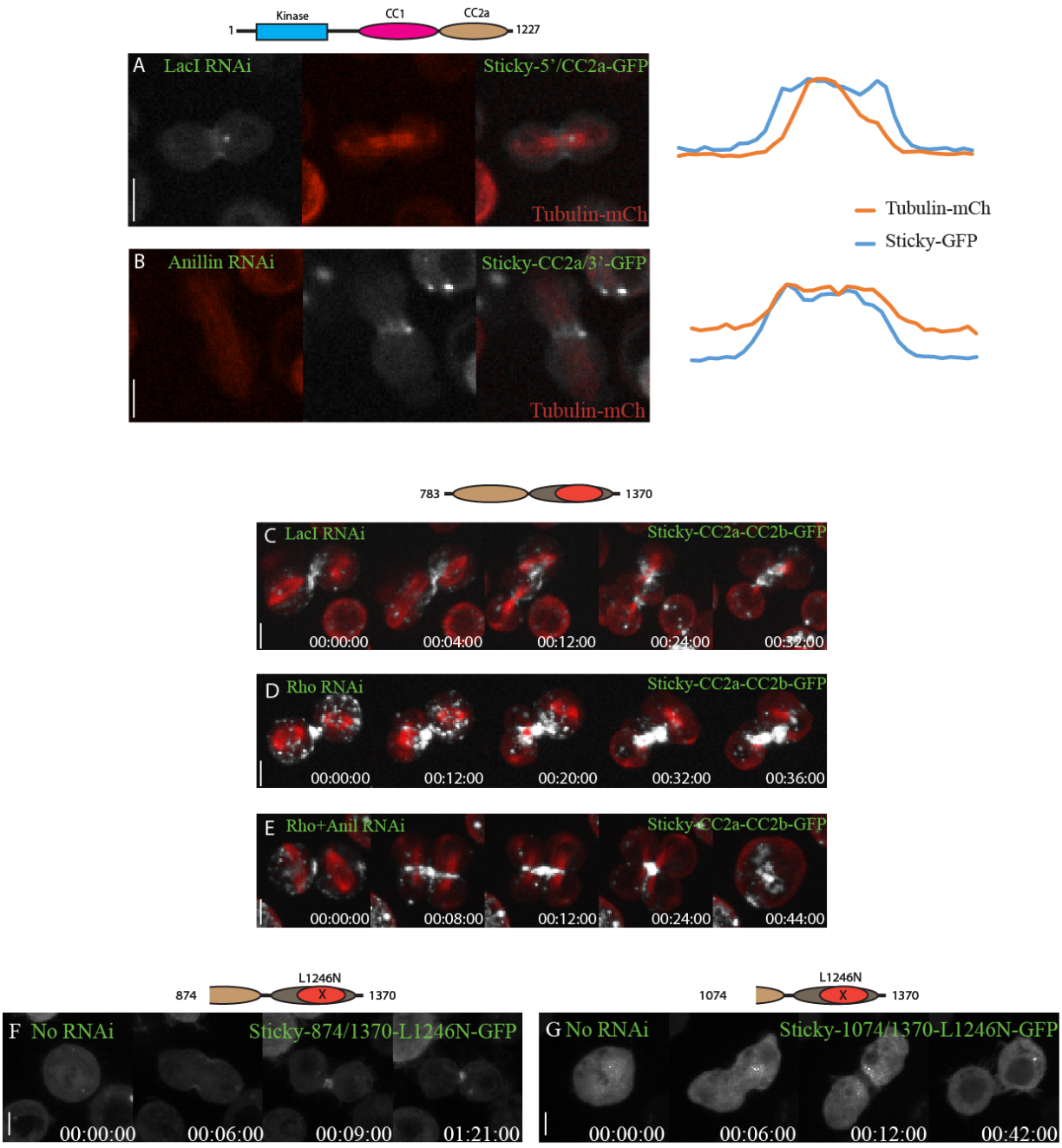

Figure S5. Joint Anillin- and RBD-dependent inputs on Sticky have stronger localization to the cortex.

(A and B) Left panels: time-lapse sequence of a cell co-expressing Tubulin-mCherry and Sticky-(5'-CC2a)-GFP treated with (A) LacI or (B) Anilin dsRNA. Right panels: Line profile across the equator of the cell in left panel. Pixel intensity was measured and normalized to the max intensity pixel of the line profile. (C, D and E) Time-lapse sequence of a cell co-expressing

Tubulin-mCherry and Sticky(CC2a-CC2b)-GFP treated with (C) LacI or (D) Rho or (E) Rho+Anillin dsRNA. (F and G) Time-lapse sequence of a cell co-expressing Tubulin-mCherry and (F) Sticky(874-1370)-L1246N-GFP or (G) Sticky(1074-1370)-L1246N-GFP. Times are h:min:sec. (A-E) 40× objective 0.85 NA, binning 2x2; (F-G) 100× objective 1.4 NA. Scale bars (A-E) 8 µm; (F-G) 3.3 µm

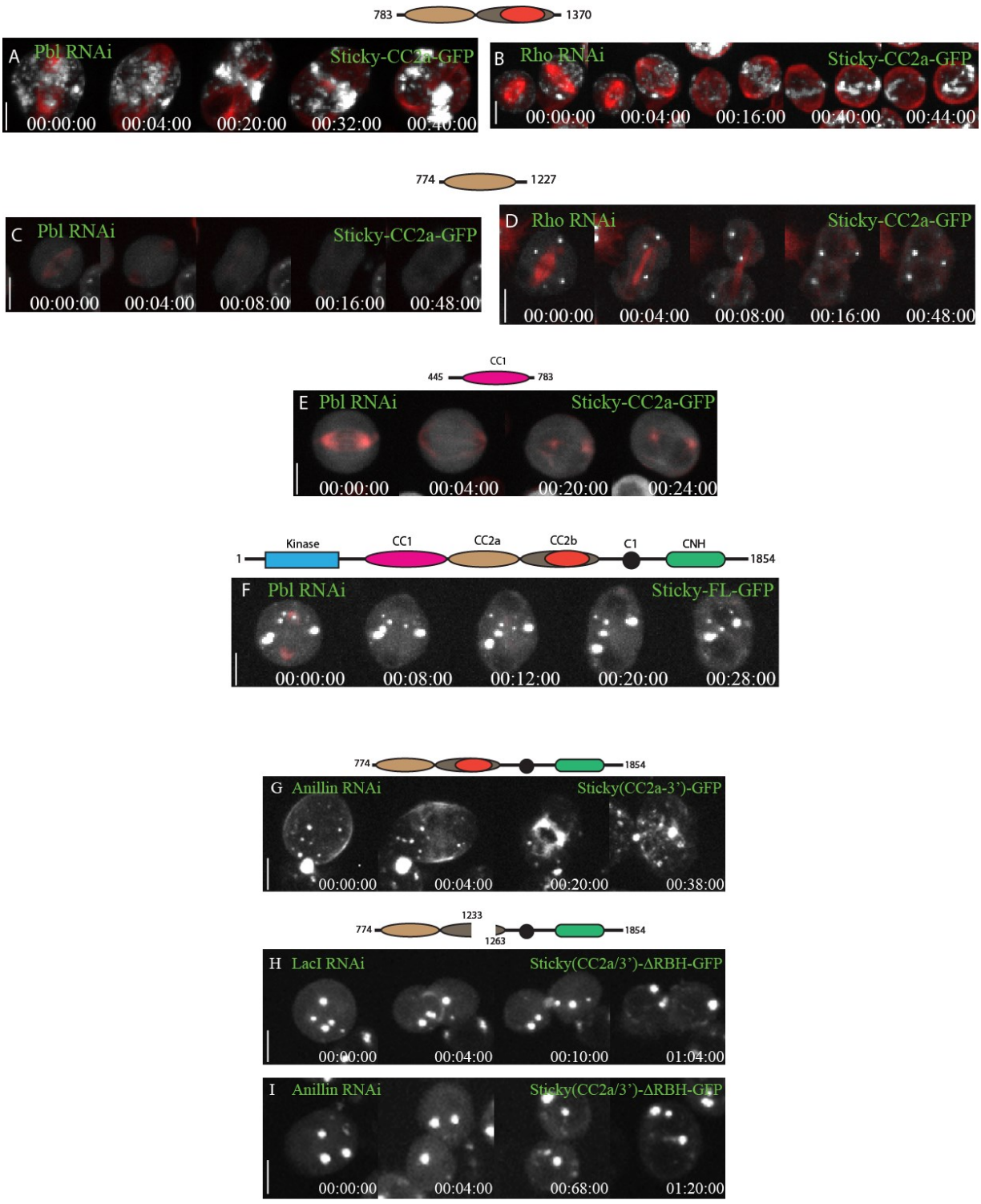

Figure S6. Rho1 and the RhoGEF Pebble are required for all inputs into Sticky localization to cytokinesis structures.

(A and B) Time-lapse sequence of a cell co-expressing Tubulin-mCherry and Sticky-CC2-GFP treated with (A) LacI or (B) Pebble dsRNA. (C and D) Time-lapse sequence of a cell co-expressing Tubulin-mCherry and Sticky-CC2a-GFP treated with (C) Pebble or (D) LacI dsRNA. (E and F) Time-lapse sequence of a cell co-expressing Tubulin-mCherry and (E) StickyCC1-GFP or (F) Sticky-FL-GFP treated with Pebble dsRNA. (G) Time-lapse sequence of a cell co-expressing Tubulin-mCherry and Sticky(CC2a-3')-GFP treated with Anillin dsRNA. (H and I) Time-lapse sequence of a cell co-expressing Tubulin-mCherry and Sticky(CC2a-3')-ΔRBH -GFP treated with (I) LacI or (J) Anillin dsRNA. 40× objective 0.85 NA, binning 2x2 Times are h:min:sec. Scale bars 8 μm

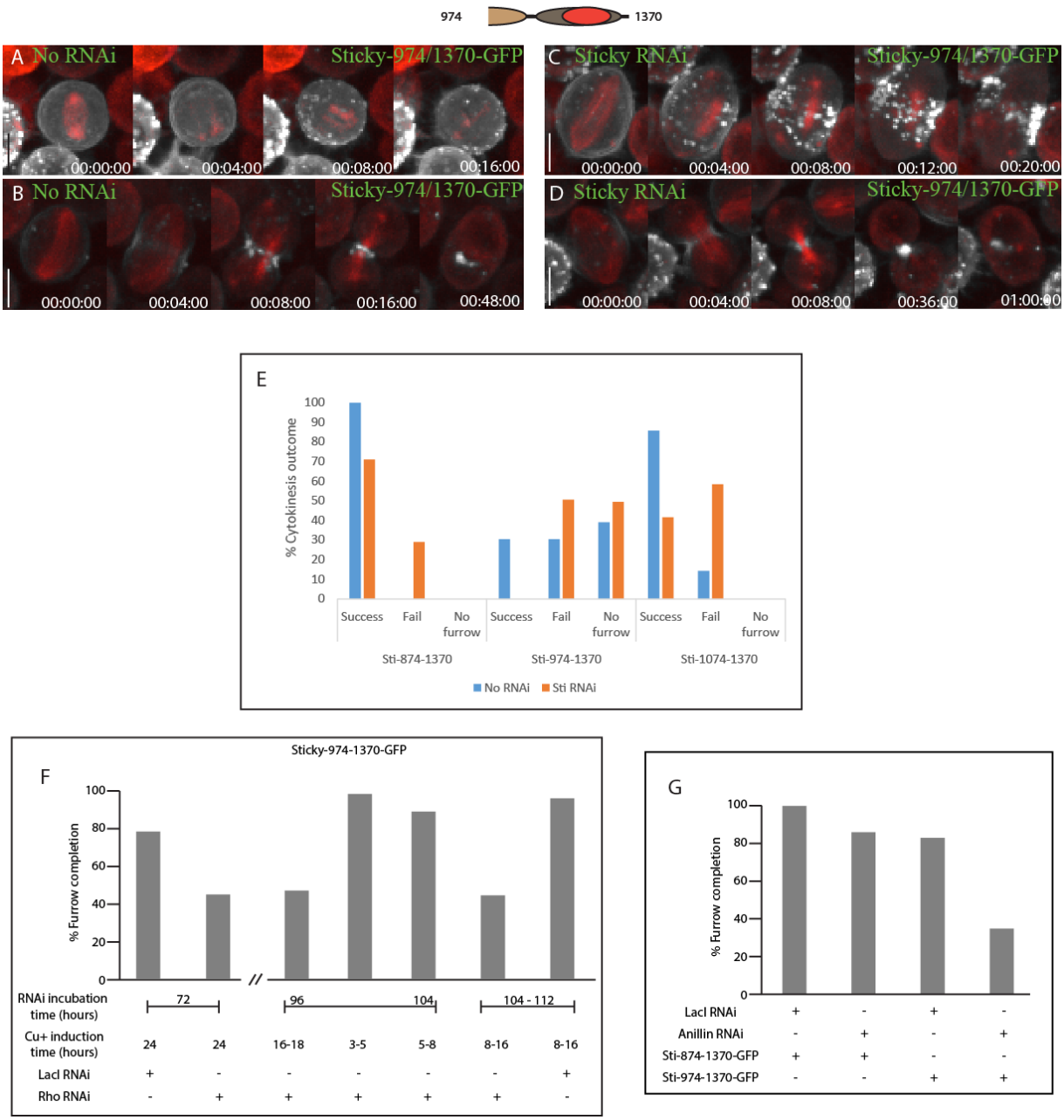

Figure S7. Different truncations extending the RBD of Sticky differentially perturb cytokinesis and differentially synergize with Rho1 RNAi.

(A-D) Time-lapse sequence of a cell co-expressing Tubulin-mCherry and Sticky(974-1370)-GFP treated with (A-B) No dsRNA or (C-D) Sticky dsRNA. (E) Quantification from live time lapse imaging of cytokinesis outcome in cells co-expressing Tubulin-mCherry and either Sticky(874-1370)-GFP (n=71), Sticky(974-1370)-GFP (n=154) or Sticky(1074-1370)-GFP

(n=26) not treated with dsRNA or treated with Sticky dsRNA. Data are from an individual experiment representative of 2 independent experiments (F) Quantification from live time lapse imaging of failure to form a furrow in cells co-expressing Tubulin-mCherry and Sticky(974-1370)-GFP, treated with either LacI or Rho1 dsRNAi, induced with $CuSO_4$ at indicated times (n≥52). Data combine two individual datasets from independent experiments separated by //. (G) Quantification from live time lapse imaging to form a furrow in cells co-expressing Tubulin-mCherry and either Sticky(974-1370)-GFP or Sticky(874-1370)-GFP, treated with either LacI or Anillin dsRNAi, induced with $CuSO_4$ at indicated times (n≥35). Data is from an individual experiment. Times are h:min:sec. Scale bars 8 μm

5.7. Materials and Methods

5.7.1. Live-cell microscopy

Live-cell imaging of *Drosophila* S2 cells in Schneider's medium was done at room temperature with a spinning-disc confocal system (Ultra-VIEW Vox; PerkinElmer) using a scanning unit (CSU-X1; Yokogawa Corporation of America) and a charge-coupled device camera (ORCA-R2; Hamamatsu Photonics) fitted to an inverted microscope (DMI6000 B; Leica) equipped with a motorized piezoelectric stage (Applied Scientific Instrumentation). Image acquisition was performed using Volocity version 6.3 (PerkinElmer). Time-lapse imaging was performed using a Plan Apochromat 40×, 0.85 NA air objective with camera binning set to 2 × 2 or when indicated in the figure legends by using a Plan Apochromat 63 or 100× oil immersion objectives, NA 1.4, at camera binning set to 2 × 2 or no binning. Using 250 μM of $CuSO_4$ we induced expressions of FP fusions under the control of the metallothionein promoter (pMT plasmids) induction occurred 12 to 16 hours before imaging unless indicated in the figures legends.

5.7.2. Image analysis

Statistical analysis was performed using Prism (GraphPad Software), by conducting an unpaired t test. Intensity measurements were done using the Volocity (Perkin Elmer) line profile measurements tool of the Volocity Quantitation and Analysis module as follows. A line was drawn across the equator of a single optical section. Max percentage values were found empirically for each line profile. The rest of the intensity values were then expressed as percentages relative to that value. Images were processed for publication using Photoshop CS (Adobe) and assembled as figures using Illustrator CS (Adobe). Video files were exported from Volocity as QuickTime videos (Apple).

5.7.3. Pull down assay

Protein purification: 3 ml *Escherichia coli* strain BL21 were inoculated overnight LB/Amp culture in 300 ml of fresh LB/Amp for 5 hours at 37 ºC at an OD of 0.6, induced with 0.5 mM of IPTG for 4 hours (at 37ºC). After induction, cells were centrifuged at 6000 rpm for 15minutes

at 4ºC. Pellets were frozen before lysis to improve cell lysis. Bacterial pellets were lysed for 1 h on ice using (75 mM PBS, 150 mM DTT, 2 mM pefabloc, 5% EDTA 0.5M, 0.2% lysozyme, 1mM protease inhibitor cocktail [Roche]). Lysates were sonicated on ice for 10min using a 30 seconds cycle on and 30 seconds off at a 50% amplitude. Sonicated pellets were centrifuged at 10000 rpm for 20 minutes at 4ºC. Supernatant were incubated overnight at 4ºC on a shaker with 500 µL of 3x PBS washed beads. Beads were next day centrifuged at 1500rpm for 10 minutes at 4ºC. Beads were washed 3x with PBS at 4ºC.

S2 harvesting/lysis: Each T75 flask of S2 cells were washed once with PBS. Cells were collected by 5 minutes centrifugation at 4ºC. Pellets were lysed for 15 minutes on ice in 1 mL of lysis buffer (50 mM Tris-HCl, pH 7.5, 150 mM NaCl, and 1% Triton X-100 completed with protease inhibitor cocktail [Roche]). Triton insoluble fraction was collected following a 15 minute 12000 rpm centrifugations at 4ºC.

Pull-down: 500 µL of whole cell lysate was added to 200 µL of GST bound beads and incubate on a shaker overnight at 4ºC. The next day, the supernatant were split from the beads by centrifugation at 10000 rpm for 5 minutes at 4ºC. Beads were washed 3x with PBS then resuspended in an estimated 1 for 1 ratio of PBS and beads.

5.7.4. Immunoblotting

Equal amount of proteins from different samples were subjected to SDS-PAGE (8–15% polyacrylamide). Proteins were transferred to a nitrocellulose membrane and blocked with 5% milk in TBS containing 0.2% Tween 20 (TBST). The membrane was cut at the appropriate molecular weight marker with the upper molecular weight part immunoblotted with affinity-purified anti-Anillin antibodies (1:1,000; generated in rabbits against amino acids 1–409 of Anillin fused to GST; a gift from J. Brill, The Hospital for Sick Children [SickKids], Toronto, Ontario, Canada; Goldbach et al., 2010) or anti-Sticky antiserum (1:3,000, generated in rabbits against a fragment of the Sticky protein [amino acids 531–742] fused to a C-terminal 6×His tag, a gift from P. D'Avino, Cambridge University, Cambridge, England, UK; (D'Avino et al., 2004). The blots were washed in TBST, incubated with horseradish peroxidase–coupled donkey anti–rabbit or anti–mouse secondary antibodies (1:5000; GE Healthcare), and washed again before detection of signals using Western ECL substrate (Clarity; Bio-Rad Laboratories).

5.7.5. Constructs, cell lines and RNAi

All constructs were generated by PCR amplification of the ORF, without stop codons, followed by cloning into pENTR-D-TOPO (Invitrogen) then by recombination using LR Clonase into appropriate destination vectors (Drosophila Gateway Vector Collection; T. Murphy, Carnegie Institution for Science, Washington, DC). Anillin-GFP (pMT-WG, driven by the metallothionein promoter), Anillin-mCh (pAc-WCh, driven by the constitutive Act05C promoter), mCh-tubulin (pAc-ChW), Anillin-ΔMyoBD-GFP (pMT-WG), Sticky-FP (pMT-WG or pMT-WCh) have been described previously (Echard et al., 2004; El-Amine et al., 2013; Hickson and O'Farrell, 2008b; Kechad et al., 2012). Sticky internal deletions and site-directed mutagenesis were performed by PCR by overlap extension followed by cloning into pENTR-D-TOPO and subsequent recombination into pMT-WG. All Anillin constructs derive from clone LD23793 (Berkeley Drosophila Genome Project Gold collection; Drosophila Genomics Resource Center) that encodes the CG2092-RB polypeptide. Note that CG2092-RB has an additional 27 residues within the actin-binding domain that is absent in CG2092-RA (Field and Alberts, 1995), but CG2092-RB is better supported by sequencing data. Anillin-ActBD encodes amino acids 256–409 as defined in Field and Alberts (1995). Anillin-M/ABD encodes amino acids 146-409. Anillin-ΔMyoBD encodes amino acids 1–145 and 238–1,239 and lacks 92 amino acids homologous to the Xenopus MyoBD defined in (Straight et al., 2005). Anillin NTD-MBD encodes amino acids 1-237. Anillin-M/ABD encodes amino acids 1-409. The sticky (CG10522) ORF was PCR amplified from clone RE26327 (Drosophila Gene Collection release 2 collection; Drosophila Genomics Resource Center). The Sticky L1246N point mutation was generated by site-directed mutagenesis using primers 5'-GCGCAGCACAAAAAGgcgATTGACTACCTTCAG-3' and 5'-CTGAAGGTAGTCAATcgcCTTTTTGTGCTGCGC-3'. Rest of Sticky contructs have an indicated encoded amino acid in the figures. All constructs were verified by sequencing. Plasmids were used to transfect *Drosophila* Schneider's S2 cells using Cellfectin reagent (Invitrogen), together with pCoHygro and additional plasmids as needed to generate stable, hygromycin-resistant cell lines following established protocols (Invitrogen). After selection, cells were cultured in Schneider's medium supplemented with 10% fetal calf serum (Invitrogen)

and penicillin/streptomycin. dsRNAs were generated using in vitro transcription kits (RiboMAX; Promega), and DNA templates were generated in a two-step PCR amplification from cDNA or genomic DNA, as described previously (Echard et al., 2004; El-Amine et al., 2013). In brief, in the first-round PCR, gene-specific primer sequences included a 5' anchor sequence (5'-GGGCGGGT-3'), whereas the second-round PCR used a universal T7 anchor primer (5'-TAATACGACTCACTATAGGGAGACCACGGGCGGGT-3'). Gene-specific primer sequences were previously described for anillin dsRNA (Echard et al., 2004; Hickson and O'Farrell, 2008b), Anillin 3′ UTR dsRNA (Hickson and O'Farrell, 2008b), and sticky dsRNAs (Echard et al., 2004; El-Amine et al., 2013). RNAi experiments were performed as follows: cells were plated in 96-well dishes and incubated with 1 µg/ml dsRNA. 12–24 h before imaging, cells were transferred to 8-well chambered coverglass dishes (Lab-Tek; Thermo Fisher Scientific). Live imaging was performed between 30 and 72 h for Anillin dsRNAs, between 30 and 60 h for Sticky dsRNAs, between 96 and 120 h for Pbl or Rho dsRNA, in which case cells were split and fresh dsRNA added on the third day. These dsRNA incubation times were maintained for codepletion experiments, but the individual dsRNA incubations were performed in the presence of irrelevant LacI control dsRNAs to control for possible effects of combining dsRNAs.

5.7.6. Primers list

Sticky-455 F: 5'-CACCATGATTTCCGCTACCACCGATGAA-3'

Sticky-774 F: 5'-CACCATGCCTGGATCTTTGACCGAACTG-3'

Sticky-783 R: 5'-AATGGCATTCAGTTCGGTCAA-3'

Sticky-1228 F: 5'-CACCATGTACGTGCAGCGGGACATTAAA-3'

Sticky-1227 R: 5'-GAACTGCTCCTTCTCGGCCAA-3'

Sticky-1370 R: 5'-CGTCGTCTTCAGCTCCACCTG-3'

Sticky-1450 R: 5'-GCTAAGATCATCGGCTGACGG-3'

Sticky-dRBH F: 5'-CAGCGGGACATTACATTGGCGGACAAACTTTTC-3'

Sticky-dRBH R: 5'-GTCCGCCAATGTAATGTCCCGCTGCACGTAGAA-3'

CC2a-50 F: 5'-CACCATGGAGCAGAGTCTTTCACCCACG-3'

CC2a-100 F: 5'-CACCATGACAGCGAATCTATCGCTCTGG-3'

CC2a-150 F: 5'-CACCATGTCACAGGAGGAAACTCGCCAG-3'

CC2a-200 F: 5'-CACCATGTTGGCCAATGTGCACAGATTA-3'

CC2a-250 F: 5'-CACCATGGACTCTTGTTTGGTCTTACAG-3'

CC2a-300 F: 5'-CACCATGCAACTTGATACCCTTCATGAG-3'

CC2a-350 F: 5'-CACCATGCTCAAGGAGCAGCAGAAGAAG-3'

CC2a-400 F: 5'-CACCATGGTTAGTTTGAAGGAGGAAAAT-3'

CC2b+50 R: 5'-TGAAAGACTCTGCTCGTTGAA-3'

CC2b-100 R: 5'-CGATAGATTCGCTGTACGCGC-3'

CC2b-150 R: 5'-AGTTTCCTCCTGTGACGTCTT-3'

CC2b-200 R: 5'-GTGCACATTGGCCAAGTGCTC-3'

CC2b-250 R: 5'-GACCAAACAAGAGTCATTCGC-3'

CC2b-300 R: 5'-AAATCTCAACTTGATACCCTT-3'

CC2b-350 R: 5'-CTGCTGCTCCTTGAGATTGAG-3'

CC2b-400 R: 5'-CTCCTTCAAACTAACCATTTC-3'

Sticky L1246N F: 5-GCGCAGCACAAAAAGgcgATTGACTACCTTCAG-3'

Sticky L1246N R: 5'-CTGAAGGTAGTCAATcgcCTTTTTGTGCTGCGC-3'

5.8. References

Bassi, Z. I., M. Audusseau, M. G. Riparbelli, G. Callaini and P. P. D'Avino (2013). "Citron kinase controls a molecular network required for midbody formation in cytokinesis." Proc Natl Acad Sci U S A **110**(24): 9782-9787.

Bassi, Z. I., K. J. Verbrugghe, L. Capalbo, S. Gregory, E. Montembault, D. M. Glover and P. D'Avino (2011). "Sticky/Citron kinase maintains proper RhoA localization at the cleavage site during cytokinesis." The Journal of Cell Biology **195**(4): 595-603.

Cunto, D. F., E. Calautti, J. Hsiao, L. Ong, G. Topley, E. Turco and G. P. Dotto (1998). "Citron rho-interacting kinase, a novel tissue-specific ser/thr kinase encompassing the Rho-Rac-binding protein Citron." The Journal of biological chemistry **273**(45): 29706-29711.

D'Avino, P., M.S. Savoian, and D.M. Glover. 2004. Mutations in sticky lead to defective organization of the contractile ring during cytokinesis and are enhanced by Rho and suppressed by Rac. *The Journal of Cell Biology*. 166:61-71.

D'Avino, P., M. Giansanti and M. Petronczki (2015). "Cytokinesis in Animal Cells." Cold Spring Harbor Perspectives in Biology **7**(4).

Dvorsky, R., L. Blumenstein, I.R. Vetter, and M.R. Ahmadian. 2004. Structural insights into the interaction of ROCKI with the switch regions of RhoA. *J Biol Chem*. 279:7098-7104.

El-Amine, N., A. Kechad, S. Jananji and G. Hickson (2013). "Opposing actions of septins and Sticky on Anillin promote the transition from contractile to midbody ring." The Journal of Cell Biology **203**(3): 487-504.

Echard, A., G.R.X. Hickson, E. Foley, and P.H. O'Farrell. 2004. Terminal cytokinesis events uncovered after an RNAi screen. *Current biology : CB*. 14:1685-1693.

Field, C.M., and B.M. Alberts. 1995. Anillin, a contractile ring protein that cycles from the nucleus to the cell cortex. *J Cell Biol*. 131:165-178.

Gai, M., P. Camera, A. Dema, F. Bianchi, G. Berto, E. Scarpa, G. Germena and F. Cunto (2011). "Citron kinase controls abscission through RhoA and anillin." Molecular biology of the cell **22**(20): 3768-3778.

Green, R. A., E. Paluch and K. Oegema (2012). "Cytokinesis in animal cells." Annual review of cell and developmental biology **28**(1): 29-58.

Gruneberg, U., R. Neef, X. Li, E. Chan, R. B. Chalamalasetty, E. A. Nigg and F. A. Barr (2006). "KIF14 and citron kinase act together to promote efficient cytokinesis." The Journal of Cell Biology **172**(3): 363-372.

Hickson, G. and P. H. O'Farrell (2008). "Rho-dependent control of anillin behavior during cytokinesis." The Journal of Cell Biology **180**(2): 285-294.

Kechad, A., S. Jananji, Y. Ruella and G. R. Hickson (2012). "Anillin acts as a bifunctional linker coordinating midbody ring biogenesis during cytokinesis." Curr Biol **22**(3): 197-203.

Madaule, P., M. Eda, N. Watanabe, K. Fujisawa, T. Matsuoka, H. Bito, T. Ishizaki and S. Narumiya (1998). "Role of citron kinase as a target of the small GTPase Rho in cytokinesis." Nature **394**(6692): 491-494.

Madaule, P., T. Furuyashiki, M. Eda, H. Bito, T. Ishizaki and S. Narumiya (2000). "Citron, a Rho target that affects contractility during cytokinesis." Microscopy research and technique **49**(2): 123-126.

Madaule, P., T. Furuyashiki, T. Reid, T. Ishizaki, G. Watanabe, N. Morii and S. Narumiya (1995). "A novel partner for the GTP-bound forms of rho and rac." FEBS letters **377**(2): 243-248.

McKenzie, C., Z. I. Bassi, J. Debski, M. Gottardo, G. Callaini, M. Dadlez and P. P. D'Avino (2016). "Cross-regulation between Aurora B and Citron kinase controls midbody architecture in cytokinesis." Open Biol **6**(3).

Piekny, A., M. Werner and M. Glotzer (2005). "Cytokinesis: welcome to the Rho zone." Trends Cell Biol **15**(12): 651-658.

Schroeder, T. E. (1972). "The contractile ring. II. Determining its brief existence, volumetric changes, and vital role in cleaving Arbacia eggs." J Cell Biol **53**(2): 419-434.

Serres, M.P., U. Kossatz, Y. Chi, J.M. Roberts, N.P. Malek, and A. Besson. 2012. p27(Kip1) controls cytokinesis via the regulation of citron kinase activation. *J Clin Invest*. 122:844-858.

Sgro, F., F. T. Bianchi, M. Falcone, G. Pallavicini, M. Gai, A. M. Chiotto, G. E. Berto, E. Turco, Y. J. Chang, W. B. Huttner and F. Di Cunto (2016). "Tissue-specific control of midbody microtubule stability by Citron kinase through modulation of TUBB3 phosphorylation." Cell Death Differ **23**(5): 801-813.

Shimizu, T., K. Ihara, R. Maesaki, M. Amano, K. Kaibuchi, and T. Hakoshima. 2003. Parallel coiled-coil association of the RhoA-binding domain in Rho-kinase. *J Biol Chem*. 278:46046-46051.

Shandala, T., S. L. Gregory, H. E. Dalton, M. Smallhorn and R. Saint (2004). "Citron Kinase is an essential effector of the Pbl-activated Rho signalling pathway in Drosophila melanogaster." Development **131**(20): 5053-5063.

Straight, A.F., C.M. Field, and T.J. Mitchison. 2005. Anillin Binds Nonmuscle Myosin II and Regulates the Contractile Ring. *Molecular Biology of the Cell*. 16:193-201.

Thumkeo, D., S. Watanabe and S. Narumiya (2013). "Physiological roles of Rho and Rho effectors in mammals." Eur J Cell Biol **92**(10-11): 303-315.

Watanabe, S., T. De Zan, T. Ishizaki and S. Narumiya (2013). "Citron kinase mediates transition from constriction to abscission through its coiled-coil domain." J Cell Sci **126**(Pt 8): 1773-1784.

6. Discussion

La cytokinèse est un processus universel qui se passe dans une forme ou une autre chez le vivant. Sa régulation est importante pour le développement des organismes. Il est donc important de comprendre ce processus en détail. Cet ouvrage s'intéresse plus spécifiquement à mieux comprendre la transition de l'anneau contractile à l'anneau du midbody. Notre contribution dans ``*opposing actions of septins and Sticky on Anillin promote the transition from contractile to midbody ring*`` *(Ch. 4)* démontre que suite à l'ingression, un processus de maturation de la transition de l'anneau contractile dynamique à l'anneau du midbody stable est nécessaire pour éviter une régression du sillon de clivage. Comment peut-on définir ce mécanisme de maturation? Quels en sont les éléments qui régulent la transition de l'anneau contractile à l'anneau du midbody? Ce sont deux questions abordées lors de cet ouvrage. Parmi les protéines largement impliquées dans ce processus, nous retrouvons Citron Kinase ou Sticky chez la *Drosophile*. Citron Kinase/Sticky semble avoir un rôle à plusieurs niveaux :

- Au niveau de la stabilisation de l'ingression de l'anneau contractile (El-Amine et al., 2013; Gai et al., 2011; Madaule et al., 1998)
- Au niveau du cytosquelette (Bassi et al., 2011; Yamashiro et al., 2003)
- Au niveau membranaire et cortical (El-Amine et al., 2013)(El-amine et al. 2016)
- Au niveau de la stabilisation du pont intercellulaire (Bassi et al., 2013; McKenzie et al., 2016)
- Au niveau de la régulation du temps requis pour l'abscision (El-Amine et al., 2013; Gai et al., 2011; Sgro et al., 2016)

Comment Citron Kinase pourrait être impliqué à tous ces niveaux si sa localisation est principalement corticale? Nous avons exploré les mécanismes nécessaires pour sa localisation au cortex à l'aide d'une étude structurelle fonctionnelle de Citron Kinase. Les résultats dans ``Distinct Anillin- and Rho-dependent contributions to Citron Kinase localization and function are required for cytokinesis`` *(Ch. 5)*, sont les premiers à identifier et caractériser deux mécanismes distincts responsables de cette localisation corticale.

La Figure 11 propose un modèle de travail tiré des résultats de cette thèse. Ce modèle représente les interactions directes ou indirectes qui ont été confirmées par la littérature. Une contribution Citron Kinase/Sticky-dépendante de la rétention de ce complexe est représentée par une flèche en direction du fuseau central. Une flèche dans le sens opposé représente une force Septin^{Peanut}-dépendante qui tire ce complexe vers l'extérieur de la cellule. À noter que cette force peut également se manifester par des glissements le long de la membrane ou une internalisation vers le cytoplasme des deux cellules filles. Citron Kinase/Sticky, se trouve à proximité de RhoA et Anillin. Anillin se trouve au centre de ce complexe interagissant à tous ces composants corticaux.

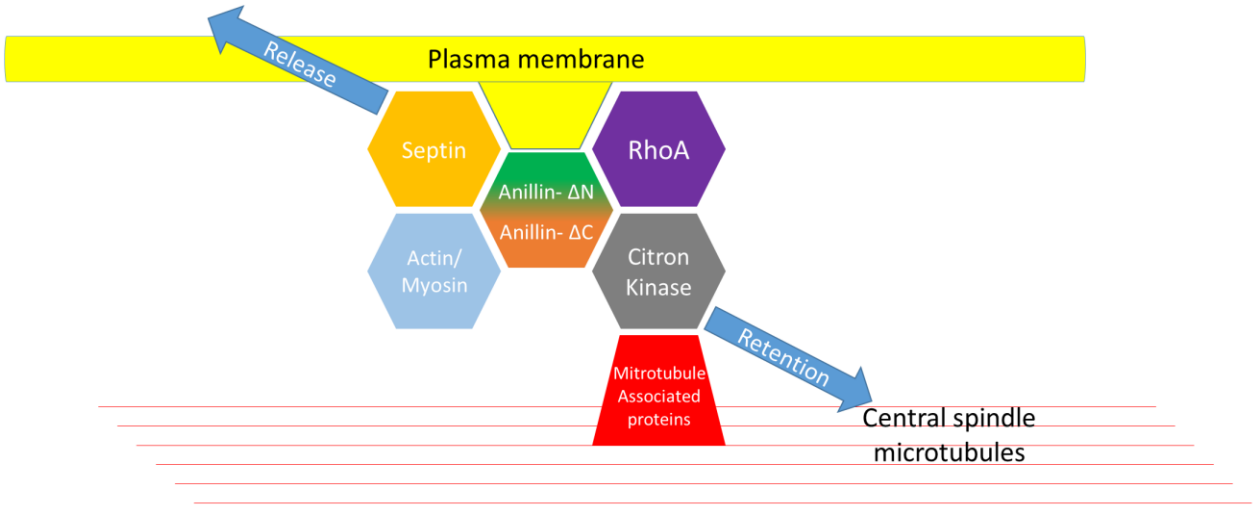

Figure 11. Modèle de mécanismes d'interactions des protéines corticales.

Chaque protéine est représentée par un hexagone. Deux segments adjacents représentent une interaction

6.1. Un enjeu double dans la localisation corticale de Sticky

Le chapitre 5 a permis de mettre en évidence deux mécanismes distincts qui confèrent à Sticky sa localisation corticale. L'un est Anillin-dépendant tandis que l'autre est Rho1-dépendant. Je propose le modèle schématique suivant pour illustrer la contribution du chapitre

5 sur la compréhension du rôle de Citron Kinase dans la cytokinèse. Ce modèle suit évidement la logique de la figure 11. L'apport ajouté dans le chapitre 5 est au niveau d'une compréhension plus approfondie des fonctions spécifiques de Citron Kinase lors de la cytokinèse. Nous avons pu démontrer que Sticky possède deux mécanismes distincts de localisation corticale à travers ses résidus Sticky-CC2a(974-1128) et Sticky-CC2b(1128-1370). La localisation corticale de chacun était différente et la perturbation de n'importe lequel de ces deux mécanismes empêche la formation d'une structure stable de l'anneau du midbody, et ce de manière similaire à la diminution d'expression de Sticky dans les cellules S2 normales.

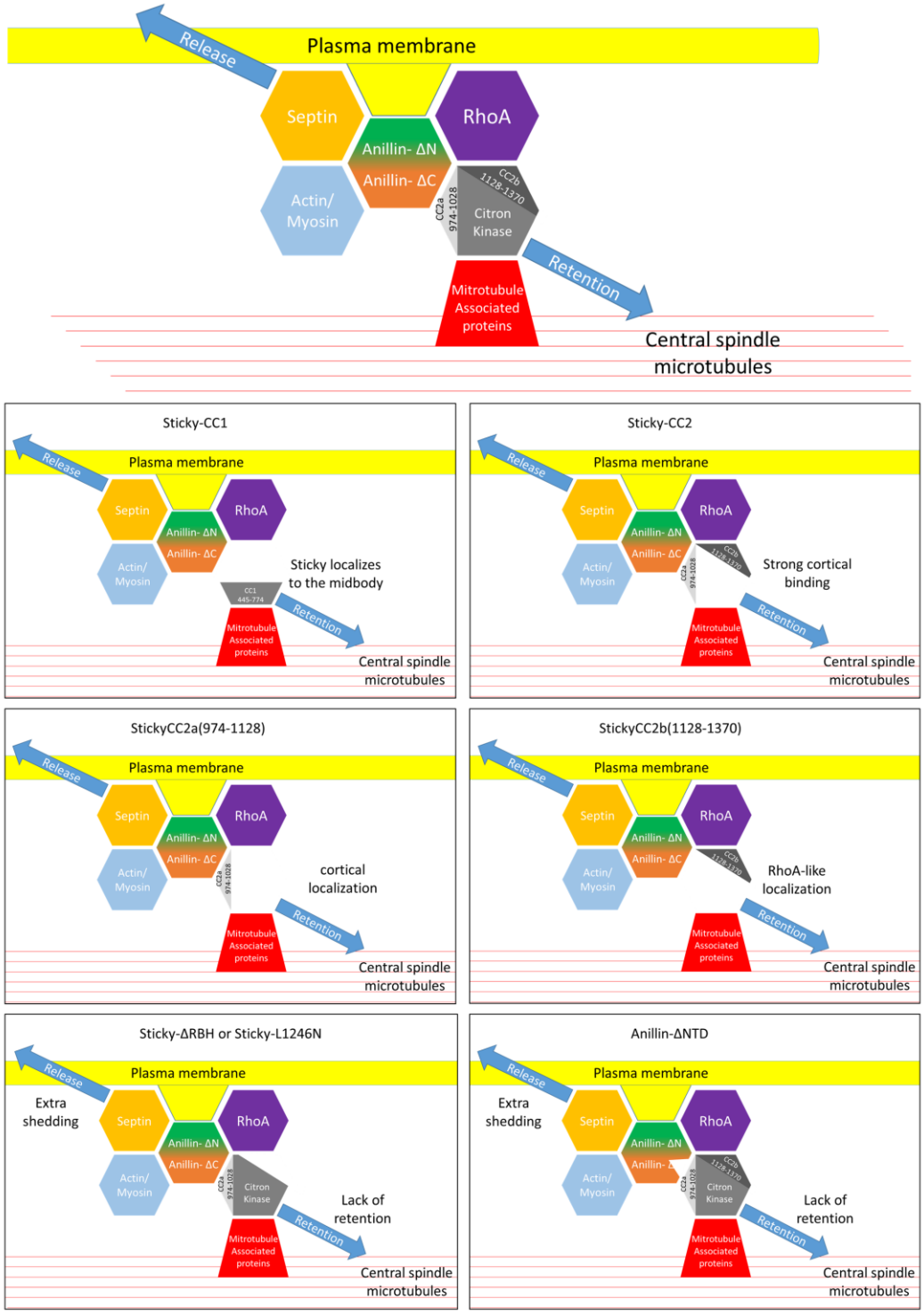

Figure 12. Modèle de localisation de Sticky lors de la cytokinèse.

Chaque protéine est représentée par un hexagone. Deux segments adjacents représentent une interaction.

6.1.1. Quelle est la relation entre ces deux modes de localisation corticaux

Une faiblesse importante de cette étude est le manque de caractérisation approfondie de la relation entre les deux modes de localisation corticaux identifies. Cependant, nous avons observé que la localisation isolée de chacun de ces mécanismes (Sticky-CC2a(973-1228) et Sticky-CC2b(1128-1370)), était différente de celle d'un mutant combinatoire de ces deux mécanismes (Sticky-CC2). Ceci suggère que les deux travaillent possiblement ensemble pour moduler la localisation de Sticky-FL. Encore plus intéressant est le fait que la protéine Sticky-FL ne ressemble pas à la forme combinée Sticky-CC2. Ceci indique que le reste de la protéine influence cette localisation. Le domaine CC1 pourrait jouer un rôle dans cet aspect. La continuation logique de ce projet devrait inclure une investigation plus approfondie de ce sujet.

Les données obtenues (*Ch.5*) suggèrent que l'une ou l'autre des contributions corticales de Sticky affectent la maturation de l'anneau par le mécanisme de rétention membranaire. Plus précisément, ce phénotype a été observé dans des cellules exprimant Anillin-ΔMyoBD, Anillin-ΔNTD, Sticky-ΔRBH ou Sticky-L1246N. Ceci signifie que les deux mécanismes ne sont pas redondants. Cependant, vu que l'analyse d'Anillin- ΔMyoBD et Anillin-ΔNTD n'est pas une observation directe du mécanisme Anillin-dépendant de Sticky, la génération et l'analyse d'un mutant Sticky-Δ(973-1128) serait important pour solidifier ces observations. On s'attend à ce que le mutant Sticky-Δ(973-1128) ce localise au cortex indépendamment d'Anillin et entièrement dépendant de RhoA. Cette dépendance RhoA devra être vérifiée via Sticky-Δ(973-1128)-L1246N.

Une note intéressante sur nos observations d'Anillin-ΔMyoBD est que les cellules exprimant ce mutant ne nécessitent plus l'expression de Sticky. Avec les données en notre possession il serait difficile de tirer une explication logique de ce phénotype. Cependant, ceci suggère que la modulation du site d'interaction Sticky/Anillin pourrait altérer le mécanisme normal et essentiel de fonctionnement de Sticky lors de la cytokinèse. L'approfondissement de nos connaissances sur ce mécanisme alternatif de fonctionnement de Citron Kinase pourrait offrir une nouvelle avenue sur notre compréhension du rôle exclusif de Citron Kinase au niveau du développement cérébral et testiculaire chez les rongeurs et l'homme.

6.1.2. Sticky-CC2a(973-1370) perturbe l'ingression du sillon de clivage

Une autre expérience surprenante est celle présentée dans la figure S7 du manuscrit (Fig. S7, chapitre 5). Comme mentionné dans l'article, nous n'avons pas exclu une troisième contribution à la localisation de Sticky lors de la cytokinèse dans le domaine CC2. Il semble que la portion minimale identifiée (Sticky-CC2a(973-1128)) qui est Anillin dépendante a une capacité plus faible de localisation corticale qu'en présence des 100 acides aminés adjacent (Sticky-CC2a(873-1128)). Des cellules exprimant Sticky-CC2a(973-1128) couplé au domaine de liaison cortical Rho-dépendant (Sticky-CC2(973-1370)) sont incapables de procéder à une cytokinèse avec succès dans près de 65% des divisions (Fig. S7A-E, chapitre 5). Cette observation n'a pas lieu ni avec Sticky-CC2a(873-1370) ou Sticky(1073-1370). Alors que Sticky-CC2a(873-1370) possède potentiellement ce troisième apport à la localisation de Sticky lors de la cytokinèse, Sticky(1073-1370) est un mutant entièrement dépendant de RhoA. Ceci indique que la localisation de Sticky corticale nécessiterait ces trois apports simultanément. De manière plus intrigante, 1/3 des cellules exprimant Sticky-CC2a(973-1370) n'étaient pas capables de former un sillon de clivage. Ce phénotype est très semblable à celui observé en absence de Rho ou de ca GEF, Pebble. Malgré que nos données soient encore une fois insuffisantes pour offrir une explication du mécanisme derrière ces observations, une hypothèse possible est que ce mutant lie très fortement RhoA ce qui conduit à sa séquestration. En accord avec cette hypothèse, une accélération du phénotype de Rho1 ARNi dans les cellules suite à l'induction d'expression de Sticky-CC2a(973-1370) a été observée (Fig. S7F, chapitre 5). L'investigation du rôle d'Anillin dans ce phénotype par réduction d'expression d'Anillin sur des cellules exprimant Sticky-CC2a(973-1370) augmenté par deux fois les nombre de cellules incapables de procéder à l'ingression du sillon de clivage (Fig. S7G, Chapitre 5). On s'attendait à un résultat inverse, ou Anillin aurait pu être capable de recouvrir ces phénotypes, puisque Sticky-CC2a(1073-1370) qui est totalement indépendant d'Anillin, n'affecte pas l'ingression du sillon de clivage. Ces observations préliminaires indiquent qu'une caractérisation plus complexe de l'interaction de Sticky avec Anillin ou RhoA est nécessaire.

6.1.3. La nature de l'interaction Sticky/Anillin et Sticky/Rho1 est une avenue à exploiter

Parmi, les expériences qui feraient la suite logique du deuxième manuscrit, seraient de tester la nature de l'interaction physique de Sticky/Anillin et Sticky/Rho1. Les expériences du chapitre 5, démontrent qu'Anillin interagit avec Sticky mais on ne sait toujours pas si cette interaction est directe ou indirecte. Pour ce qui est de l'interaction Sticky/Rho1 des difficultés techniques nous ont empêché d'exploiter cette interaction. Cette expérience est cruciale pour prouver qu'il y a en effet une interaction Sticky/Rho1. Nos résultats de Sticky-ΔRBH et Sticky-L1246N suggèrent fortement que cette interaction existe surtout avec la conservation évolutive de la séquence du domaine d'interaction. Cependant, ceci n'est pas suffisant pour en faire une conclusion. Maintenant, que les domaines minimaux requis pour les localisations corticales ont été identifiés, ces expériences d'interactions pourraient être encore plus précises et potentiellement plus faciles à tester par la technique Pull-Down. Ainsi, nous pourrions vérifier si Sticky-CC2a(973-1128) est capable de lié Anillin d'une part. D'autre part, nous pourrions vérifier si Sticky-CC2b(1128-1370) contrairement à Sticky-CC2b(1128-1307)-L1246N soit capable de se lier Rho1.

6.2. Un rôle précoce ou tardif de Citron Kinase lors de la cytokinèse?

Selon les observations initiales, il était clair que Citron Kinase ou plutôt Sticky dans les cellules S2 joue un rôle essentiel dans les étapes tardives de la cytokinèse (Echard et al., 2004). À ma connaissance, il n'existe que deux mentions dans la littérature d'une implication de Citron Kinase tôt en cytokinèse. Dans ces deux cas on observe des oscillations du sillon de clivage en surexprimant Citron Kinase (Gai et al., 2011) ou un mutant de Citron Kinase (Madaule et al., 1998). Toute autre étude de réduction d'expression (ARNi) de Citron Kinase/Sticky suggère un rôle tardif lors de la cytokinèse. De plus, dans Gai et al. 2011, 65% des cellules Citron ARNi

n'ont pas été subi à des mouvements oscillatoires ont plutôt une prolongation du temps d'abscission des cellules qui surexpriment Citron Kinase.

6.2.1. Comment ont lieu les oscillations de l'anneau contractile Sticky-dépendants?

En ce qui a trait à son rôle initial, nous avons tout d'abord démontré que Sticky a un enjeu redondant à ce niveau. Plus précisément les actions de Sticky qui peuvent causer des oscillations de l'anneau contractile, sont compensées par l'extrémité C-terminale d'Anillin ainsi que par Peanut (Fig. 13D, 13I). Cette extrémité C-terminale permet à Anillin de se lier à la membrane plasmique, interagir et recruter les septines ainsi que se lier à Rho-GTP. Intéressement, nous avons démontré que Sticky interagit avec le domaine N-terminal (NTD) d'Anillin. En quoi l'extrémité C-terminale d'Anillin pourrait-elle compenser pour le rôle précoce de Sticky si ce dernier interagit plutôt avec le bout N-terminal (Fig. 13I)? De manière similaire, comment Peanut peut-il de manière redondante contribuer au rôle précoce de Sticky (Fig. 14D)?

Une série de situations qui résument des observations de cette thèse permettent de proposer une explication (Figure 13). Ainsi, il serait possible que les oscillations observées tôt en cytokinèse soient dépendantes de la capacité d'une cellule à renforcer le lien entre trois facteurs ensemble : le cytosquelette d'actomyosine, Rho activé et la membrane plasmique. Anillin se trouve au centre de l'action par sa capacité à interagir avec ces trois facteurs. Cependant, son rôle est consolidé par des contributions similaires et possiblement indépendantes.

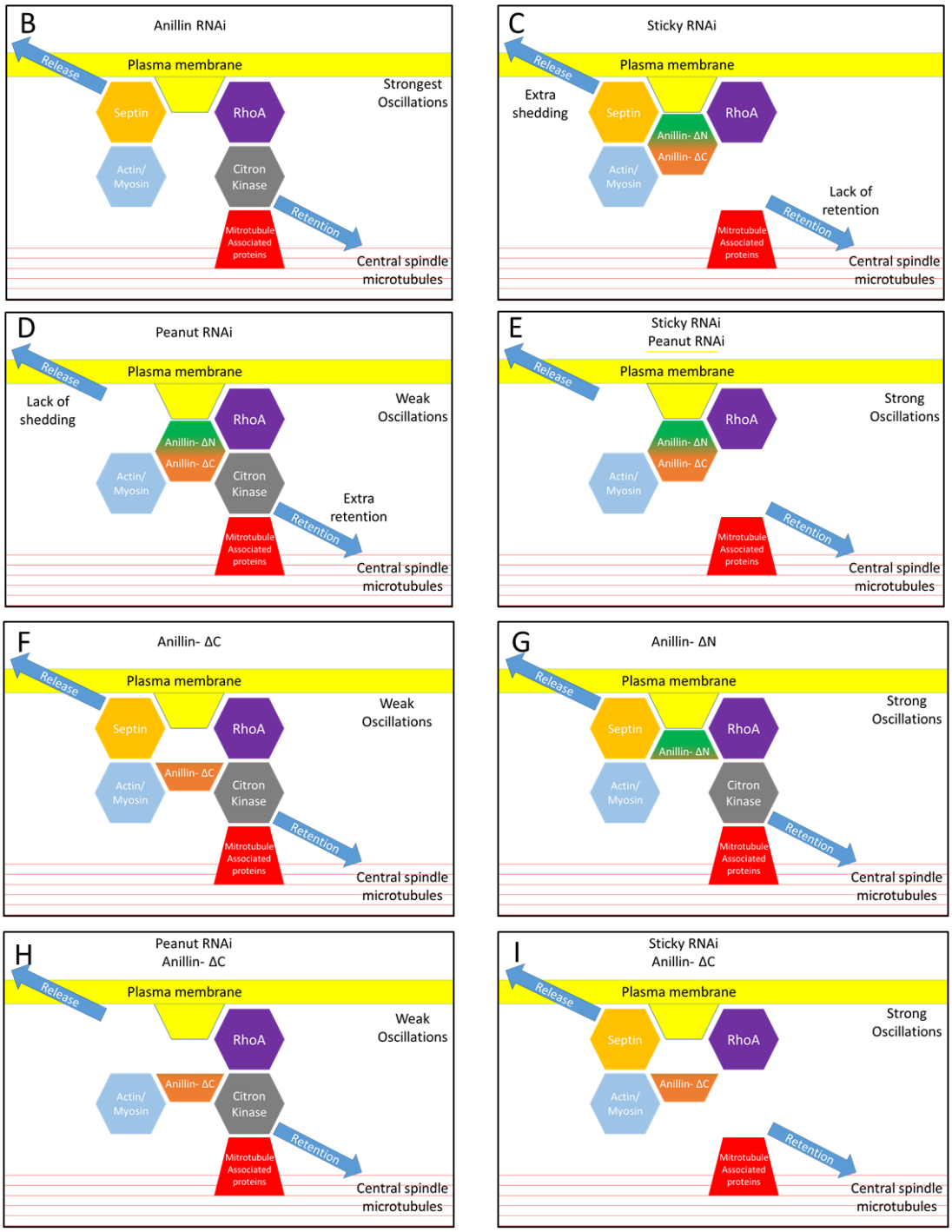

Figure 13. Modèle de stabilisation de l'anneau contractile

Chaque protéine est représentée par un hexagone. Deux segments adjacents représentent une interaction. 'Weak Oscillations' oscillations signifie un phénotype plus faible d'oscillation ou une fréquence moins élevée. Le contraire s'applique pour le terme 'Strong'.

6.2.1.1. Une stabilisation redondante Anillin-dépendante

Des cellules traitées à Anillin ARNi, sont soumises aux oscillations les plus fortes (Fig. 13B). Celles-ci sont souvent incapables de former un anneau contractile. Anillin agit comme protéine d'échafaudage pour relier le cytosquelette d'actomyosine (par Anillin-ΔC) à la membrane plasmique (par Anillin-ΔN) (Kechad et al., 2012). Le phénotype d'oscillations est plus fort avec des cellules exprimant un mutant Anillin-ΔN (Fig. 13F) comparé à Anillin-ΔC (Fig. 13G) (Kechad et al., 2012). Malgré qu'en temps normal la réduction d'expression de Sticky n'affecte pas directement la stabilisation de l'anneau contractile (Fig. 13E), les cellules exprimant Anillin-ΔN nécessitent Sticky pour stabiliser l'anneau contractile (Fig. 13I). Cet effet synergique signifie que la contribution à la stabilisation précoce de la cytokinèse par le bout C-terminal d'Anillin et Sticky sont redondantes, mais également indépendants (Fig. 13C vs F vs I). Sticky pourrait possiblement renforcer le lien entre Anillin et RhoA. Ainsi, en absence du domaine de liaison à la membrane et RhoA, présents dans le bout C-terminal d'Anillin, Sticky est capable de compenser cette faiblesse. Ceci expliquerait le faible phénotype d'oscillation Anillin-ΔC comparé à Anillin-ΔN puisque le cytosquelette serait toujours relié à RhoA et la membrane plasmique d'une manière Sticky-dépendante plus indirecte (Fig.13F vs 13G vs I). Les oscillations observées par d'autres groupes (Gai et al., 2011; Madaule et al., 1998) peuvent également être expliquées par ce modèle. Une surexpression de Sticky pourrait séquestrer la liaison d'Anillin à RhoA, ce qui affaiblirait l'apport d'Anillin dans le regroupement de la membrane, RhoA et le cytosquelette.

6.2.1.2. Une stabilisation redondante Peanut-dépendante

D'autre part, tout comme Anillin-ΔC, la déplétion de Peanut conduit les cellules vers une fréquence d'oscillation faible, cette fréquence est drastiquement augmentée lorsque co-traité à Sticky ARNi (Fig. 13C vs D vs E). Une conclusion similaire à Anillin-ΔC peut en être tirée. Sticky et Peanut ont des rôles redondants, mais aussi indépendants dans la stabilisation de l'anneau contractile. Cette redondance à probablement lieu à travers la capacité d'Anillin à lier le cytosquelette à la membrane et RhoA indépendamment de Sticky et Peanut. Mes collègues dans Kechad et al. 2011, ont démontré que la diminution d'expression de Peanut couplée avec

l'expression d'Anillin-ΔN était suffisante pour engendrer un phénotype fort d'oscillation à fréquence plus élevée que le phénotype identiquement observé en absence d'Anillin. Ceci indique que malgré la contribution Anillin-dépendante de Peanut, ce dernier possède une contribution Anillin-indépendante dans la stabilisation de l'anneau contractile. Sticky est impliqué dans ce mécanisme Anillin-indépendant. Il faudrait plus d'expérimentation pour en expliquer son mécanisme d'action.

6.2.1.3. Caractérisation de l'implication de Sticky précoce en cytokinèse

Il serait intéressant de voir l'effet suite à la diminution d'expression de Sticky simultanément avec Anillin sur la gravité des oscillations. Cette expérience permettrait de démontrer si le rôle Peanut-dépendant de Sticky se fie également à Anillin. L'étude présentée dans le chapitre 5 a permis de déterminer les domaines de Sticky responsables de ses interactions et localisations variés au niveau du cortex. Ainsi, il serait intéressant de voir quelle partie de Sticky est importante dans la stabilisation Peanut-dépendant de l'anneau contractile. Similairement, il faudrait caractériser l'implication Anillin-dépendante de Sticky. Il est fort probable que Sticky-ΔRBH ou Sticky-L1246N soient capables de se localisés au cortex d'une manière Anillin-indépendante en présence de Anillin-ΔC. En plus de l'importance de tester cette hypothèse, il serait très intéressant de savoir si cette expérience génère des oscillations similaires à ceux en diminution de l'expression de Sticky avec des cellules exprimant Anillin-ΔC. Cette expérience permettrait de tester l'hypothèse que le rôle Anillin-dépendant de Sticky dans la stabilisation précoce de la cytokinèse est d'offrir à Anillin une alternative de liaison indirecte à RhoA. Similairement, un mutant Sticky-Δ(973-1128) devrait ne pas être incapable de se lier à Anillin. De plus, l'expression de ce mutant couplée avec la diminution d'expression de Peanut et Sticky endogène permettrait de tester si Sticky possède une contribution tôt en cytokinèse indépendamment d'Anillin. Ainsi, sous ces conditions expérimentales, l'absence d'oscillation en ferait la suggestion.

6.2.2. Un mécanisme de rétention et excrétion de l'anneau du midbody essentiel pour son processus de maturation

Des expériences de microscopie électronique ont déjà décrit des excrétions à l'origine de l'anneau du midbody lors de la cytokinèse dans un modèle d'oursin marin d'Echinoidea (Shcroeder 1972) et dans un modèle cellulaire humain D98S (Mullins and Biesle 1976). L'existence de ces évènements a été ignorée pendant de très longues périodes de temps. La caractérisation approfondie de cet évènement constitue une première étude de la sorte. Ces évènements sont similaires à ceux décrits par Dubreuil et al. (2007) qui montrent que des particules d'Anillin et prominin-1 entourés de membrane sont excrétés de l'anneau contractile de cellules neuroepithéliales. Des évènements d'excrétion, semblables à nos observations, ont également été décrits au niveau du midbody dans l'embryon de *Caenorhabditis elegans* (Green et al. 2013). Suite à notre publication, une étude dans des cellules HeLa a également décrit des événements d'excrétion d'Anillin et de Septines du midbody (Renshaw et al. 2014). Ces descriptions multiples apportent un soutien à l'importance de notre étude vue que ce mécanisme semble être conservé lors de l'évolution.

Brièvement, nos résultats ont pu démontrer que ces excrétions entourées de membranes contiennent plusieurs protéines impliquées dans la cytokinèse comme l'Anillin, MKLP1/Pavarotti, MgcRacGAP/Tumbleweed, Aurora B, Septin/Peanut, Citron kinase/Sticky et Rho1. Ils semblent également être dépourvus d'Actine. De manière intéressante, la réduction d'expression de Sticky a largement augmenté la fréquence de ces événements et au contraire, la présence de Peanut est indispensable à l'occurrence de ces évènements. L'ensemble de ce travail a permis de conclure que ce mécanisme de perte membranaire fait partie d'un processus de maturation de l'anneau du midbody et l'un des rôles essentiels de Citron Kinase est d'agir comme frein à ce processus.

6.2.2.1. Le passage à deux cellules requiert une perte membranaire ?

Il est clair que le passage d'une cellule à deux cellules nécessitera une augmentation de tout le contenu cellulaire. On pourrait facilement se demander pourquoi la cellule perd de la membrane lors de la cytokinèse, étape où l'on s'attend à une augmentation de la membrane

plasmique. Des études ont décrit la nécessité de cet élargissement membranaire global. Cependant, au niveau de l'anneau contractile et plus spécifiquement de l'anneau du midbody qui sont en mode compaction, on s'attendrait à une perte locale de la membrane. L'ingression du midbody vers une structure de 1-2 μm est bien documentée (Schroeder 1972 et Carvalho 2009). Ainsi ce resserrement local devrait en principe nécessiter une perte membranaire qui selon nous se manifeste par les évènements d'excrétions caractérisés dans cette thèse.

6.2.2.2. Citron Kinase peut retenir le tout, mais comment?

Il aurait été intéressant de comprendre le mécanisme de rétention de Citron Kinase. Ainsi, lors du chapitre 5, nous avons décrit l'implication des deux domaines de localisations corticales dans ce mécanisme de maturation de l'anneau du midbody. Les deux mécanismes de localisations corticales de Citron Kinase semblent être importants dans son rôle de rétention membranaire. Une des faiblesses de cette deuxième étude était au niveau de la robustesse de cet énoncé. En effet, cette étude n'inclut aucune quantification pour supporter les conclusions. Le fait que les cellules exprimant Sticky-L1246N ou Sticky-ΔRBH aient un détériorèrent de l'anneau du midbody graduel jusqu'à la disparition de ce dernier coïncidant avec la régression sillon de clivage en était la suggestion. Les quantifications du matériel excrété comme ceux faits dans l'article publié auraient solidifié les observations décrites. De plus, la seule évidence que le mode de recrutement cortical Anillin-dépendant soit impliqué dans ce processus est au niveau des observations de Anillin-ΔNTD et Anillin-ΔNTD qui en principe n'interagissent pas aussi bien avec Sticky que la forme non modifiée d'Anillin. Cependant, ceci n'est pas suffisant pour conclure que l'observation des excrétions d'Anillin-ΔNTD est en fonction de la localisation Anillin-dépendante corticale de Sticky. Idéalement, un mutant Sticky(Δ973-1128) devrait être étudié pour ce phénotype. On s'attend tout d'abord à ce que ce mutant puisse se localiser au cortex et qu'il soit important pour la rétention membranaire. Il faudrait également tester l'importance de l'interaction de Sticky avec le fuseau central et ses protéines interactives dans le mécanisme de rétention. Nous avons répliqué ce qui a déjà été décrit dans la littérature quant à l'importance de Nebbish (KIF14) dans la localisation de Sticky au fuseau central. Ces données ne sont pas incluses dans cette thèse, mais démontrent toutefois que la réduction d'expression

de Nebbish empêche le recrutement du bout CC1 de Sticky qui est normalement uniquement localisé au midbody. La réduction d'expression de Nebbish pourrait donc être utilisée pour quantifier les excrétions membranaires. La littérature suggère que Nebbish ARNi pourrait phénocopier Sticky dans un de ses rôles lors de la cytokinèse. Si c'est également le cas dans la rétention membranaire, on pourrait donc l'étudier à l'aide de ces expériences. Une étude alternative serait l'étude d'un mutant Sticky qui ne contient pas le domaine de localisation au fuseau central. Si ce domaine est important pour la rétention membranaire, ceci pourrait suggérer que le mécanisme de rétention membranaire Sticky-dépendant a lieu par renforcement de la liaison corticale de l'anneau du midbody au fuseau central et ses protéines interactives par le biais de Sticky. Ces résultats offriraient des avancements majeurs dans notre compréhension de la stabilisation et la maturation de l'anneau contractile ou Sticky en serait un élément central.

6.2.3. L'impact sur le temps d'abscission

L'implication de Citron Kinase dans la stabilisation des microtubules du pont intercellulaire a également contribué à notre compréhension du rôle très tardif de Citron Kinase lors de l'abscision. En effet, la surexpression de Citron Kinase qui cause des délais d'abscission semble directement reliée à une surstabilisation du pont intercellulaire. Les résultats de cette thèse ont pu contribuer à notre compréhension de ce sujet.

Nos données de temps d'abscission ou d'échec de la cytokinèse en présence de Sticky ARNi montrent clairement que ces deux évènements ont lieu dans une période de temps identique. Malgré mon analyse de plusieurs centaines d'exemples de ces cellules en temps réel, quelques minutes avant l'évènement d'abscission ou d'échec sous cette condition, il était impossible de prédire l'un ou l'autre de ces destins. Ceci est remarquable pour plusieurs raisons. Tout d'abord nous savons très bien que chez les mammifères, Citron Kinase n'est pas requis pour tous les types cellulaires. Dans notre étude, le traitement à Sticky ARNi, semble fragiliser l'exigence en termes de maturation de l'anneau du midbody nécessaire pour le succès de la cytokinèse. Ainsi, certains tissus qui ont des conditions légèrement compensatoires de Citron Kinase seraient adéquats pour s'en passer de l'absence de Citron Kinase. D'autres conditions plus déstabilisées échoueraient ainsi la cytokinèse. Intéressement, une étude récente propose un

enjeu de phosphorylation Citron Kinase/Aurora B (McKenzie et al., 2016). Cette étude montre que Citron Kinase phosphoryle le complexe INCENP du complexe CPC qui contient Aurora B pour stimuler l'activité d'Aurora B. Ceci serait suffisant pour offrir une justification de l'impact de Citron Kinase sur le temps d'abscission. Ainsi, il serait intéressant d'effectuer une étude dose/réponse de l'activité Aurora B en fonction du temps d'abscission suite à une réduction graduelle de niveaux de Sticky par ARNi.

7. Conclusion

La contribution de cette thèse à notre compréhension générale de la cytokinèse est considérable. Ainsi, cet ouvrage laisse envisager que l'anneau contractile dynamique se stabilise en un anneau du midbody stable par un mécanisme de maturation qui requiert un équilibre entre la rétention et la relâche de la membrane plasmique au niveau du midbody. D'autre part, cet ouvrage à mis à jour nos connaissances sur le mode d'action de la protéine Citron Kinase, Sticky lors de la cytokinèse. Notre apport à cette compréhension de Sticky vient de nos données qui suggèrent que la contribution principale de Sticky au niveau de la cytokinèse est par son rôle d'échafaudages. Les fonctions essentielles de Sticky passent par deux enjeux qui permettent à Sticky de se localiser à l'anneau contractile d'une manière Anillin- et Rho1- dépendant.

8. Bibliographie

Amano, M., M. Nakayama, and K. Kaibuchi. 2010. Rho-kinase/ROCK: A key regulator of the cytoskeleton and cell polarity. *Cytoskeleton*. 67:545-554.

Atilla-Gokcumen, G.E., E. Muro, J. Relat-Goberna, S. Sasse, A. Bedigian, M.L. Coughlin, S. Garcia-Manyes, and U.S. Eggert. 2014. Dividing cells regulate their lipid composition and localization. *Cell*. 156:428-439.

Basit, S., K.M. Al-Harbi, S.A. Alhijji, A.M. Albalawi, E. Alharby, A. Eldardear, and M.I. Samman. 2016. CIT, a gene involved in neurogenic cytokinesis, is mutated in human primary microcephaly. *Hum Genet*. 135:1199-1207.

Bassi, Z.I., M. Audusseau, M.G. Riparbelli, G. Callaini, and P.P. D'Avino. 2013. Citron kinase controls a molecular network required for midbody formation in cytokinesis. *Proc Natl Acad Sci U S A*. 110:9782-9787.

Bassi, Z.I., K.J. Verbrugghe, L. Capalbo, S. Gregory, E. Montembault, D.M. Glover, and P. D'Avino. 2011. Sticky/Citron kinase maintains proper RhoA localization at the cleavage site during cytokinesis. *The Journal of Cell Biology*. 195:595-603.

Bastos, R.N., and F.A. Barr. 2010. Plk1 negatively regulates Cep55 recruitment to the midbody to ensure orderly abscission. *J Cell Biol*. 191:751-760.

Bauer, C.R., A.M. Epstein, S.J. Sweeney, D.C. Zarnescu, and G. Bosco. 2008. Genetic and systems level analysis of Drosophila sticky/citron kinase and dFmr1 mutants reveals common regulation of genetic networks. *BMC Syst Biol*. 2:101.

Bement, W.M., H.A. Benink, and G. von Dassow. 2005. A microtubule-dependent zone of active RhoA during cleavage plane specification. *The Journal of Cell Biology*. 170:91-101.

Ben El Kadhi, K., C. Roubinet, S. Solinet, G. Emery, and S. Carreno. 2011. The inositol 5-phosphatase dOCRL controls PI(4,5)P2 homeostasis and is necessary for cytokinesis. *Curr Biol*. 21:1074-1079.

Bendris, N., B. Lemmers, and J.M. Blanchard. 2015. Cell cycle, cytoskeleton dynamics and beyond: the many functions of cyclins and CDK inhibitors. *Cell Cycle*. 14:1786-1798.

Bhutta, M., C. McInerny, and G. Gould. 2014. ESCRT Function in Cytokinesis: Location, Dynamics and Regulation by Mitotic Kinases. *International Journal of Molecular Sciences*. 15:21723-21739.

Bieling, P., I.A. Telley, and T. Surrey. 2010. A minimal midzone protein module controls formation and length of antiparallel microtubule overlaps. *Cell*. 142:420-432.

Bringmann, H., and A.A. Hyman. 2005. A cytokinesis furrow is positioned by two consecutive signals. *Nature*. 436:731-734.

Cabernard, C., K.E. Prehoda, and C.Q. Doe. 2010. A spindle-independent cleavage furrow positioning pathway. *Nature*. 467:91-94.

Cao, L.G., and Y.L. Wang. 1996. Signals from the spindle midzone are required for the stimulation of cytokinesis in cultured epithelial cells. *Mol Biol Cell*. 7:225-232.

Capalbo, L., E. Montembault, T. Takeda, Z.I. Bassi, D.M. Glover, and P.P. D'Avino. 2012. The chromosomal passenger complex controls the function of endosomal sorting complex required for transport-III Snf7 proteins during cytokinesis. *Open Biol*. 2:120070.

Carlton, J.G., A. Caballe, M. Agromayor, M. Kloc, and J. Martin-Serrano. 2012. ESCRT-III governs the Aurora B-mediated abscission checkpoint through CHMP4C. *Science*. 336:220-225.

Carreno, S., I. Kouranti, E.S. Glusman, M.T. Fuller, A. Echard, and F. Payre. 2008. Moesin and its activating kinase Slik are required for cortical stability and microtubule organization in mitotic cells. *J Cell Biol*. 180:739-746.

Carvalho, A., A. Desai, and K. Oegema. 2009. Structural memory in the contractile ring makes the duration of cytokinesis independent of cell size. *Cell*. 137:926-937.

Chang, Y., O. Klezovitch, R.S. Walikonis, V. Vasioukhin, and J.J. LoTurco. 2010. Discs large 5 is required for polarization of citron kinase in mitotic neural precursors. *Cell Cycle*. 9:1990-1997.

Cheeseman, I.M., and A. Desai. 2008. Molecular architecture of the kinetochore-microtubule interface. *Nat Rev Mol Cell Biol*. 9:33-46.

Chesneau, L., D. Dambournet, M. Machicoane, I. Kouranti, M. Fukuda, B. Goud, and A. Echard. 2012. An ARF6/Rab35 GTPase cascade for endocytic recycling and successful cytokinesis. *Curr Biol*. 22:147-153.

Chircop, M. 2014. Rho GTPases as regulators of mitosis and cytokinesis in mammalian cells. *Small GTPases*. 5.

Crowell, E.F., A.L. Gaffuri, B. Gayraud-Morel, S. Tajbakhsh, and A. Echard. 2014. Engulfment of the midbody remnant after cytokinesis in mammalian cells. *J Cell Sci*. 127:3840-3851.

Cunto, D.F., E. Calautti, J. Hsiao, L. Ong, G. Topley, E. Turco, and G.P. Dotto. 1998. Citron rho-interacting kinase, a novel tissue-specific ser/thr kinase encompassing the Rho-Rac-binding protein Citron. *The Journal of biological chemistry*. 273:29706-29711.

Cunto, F., S. Imarisio, P. Camera, C. Boitani, F. Altruda, and L. Silengo. 2002. Essential role of citron kinase in cytokinesis of spermatogenic precursors. *Journal of Cell Science*. 115:4819-4826.

Cunto, F., S. Imarisio, E. Hirsch, V. Broccoli, A. Bulfone, A. Migheli, C. Atzori, E. Turco, R. Triolo, G. Dotto, L. Silengo, and F. Altruda. 2000. Defective Neurogenesis in Citron Kinase Knockout Mice by Altered Cytokinesis and Massive Apoptosis. *Neuron*. 28:115-127.

D'Avino, P., M.S. Savoian, and D.M. Glover. 2004. Mutations in sticky lead to defective organization of the contractile ring during cytokinesis and are enhanced by Rho and suppressed by Rac. *The Journal of Cell Biology*. 166:61-71.

D'Avino, P.P., M.G. Giansanti, and M. Petronczki. 2015. Cytokinesis in animal cells. *Cold Spring Harb Perspect Biol*. 7:a015834.

D'Avino, P.P., T. Takeda, L. Capalbo, W. Zhang, K.S. Lilley, E.D. Laue, and D.M. Glover. 2008. Interaction between Anillin and RacGAP50C connects the actomyosin contractile ring with spindle microtubules at the cell division site. *J Cell Sci*. 121:1151-1158.

D'Avino, P., M. Giansanti, and M. Petronczki. 2015. Cytokinesis in Animal Cells. *Cold Spring Harbor Perspectives in Biology*. 7.

Dean, S.O., S.L. Rogers, N. Stuurman, R.D. Vale, and J.A. Spudich. 2005. Distinct pathways control recruitment and maintenance of myosin II at the cleavage furrow during cytokinesis. *Proceedings of the National Academy of Sciences of the United States of America*. 102:13473-13478.

Dean, S.O., and J.A. Spudich. 2006. Rho kinase's role in myosin recruitment to the equatorial cortex of mitotic Drosophila S2 cells is for myosin regulatory light chain phosphorylation. *PLoS One*. 1:e131.

DeBiasio, R.L., G.M. LaRocca, P.L. Post, and D.L. Taylor. 1996. Myosin II transport, organization, and phosphorylation: evidence for cortical flow/solation-contraction coupling during cytokinesis and cell locomotion. *Mol Biol Cell*. 7:1259-1282.

Dorn, J.F., L. Zhang, T.T. Phi, B. Lacroix, P.S. Maddox, J. Liu, and A.S. Maddox. 2016. A theoretical model of cytokinesis implicates feedback between membrane curvature and cytoskeletal organization in asymmetric cytokinetic furrowing. *Mol Biol Cell*. 27:1286-1299.

Douglas, M.E., T. Davies, N. Joseph, and M. Mishima. 2010. Aurora B and 14-3-3 Coordinately Regulate Clustering of Centralspindlin during Cytokinesis. *Current Biology*. 20:927-933.

Dubreuil, V., A.M. Marzesco, D. Corbeil, W.B. Huttner, and M. Wilsch-Brauninger. 2007. Midbody and primary cilium of neural progenitors release extracellular membrane particles enriched in the stem cell marker prominin-1. *J Cell Biol*. 176:483-495.

Dvorsky, R., L. Blumenstein, I.R. Vetter, and M.R. Ahmadian. 2004. Structural insights into the interaction of ROCKI with the switch regions of RhoA. *J Biol Chem*. 279:7098-7104.

Echard, A. 2012. Phosphoinositides and cytokinesis: the "PIP" of the iceberg. *Cytoskeleton (Hoboken)*. 69:893-912.

Echard, A., G.R.X. Hickson, E. Foley, and P.H. O'Farrell. 2004. Terminal cytokinesis events uncovered after an RNAi screen. *Current biology : CB*. 14:1685-1693.

Eda, M., S. Yonemura, T. Kato, N. Watanabe, T. Ishizaki, P. Madaule, and S. Narumiya. 2001. Rho-dependent transfer of Citron-kinase to the cleavage furrow of dividing cells. *Journal of cell science*. 114:3273-3284.

Eggert, U.S., T.J. Mitchison, and C.M. Field. 2006. Animal Cytokinesis: From Parts List to Mechanisms. *Biochemistry*. 75:543-566.

Eikenes, A.H., L. Malerod, A.L. Christensen, C.B. Steen, J. Mathieu, I.P. Nezis, K. Liestol, J.R. Huynh, H. Stenmark, and K. Haglund. 2015. ALIX and ESCRT-III coordinately control cytokinetic abscission during germline stem cell division in vivo. *PLoS Genet*. 11:e1004904.

El-Amine, N., A. Kechad, S. Jananji, and G. Hickson. 2013. Opposing actions of septins and Sticky on Anillin promote the transition from contractile to midbody ring. *The Journal of Cell Biology*. 203:487-504.

Estey, M.P., C. Ciano-Oliveira, C.D. Froese, M.T. Bejide, and W.S. Trimble. 2010. Distinct roles of septins in cytokinesis: SEPT9 mediates midbody abscission. *The Journal of Cell Biology*. 191:741-749.

Ettinger, A.W., M. Wilsch-Brauninger, A.M. Marzesco, M. Bickle, A. Lohmann, Z. Maliga, J. Karbanova, D. Corbeil, A.A. Hyman, and W.B. Huttner. 2011. Proliferating versus differentiating stem and cancer cells exhibit distinct midbody-release behaviour. *Nat Commun*. 2:503.

Fededa, J., and D.W. Gerlich. 2012. Molecular control of animal cell cytokinesis. *Nature Cell Biology*. 14:440-447.

Fehon, R.G., A.I. McClatchey, and A. Bretscher. 2010. Organizing the cell cortex: the role of ERM proteins. *Nat Rev Mol Cell Biol*. 11:276-287.

Field, C.M., and B.M. Alberts. 1995. Anillin, a contractile ring protein that cycles from the nucleus to the cell cortex. *J Cell Biol*. 131:165-178.

Field, C.M., M. Coughlin, S. Doberstein, T. Marty, and W. Sullivan. 2005. Characterization of anillin mutants reveals essential roles in septin localization and plasma membrane integrity. *Development*. 132:2849-2860.

Frenette, P., E. Haines, M. Loloyan, M. Kinal, P. Pakarian, and A. Piekny. 2012. An anillin-Ect2 complex stabilizes central spindle microtubules at the cortex during cytokinesis. *PLoS One*. 7:e34888.

Fujiwara, T., M. Bandi, M. Nitta, E.V. Ivanova, R.T. Bronson, and D. Pellman. 2005. Cytokinesis failure generating tetraploids promotes tumorigenesis in p53-null cells. *Nature*. 437:1043-1047.

Gai, M., P. Camera, A. Dema, F. Bianchi, G. Berto, E. Scarpa, G. Germena, and F. Cunto. 2011. Citron kinase controls abscission through RhoA and anillin. *Molecular biology of the cell*. 22:3768-3778.

Gai, M., and F. Di Cunto. 2016. Citron kinase in spindle orientation and primary microcephaly. *Cell Cycle*:1-2.

Glotzer, M. 2009. The 3Ms of central spindle assembly: microtubules, motors and MAPs. *Nature reviews. Molecular cell biology*. 10:9-20.

Green, R.A., E. Paluch, and K. Oegema. 2012. Cytokinesis in animal cells. *Annual review of cell and developmental biology*. 28:29-58.

Gregory, S.L., S. Ebrahimi, J. Milverton, W.M. Jones, A. Bejsovec, and R. Saint. 2008. Cell division requires a direct link between microtubule-bound RacGAP and Anillin in the contractile ring. *Curr Biol*. 18:25-29.

Gruneberg, U., R. Neef, X. Li, E. Chan, R.B. Chalamalasetty, E.A. Nigg, and F.A. Barr. 2006a. KIF14 and citron kinase act together to promote efficient cytokinesis. *The Journal of Cell Biology*. 172:363-372.

Gruneberg, U., R. Neef, X. Li, E.H. Chan, R.B. Chalamalasetty, E.A. Nigg, and F.A. Barr. 2006b. KIF14 and citron kinase act together to promote efficient cytokinesis. *J Cell Biol*. 172:363-372.

Guizetti, J., and D.W. Gerlich. 2010. Cytokinetic abscission in animal cells. *Seminars in cell & developmental biology*. 21:909-916.

Guizetti, J., L. Schermelleh, J. Mantler, S. Maar, I. Poser, H. Leonhardt, T. Muller-Reichert, and D.W. Gerlich. 2011. Cortical constriction during abscission involves helices of ESCRT-III-dependent filaments. *Science*. 331:1616-1620.

Hall, P.A., C.B. Todd, P.L. Hyland, S.S. McDade, H. Grabsch, M. Dattani, K.J. Hillan, and S.E. Russell. 2005. The septin-binding protein anillin is overexpressed in diverse human tumors. *Clin Cancer Res*. 11:6780-6786.

Hanson, P.I., S. Shim, and S.A. Merrill. 2009. Cell biology of the ESCRT machinery. *Curr Opin Cell Biol*. 21:568-574.

Harding, B.N., A. Moccia, S. Drunat, O. Soukarieh, H. Tubeuf, L.S. Chitty, A. Verloes, P. Gressens, V. El Ghouzzi, S. Joriot, F. Di Cunto, A. Martins, S. Passemard, and S.L. Bielas. 2016. Mutations in Citron Kinase Cause Recessive Microlissencephaly with Multinucleated Neurons. *Am J Hum Genet*. 99:511-520.

Hickson, G., and P.H. O'Farrell. 2008a. Anillin: a pivotal organizer of the cytokinetic machinery. *Biochemical Society Transactions*. 36:439-441.

Hickson, G., and P.H. O'Farrell. 2008b. Rho-dependent control of anillin behavior during cytokinesis. *The Journal of Cell Biology*. 180:285-294.

Hochegger, H., S. Takeda, and T. Hunt. 2008. Cyclin-dependent kinases and cell-cycle transitions: does one fit all? *Nature reviews. Molecular cell biology*. 9:910-916.

Hoffmann, I., P.R. Clarke, M.J. Marcote, E. Karsenti, and G. Draetta. 1993. Phosphorylation and activation of human cdc25-C by cdc2--cyclin B and its involvement in the self-amplification of MPF at mitosis. *EMBO J*. 12:53-63.

Horton, J.S., C.T. Wakano, M. Speck, and A.J. Stokes. 2015. Two-pore channel 1 interacts with citron kinase, regulating completion of cytokinesis. *Channels (Austin)*. 9:21-29.

Hu, C.-K., M. Coughlin, and T.J. Mitchison. 2012. Midbody assembly and its regulation during cytokinesis. *Molecular Biology of the Cell*. 23:1024-1034.

Hyenne, V., N.T. Chartier, and J.C. Labbe. 2010. Understanding the role of asymmetric cell division in cancer using C. elegans. *Dev Dyn*. 239:1378-1387.

Jiang, W., G. Jimenez, N.J. Wells, T.J. Hope, G.M. Wahl, T. Hunter, and R. Fukunaga. 1998. PRC1 A Human Mitotic Spindle–Associated CDK Substrate Protein Required for Cytokinesis. *Molecular Cell*. 2:877-885.

Jordan, S.N., and J.C. Canman. 2012. Rho GTPases in animal cell cytokinesis: an occupation by the one percent. *Cytoskeleton (Hoboken)*. 69:919-930.

Kamasaki, T., M. Osumi, and I. Mabuchi. 2007. Three-dimensional arrangement of F-actin in the contractile ring of fission yeast. *J Cell Biol*. 178:765-771.

Kamijo, K., N. Ohara, M. Abe, T. Uchimura, H. Hosoya, J.-S. Lee, and T. Miki. 2006. Dissecting the Role of Rho-mediated Signaling in Contractile Ring Formation. *Molecular Biology of the Cell*. 17:43-55.

Kechad, A., and G.R. Hickson. 2016. Imaging cytokinesis of Drosophila S2 cells.

Kechad, A., S. Jananji, Y. Ruella, and G.R. Hickson. 2012. Anillin acts as a bifunctional linker coordinating midbody ring biogenesis during cytokinesis. *Curr Biol*. 22:197-203.

Kimura, K., M. Ito, M. Amano, K. Chihara, Y. Fukata, M. Nakafuku, B. Yamamori, J. Feng, T. Nakano, K. Okawa, A. Iwamatsu, and K. Kaibuchi. 1996. Regulation of myosin phosphatase by Rho and Rho-associated kinase (Rho-kinase). *Science*. 273:245-248.

Kitagawa, M., S. Fung, U. Hameed, H. Goto, M. Inagaki, and S. Lee. 2014. Cdk1 Coordinates Timely Activation of MKlp2 Kinesin with Relocation of the Chromosome Passenger Complex for Cytokinesis. *Cell Reports*. 7:166-179.

Kondo, T., K. Hamao, K. Kamijo, H. Kimura, M. Morita, M. Takahashi, and H. Hosoya. 2011. Enhancement of myosin II/actin turnover at the contractile ring induces slower furrowing in dividing HeLa cells. *The Biochemical journal*. 435:569-576.

Kuo, T.C., C.T. Chen, D. Baron, T.T. Onder, S. Loewer, S. Almeida, C.M. Weismann, P. Xu, J.M. Houghton, F.B. Gao, G.Q. Daley, and S. Doxsey. 2011. Midbody accumulation through evasion of autophagy contributes to cellular reprogramming and tumorigenicity. *Nat Cell Biol*. 13:1214-1223.

Lacroix, B., and A. Maddox. 2012. Cytokinesis, ploidy and aneuploidy. *The Journal of Pathology*. 226:338-351.

Lee, H.H., N. Elia, R. Ghirlando, J. Lippincott-Schwartz, and J.H. Hurley. 2008. Midbody targeting of the ESCRT machinery by a noncanonical coiled coil in CEP55. *Science*. 322:576-580.

Lee, K.-Y., T. Davies, and M. Mishima. 2012. Cytokinesis microtubule organisers at a glance. *J Cell Sci*. 125:3495-3500.

Lekomtsev, S., K.-C. Su, V.E. Pye, K. Blight, S. Sundaramoorthy, T. Takaki, L.M. Collinson, P. Cherepanov, N. Divecha, and M. Petronczki. 2012a. Centralspindlin links the mitotic spindle to the plasma membrane during cytokinesis. *Nature*. 492:276-279.

Lekomtsev, S., K.C. Su, V.E. Pye, K. Blight, S. Sundaramoorthy, T. Takaki, L.M. Collinson, P. Cherepanov, N. Divecha, and M. Petronczki. 2012b. Centralspindlin links the mitotic spindle to the plasma membrane during cytokinesis. *Nature*. 492:276-279.

Li, F., and H.N. Higgs. 2003. The mouse Formin mDia1 is a potent actin nucleation factor regulated by autoinhibition. *Current biology : CB*. 13:1335-1340.

Li, H., S.L. Bielas, M.S. Zaki, S. Ismail, D. Farfara, K. Um, R.O. Rosti, E.C. Scott, S. Tu, N.C. Chi, S. Gabriel, E.Z. Erson-Omay, A.G. Ercan-Sencicek, K. Yasuno, A.O. Caglayan, H. Kaymakcalan, B. Ekici, K. Bilguvar, M. Gunel, and J.G. Gleeson. 2016. Biallelic Mutations in Citron Kinase Link Mitotic Cytokinesis to Human Primary Microcephaly. *Am J Hum Genet*. 99:501-510.

Li, M., and P. Zhang. 2009. The function of APC/CCdh1 in cell cycle and beyond. *Cell Div*. 4:2.

Liu, H., F. Di Cunto, S. Imarisio, and L.M. Reid. 2003. Citron kinase is a cell cycle-dependent, nuclear protein required for G2/M transition of hepatocytes. *J Biol Chem*. 278:2541-2548.

Liu, J., G.D. Fairn, D.F. Ceccarelli, F. Sicheri, and A. Wilde. 2012. Cleavage furrow organization requires PIP(2)-mediated recruitment of anillin. *Curr Biol*. 22:64-69.

Liu, Z., and O.D. Weiner. 2016. Positioning the cleavage furrow: All you need is Rho. *J Cell Biol*. 213:605-607.

Logan, M.R., and C.A. Mandato. 2006. Regulation of the actin cytoskeleton by PIP2 in cytokinesis. *Biol Cell*. 98:377-388.

Lolli, G., and L.N. Johnson. 2005. CAK-Cyclin-dependent Activating Kinase: a key kinase in cell cycle control and a target for drugs? *Cell Cycle*. 4:572-577.

Lu, M.S., and C.A. Johnston. 2013. Molecular pathways regulating mitotic spindle orientation in animal cells. *Development*. 140:1843-1856.

Machida, Y.J., J.L. Hamlin, and A. Dutta. 2005. Right Place, Right Time, and Only Once: Replication Initiation in Metazoans. *Cell*. 123:13-24.

Madaule, P., M. Eda, N. Watanabe, K. Fujisawa, T. Matsuoka, H. Bito, T. Ishizaki, and S. Narumiya. 1998. Role of citron kinase as a target of the small GTPase Rho in cytokinesis. *Nature*. 394:491-494.

Madaule, P., T. Furuyashiki, M. Eda, H. Bito, T. Ishizaki, and S. Narumiya. 2000. Citron, a Rho target that affects contractility during cytokinesis. *Microscopy research and technique*. 49:123-126.

Madaule, P., T. Furuyashiki, T. Reid, T. Ishizaki, G. Watanabe, N. Morii, and S. Narumiya. 1995. A novel partner for the GTP-bound forms of rho and rac. *FEBS letters*. 377:243-248.

Maddox, A., and K. Burridge. 2003. RhoA is required for cortical retraction and rigidity during mitotic cell rounding. *The Journal of Cell Biology*. 160:255-265.

Maddox, A.S., L. Lewellyn, A. Desai, and K. Oegema. 2007. Anillin and the septins promote asymmetric ingression of the cytokinetic furrow. *Dev Cell*. 12:827-835.

Maiato, H., and M. Lince-Faria. 2010. The perpetual movements of anaphase. *Cell Mol Life Sci*. 67:2251-2269.

Matias, N.R., J. Mathieu, and J.R. Huynh. 2015. Abscission is regulated by the ESCRT-III protein shrub in Drosophila germline stem cells. *PLoS Genet*. 11:e1004653.

Matsumura, F. 2005. Regulation of myosin II during cytokinesis in higher eukaryotes. *Trends in Cell Biology*. 15:371-377.

Matsumura, F., Y. Yamakita, and S. Yamashiro. 2006. [Regulation of myosin II in cell division and cell migration]. *Tanpakushitsu Kakusan Koso*. 51:566-572.

Matthews, H.K., U. Delabre, J.L. Rohn, J. Guck, P. Kunda, and B. Baum. 2012. Changes in Ect2 localization couple actomyosin-dependent cell shape changes to mitotic progression. *Developmental cell*. 23:371-383.

Mavrakis, M., Y. Azou-Gros, F.C. Tsai, J. Alvarado, A. Bertin, F. Iv, A. Kress, S. Brasselet, G.H. Koenderink, and T. Lecuit. 2014. Septins promote F-actin ring formation by crosslinking actin filaments into curved bundles. *Nat Cell Biol*. 16:322-334.

McKenzie, C., Z.I. Bassi, J. Debski, M. Gottardo, G. Callaini, M. Dadlez, and P.P. D'Avino. 2016. Cross-regulation between Aurora B and Citron kinase controls midbody architecture in cytokinesis. *Open Biol*. 6.

Menon, M.B., and M. Gaestel. 2015. Sep(t)arate or not – how some cells take septin-independent routes through cytokinesis. *Journal of cell science*. 128:1877-1886.

Mierzwa, B., and D.W. Gerlich. 2014. Cytokinetic abscission: molecular mechanisms and temporal control. *Dev Cell*. 31:525-538.

Miller, A.L., and W.M. Bement. 2009. Regulation of cytokinesis by Rho GTPase flux. *Nat Cell Biol*. 11:71-77.

Mishima, M., S. Kaitna, and M. Glotzer. 2002. Central Spindle Assembly and Cytokinesis Require a Kinesin-like Protein/RhoGAP Complex with Microtubule Bundling Activity. *Developmental Cell*. 2:41-54.

Mishima, M., V. Pavicic, U. Grüneberg, E.A. Nigg, and M. Glotzer. 2004. Cell cycle regulation of central spindle assembly. *Nature*. 430:908-913.

Mollinari, C., J.-P. Kleman, W. Jiang, G. Schoehn, T. Hunter, and R.L. Margolis. 2002. PRC1 is a microtubule binding and bundling protein essential to maintain the mitotic spindle midzone. *The Journal of cell biology*. 157:1175-1186.

Morin, X., and Y. Bellaiche. 2011. Mitotic spindle orientation in asymmetric and symmetric cell divisions during animal development. *Dev Cell*. 21:102-119.

Mullins, J.M., and J.J. Biesele. 1973. Cytokinetic activities in a human cell line: the midbody and intercellular bridge. *Tissue Cell*. 5:47-61.

Mullins, J.M., and J.J. Biesele. 1977. Terminal phase of cytokinesis in D-98s cells. *J Cell Biol*. 73:672-684.

Naim, V., S. Imarisio, F. Di Cunto, M. Gatti, and S. Bonaccorsi. 2004. Drosophila citron kinase is required for the final steps of cytokinesis. *Mol Biol Cell*. 15:5053-5063.

Neef, R., U.R. Klein, R. Kopajtich, and F.A. Barr. 2006. Cooperation between mitotic kinesins controls the late stages of cytokinesis. *Current biology : CB*. 16:301-307.

Neto, H., L.L. Collins, and G.W. Gould. 2011. Vesicle trafficking and membrane remodelling in cytokinesis. *Biochem J*. 437:13-24.

Neufeld, T.P., and G.M. Rubin. 1994. The Drosophila peanut gene is required for cytokinesis and encodes a protein similar to yeast putative bud neck filament proteins. *Cell*. 77:371-379.

Norden, C., M. Mendoza, J. Dobbelaere, C.V. Kotwaliwale, S. Biggins, and Y. Barral. 2006. The NoCut pathway links completion of cytokinesis to spindle midzone function to prevent chromosome breakage. *Cell*. 125:85-98.

Normand, G., and R.W. King. 2010. Understanding cytokinesis failure. *Adv Exp Med Biol*. 676:27-55.

Nunes Bastos, R., S.R. Gandhi, R.D. Baron, U. Gruneberg, E.A. Nigg, and F.A. Barr. 2013. Aurora B suppresses microtubule dynamics and limits central spindle size by locally activating KIF4A. *J Cell Biol*. 202:605-621.

Oegema, K., and T.J. Mitchison. 1997. Rappaport rules: cleavage furrow induction in animal cells. *Proc Natl Acad Sci U S A*. 94:4817-4820.

Oegema, K., M.S. Savoian, T.J. Mitchison, and C.M. Field. 2000. Functional analysis of a human homologue of the Drosophila actin binding protein anillin suggests a role in cytokinesis. *J Cell Biol*. 150:539-552.

Otomo, T., C. Otomo, D.R. Tomchick, M. Machius, and M.K. Rosen. 2005. Structural basis of Rho GTPase-mediated activation of the formin mDia1. *Molecular cell*. 18:273-281.

Ou, G., C. Gentili, and P. Gonczy. 2014. Stereotyped distribution of midbody remnants in early C. elegans embryos requires cell death genes and is dispensable for development. *Cell Res*. 24:251-253.

Paramasivam, M., Y.J. Chang, and J.J. LoTurco. 2007. ASPM and citron kinase co-localize to the midbody ring during cytokinesis. *Cell Cycle*. 6:1605-1612.

Parker, L.L., P.J. Sylvestre, M.J. Byrnes, 3rd, F. Liu, and H. Piwnica-Worms. 1995. Identification of a 95-kDa WEE1-like tyrosine kinase in HeLa cells. *Proc Natl Acad Sci U S A*. 92:9638-9642.

Peters, J.M., A. Tedeschi, and J. Schmitz. 2008. The cohesin complex and its roles in chromosome biology. *Genes Dev*. 22:3089-3114.

Piekny, A., M. Werner, and M. Glotzer. 2005. Cytokinesis: welcome to the Rho zone. *Trends Cell Biol*. 15:651-658.

Piekny, A.J., and M. Glotzer. 2008. Anillin is a scaffold protein that links RhoA, actin, and myosin during cytokinesis. *Curr Biol*. 18:30-36.

Piekny, A.J., and A. Maddox. 2010. The myriad roles of Anillin during cytokinesis. *Seminars in Cell & Developmental Biology*. 21:881-891.

Ramkumar, N., and B. Baum. 2016. Coupling changes in cell shape to chromosome segregation. *Nature reviews. Molecular cell biology*. 17:511-521.

Rappaport, R. 1996. Cytokinesis in animal cells.

Renshaw, M.J., J. Liu, B.D. Lavoie, and A. Wilde. 2014. Anillin-dependent organization of septin filaments promotes intercellular bridge elongation and Chmp4B targeting to the abscission site. *Open Biol*. 4:130190.

Reyes, C.C., M. Jin, E.B. Breznau, R. Espino, R. Delgado-Gonzalo, A.B. Goryachev, and A.L. Miller. 2014. Anillin regulates cell-cell junction integrity by organizing junctional accumulation of Rho-GTP and actomyosin. *Curr Biol*. 24:1263-1270.

Salaun, P., Y. Rannou, and C. Prigent. 2008. Cdk1, Plks, Auroras, and Neks: the mitotic bodyguards. *Adv Exp Med Biol*. 617:41-56.

Santamaria, D., C. Barriere, A. Cerqueira, S. Hunt, C. Tardy, K. Newton, J.F. Caceres, P. Dubus, M. Malumbres, and M. Barbacid. 2007. Cdk1 is sufficient to drive the mammalian cell cycle. *Nature*. 448:811-815.

Schafer, K.A. 1998. The cell cycle: a review. *Vet Pathol*. 35:461-478.

Schink, K.O., and H. Stenmark. 2011. Cell differentiation: midbody remnants - junk or fate factors? *Curr Biol*. 21:R958-960.

Schroeder, T.E. 1972. The contractile ring. II. Determining its brief existence, volumetric changes, and vital role in cleaving Arbacia eggs. *J Cell Biol*. 53:419-434.

Sedzinski, J., M. Biro, A. Oswald, J.-Y. Tinevez, G. Salbreux, and E. Paluch. 2011. Polar actomyosin contractility destabilizes the position of the cytokinetic furrow. *Nature*. 476:462-466.

Serres, M.P., U. Kossatz, Y. Chi, J.M. Roberts, N.P. Malek, and A. Besson. 2012. p27(Kip1) controls cytokinesis via the regulation of citron kinase activation. *J Clin Invest*. 122:844-858.

Sgro, F., F.T. Bianchi, M. Falcone, G. Pallavicini, M. Gai, A.M. Chiotto, G.E. Berto, E. Turco, Y.J. Chang, W.B. Huttner, and F. Di Cunto. 2016. Tissue-specific control of midbody microtubule stability by Citron kinase through modulation of TUBB3 phosphorylation. *Cell Death Differ*. 23:801-813.

Shaheen, R., A. Hashem, G.M. Abdel-Salam, F. Al-Fadhli, N. Ewida, and F.S. Alkuraya. 2016. Mutations in CIT, encoding citron rho-interacting serine/threonine kinase, cause severe primary microcephaly in humans. *Hum Genet*. 135:1191-1197.

Shandala, T., S.L. Gregory, H.E. Dalton, M. Smallhorn, and R. Saint. 2004. Citron Kinase is an essential effector of the Pbl-activated Rho signalling pathway in Drosophila melanogaster. *Development*. 131:5053-5063.

Shimizu, T., K. Ihara, R. Maesaki, M. Amano, K. Kaibuchi, and T. Hakoshima. 2003. Parallel coiled-coil association of the RhoA-binding domain in Rho-kinase. *J Biol Chem*. 278:46046-46051.

Siller, K.H., and C.Q. Doe. 2009. Spindle orientation during asymmetric cell division. *Nat Cell Biol*. 11:365-374.

Steigemann, P., and D.W. Gerlich. 2009. Cytokinetic abscission: cellular dynamics at the midbody. *Trends in Cell Biology*. 19:606-616.

Straight, A.F., C.M. Field, and T.J. Mitchison. 2005. Anillin Binds Nonmuscle Myosin II and Regulates the Contractile Ring. *Molecular Biology of the Cell*. 16:193-201.

Su, K.-C., T. Takaki, and M. Petronczki. 2011. Targeting of the RhoGEF Ect2 to the Equatorial Membrane Controls Cleavage Furrow Formation during Cytokinesis. *Developmental Cell*. 21:1104-1115.

Sun, L., R. Guan, I.J. Lee, Y. Liu, M. Chen, J. Wang, J.Q. Wu, and Z. Chen. 2015. Mechanistic insights into the anchorage of the contractile ring by anillin and Mid1. *Dev Cell*. 33:413-426.

Sweeney, S.J., P. Campbell, and G. Bosco. 2008. Drosophila sticky/citron kinase is a regulator of cell-cycle progression, genetically interacts with Argonaute 1 and modulates epigenetic gene silencing. *Genetics*. 178:1311-1325.

Thumkeo, D., S. Watanabe, and S. Narumiya. 2013. Physiological roles of Rho and Rho effectors in mammals. *Eur J Cell Biol*. 92:303-315.

Tormos, A.M., R. Taléns-Visconti, and J. Sastre. 2015. Regulation of cytokinesis and its clinical significance. *Critical Reviews in Clinical Laboratory Sciences*. 52:159-167.

Uehara, R., G. Goshima, I. Mabuchi, R.D. Vale, J.A. Spudich, and E.R. Griffis. 2010. Determinants of myosin II cortical localization during cytokinesis. *Current biology : CB*. 20:1080-1085.

Uehara, R., T. Kamasaki, S. Hiruma, I. Poser, K. Yoda, J. Yajima, D.W. Gerlich, and G. Goshima. 2016. Augmin shapes the anaphase spindle for efficient cytokinetic furrow ingression and abscission. *Mol Biol Cell*. 27:812-827.

Voets, E., J. Marsman, J. Demmers, R. Beijersbergen, and R. Wolthuis. 2015. The lethal response to Cdk1 inhibition depends on sister chromatid alignment errors generated by KIF4 and isoform 1 of PRC1. *Sci Rep*. 5:14798.

von Dassow, G. 2009. Concurrent cues for cytokinetic furrow induction in animal cells. *Trends in Cell Biology*. 19:165-173.

Wagner, E., and M. Glotzer. 2016. Local RhoA activation induces cytokinetic furrows independent of spindle position and cell cycle stage. *The Journal of Cell Biology*. 213:641-649.

Watanabe, S., T. De Zan, T. Ishizaki, and S. Narumiya. 2013. Citron kinase mediates transition from constriction to abscission through its coiled-coil domain. *J Cell Sci*. 126:1773-1784.

Watanabe, S., K. Okawa, T. Miki, S. Sakamoto, T. Morinaga, K. Segawa, T. Arakawa, M. Kinoshita, T. Ishizaki, and S. Narumiya. 2010. Rho and anillin-dependent control of mDia2 localization and function in cytokinesis. *Mol Biol Cell*. 21:3193-3204.

Winey, M., and K. Bloom. 2012. Mitotic spindle form and function. *Genetics*. 190:1197-1224.

Wolfe, B.A., T. Takaki, M. Petronczki, and M. Glotzer. 2009. Polo-Like Kinase 1 Directs Assembly of the HsCyk-4 RhoGAP/Ect2 RhoGEF Complex to Initiate Cleavage Furrow Formation. *PLoS Biology*. 7.

Yamashiro, S., G. Totsukawa, Y. Yamakita, Y. Sasaki, P. Madaule, T. Ishizaki, S. Narumiya, and F. Matsumura. 2003. Citron kinase, a Rho-dependent kinase, induces di-phosphorylation of regulatory light chain of myosin II. *Mol Biol Cell*. 14:1745-1756.

Yüce, Ö., A. Piekny, and M. Glotzer. 2005. An ECT2–centralspindlin complex regulates the localization and function of RhoA. *The Journal of Cell Biology*. 170:571-582.

Zhang, Y., R. Sugiura, Y. Lu, M. Asami, T. Maeda, T. Itoh, T. Takenawa, H. Shuntoh, and T. Kuno. 2000. Phosphatidylinositol 4-phosphate 5-kinase Its3 and calcineurin Ppb1 coordinately regulate cytokinesis in fission yeast. *J Biol Chem*. 275:35600-35606.

Zhao, W.-m., and G. Fang. 2005. Anillin Is a Substrate of Anaphase-promoting Complex/Cyclosome (APC/C) That Controls Spatial Contractility of Myosin during Late Cytokinesis. *Journal of Biological Chemistry*. 280:33516-33524.

Zhu, C., and W. Jiang. 2005. Cell cycle-dependent translocation of PRC1 on the spindle by Kif4 is essential for midzone formation and cytokinesis. *Proceedings of the National Academy of Sciences of the United States of America*. 102:343-348.

9. Annexe

ELSEVIER LICENSE
TERMS AND CONDITIONS

Dec 21, 2016

This Agreement between Nour El ("You") and Elsevier ("Elsevier") consists of your license details and the terms and conditions provided by Elsevier and Copyright Clearance Center.

License Number	4013641358413
License date	Dec 21, 2016
Licensed Content Publisher	Elsevier
Licensed Content Publication	Trends in Cell Biology
Licensed Content Title	Concurrent cues for cytokinetic furrow induction in animal cells
Licensed Content Author	George von Dassow
Licensed Content Date	April 2009
Licensed Content Volume Number	19
Licensed Content Issue Number	4
Licensed Content Pages	9
Start Page	165
End Page	173
Type of Use	reuse in a thesis/dissertation
Portion	figures/tables/illustrations
Number of figures/tables/illustrations	1
Format	both print and electronic
Are you the author of this Elsevier article?	No
Will you be translating?	No
Order reference number	
Original figure numbers	Figure 2. Geometrical conditions supporting cleavage-furrow formation in C. elegans zygotes.
Title of your thesis/dissertation	Caractérisation du rôle de Citron Kinase dans la transition de l'anneau contractile à l'anneau du midbody
Expected completion date	Dec 2016
Estimated size (number of pages)	250
Elsevier VAT number	GB 494 6272 12
Requestor Location	Nour El-amine 25420 Pembroke Avenue GREAT NECK, NY 11020 United States Attn: Nour El amine
Total	0.00 USD

ELSEVIER LICENSE
TERMS AND CONDITIONS

Dec 21, 2016

This Agreement between Nour El ("You") and Elsevier ("Elsevier") consists of your license details and the terms and conditions provided by Elsevier and Copyright Clearance Center.

License Number	4013651328656
License date	Dec 21, 2016
Licensed Content Publisher	Elsevier
Licensed Content Publication	Developmental Cell
Licensed Content Title	Cytokinetic Abscission: Molecular Mechanisms and Temporal Control
Licensed Content Author	Beata Mierzwa,Daniel W. Gerlich
Licensed Content Date	8 December 2014
Licensed Content Volume Number	31
Licensed Content Issue Number	5
Licensed Content Pages	14
Start Page	525
End Page	538
Type of Use	reuse in a thesis/dissertation
Intended publisher of new work	other
Portion	figures/tables/illustrations
Number of figures/tables/illustrations	1
Format	both print and electronic
Are you the author of this Elsevier article?	No
Will you be translating?	No
Order reference number	
Original figure numbers	Figure 3. Anchorage of the Cell Cortex in the Intercellular Bridge
Title of your thesis/dissertation	Caractérisation du rôle de Citron Kinase dans la transition de l'anneau contractile à l'anneau du midbody
Expected completion date	Dec 2016
Estimated size (number of pages)	250
Elsevier VAT number	GB 494 6272 12
Requestor Location	Nour El-amine 25420 Pembroke Avenue GREAT NECK, NY 11020 United States Attn: Nour El amine

JOHN WILEY AND SONS LICENSE TERMS AND CONDITIONS

Dec 21, 2016

This Agreement between Nour El ("You") and John Wiley and Sons ("John Wiley and Sons") consists of your license details and the terms and conditions provided by John Wiley and Sons and Copyright Clearance Center.

License Number	4013410175115
License date	Dec 20, 2016
Licensed Content Publisher	John Wiley and Sons
Licensed Content Publication	Cytoskeleton
Licensed Content Title	Phosphoinositides and cytokinesis: The "PIP" of the iceberg
Licensed Content Author	Arnaud Echard
Licensed Content Date	Sep 25, 2012
Licensed Content Pages	20
Type of use	Dissertation/Thesis
Requestor type	University/Academic
Format	Print and electronic
Portion	Figure/table
Number of figures/tables	1
Original Wiley figure/table number(s)	Figure 2. Phosphoinositide-modifying enzymes are required at different steps of cytokinesis.
Will you be translating?	No
Title of your thesis / dissertation	Caractérisation du rôle de Citron Kinase dans la transition de l'anneau contractile à l'anneau du midbody
Expected completion date	Dec 2016
Expected size (number of pages)	250
Requestor Location	Nour El-amine 25420 Pembroke Avenue GREAT NECK, NY 11020 United States Attn: Nour El amine
Publisher Tax ID	EU826007151
Billing Type	Invoice
Billing Address	Nour El-amine 2540 pembroke avenue GREAT NECK, NY 11020 United States Attn: Nour El amine
Total	0.00 USD
Terms and Conditions	